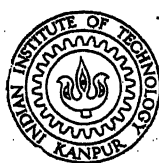


# **VIBRATIONAL SPECTRA OF CERTAIN ALIPHATIC AMINES AND ROTATIONAL ISOMERISM**

50621

BY  
**ANANDI LAL VERMA**



**DEPARTMENT OF PHYSICS**  
**INDIAN INSTITUTE OF TECHNOLOGY KANPUR**  
**JULY 1970**

I. I. T. KANPUR  
CENTRAL LIBRARY  
Acc. No: A 19807

15 JUN 1972

Ther  
547.442  
V59

V  
JUNE '76

PHY-1970-D-VER-VIB

# **VIBRATIONAL SPECTRA OF CERTAIN ALIPHATIC AMINES AND ROTATIONAL ISOMERISM**

**A Thesis Submitted  
In Partial Fulfilment of the Requirements  
for the Degree of  
DOCTOR OF PHILOSOPHY**

**BY  
ANANDI LAL VERMA**

**to the**

**DEPARTMENT OF PHYSICS  
INDIAN INSTITUTE OF TECHNOLOGY KANPUR  
JULY 1970**

Certified that the work presented in this thesis has been  
carried out by Mr. Anandi Lal Verma under my supervision.

Department of Physics  
Indian Institute of Technology  
Kanpur (INDIA)

*Putchha Venkateswarlu*  
(Putchha Venkateswarlu)  
Professor of Physics 31.7.20



## ACKNOWLEDGEMENT

I wish to keep on record my deep sense of gratitude to Professor Putcha Venkateswarlu for his inspiring guidance, continuous encouragement and many suggestions throughout the course of this work.

Thanks are due to the Director, Indian Institute of Technology, Kanpur, for his interest in the progress of the work.

Grateful acknowledgement is made to Professor J. Mahanty for his kind interest and encouragement during this investigation.

My sincere thanks are due to Mr. Kamal Kumar for many discussions and friendly cooperation.

It is impossible to acknowledge properly all of those whose cooperation and encouragement at various stages have contributed greatly to the success of the work. However, I take this opportunity to thank in particular, Drs. H.D. Bist, D.R. Rao, K.V.L.N. Sastry, P.A. Narayana and M/S J.P. Srivastava, A.N. Garg and V.N. Sarin for their interest and encouragement. The timely assistance rendered by the personnel of different technical shops is much appreciated.

I wish to thank the Department of Physics, Indian Institute of Technology, Delhi for permitting the use of their Raman Spectrophotometer and Mr. H.K. Sehgal for his help in recording the Raman spectra.

I am extremely thankful to my wife, Kala for her patience and understanding during the tenure of this work.

At the end, I would like to thank Mr. S.L. Rathore for typing the thesis patiently and efficiently and Mr. Lalloo Singh for cyclostyling the same.

(A.L. VERMA)

## CONTENTS

	<u>Page</u>
PREFACE	vi
CHAPTER	
I An Introduction to Infrared and Raman Spectroscopy	1
II Experimental Details	30
III Vibrational Spectra of Allyl Amine and Rotational Isomerism	37
IV Vibrational Spectra of Diethyl Amine and Rotational Isomerism	81
V Vibrational Spectra of Tripropargyl Amine and Rotational Isomerism	118
VI Vibrational Spectra of Triallyl Amine and Rotational Isomerism	152

## PREFACE

The thesis describes the results of investigation by the author on the infrared and Raman spectra of some aliphatic amines. The amines studied are: Allyl amine (primary amine), diethyl amine (secondary amine), tripropargyl amine and triallyl amine (tertiary amines).

The amines have many interesting properties. Very little work is reported in the literature on the structural stability of the molecules having C-N linkages ( $sp^3 - sp^3$  hybridization) as compared to those having C-C linkages. All the amines studied have one or more axes about which hindered internal rotation is possible giving rise to more than one rotational isomer. No systematic studies in this direction seem to be reported earlier with a view to determine the relationship between the precise frequencies found and the structure of the molecule as a whole for these compounds. The liable nature of the nitrogen valence electrons makes the specific assignment of group frequencies somewhat difficult. In order to find out the structure of different rotational isomers and to assign the various group frequencies with more certainty, a systematic study of the infrared spectra of the various amines in the vapour, liquid and solid phases and the Raman spectra of the liquids with depolarization measurements was undertaken.

Furthermore, the modes arising due to the  $-NH_2$  and  $-NH$  groups in the allyl amine and diethyl amine respectively are expected to be affected by the hydrogen bonding effects in various phases. The present studies are expected to yield information about the effects of temperature, solvents and change of phase on hydrogen bonding phenomenon and the deformation modes of these sub-groups.

In spite of their seemingly more complicated nature, the molecules of tripropargyl amine and triallyl amine are expected to have higher symmetries which may make the interpretation simpler. On the basis of the available information on simple propargylic and allylic compounds, it would be interesting to study the environmental and other effects on the propargyl and allyl groups when placed in somewhat more complicated molecular frames. The low temperature studies in conjunction with depolarization measurements of the Raman lines would also be helpful in determining the structure of the lower energy forms of these molecules. The assignment of the fundamental modes may become easier by attributing the observed bands to one isomer or the other. This could be made possible through the following studies: The effects of the temperature and solvent variations, the band contour studies in the vapour phase and the Raman depolarization studies.

In view of the incompleteness of the previous work on all these molecules, a systematic study of their vibrational spectra was undertaken and the results obtained are discussed in this thesis.

All the compounds were studied in infrared in the vapour, liquid and solid phases from 250 to 4000  $\text{cm}^{-1}$  using a Perkin-Elmer 521 grating infrared spectrophotometer. The Raman spectra of all the compounds in the liquid phase at room temperature were photoelectrically recorded on a Coderg PH-1 Raman spectrophotometer employing Spectra-Physics model 125 He-Ne gas laser as a source with an output at 6328 Å. Qualitative depolarization measurements for the Raman displacements were made by using incident polarized light technique. In order to study the rotational isomerism and hydrogen bonding effects in these molecules, the infrared spectra in the solid phase near liquid nitrogen temperature and in solutions of varying polarity were measured.

The thesis consists of six chapters. Chapter I is an introduction to the infrared and Raman spectroscopy. The details of calculation of the number of normal modes and the infrared and Raman active species are also given there. A brief discussion is presented about band contours in the vapour phase, effects of temperature variation and polarity of solvents, rotational isomerism, hydrogen bonding and depolarization measurements in the Raman spectra.

The experimental details regarding the spectrophotometers used in the infrared and Raman work are presented in Chapter II. The details of the low temperature cell fabricated here are also given therein. It also deals with the method of determination of Raman depolarization ratios.

Chapter III describes the vibrational spectra (ir and Raman) of allyl amine. The infrared spectra are reported in the vapour, liquid and solid phases along with the Raman spectrum and depolarization data in the liquid phase. From the observed shifts for some of the bands in various solvents ( $\text{CCl}_4$ ,  $\text{CH}_3\text{Cl}$ ,  $\text{CH}_3\text{CN}$  etc.) and in different physical states, it is shown that a weak molecular association is present in both the liquid and solid states which is caused by the intermolecular hydrogen bonding effects. In the solid phase, the  $\text{NH}_2$  deformation modes give rise to strong bands with multiplet splitting (generally into two or three components) which is probably caused due to the intramolecular interactions between the  $\text{NH}_2$  group and the  $\pi$ -electrons of the  $\text{C} = \text{C}$  double bond, or by the formation of several unequal types of bonds in a crystal or multimer unit. The spectral data suggest that two rotational isomers ('cis and trans' and 'gauche and trans') exist in the vapour and liquid phases, whereas the 'gauche and trans' form having  $\text{C}_1$  symmetry gets stabilized in the solid phase. The band contours in the vapour phase are well resolved and the calculated PR separation for the 'gauche and trans' form agrees well with the observed values.

The vibrational spectra of diethyl amine are discussed in Chapter IV. The temperature dependence of some of the bands in the infrared spectrum of diethyl amine indicates the presence of two rotational isomers (T T and T G, with T T being in more abundance)\* in the liquid and vapour phases while in the solid phase near liquid nitrogen temperature, the T G form of the molecule having no symmetry gets stabilized, presumably due to the hydrogen bonding effects. The observed data also suggest a weak molecular association in the condensed phases. The out-of-plane CNH deformation mode has been identified in the solid phase.

Chapter V gives an account of the infrared spectral measurements in the vapour, liquid and solid phases of tripropargyl amine along with the Raman data for the liquid. Various possibilities for rotational isomers with different point group symmetries are discussed. It is suggested that the GGG configuration of the molecule, having  $C_3$  point group symmetry, is the lower energy form existing in the solid phase whereas the TGG form with  $C_1$  symmetry is probably the other conformer present in lower concentration in fluid phase along with the GGG form. The bands due to the  $-C \equiv C-H$  groups are found to shift slightly with change of phase from liquid to solid thereby suggesting a very weak molecular association, probably caused due to slightly acidic nature of the acetylenic protons. A vibrational assignment for the observed bands has been attempted in view of the presence of rotational isomers in the liquid and vapour phases and the  $-CH_2$  stretching and deformation modes have been characterized.

---

\*The 'trans' (T) and 'gauche' (G) forms denote whether the skeletons  $C_4-C_3-N-C_2$  and  $C_1-C_2-N-C_3$  are in the 'trans' (dihedral angle  $0^\circ$ ) or 'gauche' (dihedral angle  $120^\circ$ ) positions respectively.

Chapter VI describes the vibrational studies made on triallyl amine. One of the interesting features of the observed spectrum of crystalline solid near 77 °K is the presence of a number of very sharp doublets for the bands corresponding to the depolarized bands in the Raman spectrum. This behaviour together with steric considerations suggests that the molecular species in the crystalline phase at low temperature possess  $C_3$  point group symmetry. The GGG (III) configuration corresponding to internal rotations about the C-N bonds with all the three N-C-C=C skeletons in the 'gauche' positions is suggested to be the lower energy form with  $C_3$  symmetry. A few bands belonging to other isomer(s) disappear at low temperature whose structure can not be established from the present data. A vibrational assignment for the observed bands has been proposed on the basis of the  $C_3$  point group symmetry for the more stable form of the molecule.

References, tables and figures are given at the end of each chapter. The Chapters III-VI in this thesis are written in a way suitable for submitting the manuscripts for publication and so repetition of certain statements has become unavoidable at some places.

July, 1970

A.L. Verma

## CHAPTER I

### AN INTRODUCTION TO INFRARED AND RAMAN SPECTROSCOPY



## INTRODUCTION

The recent developments in modern methods of spectroscopy in the different regions of electromagnetic spectrum have provided the scientists with indispensable means for the investigation of molecular structure. The choice of a particular spectroscopic method for a specific problem mostly depends on the kind of information desired. The infrared and Raman spectroscopic techniques are among the most useful and powerful physical methods available for the solution of problems connected with the molecular structure, molecular behaviour, intra- and intermolecular forces, conformational analysis and others.

Any motion of an atomic system which is associated with a change of its dipole moment leads to the emission or absorption of radiation. A change in the quadrupole moment or in the magnetic dipole moment may also lead to emission or absorption of radiation, but in general, the intensity of this emission or absorption is negligible compared to that arising from dipole moment change. When a molecule absorbs radiation of frequency  $\nu$  (cycles/sec.), its energy increases in proportion to the energy of the photon ( $h\nu$ ) under suitable circumstances. The increase in energy may be in the translational, electronic, vibrational or rotational energy of the molecule. Electronic energy transitions normally give rise to absorption or emission in the ultra-violet and visible regions of the electromagnetic spectrum. Translational motion, ordinarily, does not give rise to radiation, because classically, acceleration of charges is required for radiation. Pure rotations give rise to absorption in the microwave or far-infrared regions. If the radiation is in the medium infrared region, both the vibrational and rotational energies of the

molecular system may change simultaneously. A change in the polarizability of a molecular system may give rise to Raman scattering process.

In the present discussion, we shall be mainly concerned with the interaction of electromagnetic radiation with the molecular vibrations and rotations in its electronic ground state.

#### INFRARED SPECTRUM

The systematic study in the region of infrared radiation may be said to have been started with the classic work of Coblentz<sup>1</sup> who published the first catalogue of infrared spectra of organic compounds in 1905. In 1912, Bjerrum<sup>2</sup> presented the theory of the vibration-rotation spectra of molecules. A rapid development of the infrared spectroscopic methods took place during World War II. Substantial improvements were made in instrumentation; specially the development of refined techniques of grating spectroscopy and a mass production of easy-to-use recording type spectrophotometers was started which contributed a lot to the expansion of ir spectroscopy and is continued till to date.

If the motion of a molecule with  $N$  atoms is considered in a three dimensional space,  $3N$  coordinates are required to specify the position of each atom. Out of these, 3 coordinates are required to describe the translational motion of the system as a whole and 3 coordinates (2 for linear molecules) specify the orientation of the system (considered as rigid) in space. Therefore,  $(3N-6)$  coordinates (for linear molecules only  $3N-5$  coordinates) are left for describing the relative motion of the nuclei with fixed orientation of the system as a whole. During the vibrational motion of a molecule, the charge distribution undergoes a periodic change and therefore, in general, (but not always) the dipole

moment changes periodically. Any periodic vibrational motion of the system may be represented as a superposition of normal vibrations with appropriate amplitudes, and since normal vibrations are the only simple periodic motions, the normal frequencies are the frequencies that are emitted or absorbed by the molecules. In a normal mode of vibration, all the atoms perform simple harmonic motions with the same frequency and pass through their equilibrium positions simultaneously. If the electrical field of the molecule is vibrating or rotating at the same frequency as the incoming radiation, the transfer of energy is possible. Both the polarizability and the electric moment of the molecule may vary as the atoms change their relative positions.

#### The number and activity of modes

The number and activity of the vibrational modes of a polyatomic molecule are dependent on the symmetry of the molecule. The vibrational selection rules dictated by the symmetry of a molecule determine the spectroscopic activity, i.e., the occurrence or nonoccurrence of any given vibration in the spectrum. In order to find out which transitions occur and with what intensity, it is necessary to calculate the transition probabilities.

The probability of transition from state  $n$  to another state  $m$  is proportional to:

$$P_{nm}^2 = X_{nm}^2 + Y_{nm}^2 + Z_{nm}^2 \quad (I.1)$$

where  $X_{nm}$  is a matrix element given by

$$X_{nm} = \int \psi_n^* \mu_x \psi_m d\tau \quad (I.2)$$

with similar expression for  $Y_{nm}$  and  $Z_{nm}$ .

Here,  $\mu_x$ ,  $\mu_y$  and  $\mu_z$  are the three components of the dipole moment,

$\psi_n$  and  $\psi_m$  are the eigen functions of the system in the two states  $n$  and  $m$  respectively.

If  $P_{nm} = 0$ , the transition cannot occur, but if  $P_{nm} \neq 0$ , the transition is allowed.

In general, to evaluate the integrals of the type (I.2), one must know the wavefunctions  $\psi_n$  and  $\psi_m$  explicitly, and whenever the intramolecular forces are not harmonic, this may involve a large and laborious perturbation calculations. However, if one is interested only in vanishing or nonvanishing of the matrix elements, these could be determined from symmetry considerations alone<sup>3</sup>.

If we consider only vibrational motion of a nonrotating molecule in its electronic ground state, then it can be shown that, under the harmonic oscillator approximation,  $\Delta v = \pm 1$  for the integrals of the type (I.2) not to vanish. The net result of all these considerations can be stated as follows: If it is assumed that only linear terms in the expansion of the electric moment are important, and that the vibrational wavefunctions are the products of the harmonic oscillator functions, then only those vibrational transitions can occur with the emission or absorption of radiation in which only one quantum number changes by one unit only. Furthermore, since integrals like (I.2) are definite integrals over a whole configuration space of the molecule, they should remain unchanged by the symmetry operation permitted by the point group of the molecule. More explicitly, a vibrational transition  $v' \leftrightarrow v''$  is allowed only when there is at least one component of the dipole moment  $\vec{\mu}$  that has the same species as the product  $\psi_{v'} \cdot \psi_{v''}$ .

A number of earlier workers<sup>3a,b,c</sup> applied the principles of group theory taking into consideration the knowledge of the symmetry properties of molecules to the determination of the normal modes of vibrations and gave the following reduction formula:

$$N_i = \frac{1}{N_g} \sum n_e \chi_i(R) \quad (I.3)$$

where  $N_i$  is the number of fundamentals of vibration type  $i$ ,  $n_e$  is the number of elements in each class,  $N_g$  is the number of elements in the group, i.e., the order of the group and  $\chi_i(R)$  is the character in the character table for vibration type  $i$  and operation  $R$ .

$\chi_i(R)$  is given by

$$\chi_i(R) = (U_R - 2)(1 + 2 \cos \phi) \quad (I.4a)$$

for proper rotations

and

$$\chi_i(R) = U_R(-1 + 2 \cos \phi) \quad (I.4b)$$

for improper rotations. The number of atoms that remain unchanged by the symmetry operation is given by  $U_R$ .

#### Overtone and summation bands

Generally it is found that along with the fundamentals, some other transitions also appear in the vibrational spectra. This is due to the fact that harmonic oscillator approximation is not valid, as the contributions due to the cubic, quartic etc. terms in the potential energy (mechanical anharmonicity) are not zero. Further, the higher terms in the expansion of electric moment (electrical anharmonicity) due to non-linear changes in the dipole moment with displacement may also contribute to the observed spectra.

Overtone bands arise from vibrational transitions for which one  $\Delta v_i > 1$ . Combination bands arise from vibrational transitions for which several  $\Delta v_i \neq 0$ . It may happen sometimes that a fundamental vibration

is forbidden while certain overtone and combination bands involving the same vibration are allowed. Conclusions regarding the symmetry of a molecule may be drawn from the occurrence or non-occurrence of certain overtone bands. The activity of these overtones and summation bands are determined by the same rules as for fundamentals.

### Difference bands

When the initial state is not the vibrationless ground state of a molecule, difference bands can be observed in the vibrational spectra. If the vibration  $\nu_i$  is singly excited in the initial (lower) state and a transition takes place to a state in which the vibration  $\nu_k$  ( $> \nu_i$ ) is singly excited, the frequency of the absorption band is equal to  $\nu_k - \nu_i$ . Theoretically, the intensity of the  $\nu_k - \nu_i$  band is expected to be much smaller than that of  $\nu_k + \nu_i$  in correspondence with the Boltzmann factor  $\exp. (-\frac{hc\nu_i}{kT})$ , where  $h$  is the Planck's constant,  $k$  is Boltzmann constant,  $T$  is absolute temperature and  $c$  is the velocity of light. Another type of difference band occurs when the same low frequency vibration is excited in the upper and lower state in addition to some other vibrations in the upper state. If  $\nu_k$  is excited by one quantum in the upper state but not in the lower state and  $\nu_i$  is excited both in the lower and upper states by one quantum, a band may be obtained as  $\nu_k + \nu_i - \nu_i$ . As a result of coupling between these two vibrations ( $\nu_k$  and  $\nu_k + \nu_i - \nu_i$ ),  $\nu_k + \nu_i - \nu_i \neq \nu_k$ .

Difference bands are observed in the infrared spectra only when  $\nu_i$  is small, i.e., when the lower state is fairly near the ground state. Accordingly, the Boltzmann factor will not be too small for the lower state. The selection rules allow or forbid a difference band when the corresponding

summation band ( $\nu_k + \nu_i$ ) is allowed or forbidden. The wavenumber of a difference band  $\nu_k - \nu_i$  is exactly the difference between the wavenumbers of  $\nu_k$  and  $\nu_i$  even with anharmonicity taken into account while the wave number of a summation band needs not be exactly the sum of the wavenumbers for  $\nu_k$  and  $\nu_i$ <sup>4</sup>. The intensity of the difference bands is temperature dependent.

### Fermi resonance

In polyatomic molecules, it is possible that the two vibrational levels belonging to two different vibrations might have nearly the same energy and therefore could interact (accidental degeneracy). Such a resonant interaction leads to a perturbation of the energy levels and the mixing of the eigen functions of the two states. This interaction through anharmonic terms in potential energy produces a much greater separation of the two vibrational levels concerned and depends upon how much close the unperturbed levels are. The magnitude of the perturbation depends on the value of the second order correction to the energy level  $w_n^0$ , caused by a perturbation  $w$  and is given by

$$\frac{w_{ni} w_{in}}{w_n^0 - w_i^0} \quad (a)$$

where

$$w_{ni} = \int \psi_n^0 w \psi_i^0 d\tau \quad (b)$$

The perturbation function  $w$  is given by the anharmonic terms (cubic, quartic etc.) in the potential energy and  $\psi_n^0$ ,  $\psi_i^0$  and  $w_n^0$ ,  $w_i^0$  are the zero approximation eigen functions and energies respectively of the two vibrational levels which perturb each other. Since  $w$  has the full symmetry of the molecule (totally symmetric),  $\psi_n^0$  must have the same symmetry species as  $\psi_i^0$  in order to give a non-zero value to  $w_{ni}$ .

Therefore, Fermi resonance can occur only between the levels of the same species, and if the unperturbed frequencies are nearly alike. When resonance occurs, the two bands are perturbed in frequency and intensity and hence they appear well separated. If the resonance is close, the intensities of the two bands approximate the average of the unperturbed intensities.

If a state is in resonance with another state corresponding to the excitation of a degenerate vibration, a perturbation will usually occur only for one of the sublevels, into which the state is resolved, having the same species as that of the state in resonance.

#### THE INFRARED SPECTRA OF MOLECULES IN VARIOUS PHASES

The selection rules derived for infrared and Raman spectra apply strictly only to the isolated molecules and quite frequently forbidden bands appear weakly in condensed phase spectra due to the intermolecular perturbations. Therefore, one may expect some differences among the spectra of the same molecule in the gaseous, liquid and solid states.

##### The vapour phase

The ir spectrum of a molecule in the vapour phase can yield a great deal of information about its structure. In the vapour phase, a molecule is free to rotate as well as to vibrate since the molecular interactions via collisions are minimum at low pressures. The rotational structure is influenced at the most by the intramolecular and not by intermolecular interactions. With increasing pressure, the mean free path of the molecules is shortened and the number of collisions of the molecules per unit time increases. As a result, their rotational motions are attenuated which is manifested by the broadening and merging of rotational lines in the vibration-rotation spectrum.



For molecules possessing relatively smaller rotational constants, where the fine structure due to rotational motion is usually not resolved, a study of band shapes and PR separations may contribute a lot to the vibrational assignment of molecules. The band contours in gaseous state are determined by the orientation of the change in the molecular dipole moment in the particular vibration with respect to the principal axes of inertia tensor. A brief discussion regarding the band contours and PR separation is given below. Seth-Paul and coworkers<sup>5-8</sup> have given the modified expressions for calculating the PR separation of band envelopes in vapour phase based on the deductions of Gerhard and Dennison<sup>9</sup> for symmetric top molecules and by Badger and Zimmwalt<sup>10</sup> for asymmetric top molecules.

In the principal axes system, the three moments of inertia are denoted by  $I_A$ ,  $I_B$  and  $I_C$  such that  $I_A \leq I_B \leq I_C$  or  $A \geq B \geq C$  where  $A$ ,  $B$  and  $C$  are the rotational constants associated with the principal moments of inertia defined as:

$$A = \frac{h}{8\pi^2 c I_A} ; B = \frac{h}{8\pi^2 c I_B} \text{ and } C = \frac{h}{8\pi^2 c I_C} \quad (1.5)$$

Here  $c$  is the velocity of light and  $h$  is the Plank's constant.

Depending upon the relative values of the moments of inertia, the molecules can be divided into the following specific categories.

- (1) Linear molecules:  $I_A = 0, I_B = I_C$
- (2) Spherical top:  $I_A = I_B = I_C$
- (3) Symmetric top molecules:
  - (a) Oblate type:  $I_A = I_B < I_C$
  - (b) Prolate type:  $I_A < I_B = I_C$
- (4) Asymmetric top molecules:  $I_A \neq I_B \neq I_C$

Several molecular parameters are required for calculating the frequency difference between the maxima of the P ( $\Delta J = -1$  on lower frequency side) and R ( $\Delta J = +1$  on the higher frequency side of the Q branch ( $\Delta J = 0$ )) branches. The parameters frequently used are  $\kappa$ ,  $\beta$ ,  $\rho^*$  and  $S(\beta)$  which are either functions or simple ratios of the rotational constants. The asymmetry parameter  $\kappa$  is defined<sup>11</sup> as:

$$\kappa = \frac{2B - A - C}{A - C} \quad (I.6)$$

which implies that  $-1 \leq \kappa \leq +1$ . The molecule is called a prolate symmetrical top for  $\kappa = -1$  and an oblate symmetrical for  $\kappa = +1$  and maximally asymmetrical for  $\kappa = 0$ . When  $\kappa \approx \pm 1$ , the molecule is said to approximate to a symmetric top.  $\kappa = \frac{0}{0}$  for  $A = B = C$  which defines spherical top molecules.

The constants  $\beta$  and  $\rho^*$  are defined as follows:

$$\beta = \frac{A}{B} - 1 \text{ for prolate and } \beta = \frac{C}{B} - 1 \text{ for oblate molecules and } \rho^* = \frac{A-C}{B} \quad \dots (I.7)$$

The parameter  $S(\beta)$  introduced by Gerhard and Dennison<sup>9</sup> is a function of  $\beta$  and is defined as  $\log_{10} S(\beta) = \frac{0.721}{(\beta+4)^{1.13}}$  (I.8)

The entire PQR structure of a band is governed by two factors: The intensity of the Q branch and the PR separation. The intensity of the Q branch seems to depend on  $\beta$  and the absolute temperature, while the PR separation apparently depends upon  $\beta$ , B and the absolute temperature.

The linear molecules ( $\beta = \infty$ ) may give rise to two types of vibrational-rotational bands. A band is referred to as parallel or perpendicular when the dipole moment changes occur either parallel or perpendicular to the molecular major (a) axis of inertia respectively. The perpendicular bands generally show PQR structure with their Q branches normally being very pronounced

Gerhard and Dennison<sup>9</sup> have shown that for parallel bands of the symmetric top molecules; the ratio of the intensity of the Q-branch ( $I_Q$ ) to that of the total intensity of the band ( $I_T$ ) may be given by the expressions:

$$R(\beta) = \frac{I_Q}{I_T} = \left[ \log(\sqrt{\beta} + \sqrt{\beta+1}) - \sqrt{\beta/(\beta+1)} \right] / \left\{ \beta \sqrt{\beta/(\beta+1)} \right\} \quad (\text{I.9a})$$

$$\text{and } R(\beta) = \frac{I_Q}{I_T} = \left[ \sqrt{-\beta/(\beta+1)} - \sin^{-1} \sqrt{-\beta} \right] / \left\{ -\beta \sqrt{-\beta/(\beta+1)} \right\} \quad (\text{I.9b})$$

for  $\beta > 0$

for  $\beta < 0$

The vibrational bands of symmetric top molecules in vapour phase may give rise to both parallel and perpendicular type of bands. The parallel type bands arise from the transitions between the two non-degenerate vibrational levels while the perpendicular type bands occur by transitions from the non-degenerate ground state to the doubly degenerate first vibrational level ( $v = 1$ ). The intensities of the Q branch relative to the P and R branches may be expected to be different for different values of  $\beta$ . For parallel bands,  $I_Q = 0$  for  $\beta = \infty$  (for linear molecules) and reaches a maximum for  $\beta = -\frac{1}{2}$ . In the region  $\infty > \beta > 0$ ,  $I_Q$  increases with decreasing  $\beta$ . For  $\beta = 0$  (spherical top molecules),  $I_Q$  equals to one third of the total intensity of the band. For negative values of  $\beta$ ,  $I_Q$  increases rapidly and is maximum for  $\beta = -\frac{1}{2}$ .

For perpendicular bands, the Q branch should have comparable intensity to those of P and R branches when  $\beta \approx -\frac{1}{2}$  and might be expected to increase with increasing  $\beta$ . For positive values of  $\beta$ ,  $I_Q$  increases rapidly and all the branches (P, Q & R) become broader with their maxima lower. For sufficiently larger values of  $\beta$ , the band no longer shows PQR structure but resembles a Gauss error curve.

In the case of symmetric top molecules, it was shown by Gerhard and Dennison<sup>9</sup> that for parallel bands, the PR separation may be expressed as a product of two functions given below:

$$\Delta \nu(\text{PR}) \parallel \text{type} = S(\beta) \times 5 \left( \frac{2BT}{9} \right)^{1/2} \quad (\text{I.10})$$

Here  $S(\beta)$  is a function of  $\beta$  given by the expression (I.8) and the second part represents the PR separation for linear molecules.

For perpendicular bands; the following modified expression was given by Seth-Paul and Dijkstra<sup>5</sup> for calculating the PR separation:

$$\Delta \nu(\perp \text{PR}) = 5 S(\beta) (2\xi T/9)^{1/2} \quad (\text{I.11})$$

where  $\xi$  equals C for oblate and A for prolate symmetric top molecules within the values of  $\beta$  such that  $-\frac{1}{2} \leq \beta \leq \frac{3}{4}$ .

In the case of asymmetric top molecules, the band contours may be divided into three distinct types, A, B and C depending on whether the dipole moment change occurs along the axis of least, intermediate or greatest moment of inertia. The contours of the pure A, B, and C type bands mostly depend upon the relative values of the moments of inertia.

When the formula (I.10) is applied to predict the PR separations of type A ( $\parallel$ ) bands for near prolate and type C ( $\parallel$ ) bands for near oblate asymmetric top molecules, the calculated values are found generally higher than those observed experimentally. Lateron Seth-Paul and Dijkstra<sup>5</sup> have modified the expression (I.10) by replacing B by  $\tilde{B}$  and  $\beta$  by  $\tilde{\beta}$  where  $\tilde{B}$  equals  $BC/(B+C)$  and  $AB/(A+B)$  and  $\tilde{\beta} = \frac{A}{2\tilde{B}} - 1$  and  $\tilde{\beta} = \frac{C}{2\tilde{B}} - 1$  for prolate and oblate asymmetric top molecules respectively. The final expression thus obtained is:

$$\Delta \nu(\text{PR}) \parallel \text{type} = 10 S(\tilde{\beta}) \left( \frac{\tilde{B}T}{9} \right)^{1/2} \quad (\text{I.12})$$

which gives a better agreement between the observed and calculated values.

For perpendicular type bands of asymmetric top molecules; the above authors have given the expressions for calculating the PR separations corresponding to different values of  $\rho^*$  and asymmetry parameter  $K$ . However for low values of  $\rho^*$ , the type B( $\frac{1}{2}$ ) bands may exhibit a doublet Q branch with a PQ Q'R type structure with four maxima which gradually passes into a band structure with only two maxima (PQ and Q'R) at higher  $\rho^*$  values due to the overlapping of the P and R branches, the decrease in the intensity of the Q branch and the simultaneous broadening of all branches.

The following empirical relations for calculating the QQ' separations for oblate asymmetric top molecules were given by Seth-Paul and De Meyer<sup>6</sup>:

$$\Delta\nu(QQ') = \frac{1}{3} \rho^* S_B \sqrt{2} \text{ cm}^{-1} \text{ for molecules with } \frac{1}{3} \leq \rho^* \leq \frac{1}{2} \quad (\text{I.13})$$

$$\text{and } \Delta\nu(QQ') = \frac{2}{3} \rho^{*2} S_B \sqrt{2} \text{ cm}^{-1} \text{ for molecules with } \rho^* \geq \frac{1}{2} \quad (\text{I.14})$$

where  $S_B$  refers to the calculated PR separation of the corresponding type B( $\frac{1}{2}$ ) bands.

Sometimes it happens for molecules of low symmetry having considerably different moments of inertia that the observed and calculated values of PR separations do not agree. These differences are believed to arise from the changes in rotational and Coriolis coupling constants while going from the ground to the excited states. They could also arise because of the fact that dipole changes may not be parallel to one axis of inertia which results in the appearance of hybrid bands<sup>7</sup>.

At higher temperature in vapour phase; the separation between the maxima of the P and R branches varies approximately as the square root of the absolute temperature of the gas and the intensity of the hot bands may increase. The half-width increases and peak height decreases due to the increase in more frequent collisions of the gas molecules with increase in temperature.

### The liquid phase

In the liquid state, the molecules do not possess preferred orientations and have considerable freedom of movement for collisions. The rotational modes of the molecules no longer remain quantized and hence the symmetry of the molecule may be distorted. The fine structure of the vibration - rotation bands disappear and the vibrational bands become broader and more symmetrical. Because of the close proximity of the molecules, intermolecular effects such as dipole-dipole attraction and molecular association can occur which may give rise to frequency shifts and intensity changes in some of the vibrational bands. The close-packed molecules in liquid may become instantaneously polarized by their dynamic surroundings and hence the symmetry that exists in the gaseous state is not preserved. This may result in the appearance of new bands in liquid phase due to violation of selection rules.

### Low temperature effects and solid phase spectrum

Very significant changes in the ir spectra are observed when a substance passes from the liquid or amorphous state to the crystalline state at low temperatures. The distorting intermolecular forces in the crystalline state no longer remain random but they are controlled by the site symmetry of the molecules in the lattice. The symmetry of the building unit of the crystal lattice, the unit cell, may be different from the symmetry of the individual molecules. Accordingly a crystalline solid gives rise to: (1) Vibrations characteristic of the symmetry of the unit cell between the molecules considered as rigid entities and are called lattice vibrations (librational oscillations and translational displacement of the molecules); (2) the normal internal vibrations of the individual molecules that are in phase

with similar vibrational modes in all other unit cells. These vibrations can, in certain cases, couple with each other and may give rise to new absorptions in crystalline state spectra. If the unit cell of the crystal contains more than one chemically equivalent molecule, then the interaction between the vibrational modes of these molecules can give rise to splitting in the absorption bands associated with the vibrational modes. The stronger the attractive forces of the crystal lattice, or in other words, the more strongly polar the molecule, the greater will be the expected spectral differences between the gaseous, liquid and crystalline states.

At low temperature in solid phase, the discrete rotational fine structure of vibrational bands disappears and the lines become very sharp. The more complex spectra of the molecules having rotational isomers at normal temperatures are usually simplified at reduced temperatures due to the disappearance of the bands associated with less stable conformations. The overtone and combination bands generally become stronger and difference bands disappear at lower temperatures. In certain cases, such as those involving hydrogen bonding, there may be marked interactions between the molecules in the condensed phase which result in the frequency shifts and intensity changes of some of the bands along with many other spectral changes.

When molecules interact with each other, the potential energy of the nuclei depends not only on the internal force field of the molecule but also on the configuration of other molecules relative to the given one.

In the harmonic oscillator approximation<sup>12,13</sup>, the potential energy associated with the unit cell can be written as:

$$V = \sum_i (v_i^0 + v_i^1) + \sum_i \sum_j V_{ij} + V_L + V_{Li} \quad (I.15)$$

where the summation extends over all the molecules in the unit cell.

The various terms are:

$V_i^0$  = potential energy function of the free  $i^{\text{th}}$  molecule,

$V_i'$  = perturbation to  $V_i^0$  by the static field of the crystal at the site of the  $i^{\text{th}}$  molecule,

$V_{ij}$  represents the interaction between internal vibrations of different molecules - the dynamic field of the crystal,

$V_L$  = the potential energy function of the lattice modes (libration-translation displacements),

$V_{Li}$  = cross terms between internal and lattice coordinates.

The  $V_{Li}$  term is generally very small, and since the lattice frequencies associated with the coordinates in the  $V_L$  term are usually small in comparison with the internal frequencies of the molecule<sup>14</sup>, these terms may therefore be neglected.

The perturbation of the potential energy function of the free molecule is caused by the local equilibrium field of the crystal and is called the static crystal field effect<sup>13</sup>. Static field effects are a measure of the influence that the surrounding lattice exerts on the molecule in its equilibrium position at a site. It usually gives rise to shifts and splittings of frequencies (site-group splittings) and causes degenerate vibrational modes to split into their components.

The cross term in the dynamic crystal field effect describes the coupling between the modes of motion of the pairs of molecules within the crystals. The effect of this crystal field is that, if the unit cell contains  $N$  molecules, the  $N$ -fold degeneracy present without the  $V_{ij}$  term can be removed, so that in general a molecular mode of a single molecule will give rise to  $N$  crystal modes. This splitting is called Davydov<sup>15</sup>, exciton<sup>16</sup>, factor-group, or correlation field splitting and is usually



small (upto  $\sim 5 \text{ cm}^{-1}$ ). When the frequency of an internal mode is comparable to the lattice frequencies, the fine structure in some of the vibrational bands may arise due to interaction between these vibrations.

By considering the anharmonic terms in the potential energy expression<sup>15</sup>, the appearance of overtone and combination bands may be explained in solid phase.

#### THE RAMAN EFFECT

In 1923, Smekal<sup>17</sup> predicted theoretically the scattering of light with a change of wavelength. In 1928, Raman<sup>18</sup> observed the scattering process experimentally in some liquids in which the scattered light was found to contain the radiation of other wavelength in addition to the wavelength of the exciting light. When the photons of the exciting radiation interact with molecules of the sample being studied, the electric vector of the incident light, acting on the charges of the molecules, perturbs its wave functions. As a result, the energies of the scattered photons are either increased or decreased relative to the exciting photons by quantized increments which correspond to the energy differences in the vibrational and rotational energy levels of the molecule. For a vibration or rotation to be Raman active, there must occur a change in the "induced" dipole moment of the molecule during the vibration or rotation considered.

When a light quantum with frequency  $\nu_0$  and energy  $h\nu_0$  collides a molecule in any of its stationary states, say  $E'$  or  $E''$ , the molecule is momentarily raised to meta-stable state with energy  $h\nu_0 + E'$  or  $h\nu_0 + E''$ . If the molecule does not possess a stationary state with this energy, it may scatter a photon with the molecule either returning to its original state (Rayleigh scattering) or to a different state with the frequency of the scattered photon either less than that of the exciting photon (Stokes lines)

or greater than the exciting photon (anti-Stokes lines). The anti-Stokes lines are of lower intensity than the Stokes lines in accordance with the lower molecular population of higher energy levels compared to the levels of lower energy. Moreover, the Raman shifts do not depend upon the frequency of the exciting radiation.

The selection rules for the Raman shifts are determined by the symmetry of the molecule in its equilibrium configuration. These may be derived by using the equations (I.1 and I.2) for selection rules in infrared spectra by replacing the components of dipole moment by the components of "induced" dipole moment. One then arrives at the conclusion that only those vibrations associated with a change of polarizability may be Raman active which have  $\Delta v_i = \pm 1$ . The intensity of scattered light depends on induced dipole moment  $\vec{P}$  whose magnitude may be given by:

$$|P| = \alpha \cdot |E| \quad (I.16)$$

where  $\alpha$  is a polarizability tensor and  $E$  is the electric vector of the incident radiation. The general selection rules for vibrational Raman spectra may be stated by saying that a Raman transition between two vibrational levels  $v'$  and  $v''$  is allowed if the product of wave functions  $\psi_{v'}$ ,  $\psi_{v''}$  has the same species as at least one of the six components  $\alpha_{xx}$ ,  $\alpha_{xy}$ , ... of the polarizability tensor<sup>19</sup>.

Just as for the infrared spectrum, if the anharmonicity is taken into account, in addition to the fundamentals, overtones and combination vibrations may also appear as Raman shifts if they are associated with a change of polarizability. In general, the intensity of the overtones and combination bands is much less than the fundamentals and Raman spectrum usually contains very few of them.

The knowledge of the polarization properties of the scattered light may be very much helpful in drawing the inferences about the symmetry of the molecular vibrations. If the direction of propagation of the incident radiation is taken along the Z-axis and the scattered light is observed at right angles to the Z-axis, the depolarization ratio  $\rho$  may be defined as the ratio of the intensity of the scattered light polarized perpendicular to the XY plane,  $I_{\perp}$ , to that polarised parallel to this plane,  $I_{\parallel}$ .

For the incident unpolarized light, Born<sup>20</sup> has shown by taking average over all possible orientations of the polarizability ellipsoid that  $\rho$  for Raman scattering is given by

$$\rho_n = \frac{I_{\perp}}{I_{\parallel}} = \frac{6 \beta'^2}{45 (\alpha')^2 + 7 \beta'^2} \quad (I.17)$$

where  $\alpha'$  is the derivative of the spherical or isotropic part of the polarizability and  $\beta'$  is the change in the completely anisotropic part of the polarizability. This means that  $\rho$  for all vibrations with non-symmetric species will have the value of  $\frac{6}{7}$ , while only the totally symmetric vibrations can have a value of  $\rho$  less than  $\frac{6}{7}$ . In the case of plane polarized light;

$$\rho_1 = \frac{3 \beta'^2}{45 \alpha'^2 + 4 \beta'^2} \quad (I.18)$$

which may have maximum value of 3/4 for depolarized lines where  $\alpha' = 0$ . This property is extremely useful in identifying the totally symmetric vibrations and there is no comparable source of such information in infrared spectrum for liquid samples. However, the structural information derived from the two types of vibrational spectra (ir and Raman) are complementary to each other.

## ROTATIONAL ISOMERISM

In the case of polyatomic molecules, a multiplicity of rotational isomers is possible due to the internal rotation of one part of the molecule against the other about one or more single bonds. Out of these isomers, some may be of comparable stability. The different rotational isomers correspond to the different potential energy minima. They may be either in a fixed configuration or in a dynamic equilibrium depending upon whether the height of the potential barrier, separating the energetically more favoured conformations is greater than or comparable to the Boltzmann barrier height  $kT$ . When the barrier height is small compared to  $kT$ , the restricted rotation goes over to free rotation.

Here we shall be mainly concerned with the systems whose barrier heights are comparable to  $kT$  ( $\sim 1$  Kcal/mole.). Such conformers are sufficiently short lived and their physical separation at normal temperatures has not been possible. For complex molecules, a clear indication of more than one isomer may be expected if the nature of bonding in one form is different from those in others. This difference in the nature of bonding affects mainly those bands which are closely associated with the altered bonds.

Rotational isomers have been extensively studied by several physical methods such as microwave spectroscopy, nuclear magnetic resonance, electron diffraction, dielectric, sound dispersion, entropy and heat capacity measurements as summarized by Mizushima<sup>21</sup> and Sheppard<sup>22</sup>. Some of these techniques suffer from an inability to characterize each isomer unambiguously.

The vibrational spectroscopic techniques (ir and Raman) sometimes provide a clear characterization of each isomer, but require them to be present in relatively large amounts to give detectable absorption or scattering. Except for the 'optical' isomers which have identical vibrational

spectra, the ir and Raman spectra contain the vibrational modes corresponding to each isomer, some of which may overlap. The number of observable bands depends upon the symmetry properties of different isomers.

The relative concentration of the stable isomers is a function of the Boltzmann distribution. It is found that the vibrational spectra of molecules, which are complex in the gaseous or liquid states due to the presence of a number of isomers, often become comparatively simple at low temperature in solid phase. This is because of the fact that all parts of the molecule are not allowed to rotate in solid phase. Therefore, in general, only one conformation forms a stable lattice more readily than others. As the relative proportion of the species is also dependent on the physical environment, it may be possible to predict on the basis of thermodynamic and energetic grounds which form of the molecule exists at low temperature.

The relative intensities of the bands arising due to the isomers differing in their polarity are also markedly affected with the variation in polarity of the solvents, when spectra are observed in solutions. The intensity of the bands due to more polar forms in the medium of a high polar solvent generally increases but reverse is the case with non-polar solvents. As the polarity of the solvent is increased, the effects of solute-solvent interactions are also increased. For one particular isomeric species, the effects of solute-solvent interactions are significant in the cases of hydrogen bonding or molecular association and depend on the dielectric constant or refractive index of the solvent.

## HYDROGEN BONDING

In passing from the gas phase at low pressure to a condensed phase, intermolecular interactions may be expected to influence the group frequencies in the ir and Raman spectra. The order of these interactions may vary from the weak van der Waals type (energies  $\sim$  a few hundred calories) to the specific hydrogen bonding type interactions (energies  $\sim$  5 K cal/mole.). The hydrogen bonding interactions can therefore produce frequency shifts of the order of  $100\text{ cm}^{-1}$ .

A hydrogen bond (H-bond) is an interaction between a proton donor group (X-H) and an electron donor (proton-acceptor) atom Y in the same or a different molecule and is generally represented diagrammatically as:



where H is the hydrogen atom involved in the H-bond formation, X and Y are usually electronegative atoms; Y may be an atom with lone pair of electrons or a group with  $\pi$ -electrons. R and R' represent the remainder of the molecules in which the X-H and Y groups are present. The hydrogen bonds are mostly ionic in nature and the atoms usually involved in strong H-bond formation are those of F, O and N.

Due to the formation of the X - H ....Y bond, the force field around the hydrogen atom is modified as a result of the interactions of the electron clouds of the molecules which come close to each other. Such molecular interactions affect the vibrational spectra in a number of ways:

- (1) The X - H stretching frequencies shift to lower values on the formation of a H-bond due to decrease in the force constant of the X - H group.

(2) The X - H bending frequencies shift to higher frequencies due to increase in the restoring force tending to keep the X - H bond in a fixed orientation. The magnitude of the frequency shifts in cases (1 and 2) depends on the strength of the H-bond<sup>23-26</sup>.

(3) The intensities and the half-widths of the bands may be greatly increased on H-bond formation. Various explanations have been given for the width of the bands associated with the H-bonding<sup>27-32</sup> and a brief account of the same is given below.

According to the fluctuation theory of Badger and Bauer<sup>29</sup>, when a hydrogen bond is formed, the X...Y distance decreases and the X-H bond length increases which implies that the force constants of the X-H bond and H-bond are interdependent. This means that the vibrational motions of the X-H bond and H-bond (XH...Y) are coupled together. The range of values of X...Y distances caused by the thermal vibrations of the relatively weak H-bond gives rise to a range of X-H vibrational frequencies and hence to a broad absorption band.

The broad  $\nu_{X-H}$  band may also be taken as consisting of a series of sub-bands<sup>30-32</sup> of frequencies  $\nu_{XH} \pm n \nu(XH...Y)$ .

Hydrogen bonding effects can be studied by both the diffraction as well as spectroscopic methods. The diffraction methods (neutron, electron and X-ray diffraction etc.) give information about the position of the atoms, while the spectroscopic methods (infrared, Raman, nuclear magnetic resonance etc.) yield information about the energy levels of the system. However, the diffraction and spectroscopic methods are supplementary in the study of H-bonding.

The infrared and Raman spectroscopy provide a convenient means for studying the effects of temperature, concentration, solvent and pressure

on H-bonding effects. It is possible to differentiate between the intermolecular and intramolecular H-bonds. The former type shows the variation in position and intensity of the bands associated with the H-bonding in various solvents, while the latter type does not show such effects. In infrared measurements, it may sometimes be possible to observe the vibrational bands due to both the associated and unassociated species simultaneously in the same medium.

#### THE VIBRATIONAL ASSIGNMENT

The successful solution to the structural problems of the molecules by means of vibrational spectroscopy depends largely on the validity of the concept of group frequencies. The various factors influencing the group frequencies may be divided into external and internal ones. The external factors are related to the external environment of the vibrating groups and the important ones of them are: The change of phase, variations in temperature and crystalline form, the presence or absence of molecular association and solvent effects. The internal factors operating along the interatomic bonds or across intramolecular space include changes in the geometry or masses of the substituents, mechanical coupling between vibrations, steric and electrical effects. The electrical effects cover the inductive (due to change in electronegativity of the substituents), resonance and dipolar field effects and operate in the immediate locality of a vibrating group. These factors change the hybridization of the atoms on which they operate resulting in the change of bond lengths and hence the frequencies.

The molecule to be studied is assigned various possible structures and their symmetries are determined. The activities of their fundamental modes in both the ir and Raman spectra are deduced. A comparison of the infrared and Raman bands with depolarization measurements alongwith the



activity and number of modes allowed in the ir and Raman spectra may suffice to eliminate some structures. Moreover, the steric considerations: That no two atoms can approach each other within a distance shorter than the sum of their van der Waals radii, do not favour some configurations. The interaction of lone pair electrons and the possibility of conformation favouring or disfavouring hydrogen bond formation may also be helpful in deducing the structure of more stable forms. The band contours in vapour phase spectra may also give information about the structure of the molecular forms. The observed spectra are compared with the known spectra of similar molecules. The interpretation of the vibrational spectra may be made easy by ascribing the observed bands to one isomer or the other. For this purpose, the spectra are measured at low temperatures which may be somewhat simpler than the spectra in the vapour or liquid phases, since only one of the isomer is expected to crystallize in the lattice at low temperatures. The group frequency assignment can also be aided by a study of the intensity of both the ir and Raman bands, depolarization of Raman lines, effect of solvents of varying polarity and information about the expected location of analogous vibrations from spectra of similar molecules. Such structural deductions are of particular importance in the study of molecules exhibiting rotational isomerism.

## REFERENCES

1. W.W. Coblentz, Investigation of Infrared Spectra, Part I: Infrared Absorption Spectra, Carnegi Institute Publications, Washington, D.C. (1905)
2. N. Bjerrum, *Nerst's Festschrift*, 90 (1912)
3. (a) J.E. Rosenthal and G.M. Murphy, Revs. Modern Phys. 8, 317 (1936); (b) A.G. Meister, F.F. Cleveland and M.J. Murray, Am. J. Phys. 1, 239 (1943); (c) S. Bhagavantam and T. Venkatarayudu, Theory of Groups and its Application to Physical Problems, Andhra Univ., Waltair, India (1951)
4. D.N. Kendall, Applied Infrared Spectroscopy, Reinhold Publishing Corporation, New York (1966)
5. W.A. Seth-Paul and G. Dijkstra, Spectrochim. Acta 23A, 2861 (1967)
6. W.A. Seth-Paul and H. De Meyer, Spectrochim. Acta 25A, 1671 (1969)
7. W.A. Seth-Paul and H. De Meyer, J. Mol. Structure 3, 11 (1969)
8. W.A. Seth-Paul, J. Mol. Structure 3, 403 (1969)
9. S.L. Gerhard and D.M. Dennison, Phys. Rev. 43, 197 (1933)
10. R.M. Badger and L.R. Zumwalt, J. Chem. Phys. 6, 711 (1938)
11. B.S. Ray, Z. Physik 74, 78 (1932)
12. R.E. Hoffman and D.F. Hornig, J. Chem. Phys. 17, 1163 (1949)
13. W. Vedder and D.F. Hornig, Adv. Spectry. 2, 189 (1961)
14. T.S. Hermann, S.R. Harvey and C.N. Honts, Applied Spectry. 23, 451 (1969)
15. A.S. Davydov, Theory of Light Absorption of Molecular Crystals, Institute of Physics, Ukranian Academy of Sciences, Kiev, Ukranian (1951)
16. A. Houg, Phys. Rev. 147, 1941 (1954)
17. A. Smekal, Naturwissenschaften 11, 873 (1923)
18. C.V. Raman, Ind. J. Phys. 2, 387 (1928)
19. G. Hergberg, Infrared and Raman Spectra of Polyatomic Molecules, Van Nostrand, Princeton, New Jersey (1945)

20. M. Born, 'Optik', Edwards Brothers, Ann Arbor, Michigan (1943)
21. S. Mizushima, Structure of Molecules and Internal Rotation, Academic Press, New York (1954)
22. N. Sheppard, Advances in Spectroscopy 1, 228 (1959)
23. K. Nakamoto, M. Margoshes and R.E. Rundle, J. Am. Chem. Soc. 77, 6480 (1955)
24. N. Sheppard in Hydrogen Bonding (D. Hadzi, ed.), Pergamon Press, New York (1957), p. 85
25. C.G. Cannon, Spectrochim. Acta 10, 341 (1958)
26. J.D. Bernal in Hydrogen Bonding (D. Hadzi, ed.), Pergamon Press, New York (1957), p. 7
27. D. Hadzi, ed., Hydrogen Bonding, Pergamon Press, New York (1957)
28. G.C. Pimentel and A.L. McClellan, The Hydrogen Bond, Freeman and Co., California (1960)
29. R.M. Badger and S.H. Bauer, J. Chem. Phys. 5, 839 (1937)
30. M.I. Batuev, Izvest. Akad. Nauk. S.S.S.R., Ser, Fiz. 14, 429 (1950)
31. B.I. Stepanov, Zhurn. Fiz. Khim. 20, 408 (1946)
32. G. Herzberg, Op. cit., p. 241, 215

## GENERAL REFERENCES

1. L.J. Bellamy, The Infrared Spectra of Complex Molecules, Wiley, New York (1958)
2. E.B. Wilson, Jr., J.C. Decius and P.C. Cross, Molecular Vibrations, McGraw-Hill, New York (1955)
3. R.N. Jones and C. Sandorfy in Chemical Applications of Spectroscopy (W. West, ed.), Chapter IV, Wiley (Interscience), New York (1956)
4. R.W. Taft, Jr. in Steric Effects in Organic Chemistry (M.S. Newman, ed.), Chapter 13, Wiley, New York (1956)
5. R.M. Hochstrasser, Molecular Aspects of Symmetry, Benjamin, New York (1966)
6. M. Davies, Infrared Spectroscopy and Molecular Structure, Elsevier Publishing Co., Amsterdam (1963)
7. C.N.R. Rao, Chemical Applications of Infrared Spectroscopy, Academic Press, New York (1963)
8. N.B. Colthup and L.H. Daly, Introduction to Infrared and Raman Spectroscopy, Academic Press, New York (1964)
9. J.H. Hibben, The Raman Effect and Its Chemical Applications, Reinhold, New York (1939)
10. S. Bhagavantam, Scattering of Light and The Raman Effect, Chemical Publication Co., New York (1942)

## CHAPTER II

### EXPERIMENTAL DETAILS

All the infrared spectra were recorded on Perkin-Elmer 521 grating infrared spectrophotometer. This is a double beam instrument employing the 'optical null' photometric system. The instrument records the percent transmittance\* (or absorbance) in the range of 4000 to 250  $\text{cm}^{-1}$  on a linear wavenumber scale. Both the linear and scale change modes of operation can be used with variable scanning speeds and times. The instrument employs two gratings as the dispersing elements. The first grating is used in the first and second orders and the second grating is used in the first order only with interference filters which suppress the unwanted orders. Nerst glower is used as a source of infrared radiation and a high speed sensitive thermocouple of blackened gold leaf acts as a detector. An automatic slit control and speed suppression mechanism is incorporated in the system. For high resolution work, a compromise has to be made between the slit program, gain control and scanning speed. The resolution of the instrument at 1000  $\text{cm}^{-1}$  is 0.3  $\text{cm}^{-1}$  with a reproduction of  $\pm 0.5 \text{ cm}^{-1}$ .

The infrared spectra of the liquids and solutions in various solvents were recorded using sealed cells of fixed thicknesses of 0.025 mm, 0.05 mm and 0.1 mm. Sometimes the samples were prepared in the form of capillary films by sandwiching a thin film of the compound between two CsBr windows. The spectroscopic grade solvents of varying polarity such as  $\text{CCl}_4$ ,  $\text{CS}_2$ ,  $\text{CH}_3\text{Cl}$ ,  $\text{CH}_3\text{CN}$  etc. were used for solution spectra and the compensation due to solvent absorption was accomplished (some times partially) by placing the fixed cell of same thickness filled

---

\* The percent transmittance is defined as  $100 \times (I/I_0)$ , where  $I_0$  is the incident intensity and  $I$  is the transmitted intensity.

with solvent in the reference compartment. The vapour phase spectra at various pressures were recorded using glass cells, 5 and 10 centimeters in length and fitted with CsBr windows. The cells were generally evacuated with the help of mechanical pump followed by a diffusion pump and then the samples were introduced inside the evacuated cells at required pressures. In order to record the spectra in vapour phase at higher temperatures, the gas cells were heated by passing the current through an insulated heating tape wound on the cell. The current was varied with the help of a variac.

The spectra in the solid phase at low temperature were studied with the help of a conventional Wagner-Hornig<sup>1</sup> type cell and is shown in Figure 2.1. It consists of a double walled reservoir for coolant (liquid nitrogen) and is mounted in an evacuated cell fitted with CsBr windows. The vapour of the compound was allowed to condense on a window of CsBr which was cooled by conduction from the liquid nitrogen reservoir. The initial solid deposit was generally annealed by warming the deposit to higher temperatures (or melting it) and then cooling it slowly. This annealing process was continued until very thin and "crystalline" films were obtained, characterized by the appearance of very sharp peaks in the infrared spectra.

The calibration of the spectrophotometer was checked against the fine structure lines of HCl, CO<sub>2</sub> and the rotational bands of atmospheric water vapour below 600 cm<sup>-1</sup><sub>2</sub>. In the other regions, not covered by the above compounds, the lines of indene were recorded. The reported frequencies are estimated to be accurate upto  $\pm 2$  cm<sup>-1</sup> for sharp peaks, but for very broad, weak or diffused bands, the uncertainty may amount to as large as 5 cm<sup>-1</sup>.

The Raman spectra of the samples in liquid phase at room temperature were photoelectrically recorded on a Coderg PH-1 Raman spectrophotometer equipped with a Spectra-Physics model 125 He-Negas laser as a source with an output at  $6328 \text{ \AA}^0$ . The power level of the laser beam may be varied from 50 to 80 mw. The spectrometer employs an Ebert-Fastie double monochromator with two mechanically coupled gratings and a photomultiplier tube as a detector. The resolution of the instrument is  $0.5 \text{ cm}^{-1}$  and has an arrangement for marking the frequencies at intervals of  $50 \text{ cm}^{-1}$ . The abscissa scale is linear in wavenumber units. The Raman cell of volume 1 cc was normally used to record the spectra.

The spectrophotometer was calibrated against the prominent Raman lines of  $\text{CCl}_4$ ,  $\text{C}_6\text{H}_6$ ,  $\text{CH}_3\text{Cl}$  and  $(\text{CH}_3)_2\text{CO}$ . The frequency measurements in the Raman spectra are estimated to be accurate upto  $\pm 2 \text{ cm}^{-1}$  for sharp peaks. The intensity of the lines could be varied by changing the slit width, voltage on the photomultiplier tube and the power level of laser beam.

As summarized by Claassan<sup>3</sup>, several different schemes have been used by previous workers<sup>4,5</sup> for quantitative measurements of depolarization factors. In the present study, the depolarization data were obtained by employing a quartz half-wave plate in the path of the incident laser beam which was used to rotate the plane of polarization of the incident light. The band intensity ratios ( $R$ ) were obtained by comparing the relative band areas of the two spectral scans using incident light polarized parallel and perpendicular to the slit which is vertical. The measured intensity ratio ( $R$ ) is generally not equal to the depolarization ratio  $\rho_s$ , but is a function of  $f$  given by<sup>3,4</sup>

$$R = \rho_s \frac{(1+f)}{(f+\rho_s)} \quad (\text{II.1})$$



where  $f$  is defined as the ratio of the efficiency of the monochromator and system for the horizontally polarized light to that for the vertically polarized light and is usually less than one. For the limiting value of  $f = 1$ ;  $R = 0.86$ .

By taking into account the various factors such as refractive index, dielectric constant of the sample and instrumental corrections, accurate depolarization ratios can not be expected using coaxial or right angle laser excitation from samples contained in a multiple reflection cell<sup>6</sup>. This is due to the fact that the incident directional polarization of the laser beam becomes disoriented after getting reflected from the walls of the tube. Therefore, one can not expect theoretical depolarization ratios and only qualitative data are obtained in the present study.

## REFERENCES

1. E.L. Wagner and D.F. Hornig, J. Chem. Phys. 18, 296 (1950)
2. Tables of Wave Numbers for the Calibration of Infrared Spectrophotometers, Butterworth (1961)
3. H.H. Claassan, H. Selig and J. Shamir, Applied Spectry. 23, 8 (1969)
4. J. Brandmuller, K. Burchardi, H. Hacker and H.W. Schrotter, Z. Physik 22, 177 (1967)
5. A. Weber, S.P.S. Porto, L.E. Cheesman and J.J. Barrett, J. Opt. Soc. Am. 57, 19 (1967).
6. J.R. Allkins and E.R. Lippincott, Spectrochim. Acta 25A, 761 (1969)

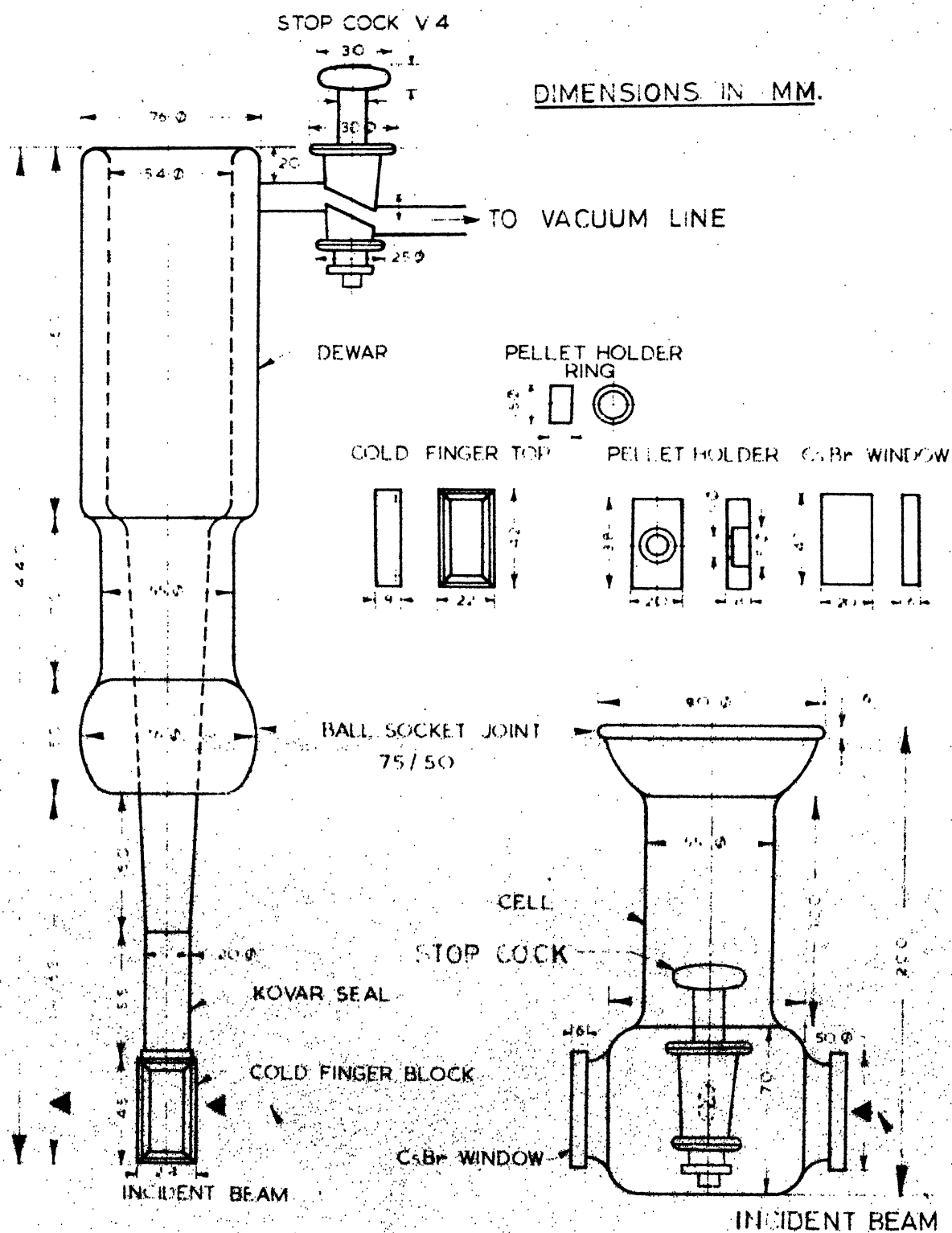


Fig. 2-1 LOW TEMPERATURE CELL

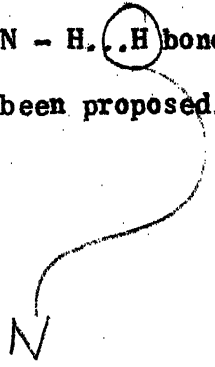
### CHAPTER III

#### VIBRATIONAL SPECTRA OF ALLYL AMINE AND ROTATIONAL ISOMERISM

## ABSTRACT

The infrared spectra of allyl amine in the vapour, liquid and solid phases have been measured between 4000 and  $250\text{ cm}^{-1}$ . The Raman spectrum in the liquid state has also been recorded photoelectrically and qualitative depolarization measurements are made. The infrared spectrum of solid allyl amine obtained near liquid nitrogen temperature reveals the existence of rotational conformers in the fluid phase. The interpretation of the spectral data suggests the presence of two rotational isomers ('cis and trans' and 'gauche and trans') in the vapour and liquid phases whereas the form having asymmetrical structure ('gauche and trans',  $C_1$  symmetry) gets stabilized in the solid state at low temperature.

It is deduced from the shifts of some of the bands in various solvents ( $\text{CCl}_4$ ,  $\text{CH}_3\text{Cl}$ ,  $\text{CH}_3\text{CN}$  etc.) and in different physical states that a weak molecular association is present in both the liquid and solid states caused by intermolecular hydrogen bonding effects. The strong and broad band at  $3170\text{ cm}^{-1}$  in the solid spectrum has been interpreted as resulting primarily from the associated  $\text{N} - \text{H} \cdots \text{H}$  bond. A vibrational assignment for the observed bands has been proposed.



## INTRODUCTION

Numerous studies have been directed at establishing the nature of rotational isomers about single bonds joining trigonal carbon to tetrahedral carbon atom. Allyl halides have been examined by Bowen, Gilchrist and Sutton<sup>1</sup> using electron diffraction technique. They were able to exclude definitely the two forms in which all heavy atoms are coplanar. Bothner-By and coworkers<sup>2a,2b,2c</sup> have shown by using nuclear magnetic resonance techniques that as the size of the substituent on the methylene carbon atom in allylic compounds is increased, the relative population of the 'cis' form decreases. Microwave studies of allyl fluoride<sup>3</sup> indicate that the molecule exists only in the 'cis' and 'gauche' forms without any indication of the 'trans' form. Sastry, Rao and Dass<sup>4</sup> reported the presence of only two isomers, 'cis' and 'gauche', in allyl cyanide. The recent microwave studies of allyl alcohol by Murty and Curl<sup>5</sup> and of allyl mercaptan by Sastry et al.<sup>6</sup> have shown that these molecules appear only in 'gauche' forms. These results are further supported by a similar conclusion drawn from a study of the vibrational spectra of allyl halides by McLachlan and Nyquist<sup>7</sup> who showed that the more stable isomers of allyl chloride, bromide and iodide exist in 'gauche' forms, while the 'cis' isomer is more stable for allyl fluoride. Since allyl amine may have rotational isomers resulting from rotations of the  $-\text{CH}_2\text{NH}_2$  group about the C-C single bond and from the additional rotations of the  $-\text{NH}_2$  group about the C-N bond (Figure 3.1), it was expected that more than one form of the molecule would be observed.

So far no data have come to the author's attention on the structural form of allyl amine. Kohlrausch and Stockmair<sup>8</sup> as well as Kahovec and Kohlrausch<sup>9</sup> have reported the Raman spectrum of allyl amine

without depolarization measurements. The near infrared spectrum of allyl amine was reported by Freymann<sup>10</sup>. The infrared spectra of this compound were first studied by Yagudaev and coworkers<sup>11</sup> and later by Gross and Forel<sup>12</sup>, but the data did not show the existence of rotational isomers. The latter authors proposed a partial vibrational assignment based on their infrared spectra and earlier Raman data. However, the previous vibrational assignments are partially invalid, because the bands arising from different rotational isomers were assigned to only one geometric structure.

The capacity of molecular association through hydrogen bonding effects of nitrogen-hydrogen containing compounds is also of practical interest. Some of the bands associated with the  $-NH_2$  group may be affected in position and intensity in various solvents at different concentrations, due to variations in temperature and physical state of the compound etc. and thereby indicating the effects of hydrogen bonding.

As a result of the incompleteness of the previous work on allyl amine, a complete investigation of the vibrational spectra for this molecule has been undertaken in this study and the results obtained are discussed, keeping in view the presence of rotational isomers in fluid phase.

#### EXPERIMENTAL

The compound studied was a commercial material (Aldrich product) and vacuum distilled prior to use. Only the middle fraction was always used.

The infrared spectra were recorded on a Perkin-Elmer 521 grating infrared spectrophotometer. The vapour phase spectra at variable pressures were investigated using 5 and 10 cm gas cells fitted with

CsBr windows. The infrared spectra of the liquid sample were recorded as capillary films by sandwiching a small quantity of the compound between two CsBr windows. For the spectra in various solutions ( $\text{CCl}_4$ ,  $\text{CH}_3\text{Cl}$ ,  $\text{CH}_3\text{CN}$  etc.), Perkin-Elmer's sealed liquid cells of 0.025 mm, 0.05 mm and 0.5 mm thickness with CsBr windows were utilized. Adequate solvent compensation was obtained with the reference cells of equal thickness placed in the reference beam. The sample of crystalline solid allyl amine was prepared by freezing the vapour of the compound onto a cold finger of CsBr cooled by conduction from a liquid nitrogen reservoir and mounted in an evacuated cell fitted with CsBr windows. Sometimes the initial solid deposit had to be annealed to get a crystalline film, characterized by the appearance of very sharp peaks. The tracings of the infrared spectra for the liquid, gaseous and solid allyl amine are shown in Figures 3.2, 3.3 and 3.4 respectively (given at the end of the Chapter) and the frequencies of the observed bands are listed in Table 3.2.

A Spectra - Physics model 125 He-Ne gas laser with an output at  $6328 \text{ \AA}$  was used to excite the Raman spectrum. The spectra were photoelectrically recorded with the help of a Coderg model FH-1 Raman spectrophotometer equipped with an Ebert-Fastie double monochromator blazed for  $7500 \text{ \AA}$  wavelength. The Raman cell of volume 1 cc was used to record the spectrum of the liquid sample at room temperature. Qualitative depolarization measurements on the Raman displacements were made in the same way as described in Chapter II. The tracings of the Raman spectrum are shown in Figure 3.5 and the wave number shifts, intensities and depolarization of the lines are entered in Table 3.2.



## DISCUSSION

Several absorption bands which are present in the vapour or the liquid phase have been found to disappear in the solid phase. This behaviour shows clear evidence for the presence of more than one rotational isomer in fluid phase. This is further supported by the study of the relative intensities of the pairs of bands, which may be assigned to the same type of vibrations in different rotational isomers, in a series of solvents. Although changes occur in various regions of the spectrum, the two moderately strong bands in the liquid spectrum at 578 and 645  $\text{cm}^{-1}$  are of particular interest. In dilute solutions with  $\text{CCl}_4$ , the 578  $\text{cm}^{-1}$  line increases in intensity relative to that at 645  $\text{cm}^{-1}$ , while with polar solvents ( $\text{CH}_3\text{Cl}$ ,  $\text{CH}_3\text{CN}$ ), the reverse effect on intensity variation is observed. The lower frequency band of this pair disappears on crystallization. The temperature-intensity behaviour of the two bands in the spectrum of vapour phase allyl amine at higher temperatures confirms that the two bands are due to two different isomers. From these observations it may be inferred that the more polar form gets stabilized in the solid phase.

The question of the detailed structures of the possible conformers of allyl amine is not yet resolved. In this case, the planarity of the ethylenic group ( $\text{CH}_2 = \text{CH}-\text{C}-$ ) is assumed and the plane is determined by the points, the  $\text{H}_1$ ,  $\text{H}_2$  and  $\text{C}_2$  atoms. Each atom in the molecule is given a particular number as indicated in Figure 3.1. In an attempt to assign all the observed transitions in the infrared and Raman spectra of allyl amine, one has to consider all the spectroscopically distinguishable conformers of this molecule.

In the case of allyl amine, out of the two carbon atoms forming the rotation axis, one atom has  $sp^3$  hybridization whereas the other carbon atom is in the binding state of  $sp^2$ . In cases similar to this,  $sp^3$ - $sp^2$  combination, the stable positions are always 'cis' and 'gauche' where one of the three single bonds attached to the  $sp^3$  carbon atom eclipses nearly or exactly with the double bond to the  $sp^2$  carbon atom. Therefore, at the outset, only two different type of conformations about the C-C single bond were considered plausible-namely, the 'cis' and two equivalent 'gauche' or 'gauche'' (corresponding to a rotation by about  $+120$  or  $-120$  degrees from the 'cis' position) forms depending upon the orientation of the  $-CH_2NH_2$  group with respect to the ethylenic  $CH_2 = CH-C-$  group. The C=C-C-N dihedral angle is taken to be zero for the 'cis' position.

The two fold symmetry axis of the  $-NH_2$  group does not lie in the direction of the third nitrogen valence bond. Therefore, a rotation of the  $-NH_2$  group around the axis of C-N bond in allyl amine should give rise to different molecular configurations. Hence corresponding to each conformation about C-C bond, there are several possible conformations about the C-N bond. The possibility of rotational isomerism about C-N bond may be considered similar to that about C-C bond with the  $sp^3$  -  $sp^3$  hybridization. If it is assumed that the lone pair orbitals of nitrogen atom point in the direction of the vacant corner of the nitrogen tetrahedron, the stable positions corresponding to the rotations of the  $-NH_2$  group about C-N axis may be expected as 'trans' and 'gauche' or 'gauche''. The 'cis' configuration is taken as the zero of the dihedral angle of C-C-N- and lone pair orbitals of nitrogen atom. Therefore, for both the 'cis' as well as 'gauche' forms of the C=C-C-N skeleton, three orientations of the  $-NH_2$  group were considered plausible. The

projections of the probable configurations in the a-b plane of the principal axes system are shown in Figure 3.1.

The most symmetrical 'cis and trans' form, with staggered positions of the hydrogen atoms of the  $\text{-NH}_2$  and  $\text{-CH}_2$  groups, is expected to have a plane of symmetry ( $C_s$  point group) with the carbon atoms, nitrogen atom and vacant corner of nitrogen tetrahedron all being coplanar except the hydrogen atoms of the  $\text{-CH}_2$  and  $\text{-NH}_2$  groups which lie symmetrically below and above the plane. In this case, the lone pair orbitals of nitrogen atom point between the space of hydrogen atoms of  $\text{-CH}_2$  group and thereby decrease the steric interactions. The two equivalent 'cis and gauche' or 'cis and gauche'' forms differ from this by a rotation of  $\text{-NH}_2$  group by  $\pm 120$  degrees about the C-N bond.

For the 'gauche' form, the planarity of the ethylenic group ( $\text{CH}_2=\text{CH-C-}$ ) is assumed and the  $\text{-CH}_2\text{NH}_2$  group is rotated about the C-C axis by  $127^\circ$  (as in allyl fluoride<sup>3</sup> and allyl alcohol<sup>5</sup>). The 'gauche and trans' is the form in which the  $\text{-NH}_2$  group points towards the ethylenic group. The 'gauche and gauche' and 'gauche and gauche' \* are the forms in which the  $\text{-NH}_2$  group is pointed away from the ethylenic group. These forms differ from the 'gauche and trans' form by a rotation of  $\text{-NH}_2$  group by  $+120$  or  $-120$  degrees about the C-N bond. The interaction between lone pair and hydrogen atoms of the  $\text{-CH}_2$  and  $\text{-NH}_2$  groups seems small in the 'gauche and trans' form as compared to the other two forms.

By assuming a reasonable set of parameters from comparable molecules<sup>3,13</sup>, the rotational constants were computed for allyl amine as a function of internal rotation angle  $\phi$  of the C=C-C-N frame, where  $\phi$  was taken to be zero at the 'cis' position. The molecule is a near prolate symmetric rotor for any value of  $\phi$ . If the molecule exists in the configuration which has a plane of symmetry ('cis and trans',

$C_s$  point group), the expected 27 vibrational modes may be divided into seventeen of species  $a'$  which are symmetrical with respect to the plane of symmetry and ten of species  $a''$ . All the modes are allowed in both the Raman and infrared spectra. In the Raman spectrum, the  $a'$  fundamentals are expected to be polarized and the  $a''$  modes depolarized. The three moments of inertia for this form of the molecule are such that intermediate and greatest moments are nearly the same, whereas the least moment of inertia is considerably smaller than the other two. The molecule therefore resembles a nearly prolate symmetric top. The Badger and Zumwalt<sup>14</sup> asymmetry parameters for this structure are:

$$\rho^* = \frac{A-C}{B} = 1.694 \text{ and } \kappa = \frac{2B-A-C}{A-C} = -0.7014$$

where A, B and C are the rotational constants associated with the principal moments  $I_A$ ,  $I_B$  and  $I_C$  respectively. Recently Seth-Paul and Dijkstra<sup>15</sup> have given the modified expressions for calculating P-R separation of band envelopes in vapour phase spectrum of asymmetric top molecules. The molecule is expected to show up three types of band contours in vapour phase. The axis of largest moment is perpendicular to the molecular symmetry plane. Thus the  $a''$  modes are expected to show type-C band contours with a pronounced Q branch and P-R separation of  $\sim 32 \text{ cm}^{-1}$ . The  $a'$  modes are expected to have contours of the types A, B or hybrid A-B. The bands arising from vibrations of the molecular dipole moment parallel to the plane of symmetry and approximately along the axis of the intermediate moment of inertia may be expected to show a central minimum with a P-R separation of  $\sim 17 \text{ cm}^{-1}$ . These are the so-called type-B bands. The type-A contours have a PQR structure with a medium intense Q branch and P-R separation of  $\sim 21 \text{ cm}^{-1}$  at room temperature. These bands arise from the vibrations of the dipole moment in

the molecular symmetry plane and roughly parallel to the axis of least moment of inertia. There is, however, no symmetry requirement forbidding dipole moment changes at angles between the directions of  $I_A$  and  $I_B$ . The  $a'$  modes will therefore, in general, have hybrid A-B band shapes and the  $a''$  modes will have type-C band envelopes.

However, if the molecule exists in the configurations belonging to the point group  $C_1$  (Figures 3.1B, C, D and E), all the 27 modes belong to the same symmetry class and should appear in both the infrared and Raman, with all the Raman bands being polarized. Calculations of Badger and Zumwalt parameters<sup>14</sup> for the least hindered and hence more probable form 'gauche and trans' give  $\rho^* = 4.578$  and  $K = -0.9863$ . The  $K$  value clearly characterises the molecule to be a symmetric spindle. In this case, the type-A bands are expected to have a medium intense Q branch and the calculated value of P-R separation from the molecular geometry comes out to be  $\sim 17 \text{ cm}^{-1}$ . The type-B bands, in principle should show up a PQ-Q'R type structure with a P-R separation of  $\sim 15 \text{ cm}^{-1}$ . But this type of structure is clear only in molecules having  $\rho^* \leq 3/4$  while for larger values of  $\rho^*$ , the overlapping of the P and R branches coupled with a decrease in intensity obstruct a clear distinction between a Q-Q' and P-R separation. The type-C bands should have a much pronounced Q branch and a P-R separation of  $\sim 26 \text{ cm}^{-1}$ . Most of the bands (except those which are very weak) in the vapour phase show a well resolved PQR structure.

Except the two bands which seem depolarized, all other observed bands in the Raman spectrum are polarized and therefore suggest the presence of at least one form having unsymmetrical structure ( $C_1$  symmetry). The vibrational spectra give no clue as to which one of the unsymmetrical

forms is predominant. The steric considerations suggest that the 'gauche and trans' form is least hindered and hence may be energetically favoured as compared to the other possible forms. The values for P-R separation in Table 3.2 show that the average of the observed P-R separation for the bands which are not badly overlapped by other vibrations, are in reasonable agreement with the calculated separation for the 'gauche and trans' isomer. At low temperature in the solid phase, the infrared bands corresponding to the Raman lines at 555 and 573  $\text{cm}^{-1}$  disappear. Both the Raman lines appear to be depolarized suggesting that they result from the symmetrical isomer ('cis and trans'). The 'cis and trans' isomer is present in lower concentration than the predominant isomer ('gauche and trans') at room temperature.

In the present discussion we shall confine our attention to the sterically favoured 'cis and trans' and 'gauche and trans' conformations only. The classification of normal modes of the symmetrical isomer ( $C_s$  symmetry) is also applied to the normal modes of the asymmetrical isomer for the sake of simplicity. The fundamental modes are described in Table 3.3.

#### ASSIGNMENT OF FUNDAMENTALS

##### Vibrational assignment of the N-H motions

Allyl amine is expected to have six internal modes which involve motions of the hydrogens joined to nitrogen. These may be classified as antisymmetric and symmetric  $\text{NH}_2$  stretching,  $\text{NH}_2$  scissoring, wagging, rocking and twisting vibrations.

The ability of primary amines to participate in the formation of intermolecular hydrogen bond has been studied by many investigators<sup>16,17</sup> (Ref. 17 may be referred to for references concerning the earlier work).

From the changes observed in the spectra of allyl amine in various phases, formation of inter-molecularly hydrogen-bonded complexes is indicated. The effects of hydrogen bonding on vibrational spectra are well known. The intensities and positions of the lines affected by hydrogen bonding show a marked temperature and concentration dependence.

In the region of NH stretch, two bands are observed at 3390 and 3312  $\text{cm}^{-1}$  with a broad shoulder at 3195  $\text{cm}^{-1}$  in the infrared spectrum of liquid allyl amine. The intensity and position of the lower frequency shoulder is far more concentration dependent than the other two lines. In dilute solutions of non-polar solvents, the intensity of the shoulder at 3195  $\text{cm}^{-1}$  goes on decreasing gradually and ultimately disappears for very dilute solutions. The observed shifts for the 3312  $\text{cm}^{-1}$  band of allyl amine in solutions of inert solvents are found to be larger than the shifts for the higher frequency band at 3390  $\text{cm}^{-1}$  and therefore suggest that only one N-H bond is being perturbed by the hydrogen bonding. These observations are in line with those of Zhukova and Shmanko in other aliphatic primary amines. In the vapour phase, the bands become extremely weak and only two bands are present with their centres at 3430 and 3350  $\text{cm}^{-1}$ . At very high pressures, a weak shoulder appears near 3220  $\text{cm}^{-1}$  which disappears with increase in temperature. In condensed phase at low temperature, exceptionally broad and strong bands appear at 3330, 3260 and 3170  $\text{cm}^{-1}$ . On the basis of these observations, the low frequency band cannot be interpreted as an overtone of the  $\text{NH}_2$  scissoring motion as it should not disappear with increase in dilution of solvents and temperature. Therefore this lower frequency band at 3170  $\text{cm}^{-1}$  in the solid phase is assumed to be primarily a mode resulting from the N-H...N bond. The remaining two bands may then be assigned as symmetric  $\nu_1$  (3350  $\text{cm}^{-1}$ , vapour) and asymmetric  $\nu_{18}$  (3430  $\text{cm}^{-1}$ , vapour)  $\text{NH}_2$  stretching vibrations.

The assignment of the  $\text{NH}_2$  scissoring motion  $\nu_6$ , characteristic of primary amines, is straight forward since such modes have been generally found in the  $1600\text{ cm}^{-1}$  region. A very strong and broad band is observed at  $1605\text{ cm}^{-1}$  in the liquid phase infrared spectrum of allyl amine. In condensed phase at low temperature, this appears as a very broad band at  $1599\text{ cm}^{-1}$  showing multiplet splitting. This multiplet splitting, generally into two or three components, also observed for most of the other bands arising from deformation modes of  $\text{NH}_2$  group, may be caused due to the following main reasons: The splitting may arise due to the intramolecular interactions between the  $-\text{NH}_2$  group and the  $\pi$ -electrons of the  $\text{C}=\text{C}$  double bond. The multiplicity of the bands may also be caused by the presence of several unequal types of bonds or by the vibrational coupling between the molecules in a unit cell of a crystal or multimer unit<sup>18</sup>.

The position of this  $-\text{NH}_2$  scissoring mode in the gas phase infrared spectrum at  $1627\text{ cm}^{-1}$  is in excellent agreement with the assignment of  $1623\text{ cm}^{-1}$  band in methyl amine vapour<sup>13</sup> and  $1622\text{ cm}^{-1}$  Raman line in methyl hydrazine<sup>19</sup> to this mode.

The low frequency deformation vibrations of the  $-\text{NH}_2$  group in primary amines have not been investigated in detail and their interpretation is ambiguous as they lie in the lower finger-print region of the spectrum and mixes with other skeletal modes. Gray and Lord<sup>13</sup> have placed the  $\text{NH}_2$  wagging and torsional vibrations in methyl amine at  $780$  and  $264\text{ cm}^{-1}$  respectively and have presented arguments for the occurrence of  $\text{NH}_2$  rocking mode (classified as  $\text{NH}_2$  twisting mode in their nomenclature) at  $1455\text{ cm}^{-1}$ , although this band was not actually observed in their spectrum. Stewart<sup>21</sup> has preferred to assign the symmetric and asymmetric  $\text{NH}_2$  bending (wagging and rocking) modes in



liquid primary amines in the regions 810-768 and 851-805  $\text{cm}^{-1}$  respectively. Dellepiane and Zerbi<sup>22</sup> have recently carried out normal coordinate calculations for methyl amines. The potential energy distribution in various normal coordinates suggests that the frequencies at 791 and 995  $\text{cm}^{-1}$  in monomethyl amine are predominantly associated with the  $\text{NH}_2$  wagging and rocking modes respectively.

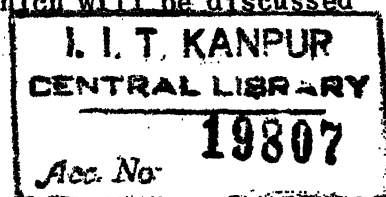
In the case of allyl amine, two strong and broad bands, showing multiplet splitting, have been observed in the crystalline state at 957 and 873  $\text{cm}^{-1}$ . The abnormal width and shape of these lines suggest that they must be associated with the  $\text{NH}_2$  group. The corresponding Raman lines in the liquid are observed at 957  $\text{cm}^{-1}$  (very weak) and 863  $\text{cm}^{-1}$  (medium intense). The infrared band in liquid phase at 860  $\text{cm}^{-1}$  is extremely broad. In the vapour phase, this band shifts to lower frequency at 780  $\text{cm}^{-1}$ . The shift to lower frequency from liquid to vapour and to higher frequency in condensed phase suggests that this band is influenced by the hydrogen bonding effects and must be associated with the  $\text{NH}_2$  group. We therefore attribute the lower frequency component to the  $\text{NH}_2$  wagging mode  $\nu_{15}$  and the higher frequency band to the  $\text{NH}_2$  rocking vibration  $\nu_{23}$  in the infrared spectrum of condensed phase.

The final NH motion to be assigned is the  $\text{NH}_2$  torsion. Scott and Crowder<sup>23</sup> have studied the far-infrared spectra of n-propyl amine, isopropyl amine and t-butyl amine and have ascribed the  $\text{NH}_2$  torsional modes in these amines at 210, 234 and 253  $\text{cm}^{-1}$  respectively. The 363  $\text{cm}^{-1}$  Raman line in methyl hydrazine<sup>19</sup> has been assigned to the  $\text{NH}_2$  torsion. The infrared spectrum of liquid allyl amine shows two bands at 355 and  $\sim 280$   $\text{cm}^{-1}$ . The higher frequency band is probably associated with the CCN bending mode and the other to  $\text{NH}_2$  torsion. The spectrum

of solid allyl amine below  $400\text{ cm}^{-1}$  is affected profoundly by hydrogen bonding, which displaces the  $\text{NH}_2$  torsion to higher wave number side where it can interact more strongly with other skeletal modes. In the solid phase at low temperature, the ir spectrum of allyl amine shows three bands at  $335$ ,  $360$  and  $376\text{ cm}^{-1}$ . The last line is very strong and shows splitting into three components. The band at  $335\text{ cm}^{-1}$  seems to arise due to an overtone of the C-N torsional mode  $\nu_{27}$  and the band at  $360\text{ cm}^{-1}$  is probably due to the CCN deformation mode  $\nu_{17}$ . Therefore the most intense one at  $376\text{ cm}^{-1}$  may be assigned to  $\text{NH}_2$  torsion.

#### Carbon hydrogen stretching vibrations

There are five carbon hydrogen bonds in allyl amine and therefore, one may expect five bands in the region of  $2800$  to  $3100\text{ cm}^{-1}$ . This region will also contain the combination and overtones of deformation modes of the vinyl and methylene groups. Two of these vibrations result from symmetric and antisymmetric C-H stretching modes of methylene group while three result from vibrations of the vinyl hydrogens. In the allyl halide series<sup>7</sup>, the symmetric  $-\text{CH}_2$  stretching vibrations occur in the range  $2935$ - $2970\text{ cm}^{-1}$  while the antisymmetric modes occur in the region  $2980$ - $2990\text{ cm}^{-1}$ . We have studied some aliphatic amines (discussed in Chapters IV, V and VI) and have been able to ascertain that the symmetric and antisymmetric C-H stretching vibrations of the methylene groups attached to nitrogen atom shift to lower frequencies and gain intensity as compared to their positions in the corresponding halides. The position of the C-H stretching vibrations of vinyl group remains nearly the same as that in other alkenes. The tripropargyl amine studied by us, which will be discussed



in Chapter V, contains only methylene groups and give rise to absorption bands at 2817 and 2928  $\text{cm}^{-1}$  corresponding to the symmetric and asymmetric  $-\text{CH}_2$  stretchings respectively.

The two strong infrared bands at 2849 and 2900  $\text{cm}^{-1}$  in the solid sample of allyl amine have been assigned to the symmetric and antisymmetric  $-\text{CH}_2$  stretching modes  $\nu_4$  and  $\nu_{20}$  respectively. In the liquid phase, these bands appear as doublets with shoulders at 2835  $\text{cm}^{-1}$  and 2928  $\text{cm}^{-1}$ . The 2835  $\text{cm}^{-1}$  shoulder, corresponding to the Raman line at 2834  $\text{cm}^{-1}$ , disappears on solidification and is believed to arise from the higher energy form ('cis and trans'). There is no Raman line corresponding to the shoulder at 2928  $\text{cm}^{-1}$  in the liquid phase ir spectrum but this band also appears in the solid phase at 2921  $\text{cm}^{-1}$  and hence may probably be the first overtone of  $-\text{CH}_2$  bending. The medium strong Raman band at 2900  $\text{cm}^{-1}$  which corresponds to the 2890  $\text{cm}^{-1}$  shoulder in vapour phase does not appear at low temperature and hence may belong to less stable isomer.

The vinyl group C-H stretching frequencies are to be expected in the 2950-3100  $\text{cm}^{-1}$  region. We have picked up the Raman lines at 2975, 3005 and 3082  $\text{cm}^{-1}$  for these modes. The infrared bands at 2982 and 3083  $\text{cm}^{-1}$  in the liquid phase and at 2970 and 3072  $\text{cm}^{-1}$  in the solid phase are assigned to the  $=\text{CH}_2$  symmetric and antisymmetric modes  $\nu_3$  and  $\nu_{19}$  respectively. The higher frequency band appears to be a type-A band in vapour phase and the lower one is a type-B band centered at 2989  $\text{cm}^{-1}$ . The medium shoulder at 3010  $\text{cm}^{-1}$  in the liquid phase corresponding to the strong Raman line at 3005  $\text{cm}^{-1}$  is ascribed to the  $=\text{CH}$  stretching mode  $\nu_2$  of vinyl group. Our assignments are in fairly good agreement with the assignment of various workers<sup>12,7</sup> for similar modes. The shoulder at 3065  $\text{cm}^{-1}$  in liquid phase, which also persists

in the solid phase at  $3060\text{ cm}^{-1}$ , does not have any Raman counterpart and is therefore suggested to appear as a result of combination mode  $1633+1436 = 3069\text{ cm}^{-1}$  in Fermi resonance with the C-H stretching vibrations.

#### Vinyl hydrogen deformations

The vinyl group is expected to have six C-H deformation modes conventionally described as three in-plane and three out-of-plane vinyl hydrogen bending modes. The two out-of-plane deformations, the vinyl wagging and twisting vibrations, have been well characterized in a large number of compounds<sup>20</sup>. The bands which may be assigned to these vibrations are found in the liquid phase infrared spectrum at  $918$  and  $995\text{ cm}^{-1}$ , corresponding to the  $920$  and  $1005\text{ cm}^{-1}$  frequencies respectively in the solid phase. A weak shoulder observed at  $928\text{ cm}^{-1}$  with the lower frequency band does not appear in the solid phase and is accordingly assigned to the higher energy isomer. The contours for these bands in the vapour phase are well resolved and have a pronounced doublet Q-branch. The very narrow doublets at  $913\text{--}916\text{ cm}^{-1}$  and  $994\text{--}997\text{ cm}^{-1}$  could hardly be regarded as B-type bands. More probably, they result from the splitting of the Q-branch of a C-type band. The origin of these splittings is uncertain: They could arise from a coupling between torsion and other vibrations through Coriolis forces, or from the presence of molecules in the vibrationally excited states (hot bands). A study of the vapour phase spectra at different temperatures suggests, however, that these doublets are primarily due to the presence of hot bands. The presence of the first overtone of these bands at  $1847$  and  $1980\text{ cm}^{-1}$  in the liquid phase also lends further support to their correct assignments.

The in-phase, out-of-plane 'cis C-H wag' vibrations generally do not give rise to characteristic absorption frequencies, as these are much more sensitive to the environment. Three bands of moderate intensity are observed at 645, 578 and 556  $\text{cm}^{-1}$  in the liquid phase infrared spectrum where this mode is expected. In the solid phase at low temperature, the higher frequency band becomes very strong and sharp while the band at 578  $\text{cm}^{-1}$  disappears completely. The band at 556  $\text{cm}^{-1}$  also decreases very much in intensity and appears only as a very weak band at low temperature. This band may probably be interpreted as a combination tone which gains intensity in liquid phase by Fermi resonance with the line at 578  $\text{cm}^{-1}$ . The disappearing band is assigned as the  $\nu_{25}$  mode due to less stable isomer and the remaining band at 643  $\text{cm}^{-1}$  is attributed to the more stable form. At higher temperatures in vapour phase, the two lower frequency bands increase in intensity as compared to the higher frequency band. This temperature intensity behaviour also suggests that these bands belong to different isomers.

The  $=\text{CH}_2$  in-plane scissoring motions absorb at relatively lower frequencies as compared to those of methylene  $-\text{CH}_2$  groups. This mode  $\nu_8$  may be safely assigned to the Raman band at 1416  $\text{cm}^{-1}$ . The corresponding infrared bands lie at 1420 and 1436  $\text{cm}^{-1}$  in liquid and solid phases respectively. The in-plane  $=\text{CH}$  bending modes in allyl halides<sup>7</sup> have been assigned in the narrow region 1289-1294  $\text{cm}^{-1}$ . In the liquid phase, a weak doublet is observed at 1275, 1285  $\text{cm}^{-1}$  in infrared, but the corresponding Raman line at 1286  $\text{cm}^{-1}$  is extremely strong and polarized. Because of its high Raman intensity, this band is assigned to the in-plane  $\nu_{10}$  mode.

Now we are left with one vinyl hydrogen in-plane deformation mode  $\nu_{11}$ . In allyl halide series, this mode has been assigned between 1187-1240  $\text{cm}^{-1}$  for the 'gauche' forms and 1022-1107  $\text{cm}^{-1}$  for the 'cis' isomers<sup>7</sup>. It seems reasonable to place this mode  $\nu_{11}$  at 1208  $\text{cm}^{-1}$  in allyl amine for the 'gauche and trans' form. The temperature-intensity behaviour of the pair 1208, 1132  $\text{cm}^{-1}$  then suggests that the lower frequency component, vanishing at low temperature, could be associated with the other isomer ('cis and trans').

In the region of C = C stretch, the infrared spectrum of liquid shows a strong band at 1640  $\text{cm}^{-1}$  with a shoulder at 1630  $\text{cm}^{-1}$ . In the solid phase, the lower frequency component disappears and may therefore arise due to other isomer. The Raman spectrum of this region shows a very strong and polarized band at 1635  $\text{cm}^{-1}$  and is assigned to the C = C stretching mode  $\nu_5$ .

#### CH<sub>2</sub>-N vibrations

The Raman band at 1448  $\text{cm}^{-1}$  is assigned to the methylene scissoring vibration  $\nu_7$ . The corresponding infrared bands lie at 1450  $\text{cm}^{-1}$  in the liquid and solid and a C-type band centred at 1467  $\text{cm}^{-1}$  in the vapour phases. The origin of the band observed at 1411  $\text{cm}^{-1}$  in solid phase is uncertain. It may probably arise as a result of combination mode. The methylene wagging mode lies somewhere in the complex band system with apparent maxima at 1328, 1346, 1365 and 1383  $\text{cm}^{-1}$  in the liquid phase. At low temperature, the lower frequency band gets intensified leaving the other bands to appear as very weak bands. This is assigned to the  $\nu_9$  mode and the other bands are interpreted as combination modes shown in Table 3.2. The methylene twisting mode  $\nu_{21}$  is placed at 1105  $\text{cm}^{-1}$  in the liquid phase ir spectrum. At low

temperature in condensed phase, a strong and broad band appears with a multiplet splitting. This mode may heavily couple with the  $\text{NH}_2$  twisting (rocking) motion and therefore gains intensity in the solid phase. The identification of the  $\text{-CH}_2$  rocking vibration is a bit difficult since they are usually weak in intensity and their frequency shifts drastically with the change of environment of the  $\text{-CH}_2$  group. This mode is tentatively associated with the shoulder at  $843\text{ cm}^{-1}$  in infrared.

Investigations on large number of amines by Stewart<sup>21</sup> have shown that aliphatic primary amines with a primary  $\alpha$ -carbon atom show medium intense bands in between  $1090\text{--}1068\text{ cm}^{-1}$ , primarily associated with the C-N stretch. The analogous mode in allyl amine may obviously be associated with the B-type band centred at  $1051\text{ cm}^{-1}$ . The corresponding polarized Raman line lies at  $1047\text{ cm}^{-1}$ . The weak shoulder on the higher frequency side at  $1080\text{ cm}^{-1}$  in the liquid phase is assigned to this mode due to less stable isomer on the basis of its behaviour at low temperature. Gross and Forel<sup>12</sup> had also observed this mode at  $1047\text{ cm}^{-1}$  in allyl amine.

#### Skeletal vibrations

The  $\text{=C-C}$  stretching vibration  $\nu_{14}$  is expected in the region of the two out-of-plane vinyl deformations and  $\text{NH}_2$  wagging modes and thus is not easy to be identified in the infrared spectrum of liquid sample. In the Raman spectrum, the band at  $889\text{ cm}^{-1}$  is relatively strong and polarized as compared to the  $\text{NH}_2$  wagging and vinyl vibrations. Therefore it is believed to arise due to the C-C stretching mode. In condensed phase, the bands become sharper and a distinct doublet corresponding to this mode appears at  $895\text{--}902\text{ cm}^{-1}$ , the doublet splitting

may probably be the result of crystal field or related effects. The two  $-C = C - C$  and  $-C - C - N$  bendings are expected to lie below  $500\text{ cm}^{-1}$ . The Raman spectrum shows three bands at  $442$ ,  $355$  and  $305\text{ cm}^{-1}$ . The  $-C = C - C$  deformation has been placed at  $428\text{ cm}^{-1}$  in propylene<sup>24</sup> and at  $438\text{ cm}^{-1}$  in allyl alcohol<sup>12</sup>. In the solid phase ir spectrum of allylamine, two bands appear in this region at  $441$  and  $472\text{ cm}^{-1}$ , the latter band being broad and strong compared to the former. The lower frequency band is assigned to this mode  $\nu_{16}$  in allyl amine, as the corresponding Raman band is medium intense. In allyl fluoride<sup>7</sup>, the  $345\text{ cm}^{-1}$  band is assigned to  $-C-C-F$  deformation mode and shows a systematic decrease in frequency with increasing mass of halogen. The similar skeletal bending mode in allyl alcohol<sup>12</sup> has also been placed at  $345\text{ cm}^{-1}$ . Therefore it is reasonable to assign the Raman and weak infrared bands at  $355\text{ cm}^{-1}$  to this mode  $\nu_{17}$ . The Raman band at  $305\text{ cm}^{-1}$  does not seem to appear in solid phase and may therefore belong to other isomer. The broad band at  $472\text{ cm}^{-1}$  in the solid phase may then be interpreted as a combination mode of  $NH_2$  torsion with some low lying intermolecular modes or torsions, as this band does not appear in the liquid and vapour phases. It is also possible that this band may arise due to some lattice mode.

The low lying mode  $\nu_{27}$ , the torsion about  $C-C$  bond, may be lying well below the limit of our infrared instrument. From the analysis of microwave data of allyl fluoride<sup>3</sup>, Hirota has calculated frequencies of  $169$  and  $84\text{ cm}^{-1}$  for the torsional vibrations of the 'cis' and 'gauche' isomers respectively. The weak band observed at  $182\text{ cm}^{-1}$  in the Raman spectrum may be associated with this mode for one isomer. The frequency for the other isomeric form could not be detected in the wing of the strong laser line.



### Overtone and combination tones

The low symmetry for the various molecular configurations of allyl amine allows all the combinations and overtones to be both infrared and Raman active. Many of the weak absorption bands in the spectra of allyl amine may be assigned as either overtones and/or combination tones of the fundamental vibrations discussed above. The most probable assignments for them are given in Table 3.2.

## REFERENCES

1. H.J.M. Bowen, A. Gilchrist and L.E. Sutton, Trans. Faraday Soc. 51, 1341 (1955)
2. (a) A.A. Bothner - By and C. Naar - Colin, J. Am. Chem. Soc. 83, 231 (1961); (b) A.A. Bothner - By, C. Naar - Colin and H. Gunther, *ibid.* 84, 2748 (1962); (c) A.A. Bothner - By and H. Gunther, Discussions Faraday Soc. 34, 127 (1962)
3. E. Hirota, J. Chem. Phys. 42, 2071 (1965)
4. K.V.L.N. Sastry, V.M. Rao and S.C. Dass, Can. J. Phys. 46, 959 (1968)
5. A.N. Murty and R.F. Curl, J. Chem. Phys. 46, 4176 (1967)
6. K.V.L.N. Sastry, S.C. Dass, W.V.F. Brooks and A. Bhaumic, J. Mol. Spectry. 31, 541 (1969)
7. R.D. McLachlan and R.A. Nyquist, Spectrochim. Acta 24A, 101 (1968)
8. K.W.F. Kohlrausch and W. Stockmair, Z. Physik. Chem. B-29, 292 (1935)
9. L. Kahovec and K.W.F. Kohlrausch, Z. Physik. Chem. B-29, 274 (1935)
10. M. Freymann, Ann. Chim. 11, (1939)
11. M.R. Yagudaev, E.M. Popov, I.P. Yakovlev and Yu. N. Sheinker, Izv. Akad. Nauk. S.S.S.R. Ser. Khim. 7, 1189 (1964)
12. B. Gross and M.T. Forel, J. Khim. Phys. 62, 1163 (1965)
13. A.P. Gray and R.C. Lord, J. Chem. Phys. 26, 690 (1957)
14. R.M. Badger and L.R. Zumwalt, J. Chem. Phys. 6, 711 (1938)
15. W.A. Seth-Paul and G. Dijkstra, Spectrochim. Acta 23A, 2861 (1967)
16. W.J.O. Thomas, A.E. Parsons and C.P. Ogden, J. Chem. Soc. 1047 (1958)
17. E.L. Zhukova and I.I. Shmanko, Opt. Spectry. 25, 279 (1968)
18. R. Blinc and D. Hadzi, in Hydrogen Bonding (D. Hadzi, ed.), p. 147, Pergamon Press, New York (1957)

19. J.R. Durig, W.C. Harris and D.W. Wertz, J. Chem. Phys. 50, 1449 (1969)
20. W.J. Potts, Jr., and R.A. Nyquist, Spectrochim. Acta 15, 679 (1959)
21. J.E. Stewart, J. Chem. Phys. 30, 1259 (1959)
22. G. Dellepiane and G. Zerbi, J. Chem. Phys. 48, 3572 (1968)
23. D.W. Scott and G.A. Crowder, J. Mol. Spectry. 26, 477 (1968)
24. R.C. Lord and P. Venkateswarlu, Opt. Soc. Amer. 43, 1079 (1953)

TABLE 3.1

MOMENTS OF INERTIA (IN ATOMIC MASS UNITS TIMES SQUARE ANGSTROM) AND ROTATIONAL CONSTANTS (IN  $\text{cm}^{-1}$  UNITS) OF THE SPECTROSCOPICALLY DISTINGUISHABLE CONFORMERS OF ALLYL AMINE

Species	'cis and trans'	'cis and gauche'	'gauche and trans'	'gauche and gauche'	'gauche and gauche' '
<u>IA</u>	33.12	31.36	21.04	20.05	19.47
<u>IB</u>	80.77	84.45	116.73	119.43	119.40
<u>IC</u>	108.05	111.40	120.49	122.38	124.47
<u>A</u>	0.5091	0.5378	0.8014	0.8111	0.8661
<u>B</u>	0.2088	0.1997	0.1444	0.1412	0.1412
<u>C</u>	0.1561	0.1514	0.1399	0.1378	0.1355
$\rho^* = \frac{A-C}{B}$	1.691	1.935	4.578	4.768	5.173
$k = \frac{2B-A-C}{A-C}$	-0.7014	-0.7500	-0.9863	-0.9903	-0.9842
Calculated P-R separation for type-A(4) bands	21.6 $\text{cm}^{-1}$	21.0 $\text{cm}^{-1}$	17.8 $\text{cm}^{-1}$	17.5 $\text{cm}^{-1}$	17.4 $\text{cm}^{-1}$

Table 3.2 Contd...

63

2742	vw	2752	vvw	2760	vw				$\nu_8 + \nu_9$
2672	vw	2681	vw						$2 \times \nu_9$
				2630	vvw				$\nu_9 + \nu_{10}$
1980	vw	1990 ) 1980 )	vw						$2 \times \nu_{22}$
1847 ) 1836 )	w sh	1851 ) 1840 )	w	1850	w				$2 \times \nu_{13}$
1640	s	1654 ) 1644 )	m	1633	sh,m	1635	vs	P	$\nu_5$ , C=C str.
1630	sh								C=C str., isomer
1605	s,br	1637 ) 1627 ) A 1618 )	vs	1603 ) 1599 ) 1595 )	s,br	1600	vvw		$\nu_6$
1450	m	1476 ) 1467 ) C 1458 )	w	1450	w	1448	mw	D?	$\nu_7$
1420	m	1440 ) 1431 ) - )	s	1438 ) 1434 )	m	1416	m	P	$\nu_8$
1408	sh	1420 ) 1410 ) B	ms	1411	w				$\nu_{12} + \nu_{17}$
1383	vw			1385	vvw				$\nu_{21} + \nu_{27}$
1365	mw	1369 ) 1360 ) A 1350 )	m	1370	vw	1368	vw	P	$\nu_{13} + \nu_{16}$
1346	w	1338	w	1346	vw	1342	vw	D	$\nu_{14} + \nu_{16}$
1328	mw	1324	vw	1330	m	1320	vw	?	$\nu_9$
1285	mw	1300 ) 1291 ) - )	m	1295	vvw	1286	s	P	$\nu_{10}$ , vinyl hydrogen i/p def.

Contd...

Contd...

Table 3.2 Contd...

65

						742	vw		$\nu_{25} + \nu_{27}$
645	m	658) 650) 639)	m	643	vs	647	w	P	$\nu_{25}$ , vinyl hydrogen o/p def.
578	m	581) 576) 568)	m			573	vw	D	vinyl hydrogen o/p def., isomer
556	m	- ) 561) 550)	m	551	vw	555	vw	D	$\nu_{17} + \nu_{27}$
						490	vw		$2X \nu_{26}$
				472	m				lattice mode?
445	mw	450) 438) C 425)	w	441	mw	442	w	P	$\nu_{16}$
355	m	340) 330) A 321)	mw	360	mw	355	w	D?	$\nu_{17}$
				335	w				$2X \nu_{27}$
						305	m	P	CCN def., isomer
280	br	275	w	380) 376) 372)	vs	255	vw	D?	$\nu_{26}$
						182	vw	P	$\nu_{27}$

Abbreviations: w, m, s, sh, br, refer to weak, medium, strong, shoulder and broad respectively. ? means an uncertain assignment. P refers for polarized and D for depolarized Raman bands. The i/p def. and o/p def. refer to in-plane deformation and out-of-plane deformation respectively. The assignment in the Table is given for the more stable 'gauche and trans' form, unless otherwise stated. The word 'isomer' stands for the less stable 'cis and trans' form.

TABLE 3.3

THE APPROXIMATE DESCRIPTION AND OBSERVED FREQUENCIES OF THE  
FUNDAMENTAL VIBRATIONS OF THE TWO CONFORMATIONS OF ALLYL AMINE

Species $C_1$ $C_s$	Number	Approximate description of vibration	Observed fundamental frequencies ( $\text{cm}^{-1}$ )				
			'cis and trans' ( $C_s$ )	'gauche and trans' ( $C_1$ )			
				Liquid (ir)	Liquid (ir)	Vapour (ir)	Solid Raman (ir) Liquid
a	$\nu_1$	N-H str. (sym.)		3312	3312	3350	3260 3305
	$\nu_2$	= CH str.		3010	3010	3012	2990 3005
	$\nu_3$	= CH <sub>2</sub> str. (sym.)		2982	2982	2989	2970 2975
	$\nu_4$	-CH <sub>2</sub> str. (sym.)		2835	2852	2855	2849 2851
	$\nu_5$	C = C str.		1630	1640	1649	1633 1635
	$\nu_6$	-NH <sub>2</sub> scissoring		1605	1605	1627	1603 ) 1599 ) 1600
	$\nu_7$	-CH <sub>2</sub> def.		1450	1450	1467	1450 1448
	$\nu_8$	= CH <sub>2</sub> def.		1420	1420	1431	1436 1416
	$\nu_9$	-CH <sub>2</sub> wag.		1328	1328	1320	1330 1335
	$\nu_{10}$	Vinyl hydrogen in-plane bending		1275	1285	1291	1295 1286
	$\nu_{11}$	Vinyl hydrogen in-plane bending		1132	1208	1210	1211 1200
	$\nu_{12}$	C-N str.		1080	1048	1051	1060 1047
	$\nu_{13}$	Vinyl hydrogen out-of- plane bending		928	918	916 ) 913 )	920 915
	$\nu_{14}$	C-C str.		892	892	901	902 ) 895 ) 889
	$\nu_{15}$	-NH <sub>2</sub> wag.		860	860	780	878 863
	$\nu_{16}$	C = C - C def.		445	445	438	441 442

Contd...



Table 3.3 Contd...

67

a''	$\nu_{17}$	C - C - N def.	(305) <sup>b</sup>	355	330		355
	$\nu_{18}$	N - H str. (asym.)	3390	3390	3430	3330	3383
	$\nu_{19}$	= CH <sub>2</sub> str. (asym.)	3083	3083	3087	3072	3082
	$\nu_{20}$	-CH <sub>2</sub> str. (asym.)	(2890) <sup>a</sup>	2910	2912	2900	2910
	$\nu_{21}$	-CH <sub>2</sub> twist	1132	1105	1116	1102 ) 1099 )	1110
	$\nu_{22}$	Vinyl hydrogen out-of-plane bending	995	995	997 ) 994 )	1005	996
	$\nu_{23}$	-NH <sub>2</sub> Rock	(965) <sup>a</sup>		965	965	957
	$\nu_{24}$	-CH <sub>2</sub> Rock	843	843		845	835
	$\nu_{25}$	Vinyl hydrogen out-of-plane def.	578	645	650	643	647
	$\nu_{26}$	-NH <sub>2</sub> torsion	280	280	275	380	(255)
	$\nu_{27}$	C - C torsion					182

<sup>a</sup>The infrared frequencies from the vapour phase ir spectrum were taken, as the corresponding bands in the liquid phase were not observed.

<sup>b</sup>The Raman data for the liquid were used, because these bands were not observed in the liquid phase ir spectrum due to the weakness of the bands.

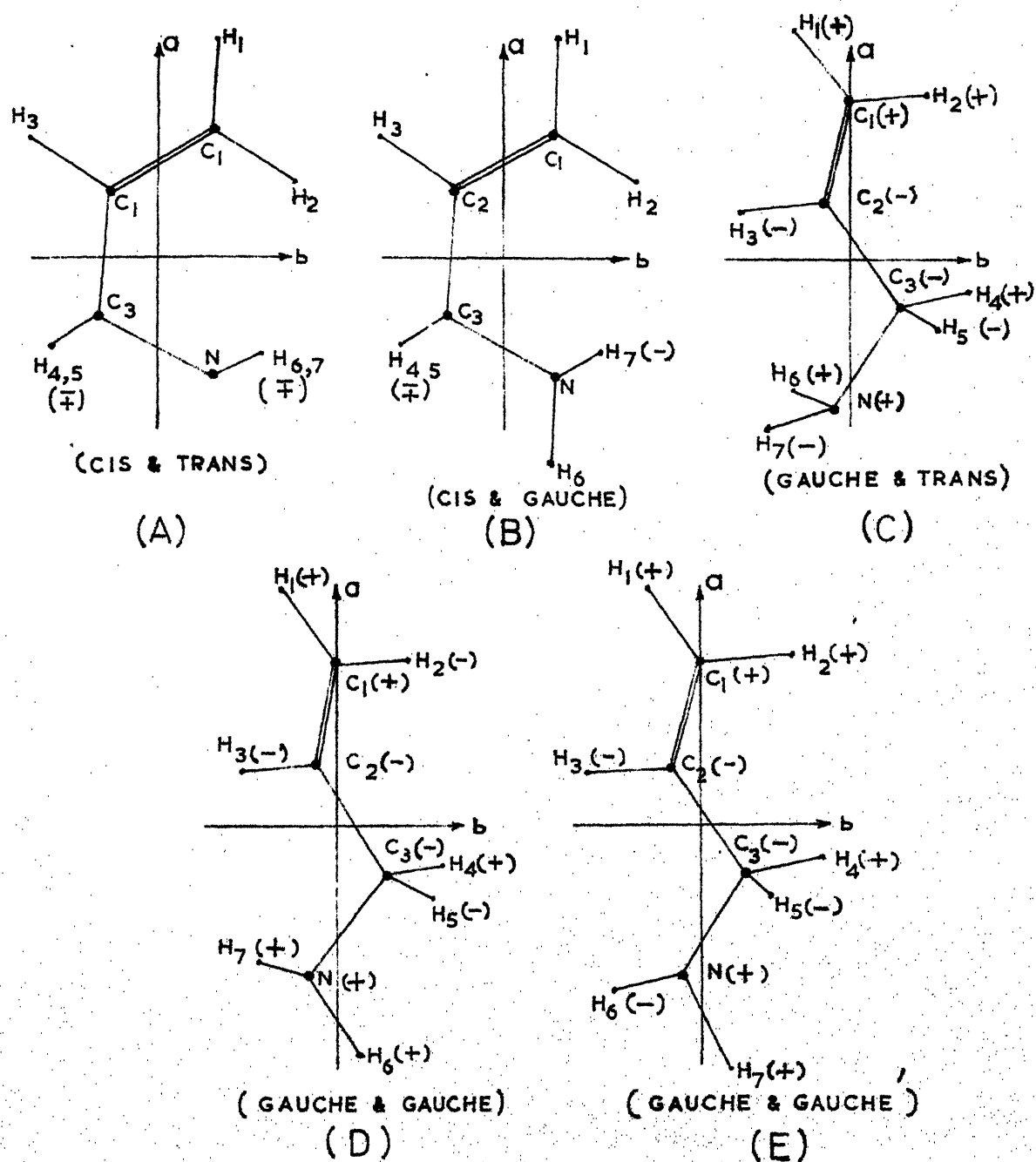


Fig. 3.1: Projections of the spectroscopically distinguishable conformers of allyl amine on  $a - b$  plane of the principal axes system. The + and - signs indicate that the atom lies above and below the  $a - b$  plane respectively.

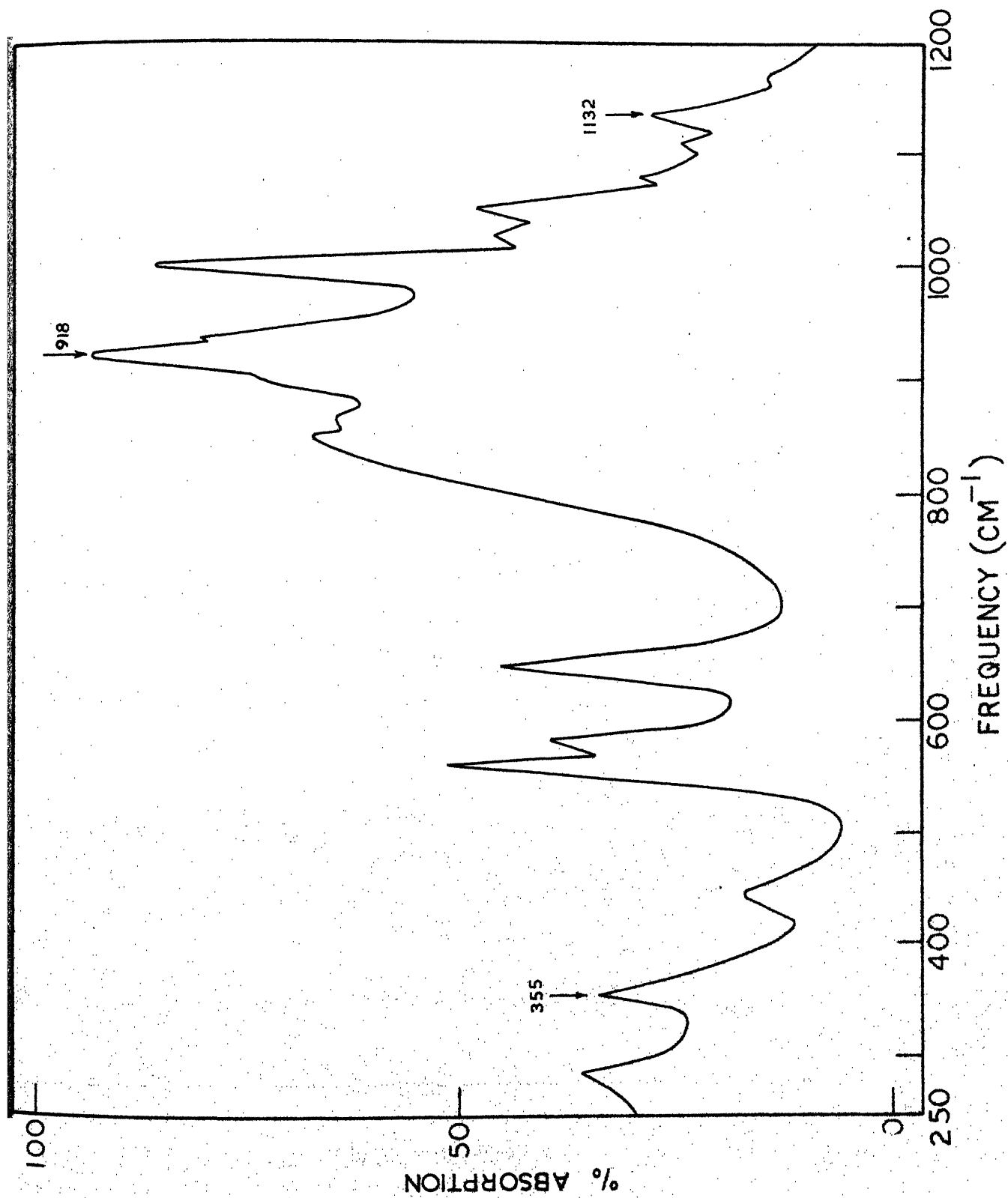


Fig. 1.2(A): The infrared spectrum of liquid allylamine (750 - 1200 cm⁻¹).

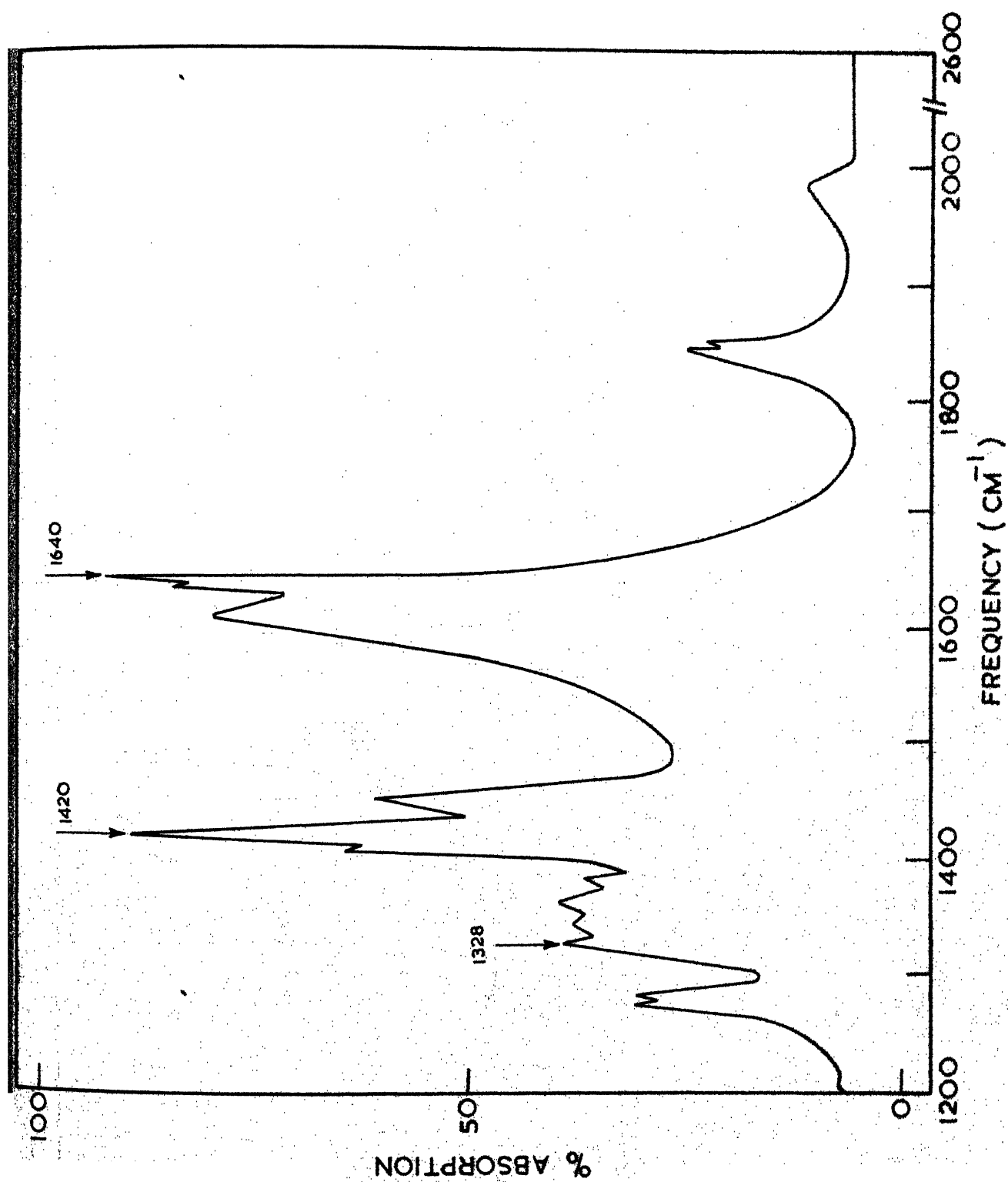


Fig. 3.2(h). The infrared spectrum of liquid allyl amine (1200 - 2600 cm<sup>-1</sup>).

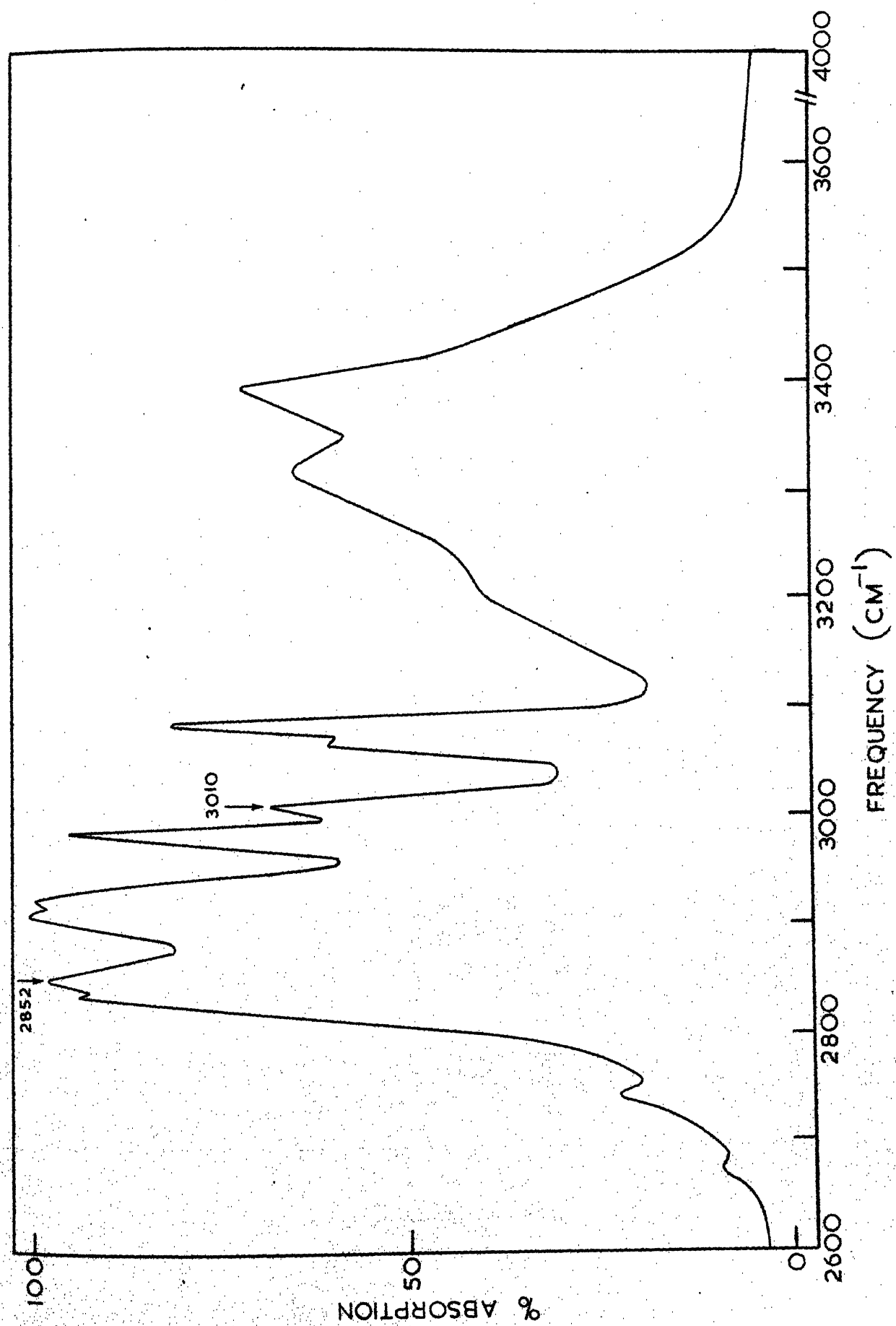


Fig. 3.2(C): The infrared spectrum of liquid allyl amine (2600-4000 cm<sup>-1</sup>).

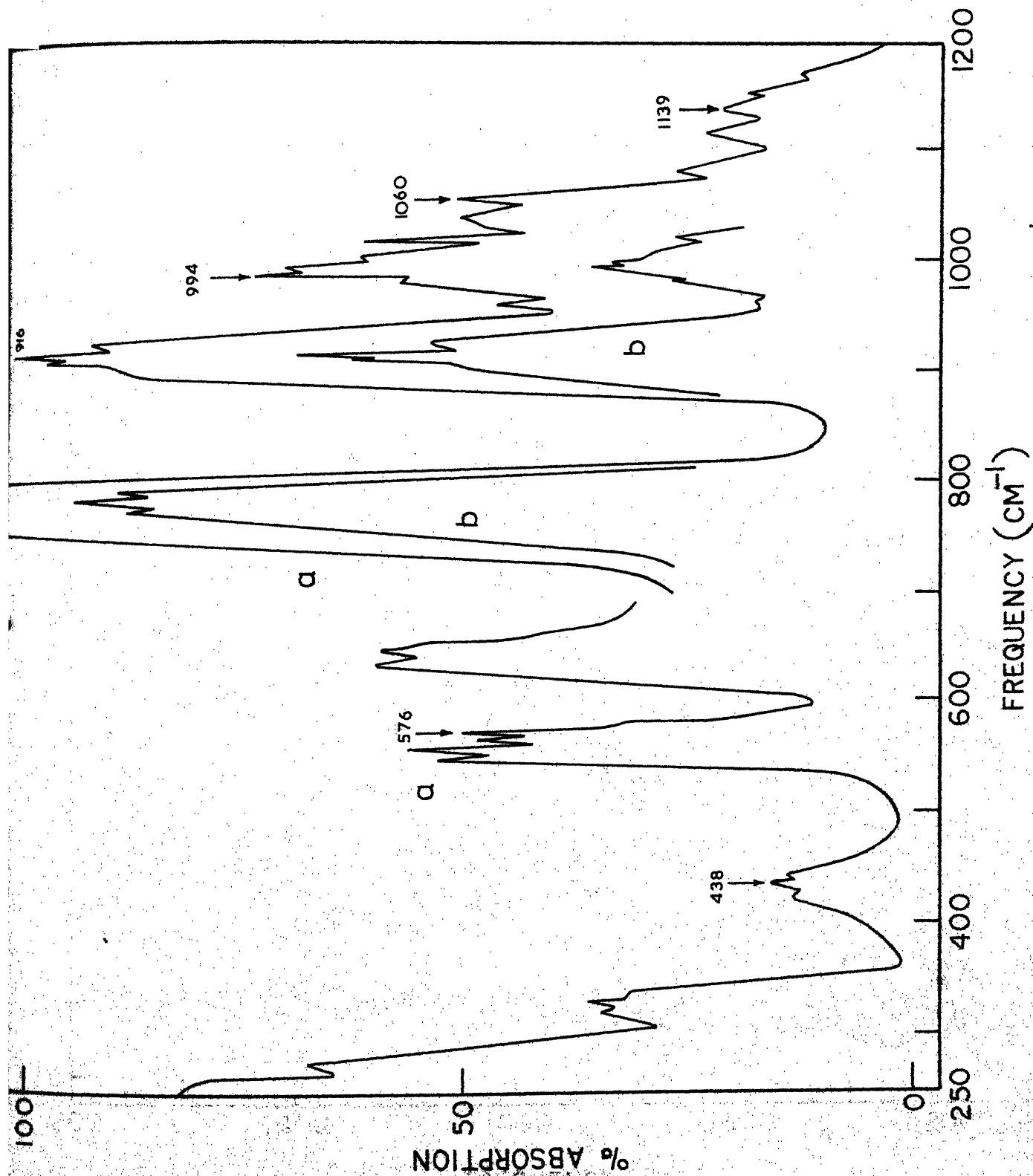


Fig. 3.3(A): The infrared spectrum of gaseous allyl amine (250-1200  $\text{cm}^{-1}$ ); 10 cm path length. (a) Pressure equals the vapour pressure at room temperature; (b) lower vapour pressure than in case (a).

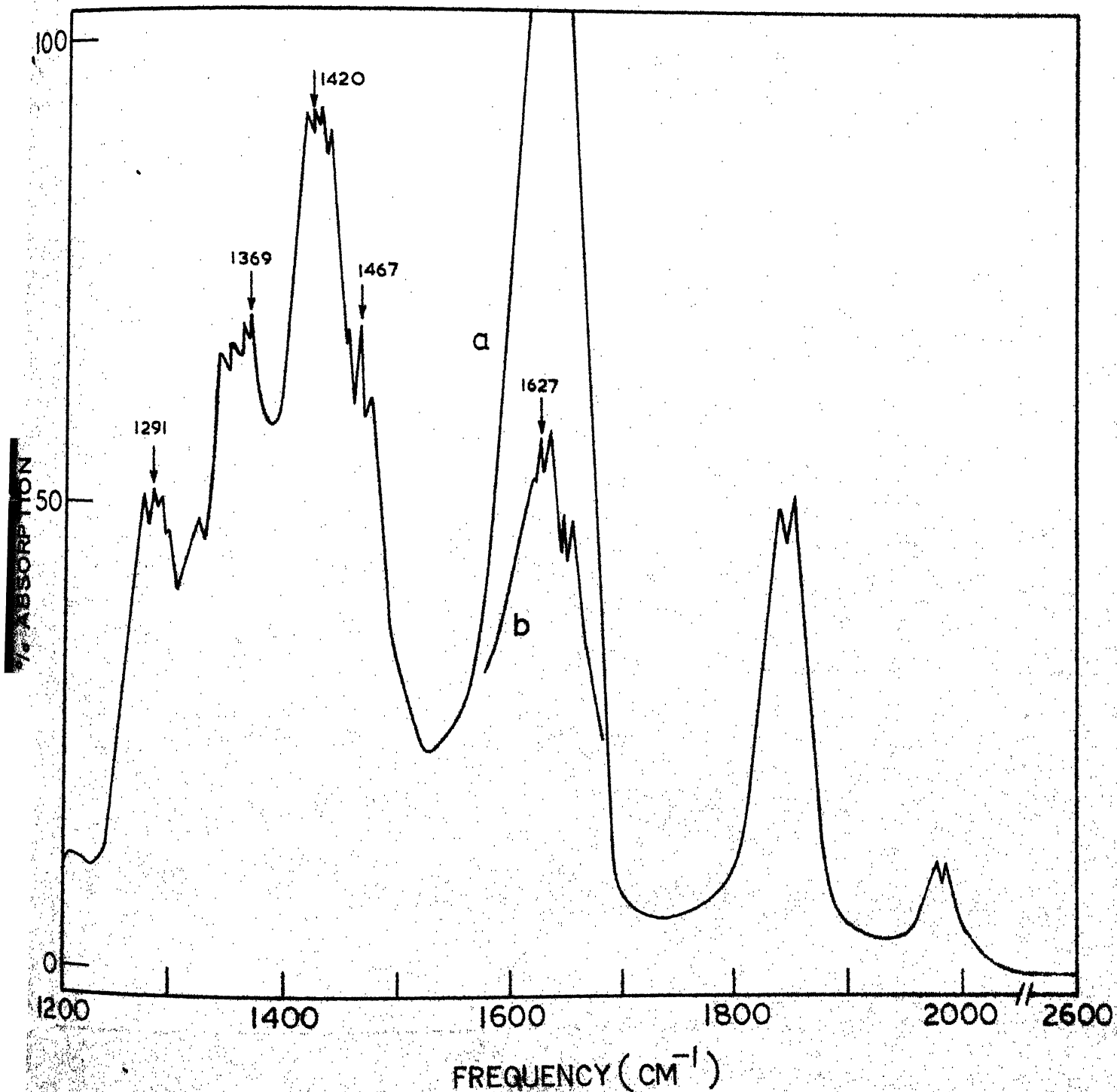


Fig. 3.3(B): The infrared spectrum of gaseous allyl amine ( $1200\text{--}2600\text{ cm}^{-1}$ ); 10 cm path length. (a) Pressure equals the vapour pressure at room temperature; (b) Lower vapour pressure than in case (a).

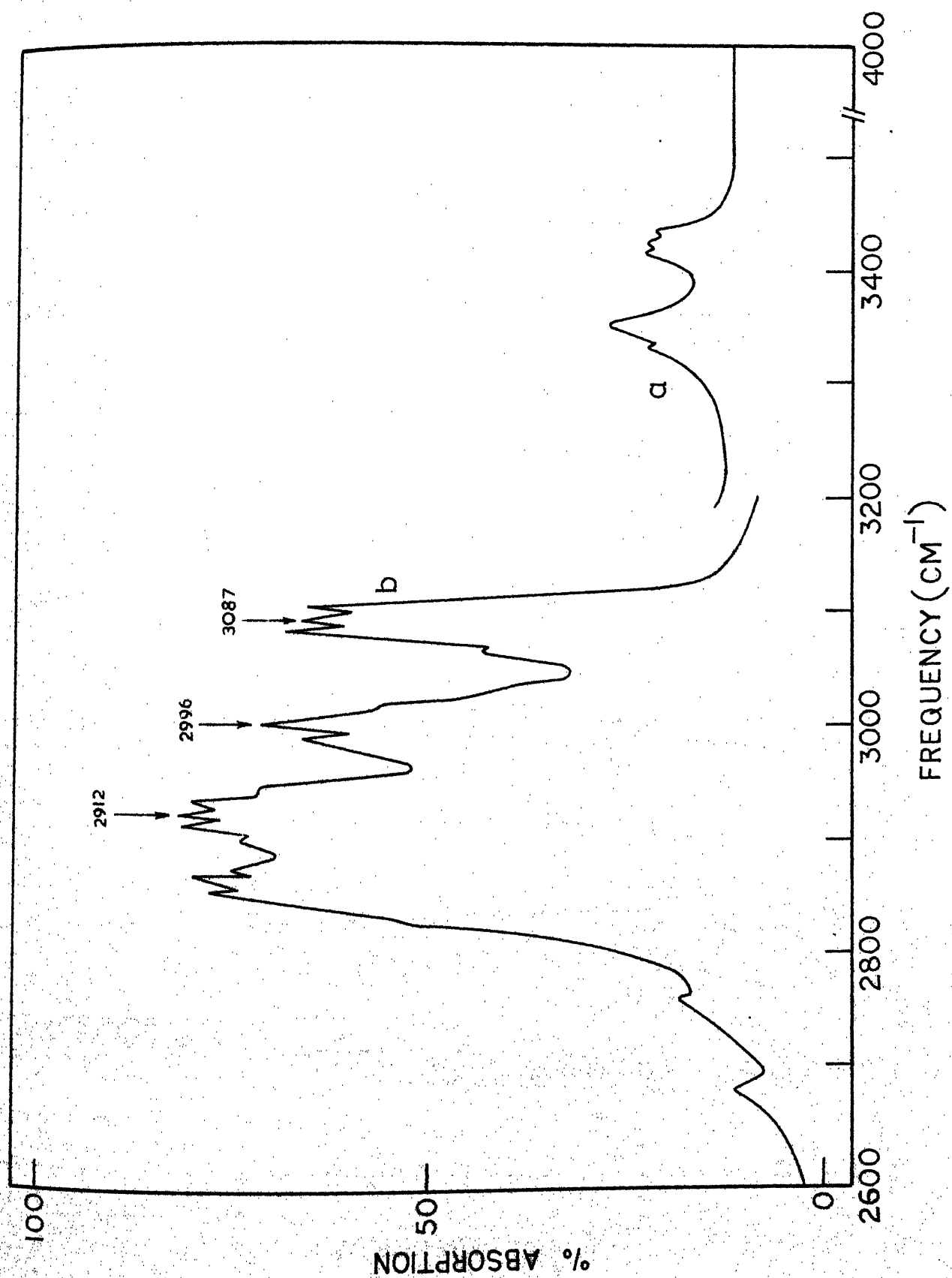


Fig. 3.3(C): The infrared spectrum of gaseous allyl aniline ( $2600-4000\text{ cm}^{-1}$ ); 10 cm path length.  
(a) Pressure equals the vapour pressure at room temperature; (b) Lower vapour pressure than in case (a).



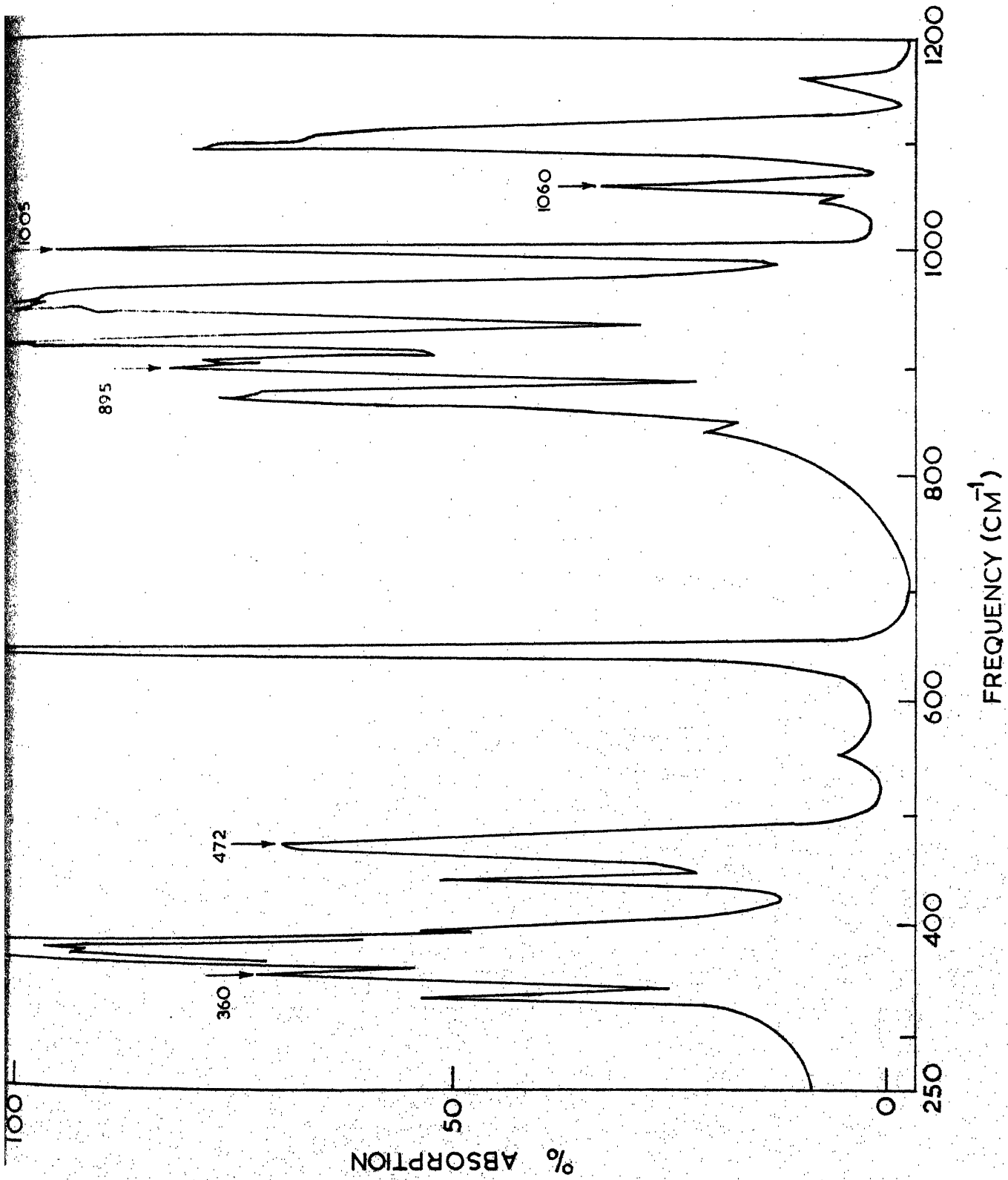


Fig. 3.4(A): The infrared spectrum of solid amine in solid phase near 77°K (250 - 1200 cm⁻¹).

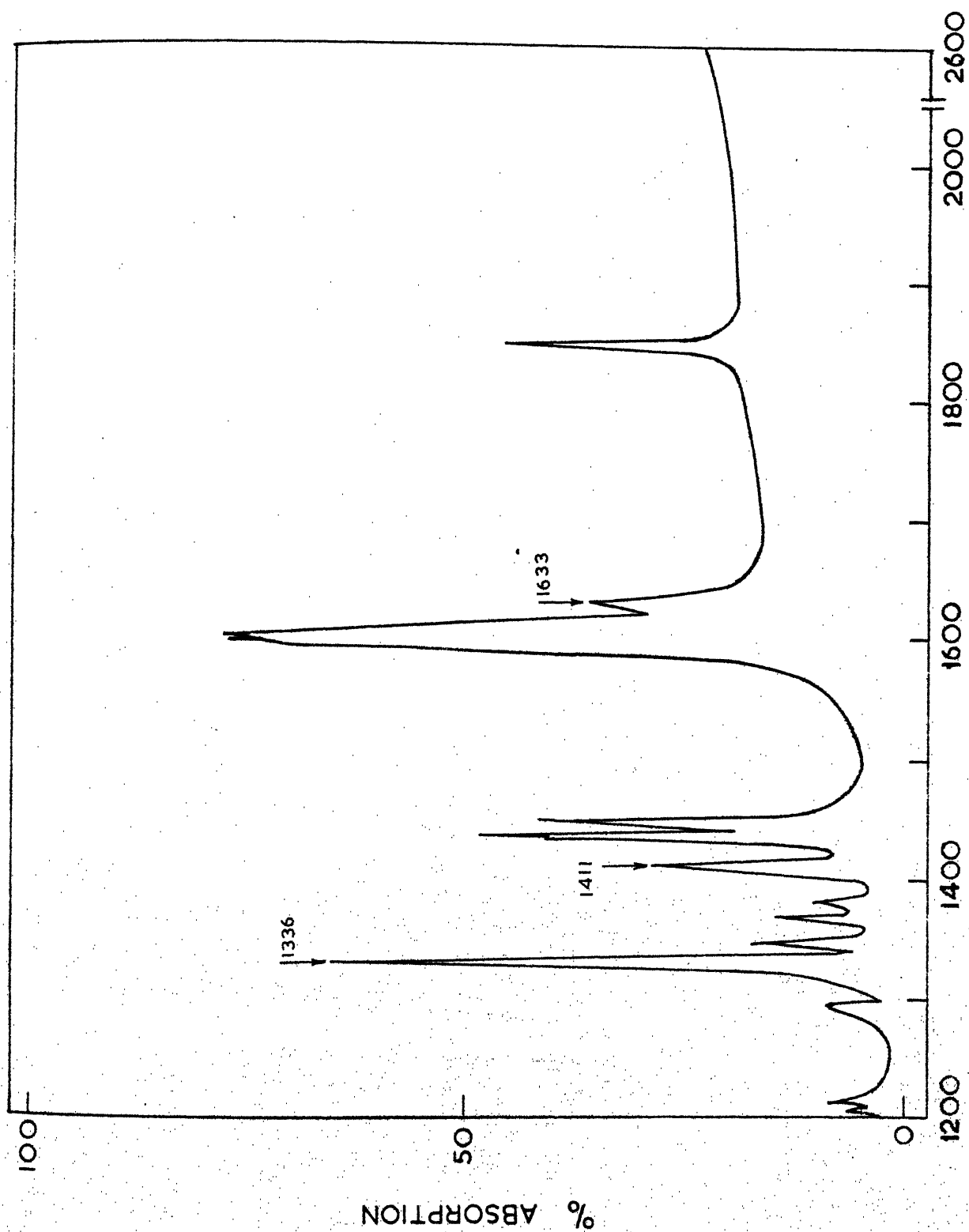


Fig. 3.4(2c). The infrared spectrum of allyl amine in solid phase near 77°K (1200-2600 cm<sup>-1</sup>).

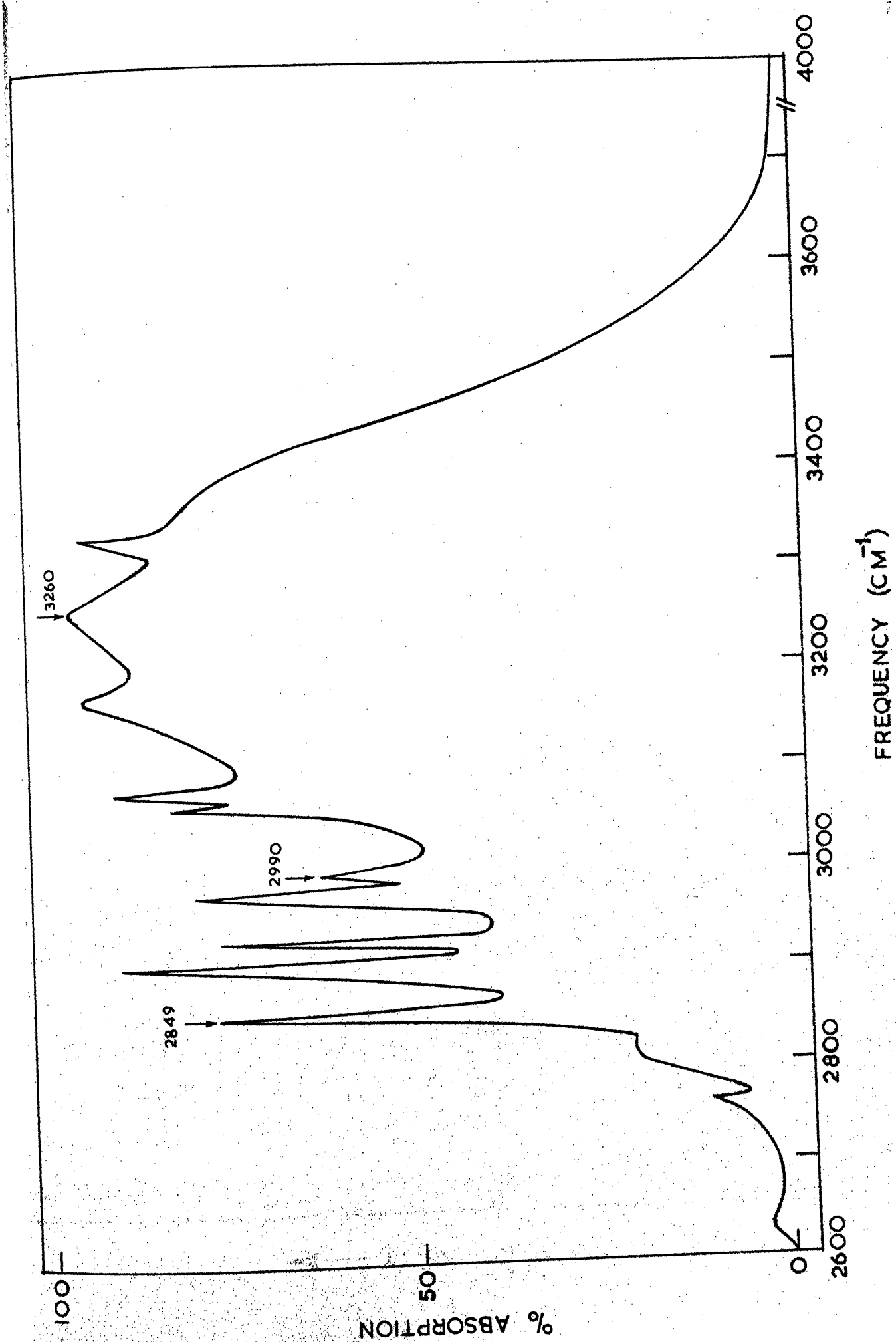


Fig. 3.4(C): The infrared spectrum of allylamine in solid phase near 77°K. (2600-4000 cm<sup>-1</sup>).

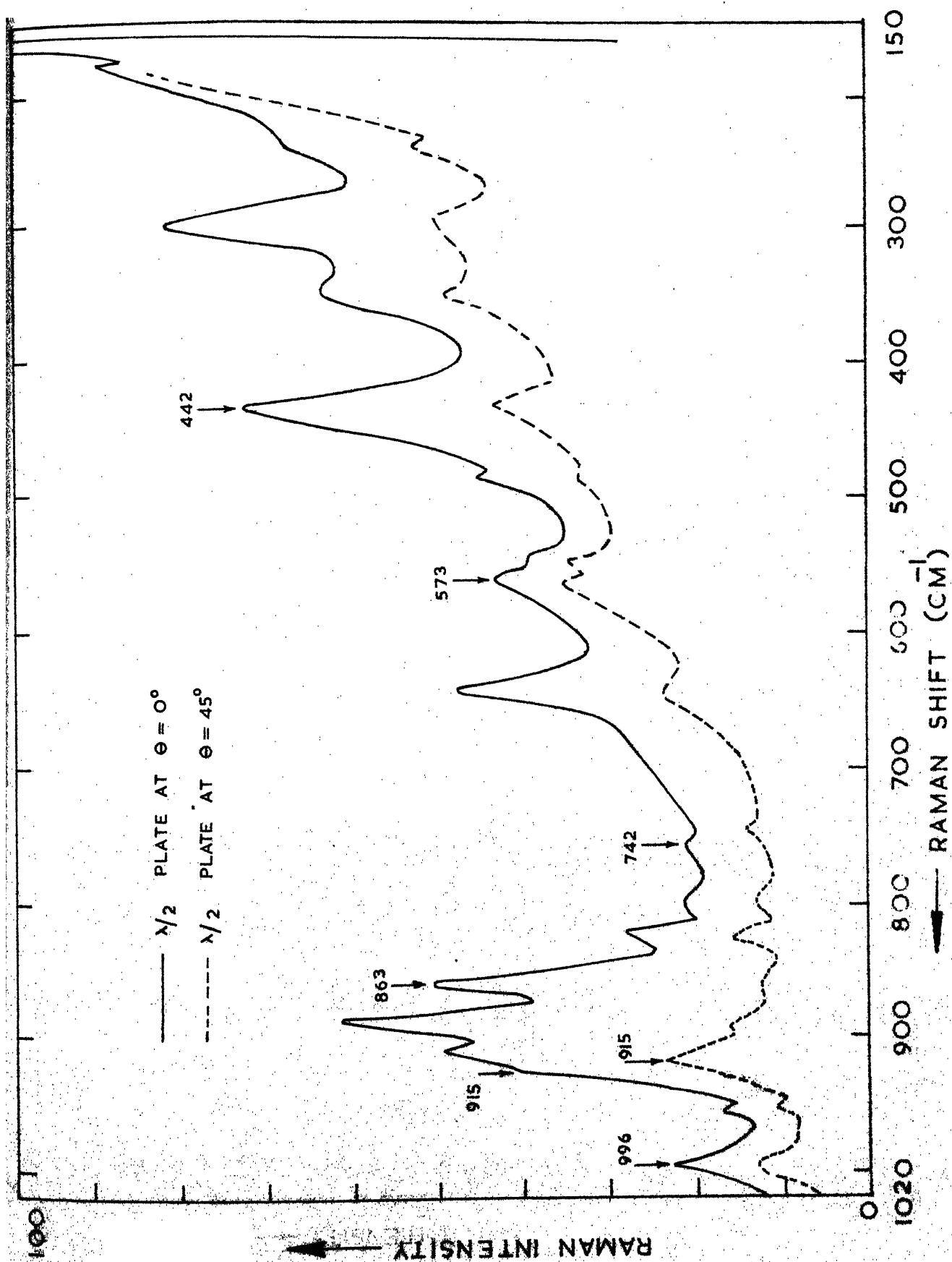


Fig. 1.5(A): The laser-Raman spectrum of liquid allylamine (150-1020 cm<sup>-1</sup>).

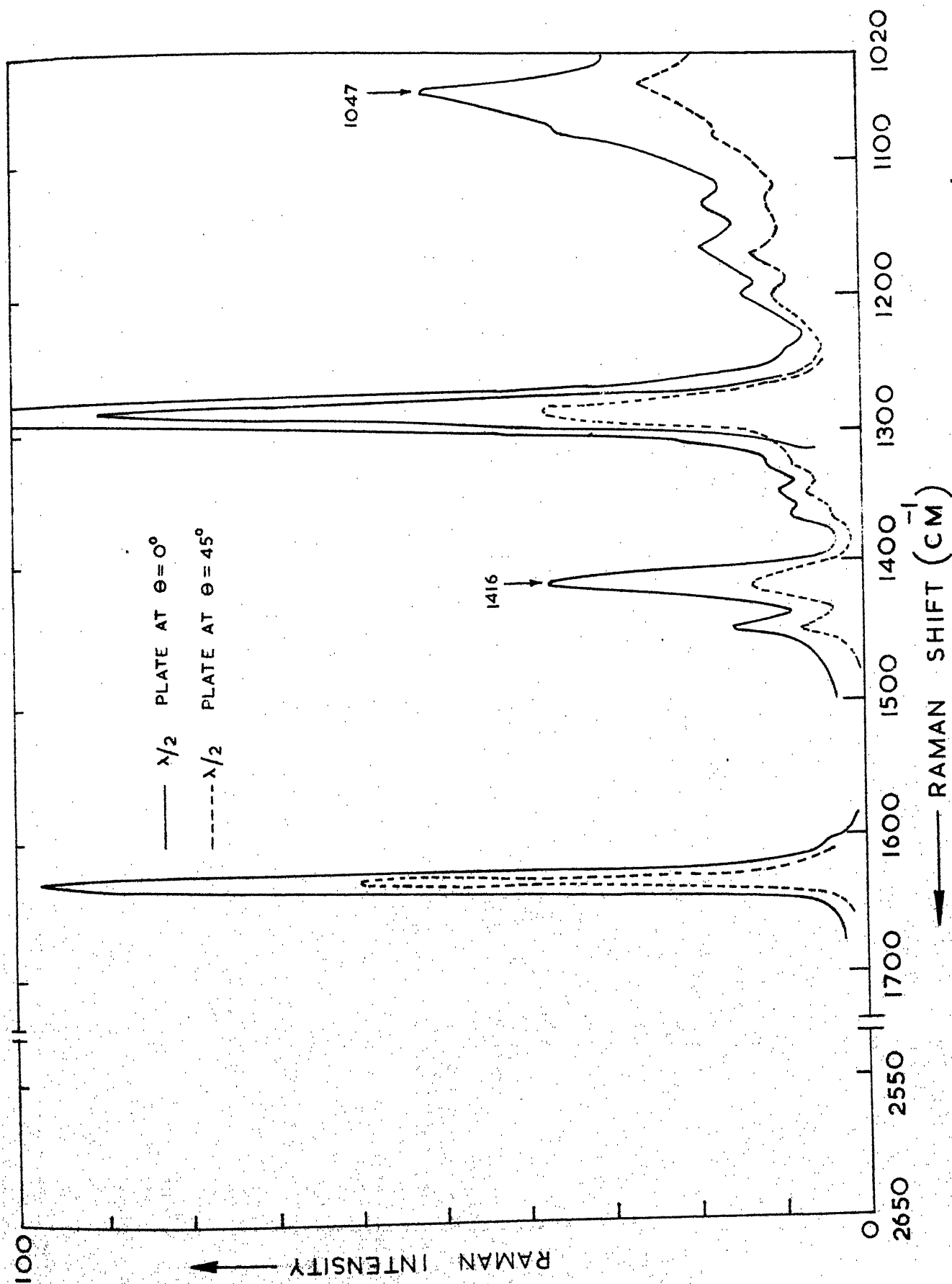


Fig. 3.5(B): The laser-Raman spectrum of liquid allyl arnine (1020-2650 cm<sup>-1</sup>).

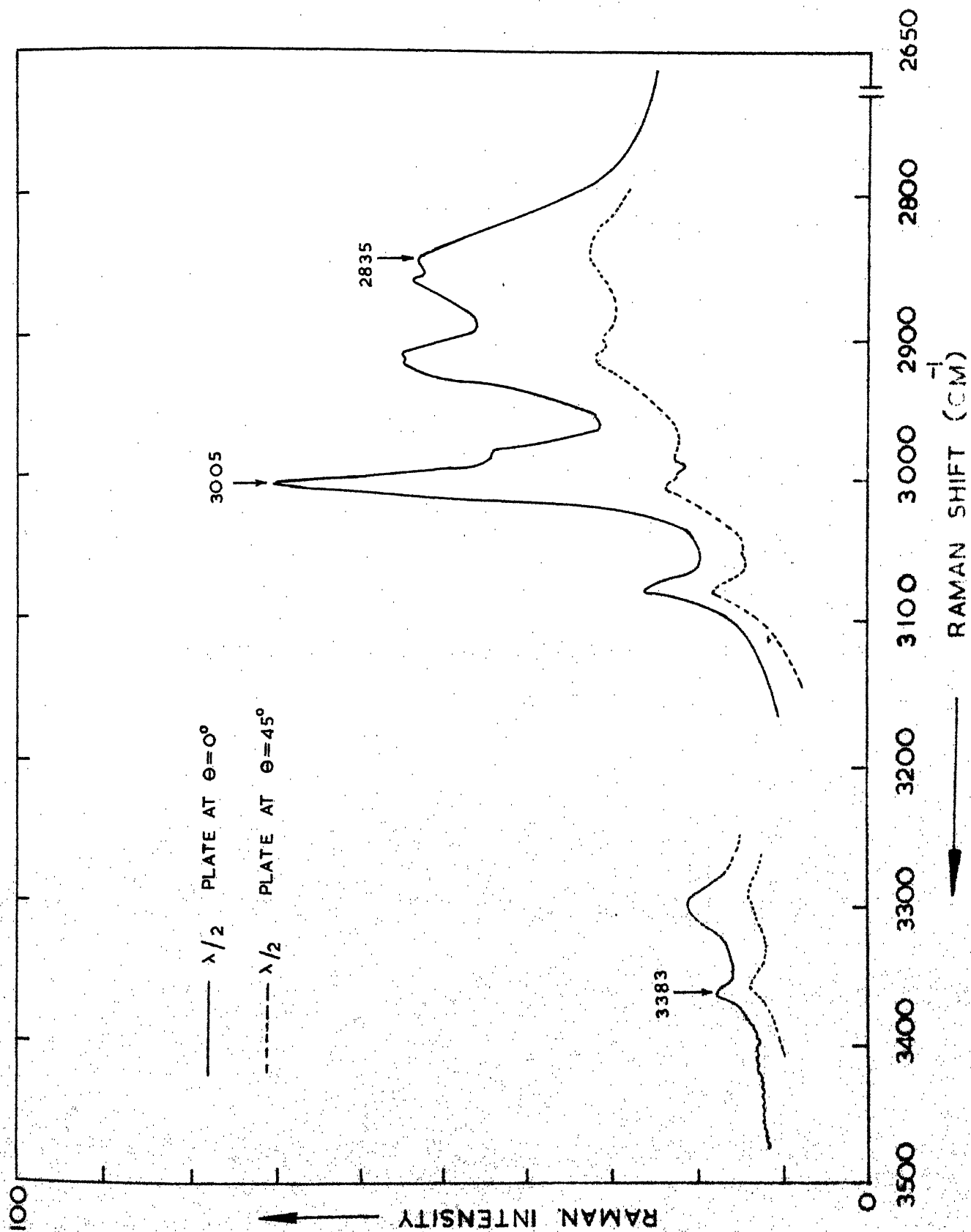


Fig. 3.5(C): The laser-Raman spectrum of liquid allyl amine (2650-3500 cm<sup>-1</sup>).

#### CHAPTER IV

#### VIBRATIONAL SPECTRA OF DIETHYL AMINE AND ROTATIONAL ISOMERISM

## ABSTRACT

The infrared spectra of diethyl amine have been investigated over the frequency range  $4000 - 250 \text{ cm}^{-1}$  in the vapour, liquid and solid phases and as solution in various solvents. The Raman spectrum of the liquid has been recorded photoelectrically and depolarization measurements have been made. The temperature dependence of some of the infrared bands indicate the presence of at least two rotational isomers ('trans-trans' and 'trans-gauche') in fluid phase, whereas in the solid phase at low temperature, the molecule assumes the 'trans-gauche' conformation having no symmetry. The vibrational assignment has been made for the observed bands, keeping in view the presence of rotational isomers.



## INTRODUCTION

Diethyl amine has been the subject of many investigations mainly concerned with the effects of hydrogen bonding in secondary amines. In contrast with many observations on the NH and CH stretching infrared bands of liquid  $(C_2H_5)_2NH$  in various solvents<sup>1-12</sup>, no detailed studies appear to have been carried out with a view to determine the relationship between the precise frequencies found and the structure of the molecule as a whole. Moreover, there does not exist a reliable interpretation of the vibrational spectra of N-H groups perturbed by hydrogen bonding.

Stewart<sup>12</sup> measured the infrared spectrum of diethyl amine in the rock salt region and suggested partial assignment for the CN stretching and CNH bending modes. Doerffel and coworkers<sup>8</sup> reported the vibrational spectrum of diethyl amine in different solvents. The Raman spectra were studied by Dadiou and Kohlrausch<sup>1</sup> and with polarisation measurements by Chaudhury<sup>2</sup>, but the reported bands are very few. There also does not seem any infrared studies made in the gaseous and solid phases for this molecule.

The skeleton of diethyl amine molecule is expected to exist in several configurations due to internal rotations about each of the two N-C bonds (Figures 4.1 and 4.2). The previous investigators have also not attempted to establish the structure of the lower energy form of the molecule.

A systematic investigation of the vibrational spectra for this molecule was planned with the aim of establishing its structure and throwing some light on the controversies regarding the bending modes

of the CNH group. An attempt has also been made to do plausible vibrational assignment for each rotational isomer.

#### EXPERIMENTAL

The compound studied was a commercial sample and was purified by vacuum distillation.

The sealed cells of CsBr of fixed thicknesses (normally 0.025 and 0.05 mm) were used for obtaining the infrared spectra for liquid and solutions in various solvents such as  $\text{CCl}_4$ ,  $\text{C}_2\text{Cl}_4$ ,  $\text{CH}_3\text{Cl}$  etc. The spectra in the vapour and solid phases were recorded in the manner described in Chapter II. The infrared spectra for the liquid, vapour and solid phases are shown in Figures 4.3, 4.4 and 4.5 respectively (given at the end of this chapter) and the observed frequencies are entered in Table 4.2.

The Raman spectrum of liquid diethyl amine at room temperature was recorded on a Coderg PH-1 Raman spectrophotometer and approximate depolarization measurements were made using the incident polarized light technique as described in Chapter II. Taking into account the different approximations for obtaining the depolarization ratios, exact theoretical ratios can not be expected. The observed Raman shifts for this molecule are entered in Table 4.2. Polarization behaviour of the lines is marked as polarized (P) or depolarized (D). In addition, a numerical value of  $\rho$  is given, whenever possible. Figure 4.6 presents the tracing of the Raman spectrum.

## DISCUSSION

The diethyl amine (DEA) molecule may be considered as a derivative of ammonia in which the two hydrogen atoms of ammonia have been replaced by the two ethyl groups. The infrared spectrum of the crystalline form of diethyl amine is found to be much simpler than that of the liquid. This is usually a clear indication of two or more isomers existing and contributing to the spectrum in the liquid phase. The possibility of rotational isomerism, giving rise to trans and gauche isomers about each of the two N-C bonds in turn, allows nine conformations for  $(C_2H_5)_2NH$  of which only six, the T T, T G, T G', G G, G G' and G' G are spectroscopically distinct. In these designations, the first letter indicates whether the  $C_4 - C_3 - N - C_2$  chain has the trans (T) or one of the two non-equivalent gauche (G and G') configurations corresponding to the rotations by + 120 or -120 degrees about the N-C bond respectively and the second letter has the same significance for the  $C_1 - C_2 - N - C_3$  chain. The numbering of the atoms is shown in Figure 4.2. The G G', G' G and G G conformations are expected to have relatively high energies because of close approach of the hydrogen atoms of the two ethyl groups and therefore are not favoured as likely low energy isomers. This evidence also finds partial support from the spectroscopic observations of diethyl ether by Snyder and Zerbi<sup>14</sup> who calculated the frequencies for the G G conformer and did not find the bands which could be attributed to this form. We may accordingly confine our attention to the remaining three isomers T T, T G and T G' only. These three conformations along with the G G and G G' are shown in Figure 4.1.

The T T conformation of DEA may have one plane of symmetry ( $C_s$  point group) which contains the N-H group and is perpendicular to the CNC plane.

The forty two normal modes of vibration should divide into symmetry species as 22  $a'$  (symmetrical with respect to the plane of symmetry) and 20  $a''$  asymmetrical modes, all vibrations being active in both the infrared and Raman spectra with the  $a'$  modes appearing as polarized and  $a''$  modes as depolarized Raman bands. The rotational constants A, B and C were calculated for all the spectroscopically distinguishable conformers of diethyl amine, assuming  $r_{C-H} = 1.09 \text{ \AA}$ ,  $r_{C-C} = 1.54 \text{ \AA}$ ,  $r_{C-N} = 1.47 \text{ \AA}$ ,  $r_{N-H} = 1.014 \text{ \AA}$  and all bond angles tetrahedral. The values of rotational constants and asymmetry parameter ( $K = \frac{2B - A - C}{A - C}$ ) are shown in Table 4.1 and indicate that the molecule is nearly a prolate symmetric top in this T T configuration. Moreover, the least moment of inertia lies along the axis at right angles to the molecular symmetry plane. Hence the  $a''$  modes may be expected to give rise to A-type band contours in the gaseous phase, while the  $a'$  modes may give rise to either pure B or C type or hybrid bands. Recently, Seth-Paul and Dijkstra<sup>15</sup> have given the modified expressions for calculating the P-R separations of band envelopes in the vapour phase for asymmetric top molecules. The calculations for the T T configuration show that the type-A ( $\dagger\dagger$ ) bands should appear with well resolved P and R branches and a weak Q-branch with P-R spacing of  $\sim 12 \text{ cm}^{-1}$ ; type-B ( $\perp$ ) bands may have a doublet Q-branch with  $\Delta \nu(\text{PR}) \sim 10 \text{ cm}^{-1}$ . The type-C bands are expected to appear with a pronounced Q-branch having weaker humps on either side corresponding to the P and R branches with  $\Delta \nu(\text{PR})$  type-C ( $\perp$ )  $\sim 17.5 \text{ cm}^{-1}$ .

The T G and T G' conformations of the molecule do not have any element of symmetry and hence belong to the trivial point group  $C_1$ . All the forty two vibrational modes should appear in both the infrared and Raman, with all the Raman bands being polarized. The values of the

asymmetry parameter  $k$  and  $\rho^* = \frac{A - C}{B}$  (given in Table 4.1) are nearly the same for both of these structures and hence the infrared band contours in the vapour phase may be expected to be of similar type for both the forms. The gaseous spectrum may be expected to exhibit three types of band contours; type-A having a medium Q-branch and P-R spacing of  $\sim 14 \text{ cm}^{-1}$ , type-B having a central minimum with a P-R separation of  $\sim 12 \text{ cm}^{-1}$  and type -C having a strong Q-branch and a P-R spacing of  $\sim 21 \text{ cm}^{-1}$ . Although the band structure is clear for some of the bands, it is not possible to distinguish the isomers on the basis of the infrared band contours, as the bands due to different isomers may lie very close to each other.

A comparative study of the infrared spectra in the vapour, liquid and solid phases of diethyl amine clearly indicates the presence of more than one rotational isomer, because several absorption bands of the liquid and vapour phases are missing in the solid phase. Some of the band pairs, which have been ascribed to different rotational isomers, lie at (289, 369), (430, 492) and (860, 890)  $\text{cm}^{-1}$  in the infrared spectrum of liquid DEA. The lower frequency components of these pairs are weak as compared to those at higher frequencies. The relative intensities of these band pairs are found to be temperature dependent. The bands corresponding to the weaker components on the low frequency side of these pairs loose in intensity relative to those on higher frequency side at elevated temperatures in the vapour phase. But at low temperature in the solid phase, only the lower frequency components persist. Moreover, the isomeric equilibrium of the various forms in solutions may be expected to vary with the polarity of the solvents. In dilute solutions with  $\text{CCl}_4$ , the intensity of the band at  $890 \text{ cm}^{-1}$  is found to increase relative to that

at  $860\text{ cm}^{-1}$  while with polar solvents ( $\text{CH}_3\text{Cl}$  and  $\text{CH}_3\text{CN}$ ), the intensities of the bands at  $430$  and  $860\text{ cm}^{-1}$  increase relative to their companion bands.

The Raman spectrum of liquid diethyl amine contains a number of depolarized lines which indicates the presence of a symmetrical isomer T T having  $C_s$  symmetry. The Raman line at  $912\text{ cm}^{-1}$  corresponding to the liquid-state ir band at  $917\text{ cm}^{-1}$  is depolarized and hence these bands are expected to arise due to an asymmetric mode in the T T form.

The infrared band of the liquid phase at  $917\text{ cm}^{-1}$  disappears and a medium strong band appears at  $958\text{ cm}^{-1}$  at low temperature whose faint indication is found in the vapour phase spectrum at  $960\text{ cm}^{-1}$ . These bands are probably associated with  $\text{CH}_3$  rocking modes. It is difficult to interpret this line in the solid phase at  $958\text{ cm}^{-1}$  as a shift of the originally found line at  $917\text{ cm}^{-1}$  in the liquid phase, because this would mean a shift of about  $40\text{ cm}^{-1}$  on change of phase from liquid to solid which is usually not observed in the spectra of organic molecules unless the group is directly involved in molecular association. On the basis of these observations, it may be inferred that the predominant form in the liquid and vapour states of diethyl amine has the T T configuration while in the solid phase, either one or both of the two asymmetrical T G or T G' forms (preferably the T G) may persist. The relative stability of these two (T G and T G') conformations is not known a priori and the present data are not sufficient to allow the selection between them. The T G form may be expected to get stabilized in the solid phase due to pronounced hydrogen bonding effects, as this T G form could be favourable for intermolecular association as compared to the T G' form. It is also not clear from the present data whether there are only two or more than two forms existing and contributing to the infrared spectra

in the vapour, liquid and solutions. However, the observed bands could be satisfactorily interpreted by assuming the presence of only two (T T and T G) forms in fluid phase.

At the outset, we have assumed in this work that the diethyl amine molecules exist only in the T T and T G conformations. The fundamental vibrations of diethyl amine are numbered (see Table 4.3) in order of their appearance in the T T isomeric form. The bands in both the infrared and Raman spectra that could be assigned to the more stable (T G) or less stable (T T) isomers or to both, are given in Table 4.2.

Many investigators<sup>3,6,9,11,13</sup> have explored the possibility of molecular association through weak hydrogen bond formation in diethyl amine. Feeney and Sutcliffe<sup>16</sup> report the nuclear magnetic resonance study of DEA and supports the occurrence of hydrogen bonding equilibrium in this molecule. The vibrational bands associated with the CNH group are expected to get affected by molecular association in various phases. In the present investigation, the changes in the intensities and positions of the bands associated with these modes are also given in Table 4.2.

#### ASSIGNMENT

##### N-H stretching frequency region (3200 - 3500 cm<sup>-1</sup>)

Extensive work has been done on the N-H stretching modes and its over-tones in order to observe the effects of anharmonicities (mechanical and electrical) on hydrogen bonding in secondary amines. The hydrogen bonding results in a shift of NH stretching bands towards lower frequencies in almost all the cases. Investigations by different workers<sup>3,6,9,11,12</sup> lead to the conclusion that diethyl amine in liquid form contains a variety of multimers. This conclusion is also supported by the measurement of

chemical shift by the NMR studies of Feeney and Sutcliffe<sup>16</sup> in different aliphatic amines including diethyl amine. The absorption due to free NH stretching vibration (monomer) is expected in very dilute solutions or in vapour phase spectrum. In liquid phase, the NH vibration band appears to be doubled. In vapour phase, this region shows three bands at 3205, 3345 and 3405  $\text{cm}^{-1}$ . It was found necessary to keep the vapour pressure very high in the gas cell in order to observe these weak bands and there was a possibility of some vapour being contaminated on the windows and thus giving the spectrum of liquid phase (multimer) along with the spectra of the vapour in this region. The lower frequency band (3205  $\text{cm}^{-1}$ ) probably arises due to the same reasons and may result due to the formation of a layer of polymers on the windows. This band shows a sharp fall in intensity at lower pressures. In crystalline state at  $\sim 77^\circ \text{K}$ , a broad band is observed with its centre at 3198  $\text{cm}^{-1}$ . On the basis of these observations, the lower frequency band at 3282  $\text{cm}^{-1}$  in the liquid phase is assigned to the N-H stretching vibration  $\nu_1$  of the TG conformer and the broad shoulder which corresponds to the 3405  $\text{cm}^{-1}$  line in the vapour phase probably arises due to the presence of the T T form. This doubling of the NH stretching vibration in liquid diethyl amine is primarily attributed to the results of rotational isomerism.

#### The C-H stretching vibrations (3000 - 2700 $\text{cm}^{-1}$ )

There are ten carbon-hydrogen stretching vibrations for diethyl amine. Since the two  $\text{CH}_3$  groups are separated by  $\text{CH}_2 - \text{N} - \text{CH}_2$ , it is expected that they may not couple with each other strongly. Therefore the six corresponding normal modes for both the  $\text{CH}_3$  groups would occur over a narrow frequency range. Wieser and coworkers<sup>17</sup> have calculated the normal vibrations of diethyl ether and shown that the methyl groups



of the T T and T G conformers absorb at nearly the same frequencies. We can expect the similar situation in the case of diethyl amine also. In the case of T T conformer, the four out-of-plane C-H bonds and the remaining two C-H bonds in the skeletal plane make the CH<sub>3</sub> groups unsymmetrical and thus remove the degeneracy of the asymmetric CH<sub>3</sub> stretching and CH<sub>3</sub> bending vibrations. The two absorptions at 2945 and 2964 cm<sup>-1</sup> in the vapour phase infrared spectrum are assigned to the asymmetric C-H stretching vibrations of CH<sub>3</sub> groups split by the anisotropic environment of the C-H bonds. Similar splittings of the asymmetric C-H stretching vibrations of CH<sub>3</sub> groups have been observed for diethyl ether<sup>17</sup> and many other molecules. The corresponding strong and depolarized Raman band lies at 2968 cm<sup>-1</sup>. For the TG conformer in the solid phase, these C-H asymmetric stretching modes lie at 2928 and 2963 cm<sup>-1</sup> respectively. The medium strong and polarized Raman band at 2815 cm<sup>-1</sup> corresponding to the resolved band at 2818 cm<sup>-1</sup> and the liquid phase ir band at 2810 cm<sup>-1</sup> may be assigned as the C-H stretching modes  $\nu_6$  and  $\nu_{27}$  of the methylene groups. In solid phase, these modes get split into a very close doublet, probably due to crystal field effects.

The remaining a' modes  $\nu_4$  and  $\nu_5$  and the two a'' stretchings  $\nu_{25}$  and  $\nu_{26}$ , all overlap in the 2850 - 2950 cm<sup>-1</sup> region. This region will also contain overtones and combination bands of the deformation modes of the CH<sub>3</sub> and CH<sub>2</sub> groups. The infrared spectra of tripropargyl amine (which contains only methylene groups and will be discussed in Chapter V) shows medium strong absorption at 2925 cm<sup>-1</sup> and is associated with the asymmetric C-H stretching of methylene groups. The strong and polarized Raman line at 2925 cm<sup>-1</sup> and the corresponding ir band at 2928 cm<sup>-1</sup> in the liquid phase may then be associated with the  $\nu_4$  and  $\nu_{25}$  modes. It has been shown

in structurally similar molecules<sup>14,17,18</sup> that the symmetric C-H stretching modes of the methyl groups give rise to only one absorption at near about  $2880\text{ cm}^{-1}$ . Thus the two bands of nearly equal intensity centred at  $2890$  and  $2870\text{ cm}^{-1}$  in the liquid phase infrared spectrum must be related in some way to the symmetric stretching vibrations of the methyl groups. Because the bands are of nearly equal intensity, it is likely that the doublet arises due to Fermi resonance interaction between the symmetric C-H stretching modes of  $\text{CH}_3$  groups and overtones of the methyl deformation modes. Since the combinations or overtones generally appear as weak bands in Raman effect, the weak and diffused shoulder in Raman spectrum at  $2893\text{ cm}^{-1}$  corresponding to the infrared band at  $2890\text{ cm}^{-1}$  may arise due to the overtones of the deformation modes of  $\text{CH}_3$  and  $\text{CH}_2$  groups. The remaining strong and polarized Raman line at  $2868\text{ cm}^{-1}$  and the related infrared band at  $2870\text{ cm}^{-1}$  may then be assigned to the symmetric C-H stretching vibrations of the methyl groups  $\nu_5$  and  $\nu_{26}$ . This discussion accounts for the C-H stretching region in a qualitative way. In most of the cases, the in-plane and out-of-plane vibrations occur in closely lying pairs, the band contours get overlapped and it becomes difficult to draw any definite conclusion about the type of the band from its contour features in the vapour phase infrared spectrum.

#### The C-H deformation vibrations ( $1500 - 1200\text{ cm}^{-1}$ )

The liquid phase infrared spectrum of diethyl amine exhibits four lines at  $1438$ ,  $1456$ ,  $1465$  and  $1481\text{ cm}^{-1}$ . The absorptions at  $1465$  and  $1481\text{ cm}^{-1}$  in the liquid phase for the T T conformer and at  $1460$  and  $1479\text{ cm}^{-1}$  for the T G conformer in solid phase may be assigned to the symmetric deformation modes of methyl groups which might have split by the anisotropic environment of the hydrogen atoms of methyl groups.

The 1438 and 1456  $\text{cm}^{-1}$  ir bands may then be correlated with the  $\text{CH}_2$  deformation modes  $\nu_9$  and  $\nu_{31}$  respectively. One of the basic difficulties in identifying these bands separately as belonging to either  $\text{CH}_3$  or  $\text{CH}_2$  groups is that many absorption bands of the methyl and methylene groups overlap severely and an infrared and Raman study of deuterated species is clearly needed in order to characterise them uniquely.

The A-type band at 1380  $\text{cm}^{-1}$  in the gas phase spectrum of diethyl amine is assigned to the symmetric methyl deformation modes  $\nu_{10}$  and  $\nu_{32}$ . At lower temperatures in solid phase, this band splits into a close doublet at 1372 and 1378  $\text{cm}^{-1}$ , probably due to crystal field effects.

The wagging,  $\nu_{11}$  and  $\nu_{33}$ , and twisting  $\nu_{12}$  and  $\nu_{34}$  modes of the methylene groups are expected to occur near 1300  $\text{cm}^{-1}$ . The infrared bands at 1286 and 1328  $\text{cm}^{-1}$  have been assigned to the methylene wagging modes  $\nu_{11}$  and  $\nu_{33}$  respectively. The lower frequency band is a type-B band and the higher frequency line shows a structure expected for the A-type band in the vapour phase. The corresponding Raman lines are very weak. The  $\text{CH}_2$  twisting modes  $\nu_{12}$  and  $\nu_{34}$  have been associated with the infrared band at 1263  $\text{cm}^{-1}$ , which lacks distinct contour features.

#### The skeletal vibrations (below 1250 $\text{cm}^{-1}$ )

The vibrational modes which are expected to occur in this region of the spectrum, are those associated with the skeletal vibrations, the methyl and methylene rocking modes and the N-H deformation modes. As regards the rocking vibrations, these may be expected to appear in the vibrational spectrum mixed with other vibrations of approximately the same magnitude and of similar species, specially with the skeletal and N-H bending modes. The in-phase and out-of-phase combinations of the in-plane methyl rocking modes for each ethyl group in DEA, coupled with some other modes, may

interact with one another leading to two separate bands. By analogy with n-pentane<sup>18</sup> and diethyl ether<sup>17</sup>, the 820 and 917  $\text{cm}^{-1}$  bands of  $(\text{C}_2\text{H}_5)_2\text{NH}$  for the T T conformer may be associated with the similar vibrational modes  $\nu_{16}$  and  $\nu_{38}$  respectively. The other two out-of-plane  $\text{CH}_3$  rocking modes (in-phase and out-of-phase combinations) have been placed at 1187 and 1068  $\text{cm}^{-1}$  for the T T isomer. The assignment for the other T G isomeric form in the solid phase is given in Table 4.2.

The band at 1146  $\text{cm}^{-1}$  in the ir spectrum of liquid diethyl amine was assigned to an asymmetric C-N stretching mode by Stewart<sup>12</sup>. In the liquid and solid phases, this line appears as a doublet in our study. The relative intensities of the component lines of this pair undergo insignificant change with variation of temperature and hence they can not be simply associated with the different isomeric forms. One component of this pair may arise due either to a suitable combination mode in Fermi resonance with the main C-N stretching mode or some fundamental vibration. The probable vibrational mode which may arise in this region is a  $\text{CH}_3$  rocking vibration. In the Raman spectrum, a single medium strong and depolarized band at 1145  $\text{cm}^{-1}$  is observed without any indication of another line or shoulder around this band which may be correlated with methyl rocking mode. And since combination bands are not so frequently observed in Raman spectrum, one of these components is assigned as a combination mode  $717 + 426 = 1143 \text{ cm}^{-1}$  in Fermi resonance with the C-N stretching mode and the other component in solid phase may be the asymmetric C-N stretching mode  $\nu_{26}$ .

The infrared and Raman spectra show a complex band system in the region where C-C stretching modes are expected. The medium intense infrared band at 1048  $\text{cm}^{-1}$  in liquid showing the A-type structure in vapour phase with its pronounced Q-branch at 1050  $\text{cm}^{-1}$  is assigned to

the asymmetric C-C stretching mode  $\nu_{37}$  for the T T conformer. For the T G form in solid phase, this band appears at  $1043\text{ cm}^{-1}$ . The two shoulders located at  $1020$  and  $1032\text{ cm}^{-1}$  on the lower frequency side of the strong band at  $1048\text{ cm}^{-1}$  in the liquid phase may be assigned to the symmetric C-C stretching mode  $\nu_{14}$ . The higher frequency component of this doublet disappears at low temperature and is accordingly associated with the T T conformer. The corresponding Raman lines at  $1015$  and  $1025\text{ cm}^{-1}$  are polarized.

The two medium strong and polarized Raman lines at  $862$  and  $890\text{ cm}^{-1}$  are to be associated with the symmetric C-N stretching modes on the basis of their Raman intensity. The corresponding infrared bands at  $860$  and  $890\text{ cm}^{-1}$  show variation in their relative intensities with temperature. In vapour phase, the higher frequency band appears as a B-type band with its centre at  $895\text{ cm}^{-1}$ . In solid phase, the higher frequency band disappears completely and the lower frequency band shifts to  $845\text{ cm}^{-1}$ . On the basis of these temperature effects, the  $845\text{ cm}^{-1}$  line may be assigned to the T G conformer and the other line should belong to the T T form. The vapour phase absorption in this region is very weak. The pair of bands at  $820$  and  $802\text{ cm}^{-1}$  in the liquid phase, however, appears to arise from mixed methyl and methylene rocking vibrations. In the solid phase at low temperature, three medium strong bands appear at  $799$ ,  $812$  and  $834\text{ cm}^{-1}$ . These bands might have got separated in the solid phase due to the sharpening of the bands at low temperature. The two lower frequency bands have been assigned as the methylene rocking modes  $\nu_{17}$  and  $\nu_{39}$  respectively and the higher frequency band at  $834\text{ cm}^{-1}$  has been taken as the methyl rocking mode  $\nu_{16}$  for the T G isomer.

Regarding the assignment of the CNH bending modes in aliphatic secondary amines, different divergent views have been put forward by various workers. In the recent study of  $(\text{CH}_3)_2\text{NH}$  and  $(\text{CH}_3)_2\text{ND}$  by

Buttler and McKean<sup>19</sup> in the gaseous and solid phases, the  $a'$  type CNH bending mode is placed at  $735\text{ cm}^{-1}$  in the vapour phase spectrum which splits into a wider doublet at  $893$  and  $868\text{ cm}^{-1}$  in the crystalline state. The other  $a''$  CNH deformation mode is located at  $1525\text{ cm}^{-1}$  in solid phase. More recently, Dellepiane and Zerbi<sup>20</sup> calculated fundamental frequencies of methyl amines and their deuterated derivatives. These calculations also support the assignment proposed by Buttler and McKean<sup>19</sup>. Perchard and coworkers<sup>21</sup> proposed an alternative assignment for dimethyl amine in disagreement with these results.

Barr and Haszeldine<sup>13</sup> investigated the infrared spectra of diethyl amine and its trifluoro derivative. They observed that the  $\text{CH}_2$  deformation band reveals a side peak at  $6.80\text{ }\mu$  for diethyl amine in liquid phase which was tentatively assigned to the NH deformation mode. Stewart<sup>12</sup> had placed one of these CNH bending modes for diethyl amine at  $735\text{ cm}^{-1}$ , while Owens and Barker<sup>22</sup> had proposed the possibility of finding both the symmetric and asymmetric CNH bending modes under the broad  $780\text{ cm}^{-1}$  band in methyl amine. In the present investigations of diethyl amine, very broad band is observed in the liquid phase at  $740\text{ cm}^{-1}$  revealing a broad shoulder at  $775\text{ cm}^{-1}$ . The Raman spectrum shows two very broad and weak bands at  $725$  and  $770\text{ cm}^{-1}$ . The higher frequency band is definitely polarized, while the polarization of the lower frequency band is not certain due to the broadness of the band. The infrared spectrum of crystalline form shows two bands at  $717$  and  $773\text{ cm}^{-1}$ , the former being sharp and strong while the higher frequency band is broad and weak showing multiplet splitting. These bands are assigned to the  $a'$  CNH bending mode of diethyl amine. The multiplet splitting of the higher frequency band at  $773\text{ cm}^{-1}$  in the solid phase may result due to the presence of several unequal types of bond formation and is believed to arise due to the presence of associated molecules in the condensed phase at low temperature.

The medium strong doublet 1500, 1508  $\text{cm}^{-1}$ , observed in the solid phase, may be assigned to the other asymmetric CNH bending mode  $\nu_{28}$ . A weak shoulder is observed in vapour phase at 1495  $\text{cm}^{-1}$ . The assignment of these two NH bending modes at frequencies near 1500 and 715  $\text{cm}^{-1}$  is supported by the similar assignments in dimethyl amine by Buttler and McKean<sup>19</sup> and by Barr and Haszeldine<sup>13</sup> in  $(\text{CF}_3)_2\text{NH}$ . The investigation of aromatic secondary amines with their deuterated derivatives has shown the presence of a weak band in the 1510  $\text{cm}^{-1}$  region, characteristic of this mode<sup>23</sup>.

The other alternate assignment may be to correlate the  $a''$  CNH bending mode with the Raman band at 725  $\text{cm}^{-1}$  (not clearly polarized) and the solid phase infrared band at 715  $\text{cm}^{-1}$ . The band at 1505  $\text{cm}^{-1}$  in the solid phase may then be interpreted as a combination or overtone of these CNH bending modes ( $\nu_{18} = 770 \text{ cm}^{-1}$  and  $\nu_{28} = 715 \text{ cm}^{-1}$  in the solid phase). The points against this assignment are that: (1) It seems unlikely for both the symmetric and antisymmetric modes to lie within such a narrow range due to high coupling among themselves and other skeletal modes, (2) this assignment conflicts with the assignments given in the literature for the similar modes<sup>13,19,20,23</sup>. Hence the former assignments are preferred for these modes.

The remaining bending modes of the skeleton of diethyl amine are expected to occur below 600  $\text{cm}^{-1}$ . In diethyl ether<sup>17</sup>, the  $\angle \text{CCO}$  bending modes are placed at 451  $\text{cm}^{-1}$  ( $B_1$ ) and 245  $\text{cm}^{-1}$  ( $A_1$ ) for the T T conformer and at 387 and 349  $\text{cm}^{-1}$  for the T G conformer. The COC bending mode for the T G conformer is located at 503  $\text{cm}^{-1}$  with nearly equal contribution from the CCO bending mode. The infrared spectrum of liquid diethyl amine shows two temperature dependent bands at 490 and 430  $\text{cm}^{-1}$ .

Only the lower frequency component of this pair persists at lower temperature and is accordingly assigned to the T G conformer. The corresponding Raman band at  $426\text{ cm}^{-1}$  is very intense and polarized and is associated with the CCN bending mode  $\nu_{40}$  for the T G form together with appreciable contribution from the CNC bending mode. The other CCN bending mode  $\nu_{19}$  for the T G configuration is placed at  $256\text{ cm}^{-1}$  in the solid phase. In the vapour phase a shoulder appears at  $421\text{ cm}^{-1}$  on the lower frequency side of the main band at  $435\text{ cm}^{-1}$ . This shoulder may be associated mainly with the CCN bending mode  $\nu_{19}$  for the T T isomer and the other  $a''$  mode  $\nu_{40}$  to the band at  $485\text{ cm}^{-1}$  in the vapour phase. The description given above is only qualitative as to their approximate nature because of the heavy mixing among these modes.

As the torsional modes show extremely weak absorptions in the infrared and Raman spectra, their location is somewhat uncertain. A very weak and diffused band at  $246\text{ cm}^{-1}$  in the Raman spectrum of diethyl amine may be correlated with the methyl torsional modes mixed with CCN bending modes in analogy with diethyl ether<sup>17</sup>. The other torsional modes about C-N bonds are expected to occur well below  $200\text{ cm}^{-1}$ . There is an indication of a very weak hump at  $\sim 130\text{ cm}^{-1}$  obscured in the wing of the exciting Raman laser line. This may be tentatively associated with the torsional modes  $\nu_{22}$  and  $\nu_{42}$ .

The other weak bands observed in the infrared and Raman spectra of diethyl amine could be satisfactorily assigned as either overtones and/or combination tones of the fundamental vibrations and are given in Table 4.2.



## REFERENCES

1. A. Dadieu and K.W.F. Kohlrausch, *Monatsh.* 57, 225 (1931)
2. B.K. Chaudhury, *Indian J. Phys.* 11, 203 (1937)
3. *The Infrared Spectra of Complex Molecules* by L.J. Bellamy (2nd Ed.), Methuen (1958)
4. C. Corin, *Bull. Soc. Roy. Sci. Liege* 10, 99 (1941)
5. V.M. Chulanovskii, *Izvest. Akad. Nauk. S.S.S.R. Ser. Fiz.* 17, 624 (1953)
6. R.A. Russell and H.W. Thompson, *J. Chem. Soc.* 483 (1955)
7. Z.M. Muldakhmetov and M.M. Sushchinskii, *Optika i Spektroskopiya* 819 (1963)
8. K. Doerffel, R. Geyer and W. Hoebold, *Wiss. Z. Tech. Hochschule Chem. Leuna Merseburg* 6, 92 (1964)
9. C. Berthomieu and C. Sandorfy, *J. Mol. Spectry* 15, 15 (1965)
10. S. Ya. Khaikin and V.M. Chulanovskii, *Opt. Spectry* 20, 126 (1966)
11. R.A. Russell and H.W. Thompson, *Proc. Roy. Soc. (London) Ser A* 234, 318 (1956)
12. J.E. Stewart, *J. Chem. Phys.* 30, 1259 (1959)
13. D.A. Barr and R.N. Haszeldine, *J. Chem. Soc.* 72, 4169 (1955)
14. R.G. Snyder and G. Zerbi, *Spectrochim. Acta* 23A, 391 (1967)
15. W.A. Seth-Paul and G. Dijkstra, *Spectrochim. Acta* 23A, 2861 (1967)
16. J. Feeney and L.H. Sutcliffe, *Proc. Chem. Soc.* 118 (1961)
17. H. Wieser, W.G. Laidlaw, P.J. Krueger and H. Fuhrer, *Spectrochim. Acta* 24 A, 1055 (1968)
18. R.G. Snyder and J.H. Schachtschneider, *Spectrochim. Acta* 19, 85 (1963)
19. M.J. Buttler and D.C. McKean, *Spectrochim. Acta* 21, 465 (1965)
20. G. Dellepiane and G. Zerbi, *J. Chem. Phys.* 48, 3372 (1968)
21. J.P. Perchard, M.T. Forel and M.L. Jasien, *J. Chim. Phys.* 62, 652 (1964)
22. R.G. Owens and E.F. Barker, *J. Chem. Phys.* 8, 229 (1940)
23. D. Hadzi and M. Skrbliak, *J. Chem. Soc.* 843 (1957)

TABLE 4.2

## VIBRATIONAL SPECTRA OF DIETHYL AMINE

Observed frequencies

T T and T G forms							T G form		Assignment for both the T T and T G forms	
Liquid (ir)		Vapour (ir)		Raman (liquid)			Solid (ir)			
(cm <sup>-1</sup> )	Int.	(cm <sup>-1</sup> )	Band Type	Int.	(cm <sup>-1</sup> )	Int.	Dep. Ratio	(cm <sup>-1</sup> )		Int.
3335	br,sh	3405		vvw						$\nu_1$ (TT), N-H str.
3282	w	3345		vvw	3315 <sup>a</sup>	w	0.25	3198	s,br	$\nu_1$ (TG), N-H str.
		3205		vw						Polymer, N-H str.
								2989	sh	2X $\nu_{28}$ (F.R.)
2965	s	2974 } 2964 } 2955 }		s	2968	m	0.81	2968 } 2959 }	vs	$\nu_2, \nu_{23}$
2952	s	2945		sh				2928	sh	$\nu_3, \nu_{24}$
2928	ms	2922 } 2911 }	B	s	2925	s	0.5	2919	sh	$\nu_4, \nu_{25}$
2890	ms	2894		m	2893	mw	P	2887 } 2881 }	s	$\nu_8 + \nu_9$ (F.R.)
2870	ms	2885	C	m	2868	s	0.18	2864	sh	$\nu_5, \nu_{26}$
2810	s	2824 } 2818 } 2809 }	C	s	2815	ms	P	2812 } 2802 }	vs	$\nu_6, \nu_{27}$
					2780	w	P			$\nu_{31} + \nu_{33}$
2770	vw	2765		vw	2765	w	P	2765	m	2X $\nu_{10}$
2732	vw	2740		vw	2730	w	P	2737 } 2731 }	m	$\nu_{11} + \nu_{31}$
2695	vw				2685	vw	P	2699	vvw	$\nu_{32} + \nu_{33}$
2672	vw	2680		vw	2666	vw	P	2670	vw	2X $\nu_{33}$
2632	vw							2640	mw	$\nu_{10} + \nu_{12}$

Contd....

Table 4.2 Contd...

		1495	sh				1508 } m v <sub>28</sub> 1500 }
1481	sh	1483	sh	(1460)			1479 s v <sub>7</sub> , v <sub>29</sub>
1465	s	1475 } 1465 }	s	1460	1.5	0.89	1460 w v <sub>8</sub> , v <sub>30</sub>
1456	s	1462 } 1455 }	C s				1445 m v <sub>31</sub>
1438	sh	1440	sh	1432	10.0	0.85	1435 } m v <sub>9</sub> 1430 }
							1386 w v <sub>38</sub> (TG)+v <sub>40</sub> (TG)
1379	ms	1386 } 1380 } 1375 }	A m	1375	vw		1378 } s v <sub>10</sub> , v <sub>32</sub> 1372 }
1360	vw	1368	vw	1355	vw		1358 mw v <sub>17</sub> (TG)+v <sub>36</sub> (TG)
1345	vw						v <sub>15</sub> (TG)+v <sub>40</sub> (TT)
1328	m	1342 } 1335 } 1326 }	A m	1325	vw		1328 s v <sub>33</sub>
1286	mw	1298 } 1289 }	B w	1283	0.5	0.64	1292 mw v <sub>11</sub>
1263	w	1265	w	1255	1.0	0.79	1255 w v <sub>12</sub> , v <sub>34</sub>
1187	mw	1200 } 1189 }	B sh	1182	1.0	0.2	1209 w v <sub>13</sub>
1148	s	1145	s	1145	3.0	0.83	1145 s v <sub>35</sub>
1141	s	1135	sh				1127 } s v <sub>18</sub> (TG)+v <sub>40</sub> (TG)(F.R.) 1121 }
1095	sh	1110 } 1100 }	w	1092	vw	D	1098 ms v <sub>36</sub> (TG), CH <sub>3</sub> rock
1068	w						v <sub>36</sub> (TT), CH <sub>3</sub> rock
1048	m	1058 } 1050 } 1041 }	A m	1045	w	D	1043 s v <sub>37</sub>
1032	sh	1028	sh	1025	m	P	v <sub>14</sub> (TT), C-C str.
1020	vw			1015	w	P	1012 vw v <sub>14</sub> (TG), C-C str.

Contd...

Table 4.2 Contd...

				1002	sh		$\nu_{15}^{(TT)} + \nu_{22}$
		960	vw			958 vs	$\nu_{38}^{(TG)}$ , CH <sub>3</sub> rock
917 mw		920	vw	912	2.0 0.86		$\nu_{38}^{(TT)}$ , CH <sub>3</sub> rock
890 m	902 } B	888	vw	890	1.5 0.48		$\nu_{15}^{(TT)}$ , C-N str.
860 sh		860	sh	862	3.5 0.1	845 m	$\nu_{15}^{(TG)}$ , C-N str.
						834 s	$\nu_{16}^{(TG)}$ , CH <sub>3</sub> rock
820 vw		818	vw	815	vw ?	812 s	$\nu_{39}$
802 vw		800	vw			799 m	$\nu_{17}$
775 sh				770	w P	773 } w	Polymer
						760 }	
						753 }	
740 vs,br		721	vs,br	725	vw D?		$\nu_{18}^{(TT)}$ , in-plane CNH def.
				712	vw	715 m	$\nu_{18}^{(TG)}$ , in-plane CNH def.
492 m	489 } B	480	m	490	1.0 0.31		$\nu_{40}^{(TT)}$ , CCN def.
430 w		435	w	426	8.0 0.23	426 w	$\nu_{40}^{(TG)}$ , CCN def.
		421	sh				$\nu_{19}^{(TT)}$ , CCN def.
369 w	361 } C	354	w	365	2.5 0.21		$\nu_{20}^{(TT)}$ , CNC def.
	345						
289 w	295 }	285	vw	292	vw P	285 vw	$\nu_{20}^{(TG)}$ , CNC def.
252 vvw		255	vvw	246	vw	256 w	$\nu_{19}^{(TG)}$ , CCN def.
				~ 130	sh		$\nu_{22}$ , $\nu_{42}$ : C-CH <sub>3</sub> torsion

a

Raman data taken from reference (2)

**Abbreviations:** w = weak, m = medium, s = strong, vw = very weak  
 vvw = very very weak, vs = very strong, mw = medium weak,  
 ms = medium strong, br = broad, sh = shoulder, p = polarized,  
 D = depolarized, (F.R.) = Fermi Resonance, ( ) means used twice.

TABLE 4.3

APPROXIMATE DESCRIPTION AND FREQUENCIES (in  $\text{cm}^{-1}$ ) OF THE  
FUNDAMENTAL VIBRATIONS OF THE T-T CONFORMER OF DIETHYL AMINE

species ( $C_s$ ) ( $C_{2v}$ ) *	Number	Approx. description of vibrations	Observed fundamental frequencies		
			Liquid (ir)	Vapour (ir)	Raman liquid
a'	$\nu_1$	N-H str. (sym.)	3335	3372	
	a <sub>1</sub> $\nu_2$	CH <sub>3</sub> str. (asym.)	2965	2964	2968
	b <sub>2</sub> $\nu_3$	CH <sub>3</sub> str. (asym.)	2952	2945	
	b <sub>2</sub> $\nu_4$	CH <sub>2</sub> str. (asym.)	2928	2917	2925
	a <sub>1</sub> $\nu_5$	CH <sub>3</sub> str. (sym.)	2870	2885	2868
	a <sub>1</sub> $\nu_6$	CH <sub>2</sub> str. (sym.)	2810	2818	2815
	a <sub>1</sub> $\nu_7$	CH <sub>3</sub> def. (asym.)	1481	1483	(1460)
	b <sub>2</sub> $\nu_8$	CH <sub>3</sub> def. (asym.)	1465	1470	1460
	a <sub>1</sub> $\nu_9$	CH <sub>2</sub> def.	1438	1440	1432
	a <sub>1</sub> $\nu_{10}$	CH <sub>3</sub> def. (sym.)	1379	1380	1375
	a <sub>1</sub> $\nu_{11}$	CH <sub>2</sub> wag.	1286	1294	1283
	b <sub>2</sub> $\nu_{12}$	CH <sub>2</sub> twist.	1263	1265	1255
	a <sub>1</sub> $\nu_{13}$	CH <sub>3</sub> rock.	1187	1195	1182
	a <sub>1</sub> $\nu_{14}$	C-C str.	1032	1028	1025
	a <sub>1</sub> $\nu_{15}$	C-N str.	890	895	890
	b <sub>2</sub> $\nu_{16}$	CH <sub>3</sub> rock.	(820)	(818)	(815)
	b <sub>2</sub> $\nu_{17}$	CH <sub>2</sub> rock.	802	800	
	$\nu_{18}$	CNH def.	740	721	725
	a <sub>1</sub> $\nu_{19}$	CCN bend.		421	
	a <sub>1</sub> $\nu_{20}$	CNC bend.	369	354	365
	b <sub>2</sub> $\nu_{21}$	CH <sub>3</sub> torsion			~130
	b <sub>2</sub> $\nu_{22}$	C-CH <sub>3</sub> torsion			

Contd....

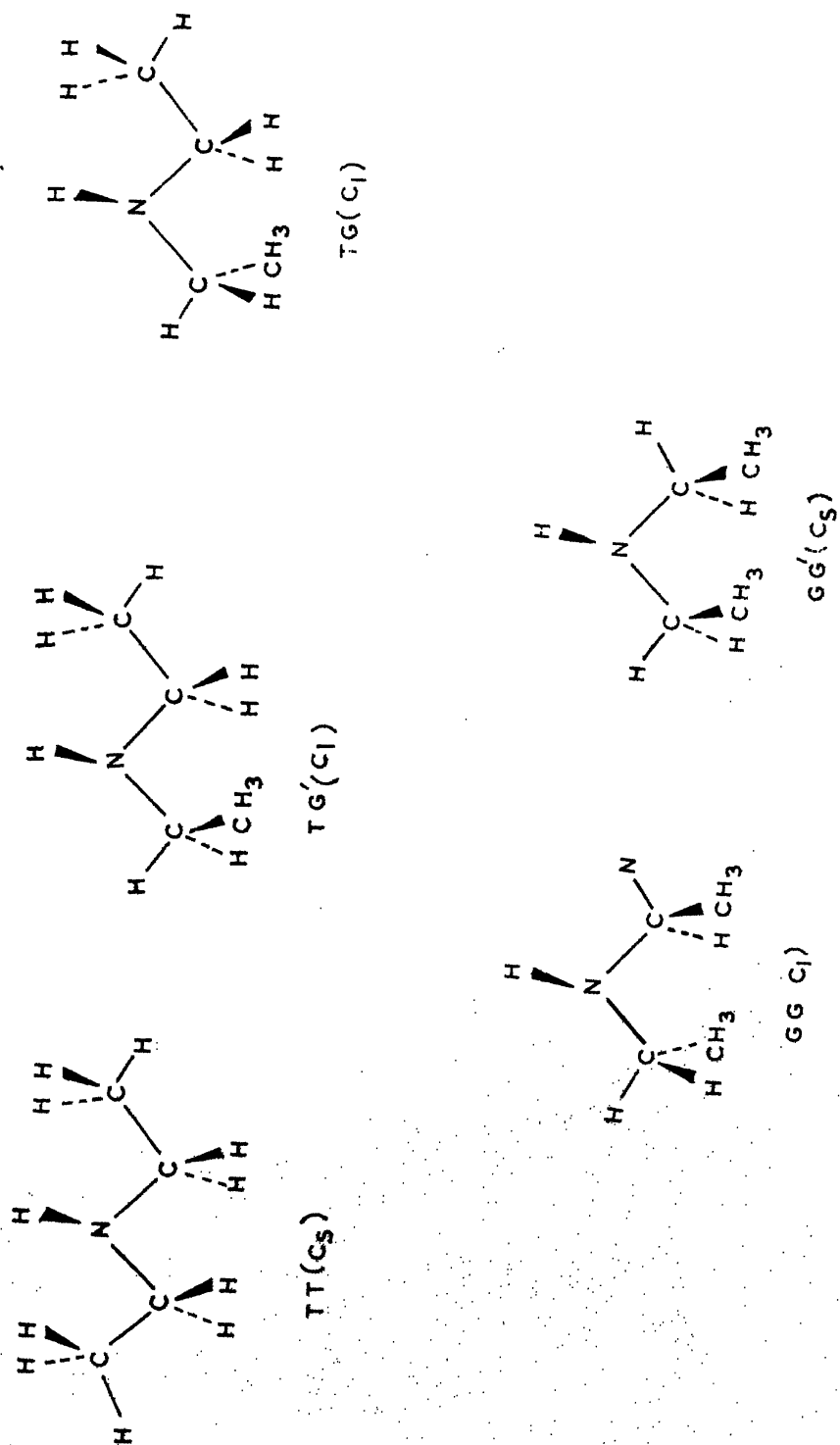


Fig. 4.1: Possible spectroscopically distinguishable conformations of 2,3-dimethylbutanamine.

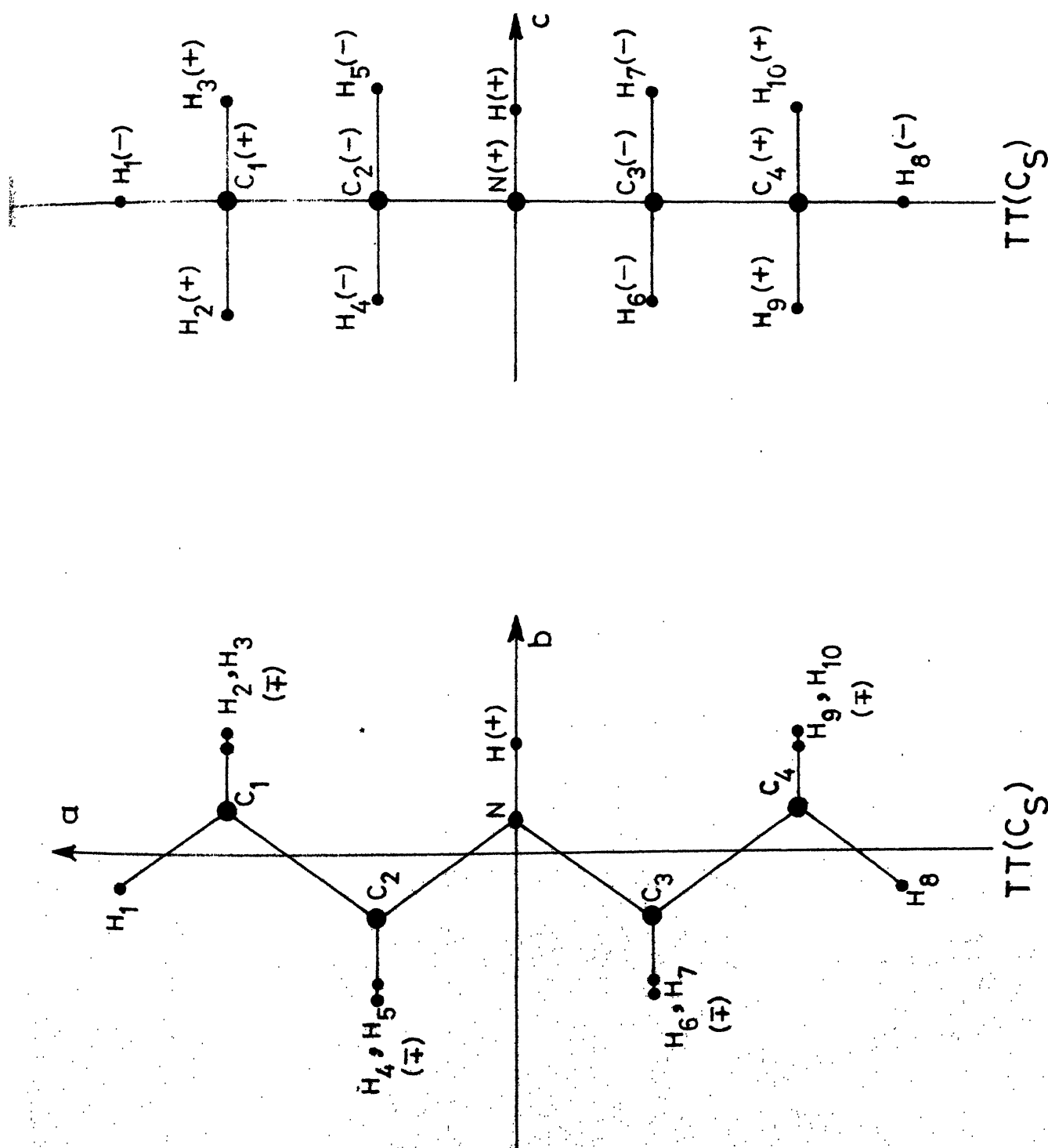


Fig. 4.2(A): Projections of the T-T form of DPA on the  $a$ - $b$  and  $a$ - $c$  planes of principal axes system. The  $+$  and  $-$  signs indicate the atoms above and below the planes respectively.

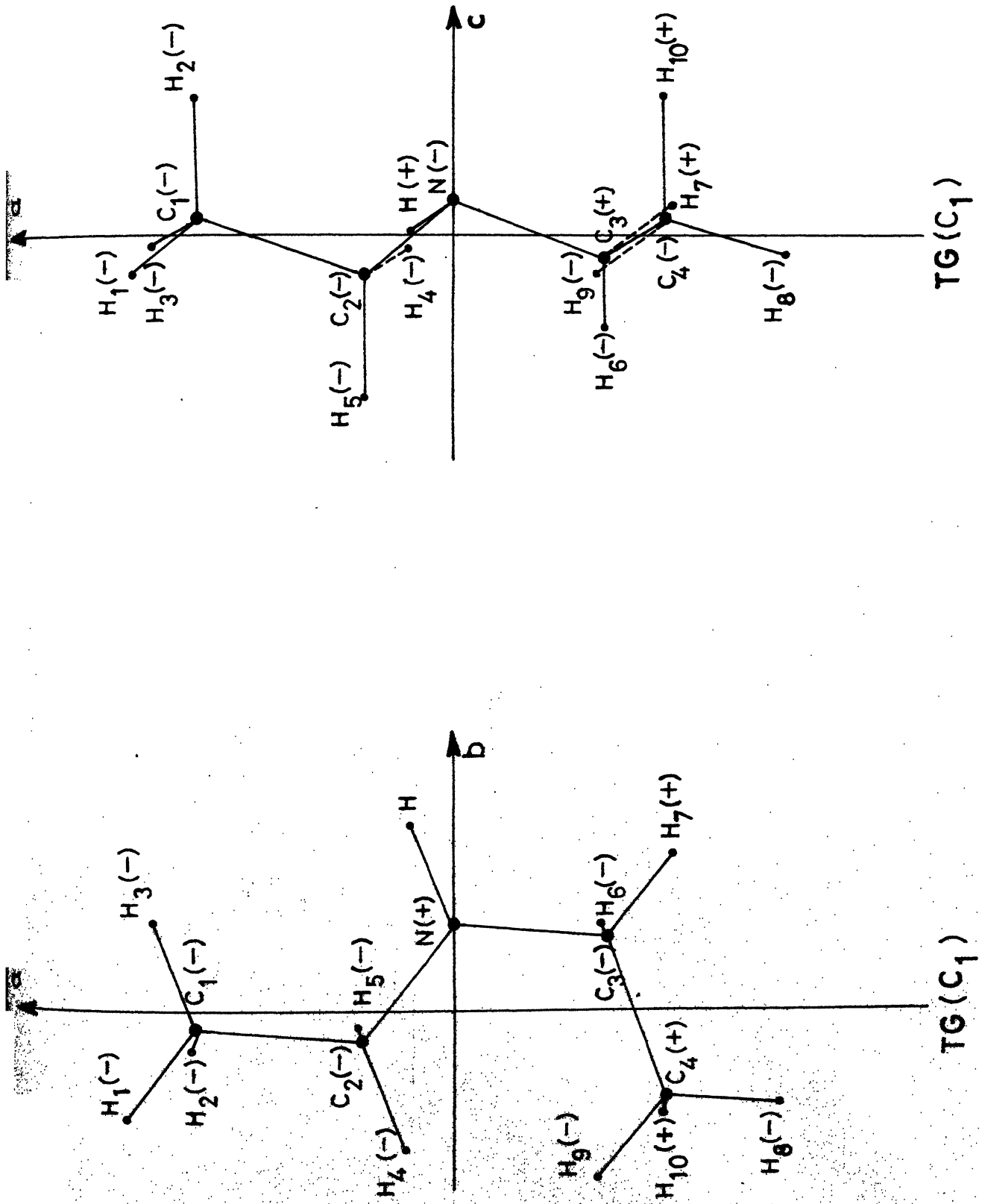


Fig. 4.2(3): Projections of the T-G form of DEA on the  $a-b$  and  $a-c$  planes of principal axes. The + and - signs indicate the atoms above and below the plane, respectively.



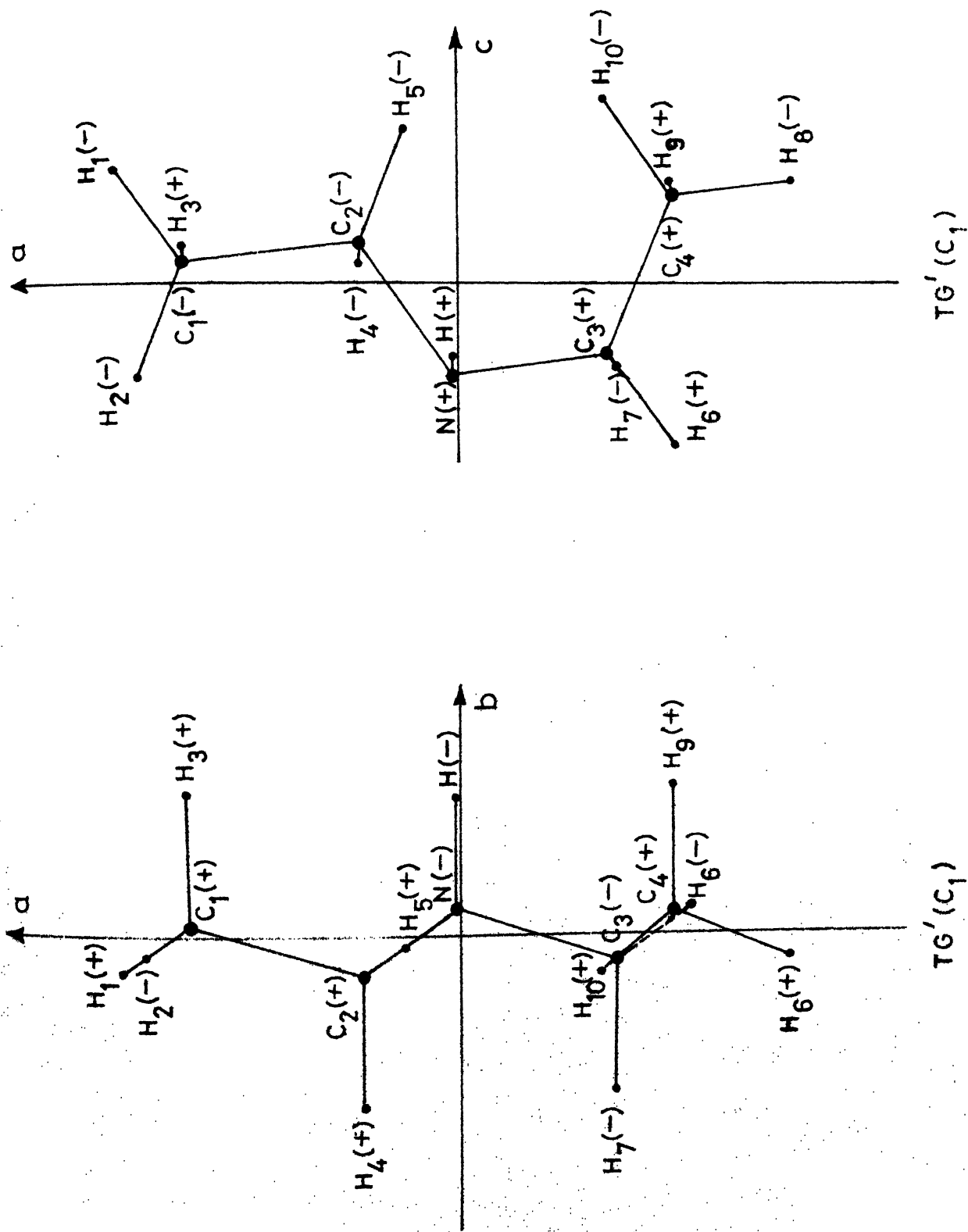


Fig. 4.2(Cu) Projection of the 1-1' direction of the crystal structure of  $TG(C_1)$  and  $TG'(C_1)$  in the  $a-b$  plane. The axes are labeled  $a$ ,  $b$ , and  $c$ . The vertices are labeled  $H_1$  through  $H_{10}$  and  $C_1$  through  $C_4$ ,  $N$ , and  $H$ . The signs (+) and (-) indicate the relative positions of the vertices.

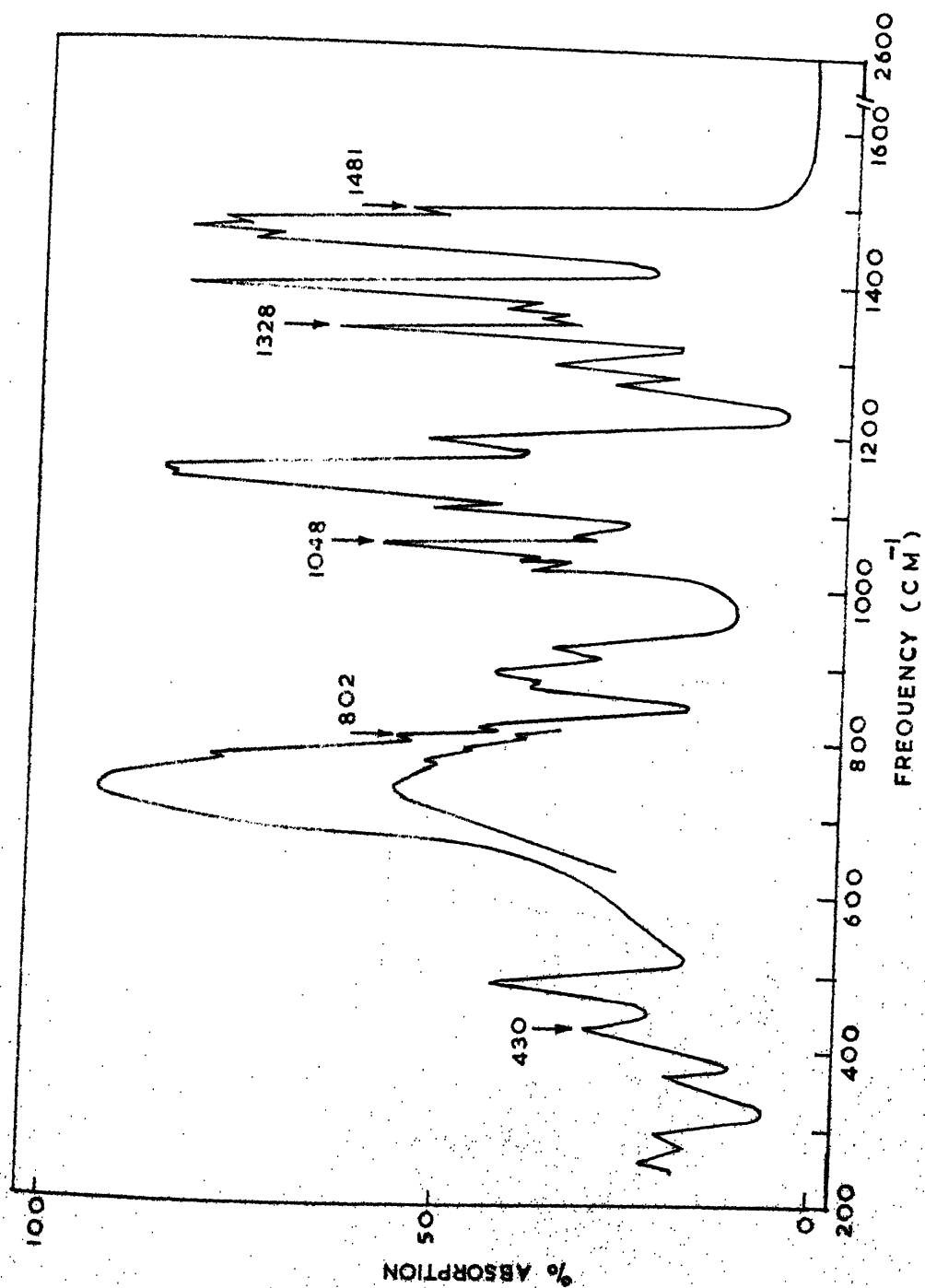


Fig. 4.3(A): The infrared spectrum of liquid diethyl amine (250-2600  $\text{cm}^{-1}$ ).

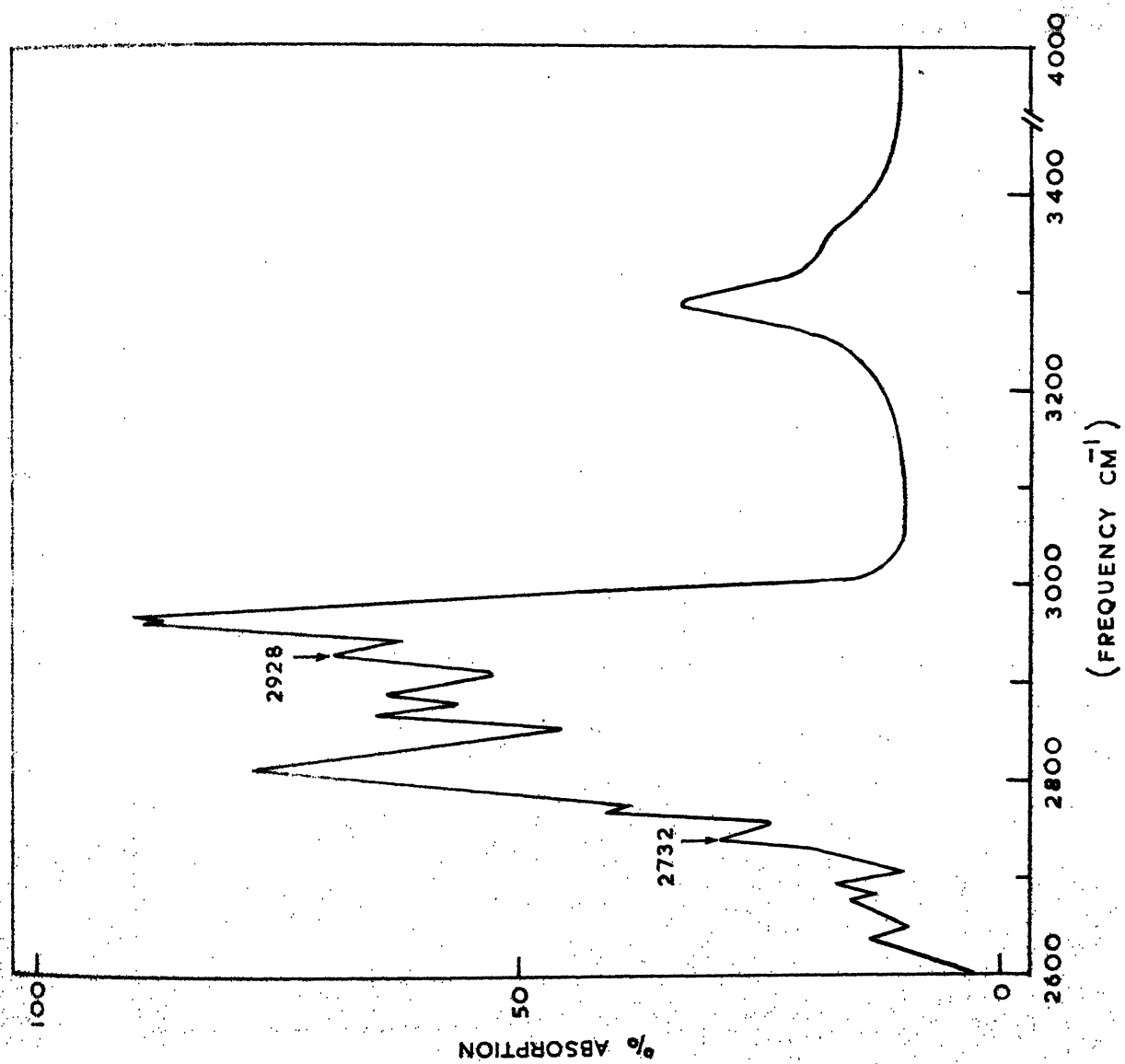


Fig. 4.3(B): The infrared spectrum of liquid diethyl amine (2600-4000 cm<sup>-1</sup>).

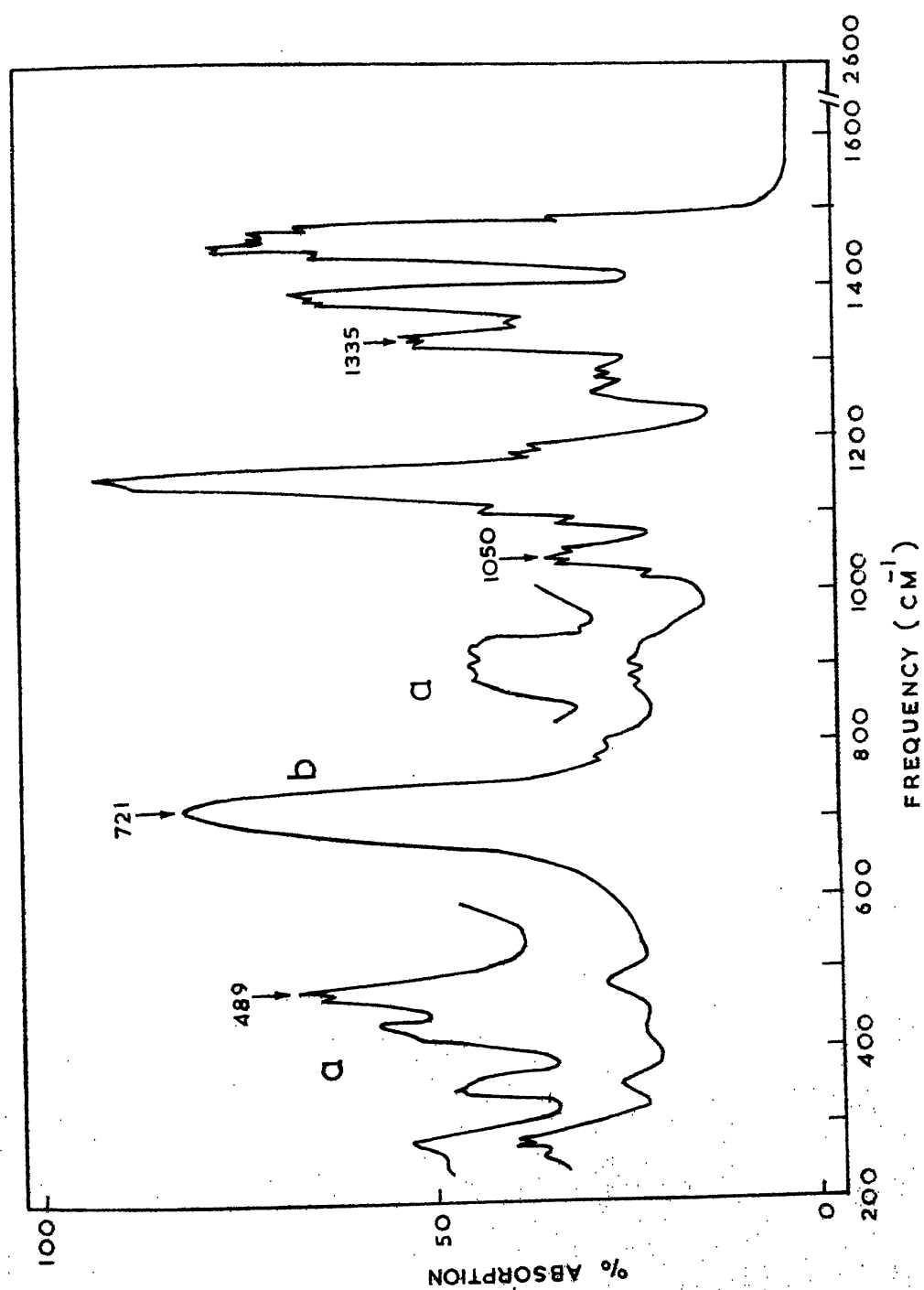


Fig. 4.4(A): The infrared spectrum of gaseous diethyl amine ( $250\text{--}3600\text{ cm}^{-1}$ ); 10 cm path length. (a) Pressure equals the vapour pressure of DEA at room temperature; (b) lower vapour pressure than in case (a).

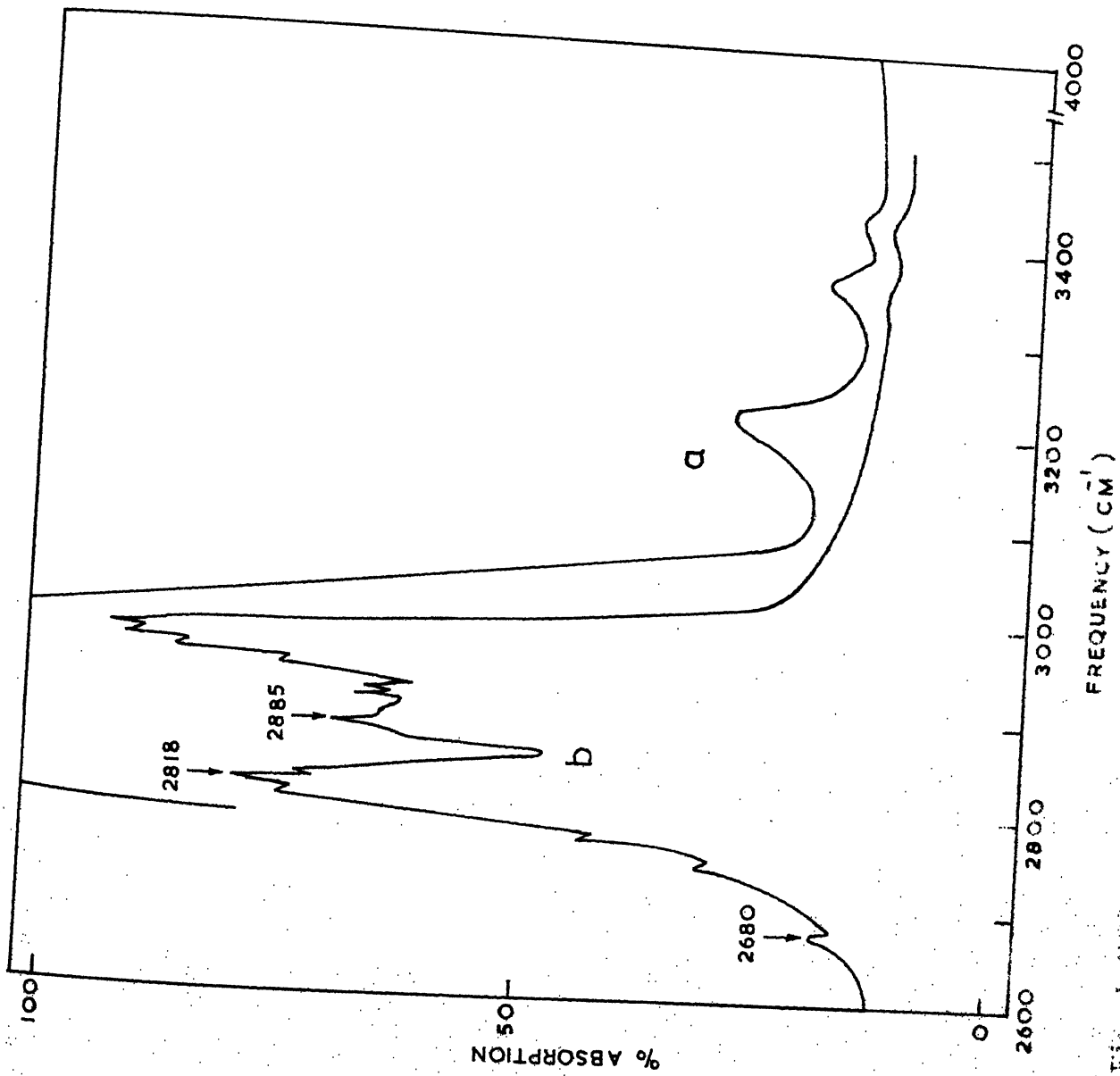


Fig. 4-100: The infrared spectrum of gamma, gamma-dithiylamine (1000-4000  $\text{cm}^{-1}$ ) in 10 cm cell (left). In P10 were equal to the vapor pressure of the liquid. In P10 were equal to the vapor pressure of the liquid.

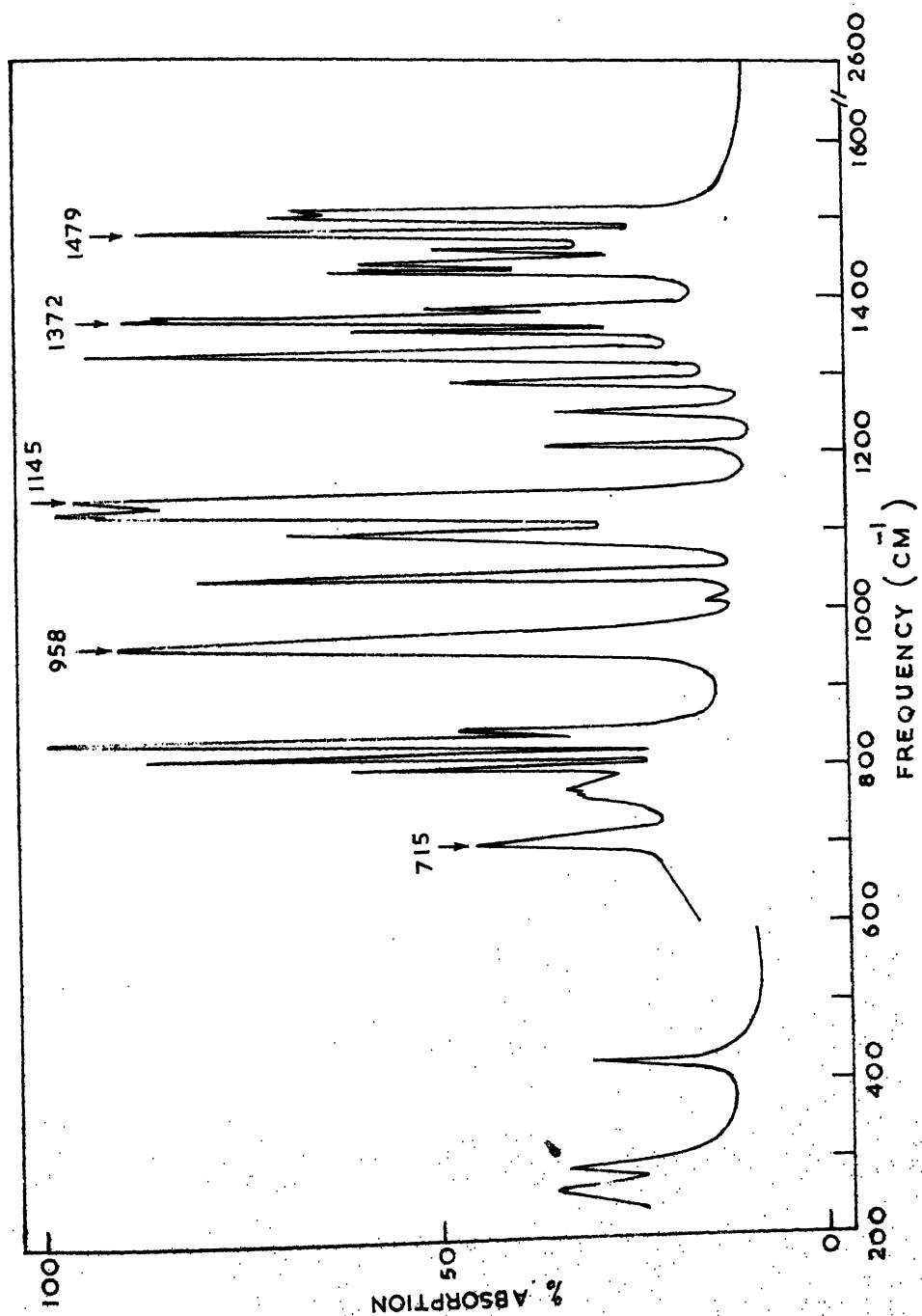


Fig. 4.5(A): The infrared spectrum of solid diethyl amine near 77°K (250-2600 cm<sup>-1</sup>).

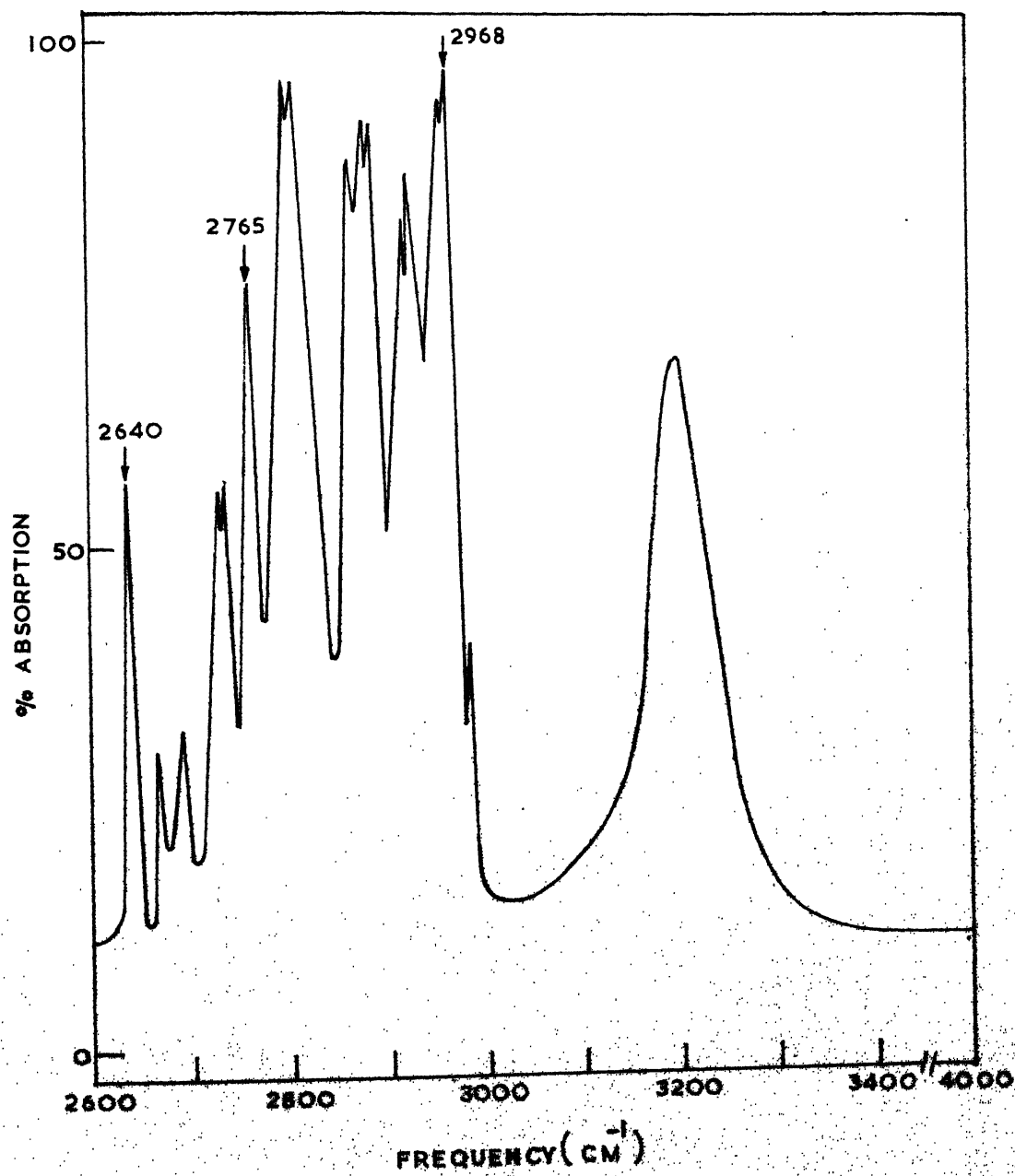


Fig. 4.5(B): The infrared spectrum of solid diethyl amine near 77°K (2600-4000 cm<sup>-1</sup>).

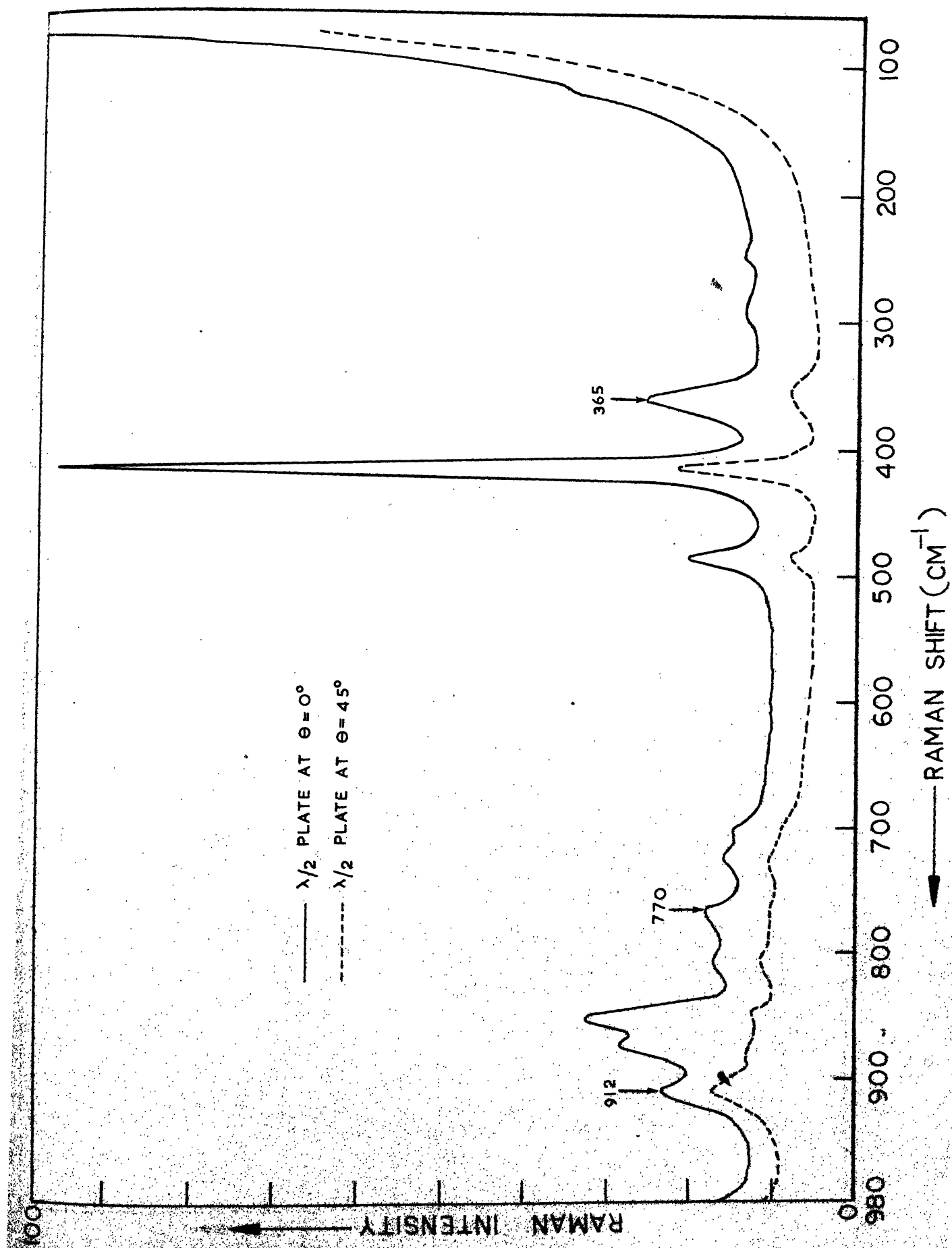


Fig. 4.6(A): The laser-Raman spectrum of liquid diethyl amine ( $100 \pm 80 \text{ cm}^{-1}$ ).



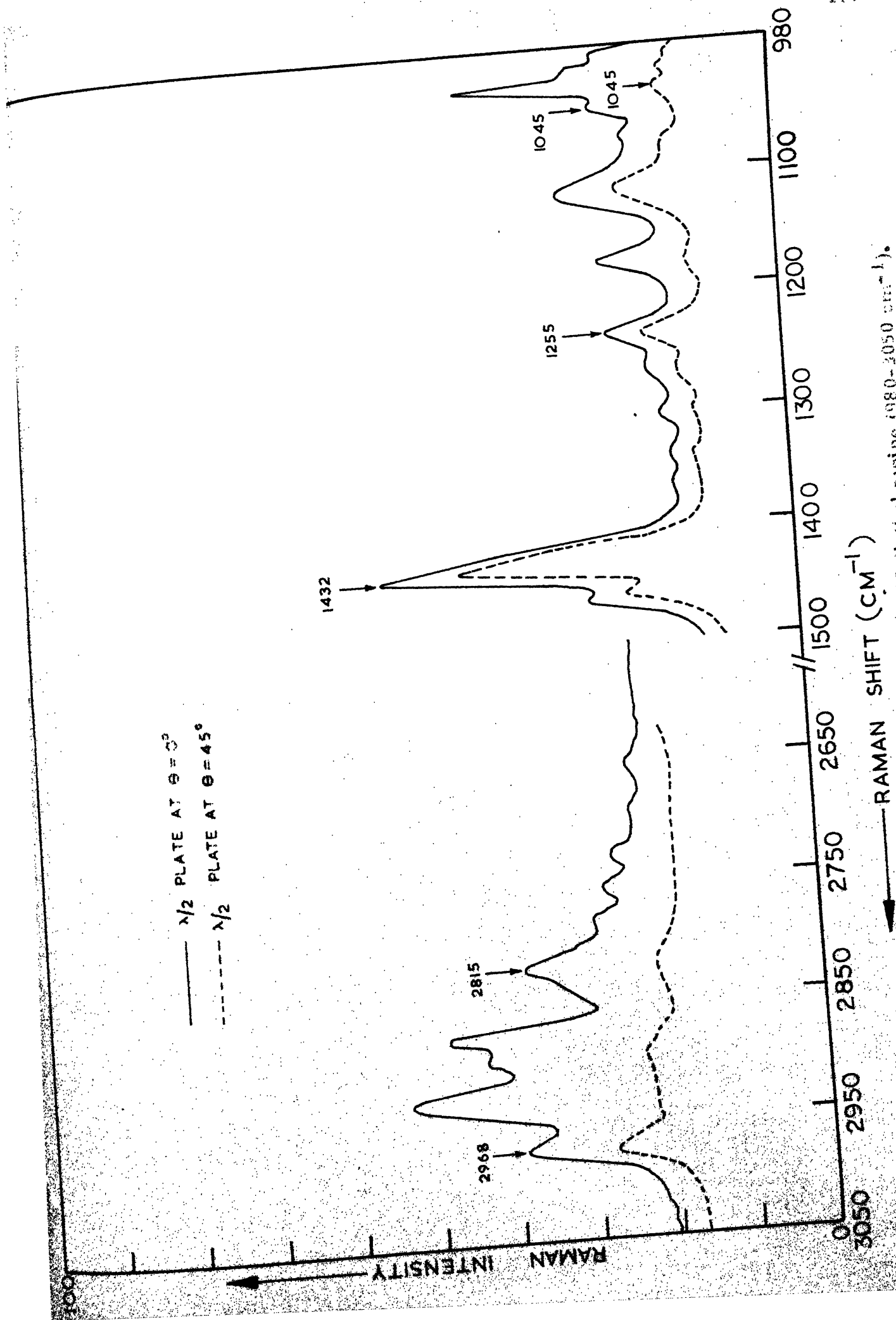


Fig. 4.6(B): The laser-Raman spectrum of liquid diethyl amine (980-3050  $\text{cm}^{-1}$ ).

## CHAPTER V

## VIBRATIONAL SPECTRA OF TRIPROPARGYL AMINE AND ROTATIONAL ISOMERISM

## ABSTRACT

The infrared spectra of tripropargyl amine were recorded from 250 to 4000  $\text{cm}^{-1}$  in the vapour, liquid and solid phases. The Raman spectrum of the liquid at room temperature was photoelectrically recorded and qualitative depolarization measurements were made. A comparative study of the infrared spectra in the fluid phase and in various solvents with that in solid phase reveals the existence of rotational isomers in the liquid and vapour phases. Various possibilities for rotational isomers with different point group symmetries are discussed.

The interpretation of the observed spectra suggests that the GGG configuration of the molecule having  $C_3$  point group symmetry is the one with lower energy and exists in the solid phase. In the vapour and liquid phases, another conformation (TGG) with  $C_1$  symmetry is also present in lower concentration. A vibrational assignment for the observed bands is proposed.

## INTRODUCTION

A correlative study of the infrared absorption bands corresponding to the terminal acetylenic groups in a large number of molecules was made by Nyquist and Potts<sup>1</sup>. The spectral variations observed in these simple acetylenic compounds associated with the  $\text{-C-C}\equiv\text{C-H}$  group were correlated with certain chemical and structural parameters. It would be interesting to study the effect of environment on acetylenic groups placed in a somewhat more complicated molecular frame. To facilitate the analysis, the choice of tripropargyl amine (TPA) molecule was made as it could be expected to have some higher order of symmetry.

Piaux and Gaudemar<sup>2</sup> reported the Raman spectra of mono-, di- and tripropargyl amines together with the spectra of some other acetylenic compounds. The bands characteristic of the  $\text{-C}\equiv\text{C}$  and  $\equiv\text{C-H}$  stretching modes were identified but no detailed assignment for other bands was attempted. The  $\text{-C-C}\equiv\text{C-H}$  group in methyl acetylene<sup>3</sup>, propargyl halides<sup>4-6</sup>, propargyl alcohol<sup>7</sup> and propargyl amine<sup>8</sup> is established to be linear. Therefore the  $\text{-C-C}\equiv\text{C-H}$  chains in the tripropargyl amine may also be considered to behave as linear sub-groups, but the skeleton about the C-N bond is expected to be bent. There is a possibility of hindered internal rotation about the C-N single bonds which may give rise to different geometrical configurations for the molecule. The infrared spectrum at low temperature may throw some light on the existence of stable isomer. To our knowledge, no structural determination for this molecule was attempted earlier. It was felt that a comparative study of the infrared spectra in the vapour, liquid and solid phases would enable us to verify the presence of rotational isomers with the identification of the lower energy form.

The point groups, to which the different reasonable structures of TPA are expected to belong, are  $C_{3v}$ ,  $C_3$ ,  $C_s$  and  $C_1$ . The  $-C \equiv C-C$  and  $-C \equiv C-H$  deformation modes are expected to give rise to different sets of absorption bands in the infrared and Raman spectra depending on the symmetry of the molecular frame. Hence the symmetry of the more stable form of the molecule may be inferred on the basis of the number of vibrational bands observed for these sub-groups. The depolarization measurements may also be helpful in this connection. Therefore a systematic vibrational study of tripropargyl amine was undertaken and the results obtained are discussed here.

#### EXPERIMENTAL

The compound used in this study was an Aldrich product and was distilled in vacuum prior to use. The infrared spectrum in the liquid phase was recorded in the form of a capillary film by sandwiching a small quantity of the compound between two CsBr plates. A part of the ir spectrum in liquid phase and the spectra in solutions of varying polarity ( $CCl_4$ ,  $CS_2$ ,  $CH_3Cl$  etc.) were measured with the help of 0.025 mm cell of fixed thickness fitted with CsBr windows. After introducing a small quantity of the compound inside the gas cell (10 cm path length), it was heated to higher temperatures to obtain sufficient vapour pressure for recording the ir spectra in the vapour phase. The spectrum in the solid phase near liquid nitrogen temperature was obtained with the help of a conventional low temperature cell. The initial solid deposit was annealed by melting the deposit and cooling it slowly. The tracings of the infrared spectra for the liquid, vapour and solid phases are shown in Figures 5.3, 5.4 and 5.5 respectively.

The laser-Raman spectrum of liquid TPA was obtained on a Coderg Raman spectrophotometer. The qualitative depolarization measurements on Raman displacements were made in the same way as described in Chapter II. The position of the Raman lines is shown in Figure 5.6.

### DISCUSSION

In the absence of any structural data, it seems reasonable to assume a pyramidal structure for TPA, as the chemical evidence rules out a planar structure. As has already been pointed out, all the atoms of  $\text{H-C} \equiv \text{C-C}$  chain lie on a straight line, and these atoms together with the nitrogen atom determine a plane. Depending upon the position and orientation of the remaining atoms of the three propargyl groups, this molecule may assume different point group symmetries. In principle, twenty seven conformations are possible for TPA corresponding to rotations, in turn, about each of the three N-C bonds. Out of these only seven, the TTT, TTG, TGG, TGG', TG'G, GGG and GGG' are spectroscopically distinguishable and are shown in Figure (5.1). In these designations, the 'trans' and 'gauche' configurations about any of the N-C bond with respect to the lone pair orbitals of nitrogen atom are denoted by T and G respectively. The steric considerations among different atoms of the groups and the  $\pi$ -orbitals of the  $\text{C} \equiv \text{C}$  triple bonds eliminate the need to consider the TTT, TTG, TG'G and GGG' forms as energetically favourable (An analysis of the observed spectra also rules out the existence of these configurations). Thus we may accordingly confine ourselves with the remaining three isomers, viz., TGG, TGG' and GGG only. The projections on the planes of the principal axes system of these configurations are shown in Figure 5.2.

In the most unsymmetrical form of the molecule (TGG) with the trivial point group symmetry  $C_1$ , all the fifty one normal modes belong to the same symmetry class. All these modes are expected to be active in both the ir and Raman spectra, with all the Raman lines being polarized. The rotational constants A, B, C and the asymmetry parameter ( $k = \frac{2B-A-C}{A-C}$ ) were calculated by assuming the parameters for propargyl group from ref. (4):  $r_{C-H} = 1.09 \text{ \AA}$ ,  $r_{\equiv C-H} = 1.06 \text{ \AA}$ ,  $r_{\equiv C-C} = 1.465 \text{ \AA}$ ,  $r_{C\equiv C} = 1.207 \text{ \AA}$ ,  $r_{C-N} = 1.472 \text{ \AA}$  and all bond angles as tetrahedral. These are tabulated for the three conformations in Table 5.1. The calculations of Badger and Zimmwalt asymmetry parameters<sup>9</sup> for the TGG form yield

$\rho^* = 0.794$  and  $k = -0.204$  and hence infrared spectrum in the vapour phase may be expected to exhibit three types of band contours. Recently, Seth-Paul and Dijkstra<sup>10</sup> gave the modified expressions for calculating PR separation of the band envelopes in vapour phase. The type -A bands are expected to exhibit a medium intense Q-branch and a PR spacing of  $\sim 9.5 \text{ cm}^{-1}$ , type -B bands will have a PQ Q'R type structure with a QQ' separation of  $\sim 4.5 \text{ cm}^{-1}$  and PR separation of  $\sim 7.6 \text{ cm}^{-1}$ , while a strong Q branch and PR spacing of  $\sim 14 \text{ cm}^{-1}$  are expected for type -C bands.

The TGG' conformation can have at the most one plane of symmetry (point group  $C_s$ ) passing through the propargyl group which has the 'trans' configuration. In this case, the fifty one normal modes may be divided into 28  $a'$  symmetrical and 23  $a''$  asymmetrical species. The  $a'$  modes should give rise to polarized Raman bands while the  $a''$  modes should yield depolarized Raman bands. The Badger and Zimmwalt parameters<sup>9</sup> for this configuration come out to be  $\rho^* = 1.418$  and  $k = -0.734$  and hence the infrared spectrum in vapour phase should

exhibit three types of band contours, type-A bands having a POR structure with a medium Q-branch and PR spacing of  $\sim 9 \text{ cm}^{-1}$ , type-B having a PR separation of  $\sim 6.7 \text{ cm}^{-1}$ , and type - C having a POR structure with medium to strong Q-branch and PR spacing of  $\sim 13 \text{ cm}^{-1}$ .

The GGG conformation may have only a  $C_3$  - axis of rotation as an element of symmetry and hence the 51 fundamental vibrations may be divided into symmetry species as  $17a + 17e$ , all the vibrations being active in both the infrared and Raman spectra. The type-a modes should appear as polarized and type-e as depolarized in the Raman spectrum. The calculation of Gerhard and Dennison<sup>11</sup> parameter gives  $\beta = -0.47$  and therefore the molecule is an oblate symmetric top in this configuration. The vapour phase spectrum may therefore be expected to consist of two types of bands: (1) The parallel bands having a strong Q branch and PR spacing of  $\sim 13 \text{ cm}^{-1}$  and (2) the perpendicular type bands having a weak Q branch with a PR spacing of  $\sim 9.5 \text{ cm}^{-1}$ .

In the vapour phase, the band contours are not resolved except for a very few bands, and hence they are not of much help in assigning the bands to particular fundamental modes. The symmetry classification of the fundamental vibrations and their selection rules for each structure with different point group symmetry are summarized in Table 5.2. Herzberg's convention<sup>12</sup> for numbering the vibrations is used.

A comparative study of the spectra in the liquid and vapour phases and in solutions reveals that a number of sets of bands display differences in their relative intensities suggesting the presence of more than one rotational isomer in fluid phase. However, in the solid phase only one isomer gets stabilized. The question of the symmetry of the more stable molecular species at low temperature can best be decided after the



proper assignment of the bands corresponding to the deformation modes of the  $-C-C \equiv C$  and  $-C \equiv C-H$  sub-groups has been made. Hence the key to the correct interpretation lies in the correct assignment of the modes arising due to these sub-groups.

#### ASSIGNMENT

In the methyl acetylene<sup>3</sup>, the  $C \equiv C -C$  and  $C \equiv C-H$  deformation modes are degenerate. With a decrease in the symmetry of the molecular frame in propargyl halides<sup>5,6</sup>, these degenerate modes split into an in-plane and an out-of-plane component giving rise to two separate bands. Since there are three such sub-groups of each type in TPA, in place of each of the corresponding in-plane and out-of-plane modes, three modes are expected which may split into separate components depending upon the symmetry properties of the molecular frame and interaction among themselves and other modes of the molecule.

In the approximation of  $C_{3v}$  point group symmetry for TPA, the bending modes associated with each of the  $-C \equiv C-C$  and  $-C \equiv C-H$  sub-groups may be divided into symmetry species as  $1a_1$ ,  $1a_2$  and  $2e$  corresponding to the three in-plane and three out-of-plane modes. The  $a_2$  modes being inactive in both the infrared and Raman spectra, three lines may be expected for each of the sub-groups in the corresponding regions of their normal occurrence. If the symmetry is reduced from  $C_{3v}$  to  $C_3$ , species  $a_1$  and  $a_2$  coalesce making the above two inactive  $a_2$  modes active in the vibrational spectra. Therefore, in place of three, four lines may now be expected for each sub-groups. If the symmetry is further reduced from  $C_3$  to  $C_s$  or  $C_1$ , each of the doubly degenerate  $e$  modes in the point group  $C_3$  are expected to split

giving rise to two components. Hence a much richer spectrum is expected upon such conversion. It is shown below that the vibrational spectra contradicts this and the results obtained can be satisfactorily interpreted in terms of the  $C_3$  point group symmetry (GGG form) for the molecule.

In comparison with other molecules containing acetylenic groups<sup>1,3,5,6,13</sup>, the  $-C \equiv C-H$  deformation modes may be expected between 600 and 700  $cm^{-1}$ . These bands are fairly strong and broad in infrared spectrum. The liquid phase infrared spectrum of TPA shows strong bands at 626 and 654  $cm^{-1}$  with a shoulder at 670  $cm^{-1}$ . The Raman lines at 608 and 659  $cm^{-1}$  appear as polarized and those at 632 and 673  $cm^{-1}$  depolarized. The solid TPA near  $\sim 77^\circ K$  shows very strong lines at 634, 648, 685 and 699  $cm^{-1}$ . These lines seem to shift to higher frequencies as compared to those in the liquid or vapour phase, probably due to a weak molecular association. As the lower frequency bands in the  $-C \equiv C-H$  deformation region were assigned to the out-of-plane modes in propargyl halides<sup>5,6</sup>, and other acetylenic compounds<sup>1,13</sup>, the in-plane modes in TPA may also be expected to occur on the higher frequency side of the out-of-plane modes. Therefore, the pair of bands at 608  $cm^{-1}$  (polarized) and 632  $cm^{-1}$  (depolarized) in the Raman spectrum, which correspond to the infrared bands at 634 and 648  $cm^{-1}$  in the solid phase, may be assigned to the out-of-plane  $-C \equiv C-H$  deformation modes. If the remaining two bands in the infrared spectrum of solid phase at 685 and 699  $cm^{-1}$  corresponding to the Raman bands at 659 and 673  $cm^{-1}$  are attributed to the in-plane modes, this assignment supports the  $C_3$  symmetry for the molecule. In liquid phase ir spectrum, probably the bands are not resolved due to large width of the absorption lines.

From the observations on different molecules<sup>5,6,14,15</sup> it may be inferred that the in-plane  $-C \equiv C-C$  bending modes lie at higher frequencies as compared to those due to out-of-plane vibrations. Therefore, a similar behaviour may be expected for the analogous modes in TPA. In the region of  $-C \equiv C-C$  bending modes, three medium strong lines have been observed in the liquid phase ir spectrum of TPA at 313, 329 and 352  $\text{cm}^{-1}$ . In the solid phase at low temperature, the ir spectrum exhibits very strong and sharp lines at 313, 327, 338 and 352  $\text{cm}^{-1}$ . The pair of bands at 311  $\text{cm}^{-1}$  (polarized) and 324  $\text{cm}^{-1}$  (depolarized) in the Raman spectrum and the corresponding bands at 313 and 327  $\text{cm}^{-1}$  in the solid phase ir spectrum may be assigned to the out-of-plane  $-C \equiv C-C$  bending modes of TPA in analogy with other molecules<sup>5,6,14,15</sup>. The in-plane  $-C \equiv C-C$  deformation modes may then be associated with the Raman lines at 334  $\text{cm}^{-1}$  (polarized ?) and 346  $\text{cm}^{-1}$  (depolarized), corresponding to the infrared bands in the solid phase at 338 and 352  $\text{cm}^{-1}$ . Since the in-plane vibrations can not interact with the out-of-plane vibrations, one can expect all the  $-C \equiv C-C$  deformation modes to occur in such a narrow frequency range.

From the consideration on the number of lines observed for these modes in the infrared (crystalline solid) and Raman spectra, it is inferred that TPA in its lower energy configuration can have at the most a  $C_3$  point group symmetry. The assignment of other bands in the assumption of  $C_3$  symmetry for the more stable form may lend further support for this configuration. The other isomer(s) present in the liquid and vapour phases belong to lower symmetry whose structures may be estimated after assigning the bands due to them. It is to be noted that these arguments are based on the features seen in the spectra and not on features that are missing.

The assignment for the observed bands is given in Table 5.3 categorically for the GGG form having  $C_3$  symmetry and a brief discussion is presented here. The interpretation of the vibrational spectra may become easier if the observed bands can be ascribed to one isomer or the other. In addition to the low temperature effects, the pair of bands belonging to separate isomers can be identified by studying the effects of solvents of varying polarity and increase in temperature on the relative intensities of such type of pairs. Although there was no significant effect of solvents, the bands at 1127 and 585  $\text{cm}^{-1}$  were found to increase in intensities relative to those at 1108 and 554  $\text{cm}^{-1}$  at higher temperatures ( $\sim 90^\circ \text{C}$ ) in the vapour phase. This variation in intensities with temperature is probably due to the change in the isomeric equilibrium of the molecules of TPA.

A medium strong and sharp doublet is observed at 828 and 839  $\text{cm}^{-1}$  in the liquid phase ir spectrum of TPA. The corresponding doublet in Raman spectrum (827 and 838  $\text{cm}^{-1}$ ) is very strong and polarized. At low temperature in solid phase, only the lower frequency component persists at 831  $\text{cm}^{-1}$  and the higher frequency component disappears completely. This band at 831  $\text{cm}^{-1}$  has been assigned to the a-type C-N stretching mode and the disappearing component may belong to other isomer(s). In the region of asymmetric C-N stretch, the liquid phase spectra show two bands at 1116 and 1126  $\text{cm}^{-1}$  (ir) and at 1108 and 1123  $\text{cm}^{-1}$  (Raman, depolarized) while at low temperature in solid phase, the higher frequency component seems to disappear and the lower frequency component at 1110  $\text{cm}^{-1}$  shows a very sharp and closely lying shoulder at 1114  $\text{cm}^{-1}$ . From its features, this splitting resembles that expected from crystal field effects. Moreover, at higher temperatures, the relative intensities of the bands at 1127 and 1108  $\text{cm}^{-1}$

in the vapour phase show reverse effect to that at low temperature. Hence the line at  $1110\text{ cm}^{-1}$  in the solid phase is assigned as the asymmetric C-N stretching mode and the missing band may be ascribed to this mode arising due to other isomer(s).

As shown by Wotiz and Miller<sup>16</sup>, the intensity of the  $\text{-C} \equiv \text{C}$  stretching modes in ir spectrum goes on decreasing with increase in the symmetry of the environment of  $\text{C} \equiv \text{C}$  bonds. The bands corresponding to the  $\text{C} \equiv \text{C}$  stretching modes are completely missing in the liquid phase ir spectrum of  $(\text{H-C} \equiv \text{C-CH}_2)_3\text{N}$ , but the Raman spectrum shows two very strong and polarized bands at  $2105$  and  $2123\text{ cm}^{-1}$ . In the vapour phase at higher temperature ( $\sim 90^\circ\text{C}$ ), very faint bands appear at  $2108$  and  $2122\text{ cm}^{-1}$ . In the solid phase, a single weak band is observed at  $2120\text{ cm}^{-1}$ . From these observations, we have associated the higher frequency component with the  $\text{C} \equiv \text{C}$  stretching modes  $\nu_4$  and  $\nu_{21}$ . Most probably, the lower frequency component, not observed in the solid phase, belongs to other isomer(s). The speculation, that both of these bands arise due to the single isomeric species having the  $\text{C}_3$  symmetry, does not seem correct, since in this case, one band is expected to appear as depolarized Raman line which is contrary to our observations. Hence we have preferred the alternate explanation given above for these bands.

The band at  $928\text{ cm}^{-1}$  in the vapour phase of methyl acetylene<sup>3</sup> has been considered principally due to  $\text{C-C} \equiv$  stretching vibration. The absorption due to this mode in propargyl halides has been assigned in the range  $940\text{-}960\text{ cm}^{-1}$  by Evans and Nyquist<sup>5</sup>. In the present study, TPA shows five absorption bands in the region  $900$  to  $1000\text{ cm}^{-1}$ . The polarized Raman line at  $897\text{ cm}^{-1}$  and a medium strong infrared band at

903  $\text{cm}^{-1}$  in the liquid phase may be associated with the symmetric C-C  $\equiv$  stretching mode  $\nu_8$ . The asymmetric C-C  $\equiv$  stretch  $\nu_{25}$  is difficult to be located because of the overlap of the region by absorption due to many other type of molecular vibrations, mainly combination and overtones. This  $\nu_{25}$  mode may be tentatively associated with the medium strong infrared band in the solid phase which shows doublet splitting with its components at 980 and 985  $\text{cm}^{-1}$ . The assignment for other bands in this region is given in Table 5.3.

Leaving aside the C-C  $\equiv$  C deformation modes, tripropargyl amine should have nine fundamentals in the frequency region below 600  $\text{cm}^{-1}$ , six corresponding to the bending modes of the CNC and CCN groups and three to the torsional modes about the C-N bonds. These modes are expected to be highly dependent on the geometry of the molecule due to a large amount of coupling between the motions of adjacent bonds and bond angles. However, their approximate description and assignment may be given as follows: The polarized Raman band at 442  $\text{cm}^{-1}$  corresponding to the liquid phase infrared band at 443  $\text{cm}^{-1}$  may be assigned to the CCN bending mode  $\nu_{13}$  for the more stable isomer. The very weak infrared band in the liquid phase at 471  $\text{cm}^{-1}$  corresponding to the polarized Raman band at 465  $\text{cm}^{-1}$  does not appear in the crystalline state and may be assigned to this mode due to less stable isomer(s). The pair of bands at 553  $\text{cm}^{-1}$  (Raman depolarized) and 583  $\text{cm}^{-1}$  (Raman polarized) corresponding to the infrared bands at 555  $\text{cm}^{-1}$  and 584  $\text{cm}^{-1}$  in the liquid phase have been associated with the other CCN bending modes. The lower frequency band is assigned to the more stable isomeric form having  $C_3$  symmetry and the higher band to the less stable form on the basis of their behaviour at low temperature. The e-type CNC bending

mode  $\nu_{33}$  may be associated with the depolarized Raman band at  $382\text{ cm}^{-1}$  whose corresponding ir band in the solid phase shows a crystal field splitting with its components at  $375$  and  $380\text{ cm}^{-1}$ . The remaining  $\delta_{\text{CNC}}$  mode  $\nu_{16}$  may be associated with the medium intense Raman band at  $172\text{ cm}^{-1}$ . The weak shoulder on the lower frequency side of this band may possibly belong to other isomer(s). A weak band, observed in the Raman spectrum of TPA at  $\sim 78\text{ cm}^{-1}$ , may be tentatively associated with the torsional modes  $\nu_{34}$  and  $\nu_{17}$ . This completes the assignment of the skeletal modes.

It is well known that the  $\equiv\text{C-H}$  stretching fundamentals occur around  $3300\text{ cm}^{-1}$  in most of the acetylenic compounds. The infrared bands are observed at  $3288$  and  $3302\text{ cm}^{-1}$  in the liquid phase and at  $3266$  and  $3283\text{ cm}^{-1}$  in the solid phase of TPA, with the last line showing a doublet nature in the solid state. The lower frequency band has been associated with the symmetric and the higher frequency component to the asymmetric  $\equiv\text{C-H}$  stretching modes respectively. The lowering in frequency for these modes in the solid phase may result due to hydrogen bonding or related effects, due to slightly acidic nature of the acetylenic proton.

The modes associated with the methylene groups are still to be identified. In the region of C-H stretch, three infrared bands are observed in the liquid phase of which two have been assigned to the methylene group stretching vibrations as given in Table 5.3. The third one has been assigned as an overtone of the  $-\text{CH}_2$  deformation modes. The a-type and e-type modes occur at nearly the same frequencies giving rise to the corresponding Raman lines a polarized nature. In the solid phase, both the bands due to the  $-\text{CH}_2$  group stretching modes split into close doublets. This is probably because of the reason that the

a- and e-type modes get separated due to the sharpening of the bands at low temperature.

The  $\text{-CH}_2$  deformation modes  $\nu_5$  and  $\nu_{22}$  may be satisfactorily associated with the infrared bands (liquid) at 1434 and 1445  $\text{cm}^{-1}$  respectively. The corresponding Raman bands at 1428  $\text{cm}^{-1}$  and 1442  $\text{cm}^{-1}$  are depolarized. The region, in which the  $\text{CH}_2$  wagging and twisting modes are expected, is heavily overlapped due to the presence of overtones and combination tones of the  $\text{-C} \equiv \text{C-H}$  deformation modes. The  $\text{-CH}_2$  wagging modes may be expected in the region 1300 - 1400  $\text{cm}^{-1}$ . The two pairs of bands at 1331/1342 and 1362/1371  $\text{cm}^{-1}$  in the liquid phase infrared spectrum may be associated with the  $\text{-CH}_2$  wagging modes in this molecule. In the solid phase at low temperature, the higher frequency component of the first pair disappears, but corresponding to the lower frequency band, the Raman line at 1330  $\text{cm}^{-1}$  is depolarized. Therefore, this is correlated with the mode  $\nu_{23}$  for the GGG form and the disappearing band may be due to other isomer(s). The Raman spectrum shows a polarized band of moderate intensity at 1359  $\text{cm}^{-1}$  with a diffused shoulder on the higher frequency side at 1372  $\text{cm}^{-1}$ . The corresponding bands in the solid phase lie at 1357 and 1367  $\text{cm}^{-1}$  respectively. The polarized Raman band may be associated with the  $\nu_6$  mode and the other component of this pair may correspond to an overtone or a combination mode.

The bands arising out of combinations or overtones may be expected to have moderate intensity at low temperature, but in vapour phase at higher temperatures, they may show a marked decrease in their intensity in absorption spectra due to lesser coupling between the molecular modes. The pair of diffused bands at 1278  $\text{cm}^{-1}$  and 1308  $\text{cm}^{-1}$  in the liquid phase infrared spectrum probably corresponds to summation bands.



The strong infrared band at  $1254\text{ cm}^{-1}$  and the corresponding weak and depolarized band in the Raman spectrum at  $1247\text{ cm}^{-1}$  may be correlated with the  $-\text{CH}_2$  twisting mode  $\nu_{24}$ . This twisting mode is probably mixed up with other skeletal modes and hence gains intensity in the infrared spectra. The other  $-\text{CH}_2$  twisting mode  $\nu_7$  may be associated with the weak band at  $1239\text{ cm}^{-1}$  in the solid phase for the GGG form.

The medium intense infrared band in the solid phase at  $747\text{ cm}^{-1}$  may be tentatively assigned to the  $-\text{CH}_2$  rocking modes  $\nu_{10}$  and  $\nu_{27}$ . This band is probably masked in the wing of the strong  $-\text{C} \equiv \text{C}-\text{H}$  deformation bands in the liquid phase.

On the basis of the above assignments, it may be inferred that the isomer having lower concentration in the liquid and vapour phases possesses the  $C_1$  symmetry (TGG form) along with the more abundant GGG form ( $C_3$  symmetry). This conclusion is based on the polarization data and the disappearance of the infrared bands corresponding to the Raman bands at  $583$ ,  $838$  and  $2105\text{ cm}^{-1}$  which could be explained only on the basis of the  $C_1$  symmetry for the molecule. From the present studies, it is not certain whether there is only one higher energy form (TGG) or more than one, although the disappearing bands at low temperature could be satisfactorily interpreted as arising due to the presence of only TGG form.

The other observed bands may be satisfactorily assigned as overtones and/or combination tones of the fundamentals discussed above.

## REFERENCES

1. R.A. Nyquist and J.W. Potts, *Spectrochim. Acta* 16, 419 (1960)
2. L. Piaux and M. Gaudemar, *Bull. Soc. Chim. Fr.* 786 (1957)
3. D.R.J. Boyd and H.W. Thompson, *Trans. Faraday Soc.* 48, 493 (1952)
4. E. Hirota and Y. Morino, *Bull. Chem. Soc. Japan* 34, 341 (1961)
5. J.C. Evans and R.A. Nyquist, *Spectrochim. Acta* 19, 1155 (1963)
6. G. Zerbi and M. Gussoni, *J. Chem. Phys.* 41, 456 (1964)
7. E. Hirota, *J. Mol. Spectry.* 26, 335 (1968)
8. K. Bolton, N.L. Owen and J. Sheridan, *Nature* 217, 164 (1968)
9. R.M. Badger and L.R. Zumwalt, *J. Chem. Phys.* 6, 711 (1938)
10. W.A. Seth-Paul and G. Dijkstra, *Spectrochim. Acta* 23A, 2861 (1967)
11. S.L. Gerhard and D.M. Dennison, *Phys. Rev.* 43, 197 (1933)
12. G. Herzberg, *Infrared and Raman Spectra of Polyatomic Molecules*,  
Van Nostrand, New York (1945)
13. N. Sheppard, *J. Chem. Phys.* 17, 74 (1949)
14. P.N. Daykin, S. Sunda Ram and F.F. Cleveland, *J. Chem. Phys.*  
37, 1087 (1963)
15. R.A. Nyquist, A.L. Johnson and Y.S. Lo, *Spectrochim. Acta* 21,  
77 (1965)
16. J.F. Wotiz and F.A. Miller, *J. Amer. Chem. Soc.* 71, 3441 (1949)

TABLE 5.1

THE MOLECULAR PARAMETERS FOR THE GGG, TGG AND TGG'  
CONFORMERS OF TRIPROPARGYL AMINE

Species	GGG	TGG	TGG'
$I_a(\text{a.m.u.}-\text{\AA}^2)$	412.5	318.8	247.4
$I_b(\text{a.m.u.}-\text{\AA}^2)$	412.5	471.0	551.6
$I_c(\text{a.m.u.}-\text{\AA}^2)$	778.1	688.5	679.6
$\rho^* = \frac{A - C}{B}$	0.470	0.794	1.418
$\kappa = \frac{2B - A - C}{A - C}$	1.00	-0.204	-0.734
$\Delta V(\text{FR})\ddagger$ type bands	13.0 $\text{cm}^{-1}$	9.5 $\text{cm}^{-1}$	8.8 $\text{cm}^{-1}$

TABLE 5.2

SYMMETRY CLASSIFICATION, ACTIVITY AND NUMBERING OF THE VIBRATIONAL MODES\*  
FOR ALTERNATE POSSIBLE STRUCTURES OF  $(\text{H}-\text{C}\equiv\text{C}-\text{CH}_2)_3 \text{N}$ .

Approximate description of vibrational modes	$\text{C}_{3v}$			$\text{C}_3$		$\text{C}_s$	
	Class $a_1$ IR, R (P)	Class $a_2$ - , -	Class e IR, R (D)	Class a IR, R (P)	Class e IR, R (D)	Class $a'$ IR, R (P)	Class $a''$ IR, R (D)
Acetylenic $\equiv\text{C}-\text{H}$ str.	$\nu_1$		$\nu_{18}$	$\nu_1$	$\nu_{18}$	$\nu_1, \nu_2$	$\nu_{29}$
Methylene $-\text{CH}_2$ str. (asym.)		$\nu_{12}$	$\nu_{19}$	$\nu_2$	$\nu_{19}$	$\nu_3$	$\nu_{30}, \nu_{31}$
Methylene $-\text{CH}_2$ str. (sym.)	$\nu_2$		$\nu_{20}$	$\nu_3$	$\nu_{20}$	$\nu_4, \nu_5$	$\nu_{32}$
$\text{C}\equiv\text{C}$ str.	$\nu_3$		$\nu_{21}$	$\nu_4$	$\nu_{21}$	$\nu_6, \nu_7$	$\nu_{33}$
$-\text{CH}_2$ def.	$\nu_4$		$\nu_{22}$	$\nu_5$	$\nu_{22}$	$\nu_8, \nu_9$	$\nu_{34}$
$-\text{CH}_2$ wagging	$\nu_5$		$\nu_{23}$	$\nu_6$	$\nu_{23}$	$\nu_{10}, \nu_{11}$	$\nu_{35}$
$-\text{CH}_2$ twisting		$\nu_{13}$	$\nu_{24}$	$\nu_7$	$\nu_{24}$	$\nu_{12}$	$\nu_{36}, \nu_{37}$
$\text{C}-\text{C}\equiv\text{C}$ str.	$\nu_6$		$\nu_{25}$	$\nu_8$	$\nu_{25}$	$\nu_{13}, \nu_{14}$	$\nu_{38}$
$\text{C}-\text{N}$ str.	$\nu_7$		$\nu_{26}$	$\nu_9$	$\nu_{26}$	$\nu_{15}, \nu_{16}$	$\nu_{39}$
$-\text{CH}_2$ rocking		$\nu_{14}$	$\nu_{27}$	$\nu_{10}$	$\nu_{27}$	$\nu_{17}$	$\nu_{40}, \nu_{41}$
$-\text{C}\equiv\text{C}-\text{H}$ def. (in-plane)	$\nu_8$		$\nu_{28}$	$\nu_{11}$	$\nu_{28}$	$\nu_{18}, \nu_{19}$	$\nu_{42}$
$-\text{C}\equiv\text{C}-\text{H}$ def. (out-of-plane)		$\nu_{15}$	$\nu_{29}$	$\nu_{12}$	$\nu_{29}$	$\nu_{20}$	$\nu_{43}, \nu_{44}$
CCN bending	$\nu_9$		$\nu_{30}$	$\nu_{13}$	$\nu_{30}$	$\nu_{21}, \nu_{22}$	$\nu_{45}$
$-\text{C}-\text{C}\equiv\text{C}$ def. (in-plane)	$\nu_{10}$		$\nu_{31}$	$\nu_{14}$	$\nu_{31}$	$\nu_{23}, \nu_{24}$	$\nu_{46}$
$-\text{C}-\text{C}\equiv\text{C}$ def. (out-of-plane)		$\nu_{16}$	$\nu_{32}$	$\nu_{15}$	$\nu_{32}$	$\nu_{25}$	$\nu_{47}, \nu_{48}$
CNC bending	$\nu_{11}$		$\nu_{33}$	$\nu_{16}$	$\nu_{33}$	$\nu_{26}, \nu_{27}$	$\nu_{49}$
Torsion along CN bond		$\nu_{17}$	$\nu_{34}$	$\nu_{17}$	$\nu_{34}$	$\nu_{28}$	$\nu_{50}, \nu_{51}$

\* The  $a_2$  type modes in  $\text{C}_{3v}$  symmetry transform into  $a''$  type modes in  $\text{C}_s$  symmetry. The corresponding transformation for the degenerate modes of the  $\text{C}_{3v}$  or  $\text{C}_3$  symmetry in  $\text{C}_s$  symmetry is ( $a' + a''$ ).

TABLE 5.3

## VIBRATIONAL SPECTRA AND ASSIGNMENT OF TRIPROPARGYL AMINE

Infrared spectra of						Raman spectrum of			Interpretation*
Liquid		Vapour		Solid		Liquid			
(cm <sup>-1</sup> )	Int.	(cm <sup>-1</sup> )	Int.	(cm <sup>-1</sup> )	Int.	(cm <sup>-1</sup> )	Int.	Qual. depol.	
3302	s	3305	s	3286 } 3280 }	s				$\nu_{18}$
3288	m	3292	m	3266	m				$\nu_1$
3262	vw	3275	vw	3241	m				$\nu_4 + 2X \nu_{29}$
				2949	vw				$\nu_9 + \nu_{28} + \nu_5$
				2935	vw				$\nu_9 + \nu_{29} + \nu_{22}$
2928	s	2945 } 2934 }	s	2924	m	2934 } 2918 }	s	P	$\nu_2, \nu_{19}$
2876 } 2867 }	m	2895 } 2888 }	w	2876 } 2863 }	diff.	2880 } 2870 }	w	D	$2X \nu_{22}$
				2831	sh				$\nu_6 + \nu_{22}$
2817	s	2826 } 2821 }	s	2822	s	2818	s	P	$\nu_3, \nu_{20}$
2757	w	2759	vw	2757	vw	2755	vw		$\nu_5 + \nu_{23}$
				2725	vw	2718	vw		$2X \nu_{28} + \nu_6$
2710	vw	2713	vw	2700	vw	2695	vw	P	$2X \nu_6$
		2645	vw	2660	vw				$2X \nu_{23}$
		2122	vw	2120	w	2123	vs	P	$\nu_4, \nu_{21} C \equiv C \text{ str.}$
		2108	vw			2105	vs	P	$C \equiv C \text{ str., Isomer}$
1682	vw	1683	vvw	1676	vw				$\nu_{15} + \nu_{22}$
1621	vw			1617	vw				$\nu_{16} + \nu_{22}$
		1504	vvw						$\nu_9 + \nu_{28}$

Contd...

Table 5.3 Contd...

138

				1474	diff.				2X $\nu_{27}$
1445	s	1454 } 1448 }	s	1442 } 1435 }	s	1442	m	D	$\nu_{22}$
1434	sh	1426	sh	1427	sh	1428	m	D	$\nu_5$
1371	sh	1370	diff.	1367	s	1372	sh	?	2X $\nu_{28}$
1362	s	1365	ms	1357	s	1359	mw	P	$\nu_6$
1342	sh	1344	ms						CH <sub>2</sub> wag., Isomer
1331	s	1333	ms	1331	s	1330	w	D	$\nu_{23}$ , CH <sub>2</sub> wag.
1308	w	1304	w	1305	ms				$\nu_{11} + \nu_{28}$
1278	w	1294	vw	1287	ms	1280	w	D	$\nu_{11} + \nu_{12}$
1254	s	1253	ms	1251	s	1247	mw	D	$\nu_{24}$
				1239	w, sh				$\nu_7$
						1214	vw	D	2X $\nu_{12}$
				1180 } 1170 }	vw				$\nu_9 + \nu_{31}$
1126	s	1127	s			1123	w	D?	C-N str., Isomer
1116	s	1108	s	1114 } 1110 }	s	1108	w	D	$\nu_{26}$ , C-N str.
1010	sh								$\nu_{15} + 2X \nu_{31}$
1001	ms	1003	sh	1002	s				$\nu_9 + \nu_{16}$
979	s	984	s	985 } 980 }	s	980 } 970 }	mw	P?	$\nu_{25}$
955	w	946	vw	944	ms	951	vw	P	$\nu_{12} + \nu_{15}$
923	sh	924	w, sh	925	sh	922	vw	?	$\nu_{30} + \nu_{33}$
903	s	904	ms	900	s	897	w	P	$\nu_8$
839	ms	841	m, sh			838	s, sh	P	C-N str., Isomer
828	s	830	m	831	ms	827	vs	P	$\nu_9$ , C-N str.
		724	w	747	m				$\nu_{10}, \nu_{27}$
670	m, sh	666	sh	699	s, sh	673	sh	D	$\nu_{28}$
654	vs	659 } 653 }	vs	685	s	659	w	P	$\nu_{11}$

Contd...

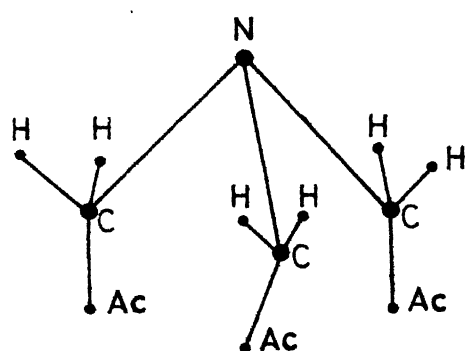
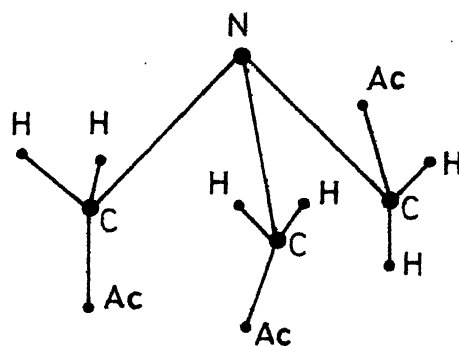
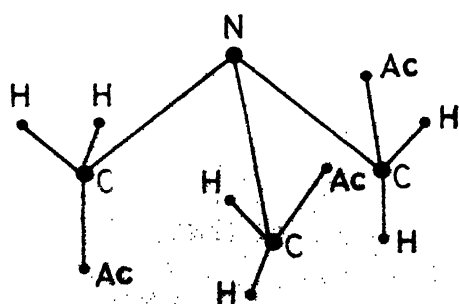
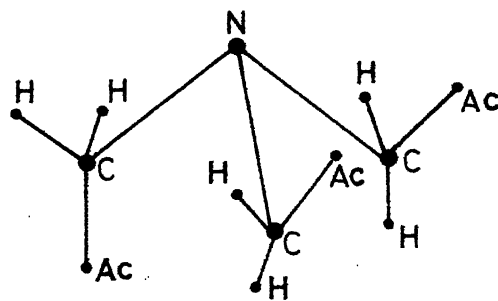
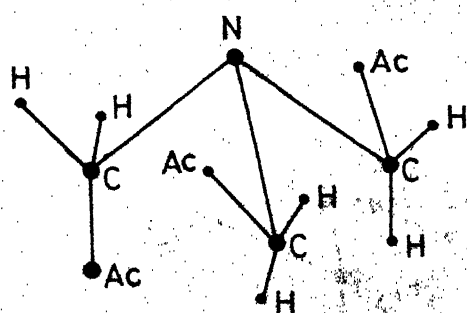
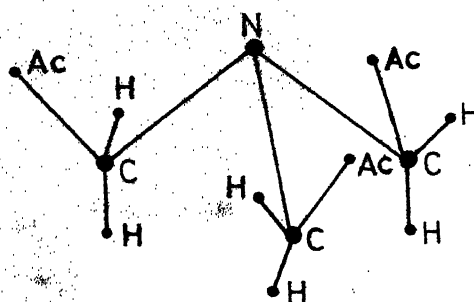
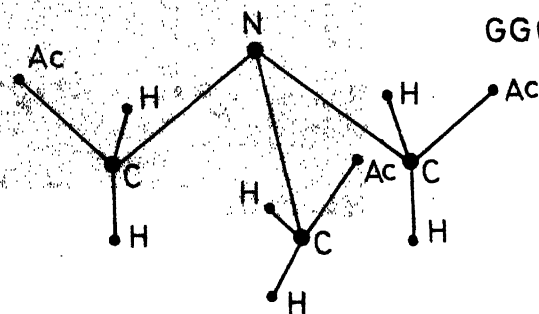
TTT ( $C_{3v}$ )TTG ( $C_1$ )TGG ( $C_1$ )TGG' ( $C_s$ )TG'G ( $C_1$ )GGG ( $C_3$ )GGG' ( $C_1$ )

Fig. 6.1: The spectroscopically distinguishable conformers and point groups of  $(N-CEC-CH_3)_3N$ . 'Ac' stands for the acetylenic  $(-CEC-N)$  group.

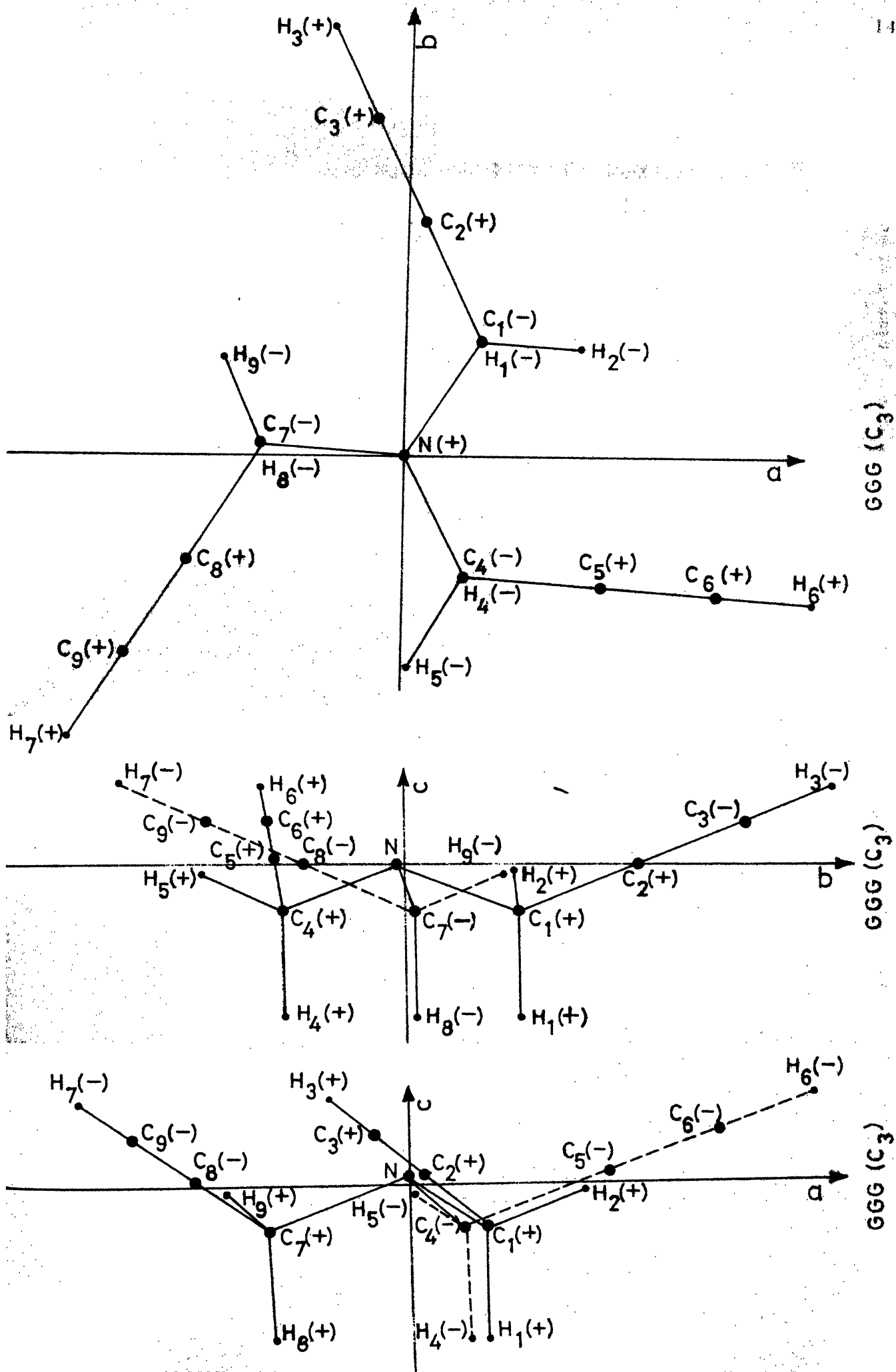


Fig. 3.2(AA): The projections of the GGG form of TPA on the three planes of principal axes. The + and - signs indicate that the atom lies above and below the plane respectively.



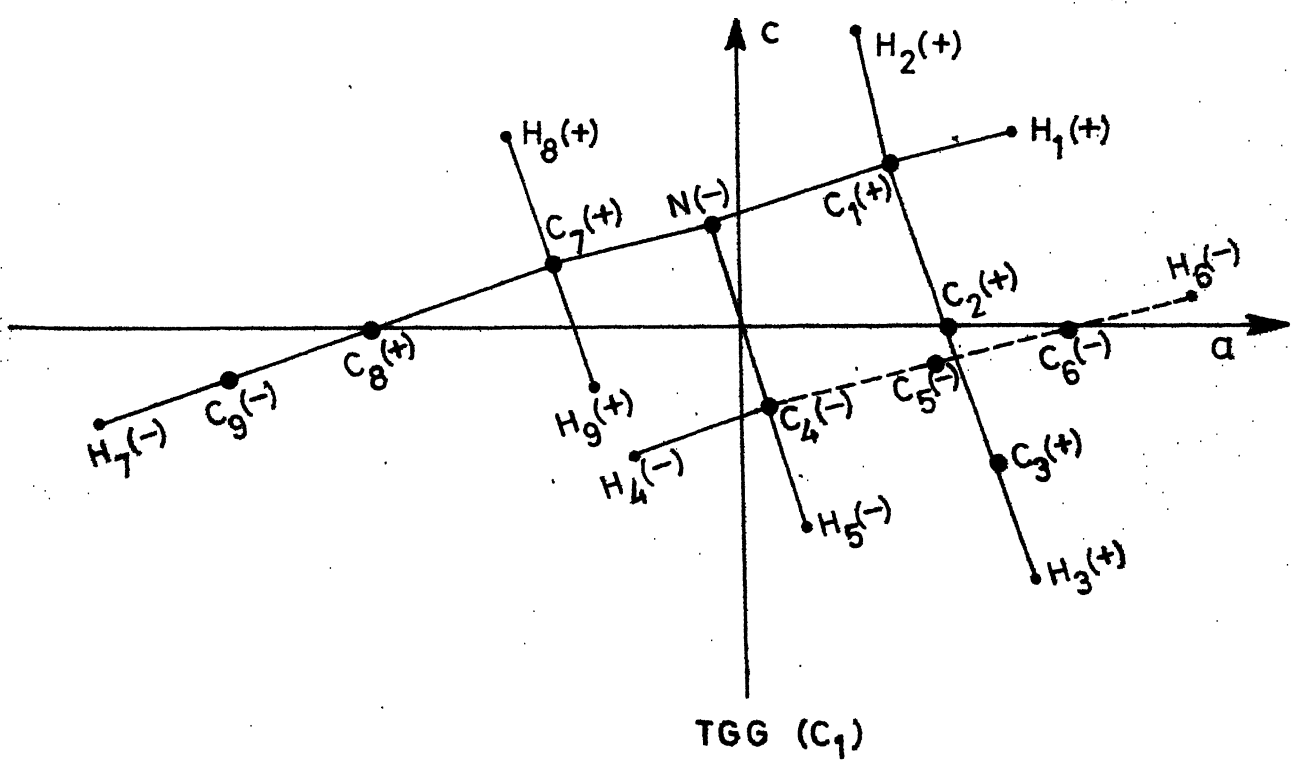
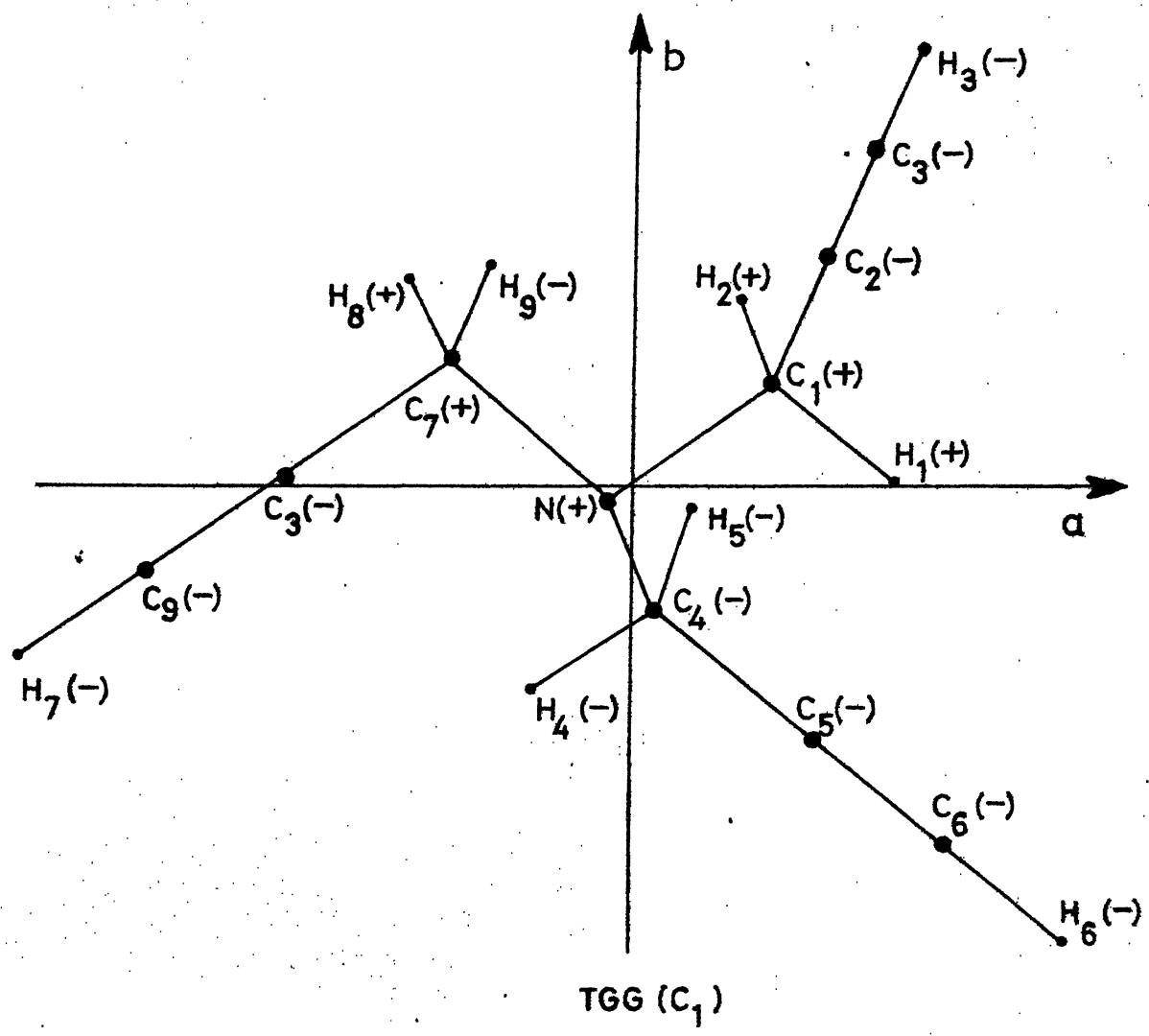


Fig. 5.2(B): The projections of the TGA form of TPA on the  $a$  -  $b$  and  $a$  -  $c$  planes of principal axes system. The + and - signs indicate that the atom lies above and below the plane respectively.

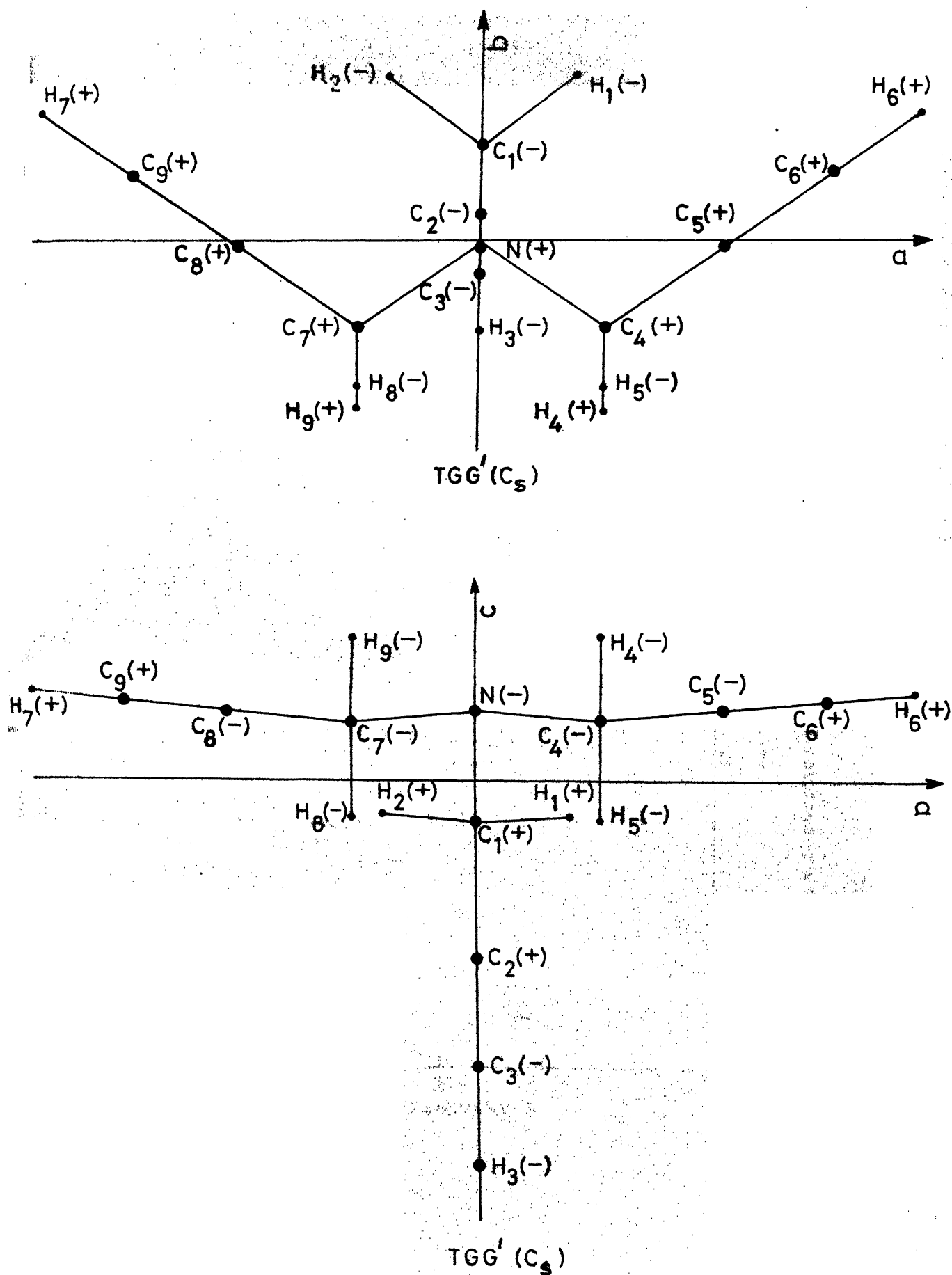


Fig. 1.24C: The projections of the TGG' form of TPA on the  $a-b$  and  $a-c$  planes of the principal axes system. The  $+$  and  $-$  signs indicate that the atom lies above and below the plane respectively.

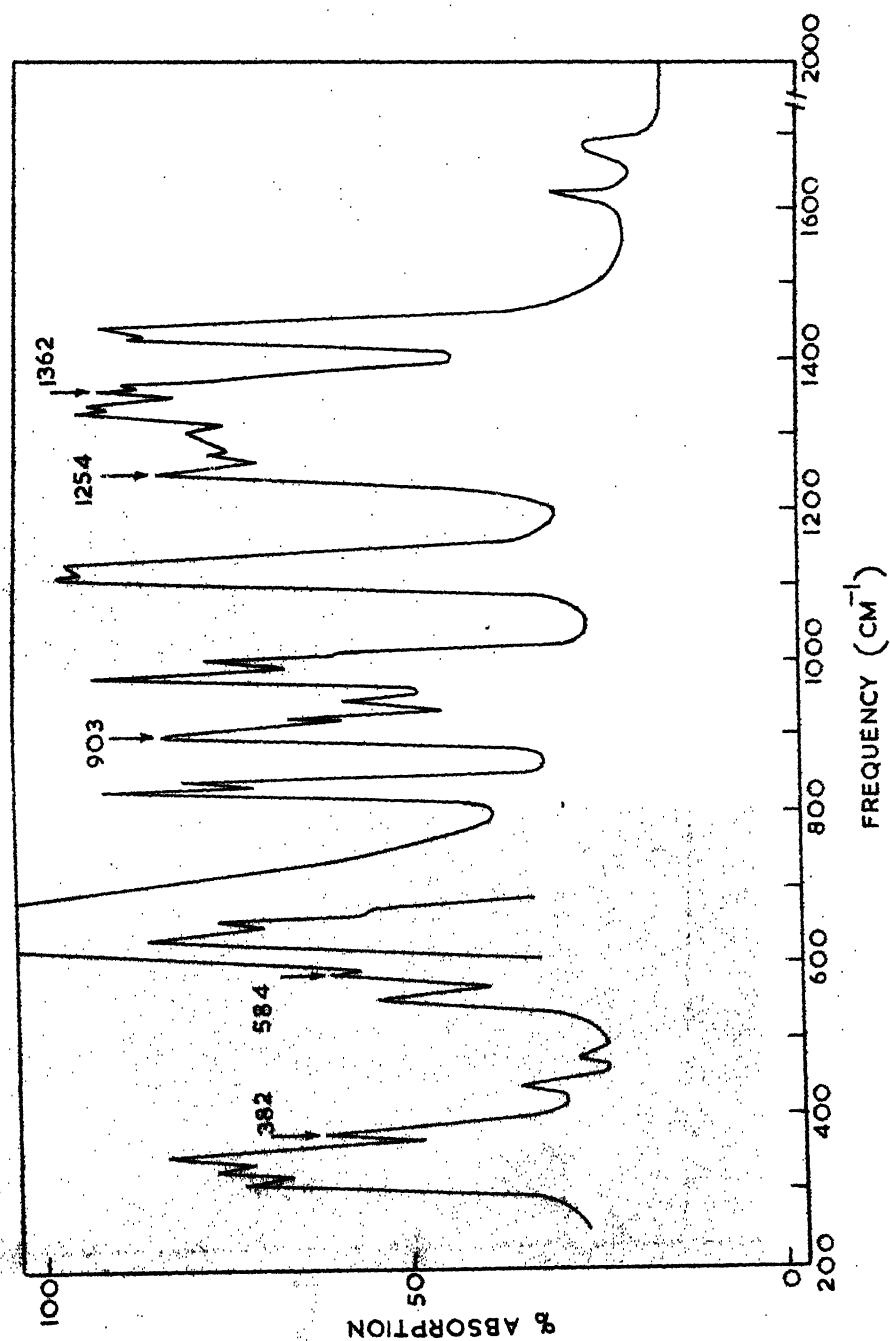


Fig. 5.3(A): Infrared absorption spectrum of liquid TPA (250-2000  $\text{cm}^{-1}$ ); thin film.

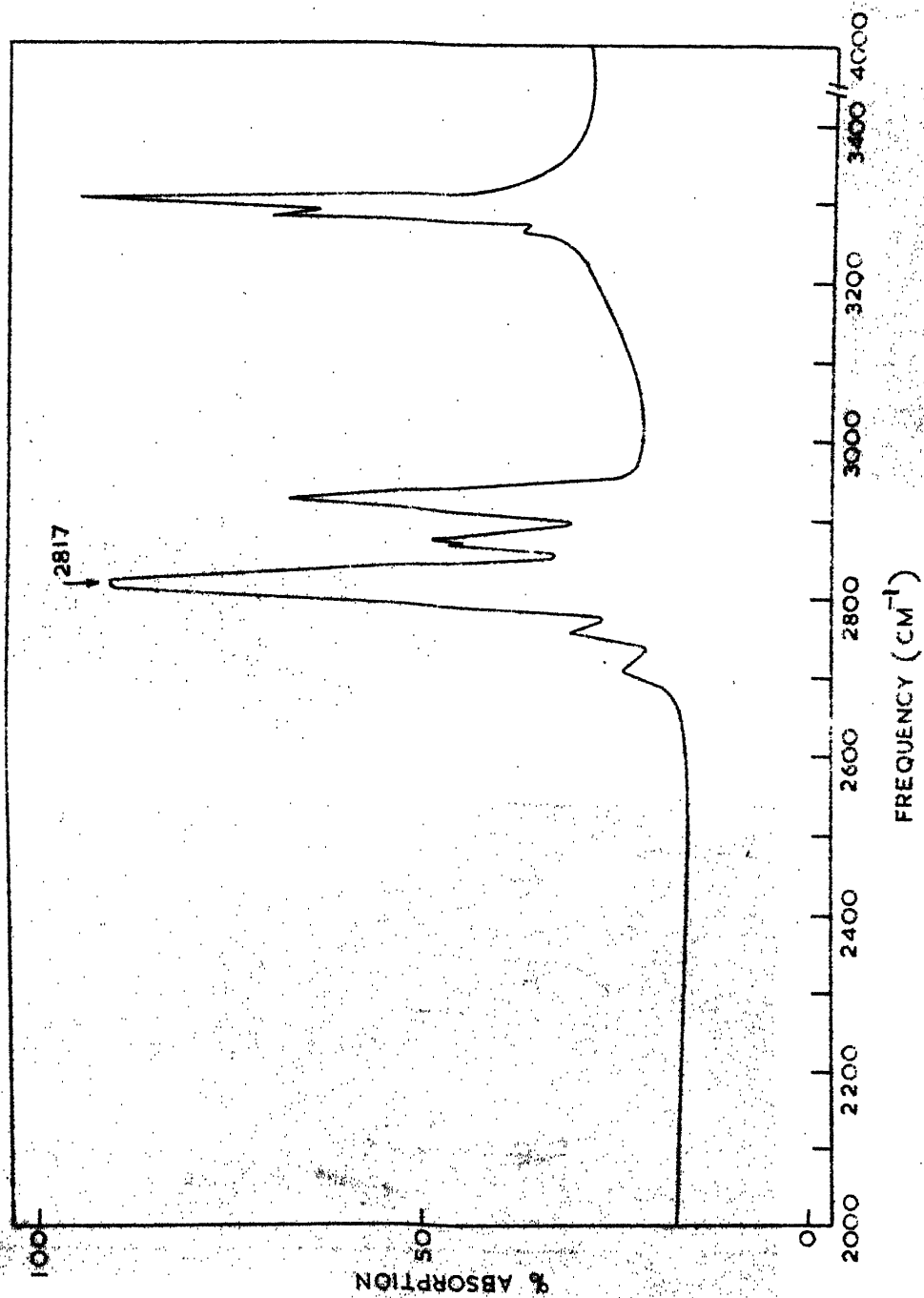


Fig. 5.3(B): Infrared absorption spectrum of liquid TPA (2000-4000  $\text{cm}^{-1}$ ); thin film.

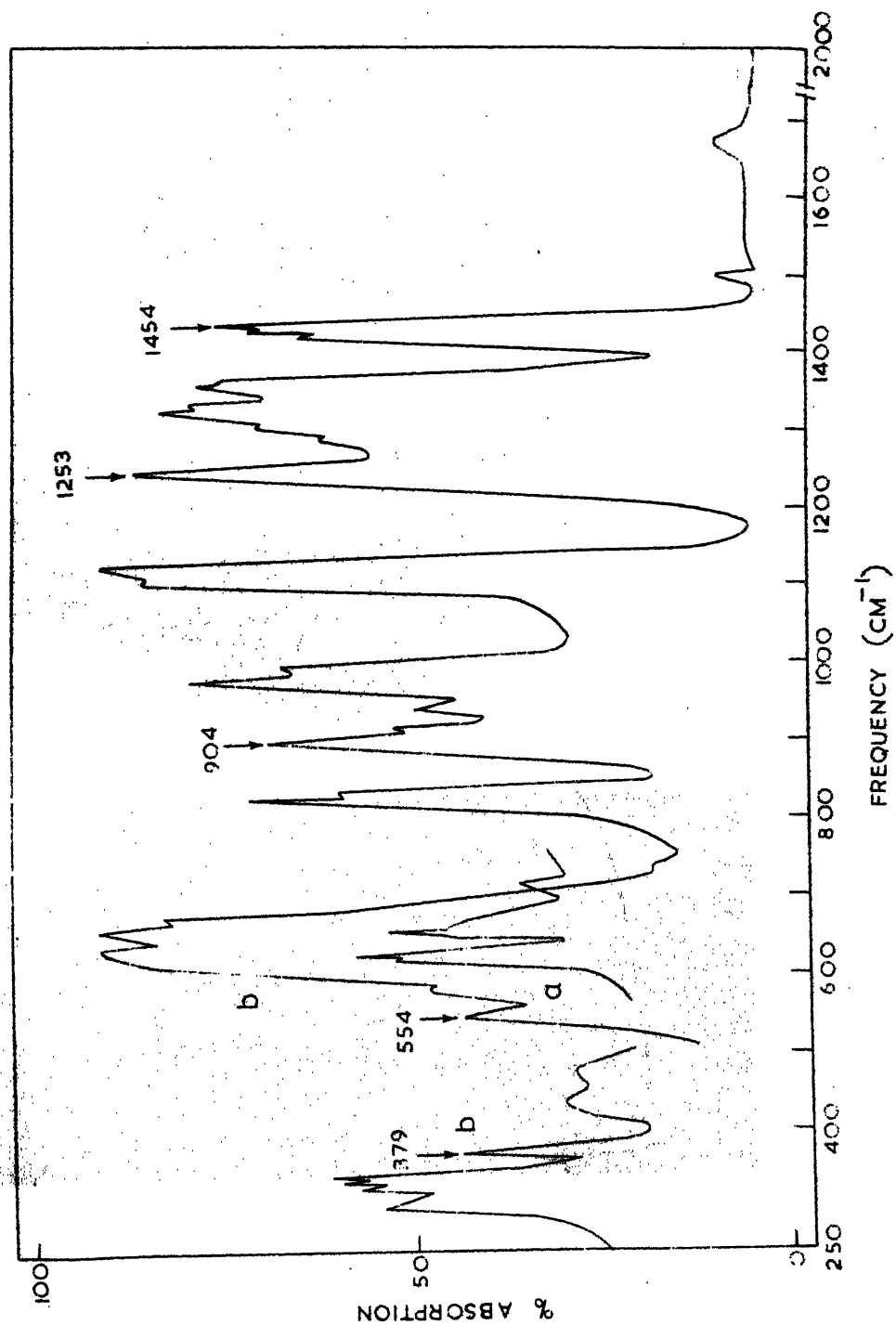


Fig. 5.4(A): Infrared absorption spectrum of TPA in the vapour phase ( $250\text{--}2000\text{ cm}^{-1}$ );  $10\text{ cm}$  path length. The letters **a** and **b** designate the saturated vapour pressures inside the gas cell at temperatures  $\sim 40^\circ$  and  $\sim 80^\circ\text{ C}$  respectively.

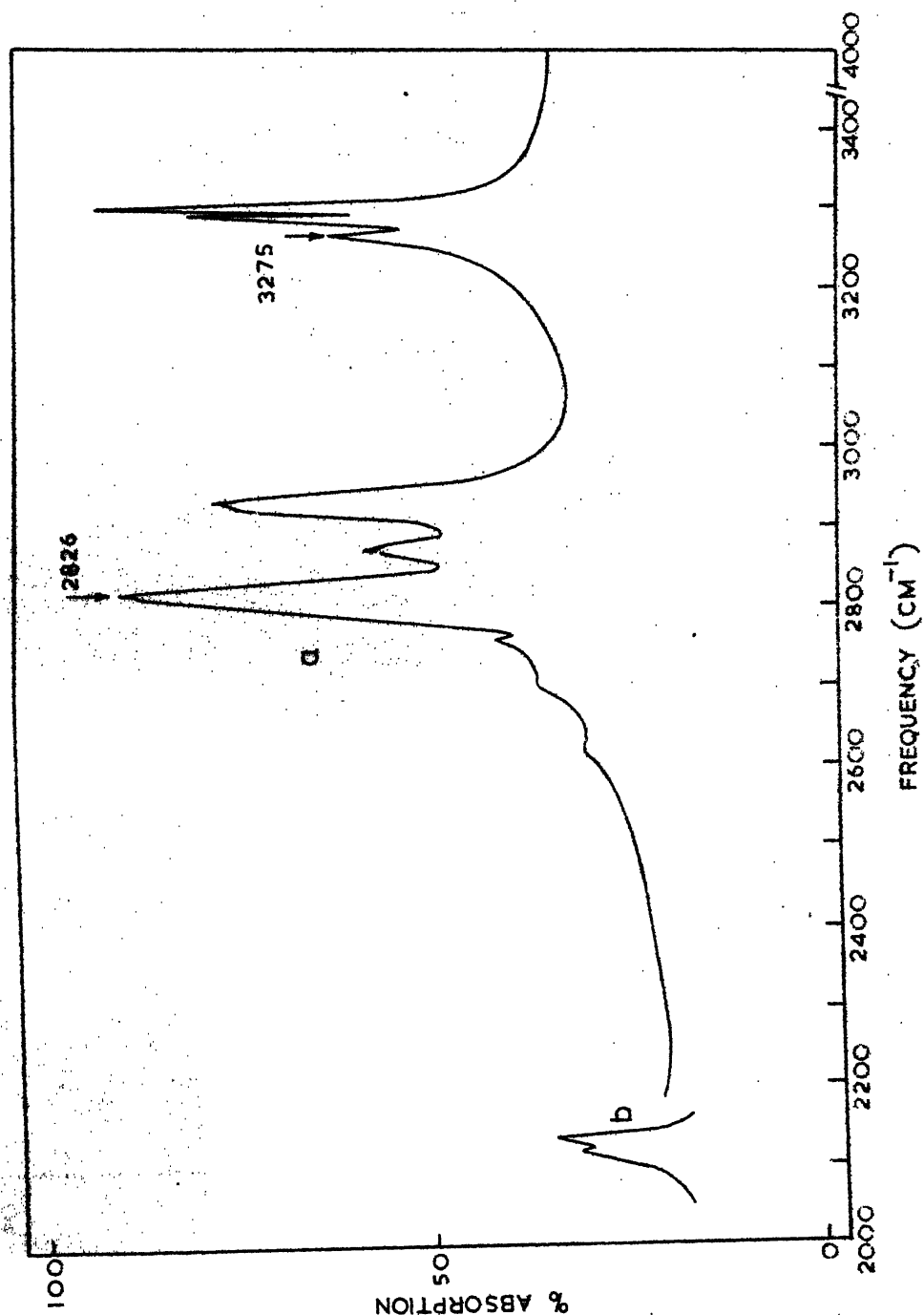


Fig. 5.4(B): Infrared absorption spectrum of TPA in the vapour phase (2000-4000  $\text{cm}^{-1}$ ); 10 cm path length. The letters a and b designate saturated vapour pressures inside the gas cell at temperatures  $\sim 40^\circ\text{C}$  and  $\sim 80^\circ\text{C}$  respectively.

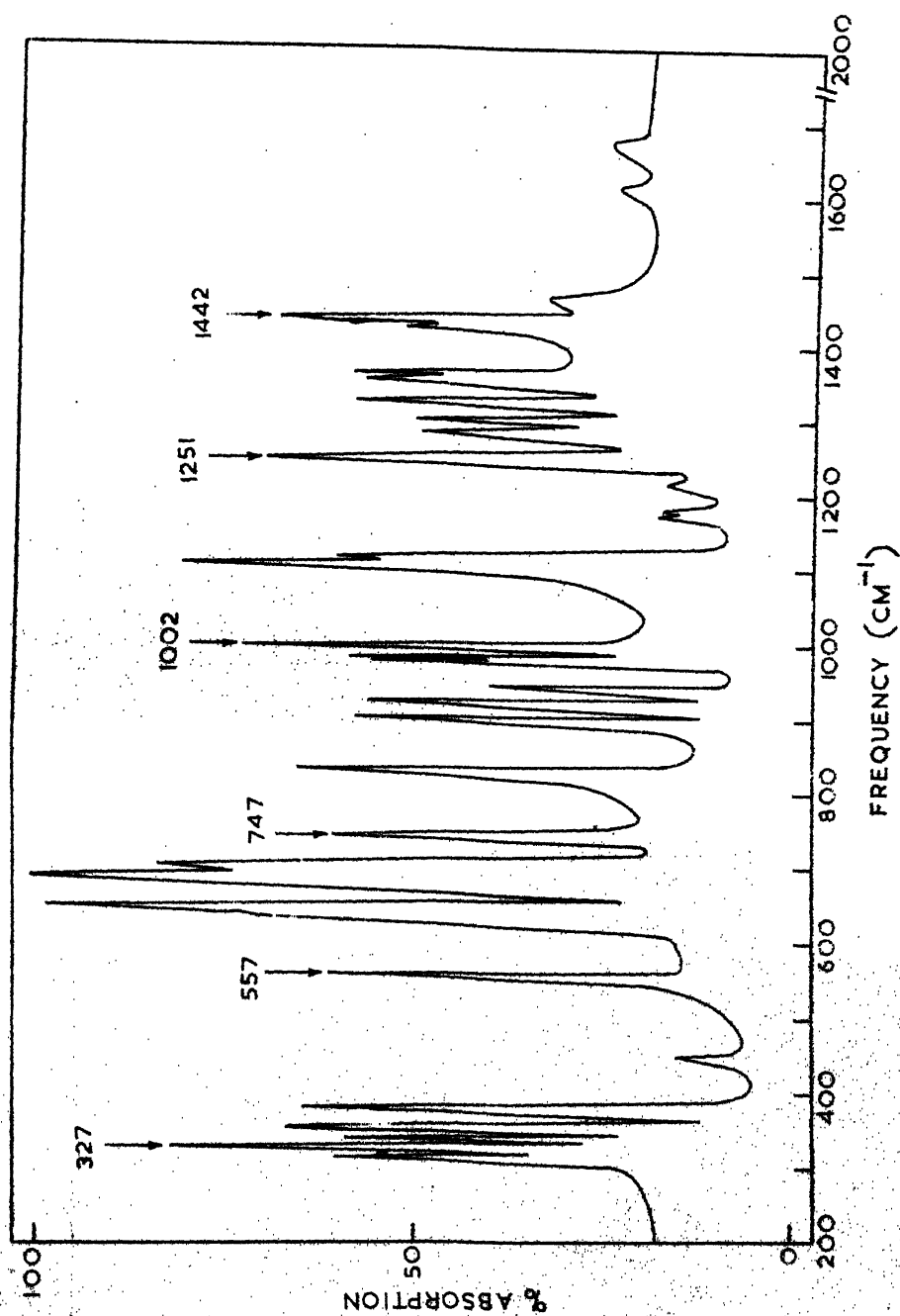


Fig. 5.5(A): Infrared absorption spectrum of a solid film of TPA near 77°K (250-2000  $\text{cm}^{-1}$ ).

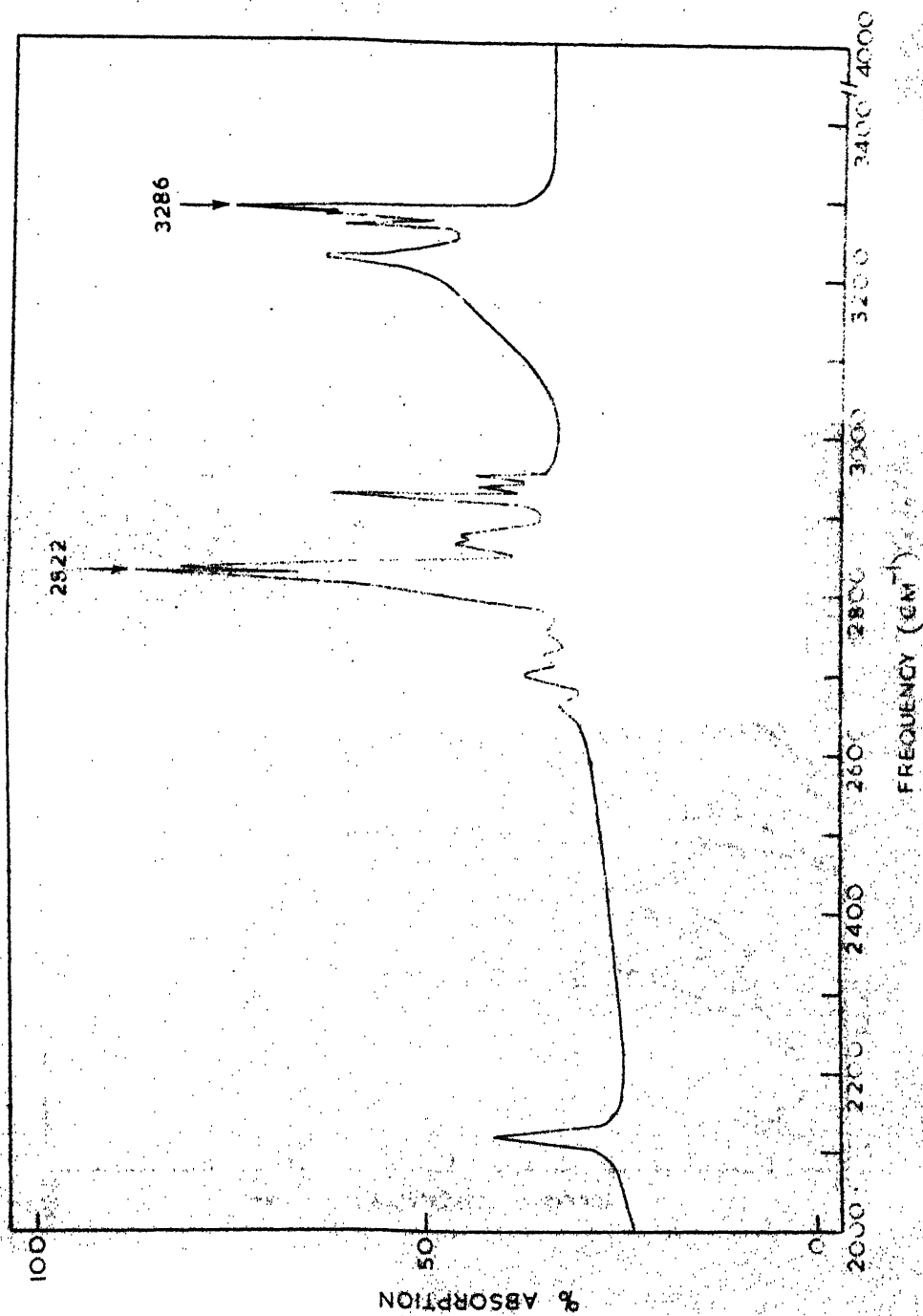


Fig. 5.5(3): Infrared absorption spectrum of a solid film of TPA near 77°K (2000-4000 cm<sup>-1</sup>).



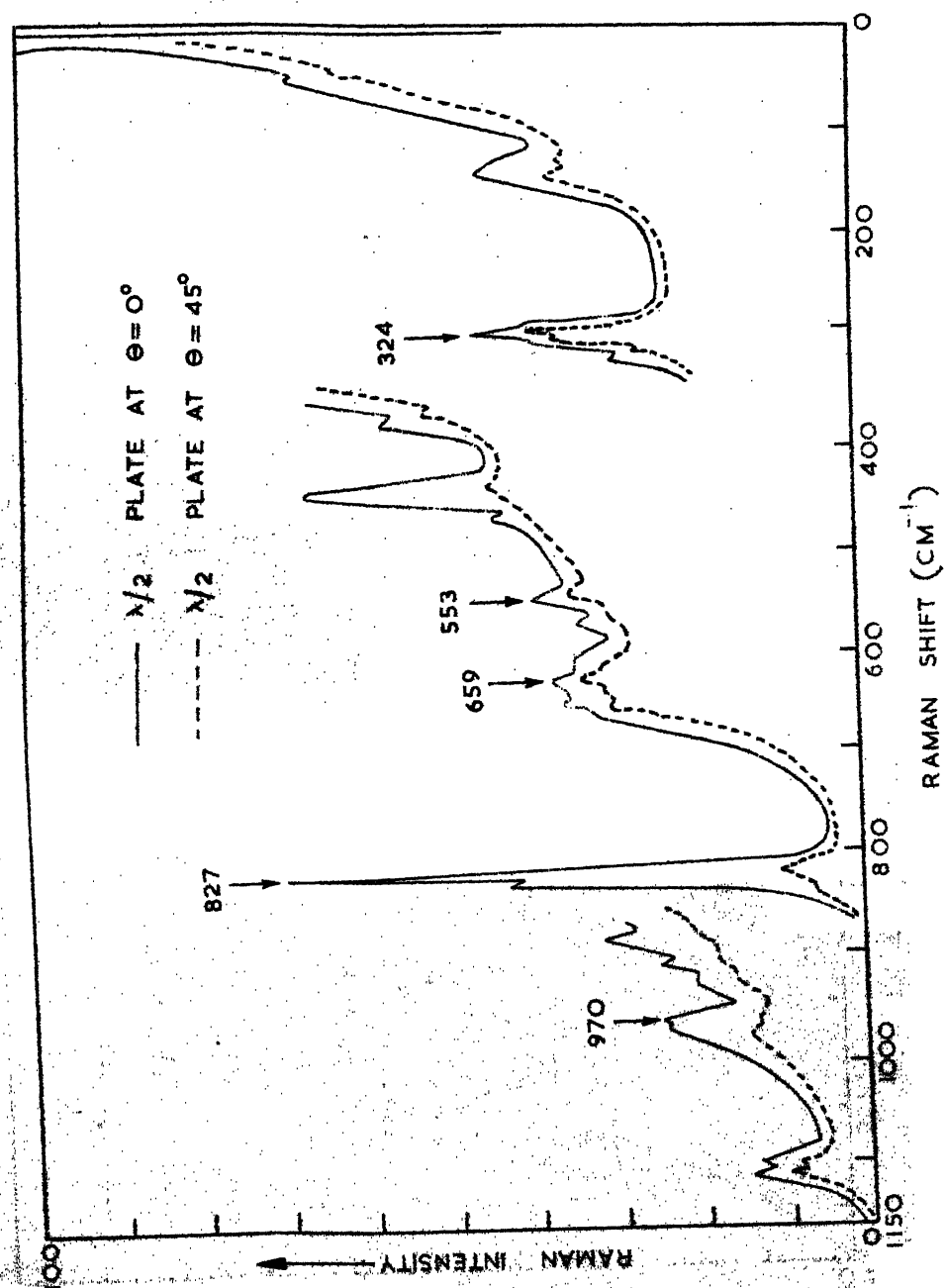


Fig. 5.6(A): The laser-Raman spectrum of the liquid TPA at room temperature (0-1150  $\text{cm}^{-1}$ ).

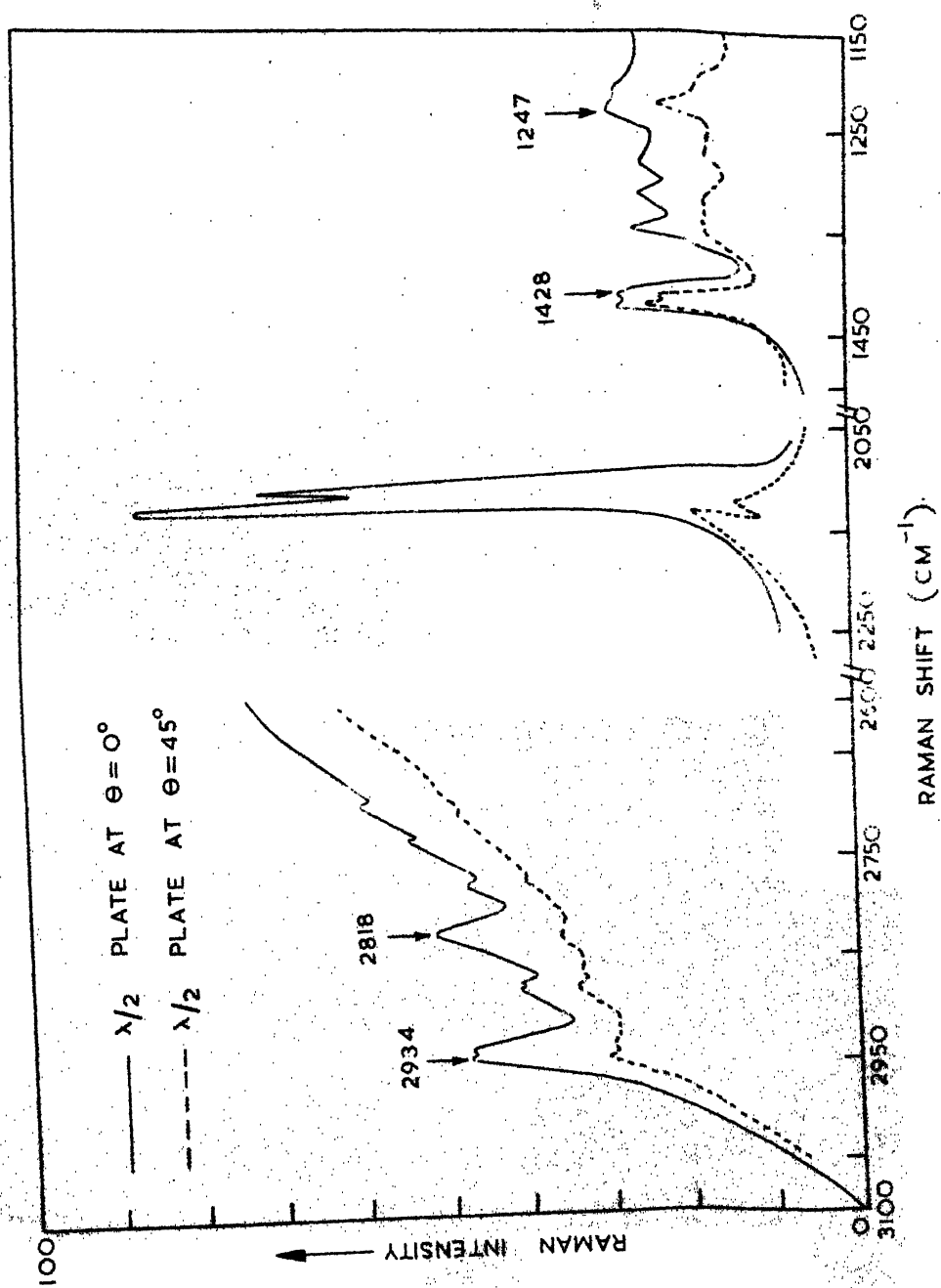


Fig. 5.6(B): The laser-Raman spectrum of liquid TPA at room temperature (1150-3100 cm<sup>-1</sup>).

## CHAPTER VI

### VIBRATIONAL SPECTRA OF TRIALLYL AMINE AND ROTATIONAL ISOMERISM

## ABSTRACT

The infrared spectra of triallyl amine in the vapour and liquid phases, as solutions in  $\text{CS}_2$ ,  $\text{CCl}_4$ ,  $\text{CH}_3\text{Cl}$  and  $\text{CH}_3\text{CN}$ , and in the solid state at low temperature were measured over the frequency range 250 to  $4000\text{ cm}^{-1}$ . The Raman spectrum of the liquid was photoelectrically recorded and qualitative depolarization measurements were made. It is shown that in the liquid and vapour phases, the molecule exists as a mixture of at least two rotational isomers while in the crystalline phase, it assumes a single configuration having point group symmetry  $\text{C}_3$ . A vibrational assignment for the observed bands in the infrared and Raman spectra is presented on the basis of the  $\text{C}_3$  point group symmetry for the more stable form of the molecule.

## INTRODUCTION

There has been considerable interest in the biological and chemical aspects of allyl amines<sup>1,2</sup>, but only a few vibrational studies seem to have been made for them. The vibrational spectra of monoallyl<sup>3,4</sup> and diallyl amines<sup>5</sup> were reported previously and only a partial vibrational assignments of the observed bands were made. In the Chapter III, the vibrational spectra of allyl amine were reported and it was shown that the molecule exists in the two rotational forms in fluid phase. In this chapter, we report and discuss the vibrational spectra of somewhat more complicated molecule of this series, viz., triallyl amine. This molecule was chosen for this study as it may be expected to have some order of symmetry which may facilitate the vibrational assignment.

The structure of triallyl amine has not been so far determined, but the steric considerations suggest the possibility of several rotational conformers in this molecule (the projections of the three GGG forms are shown in Figure 6.1). The relative proportion of different isomeric forms is expected to vary with temperature, the polarity of solvents and the change in phase of the compound. Since internal rotation is not possible in the solid phase, only one form of the molecule with lower energy is expected to get stabilized at low temperature. The depolarization data of the Raman lines would be helpful in drawing inferences about the symmetry of various forms present. Hence a correlative study of the infrared spectra in the solid phase with that of the vapour, liquid (and in solutions of various solvents) and the Raman spectrum may give information about

the isomeric forms of triallyl amine. With these facts in mind, a systematic vibrational study of triallyl amine was undertaken and the results obtained are discussed here.

#### EXPERIMENTAL

The sample of triallyl amine was a K and K laboratories product and was vacuum distilled before use. Only the middle fraction of the distillate was used for the vibrational measurements. The infrared spectra in the vapour, liquid and solid phases were recorded in the usual manner as described in Chapter II and are shown in Figures 6.2, 6.3 and 6.4 respectively (given at the end of the Chapter).

The Raman spectrum of the liquid sample at room temperature was obtained with the Raman cell of volume 1 cc and qualitative depolarization ratios were measured according to the method described in Chapter II. The corrections for the observed peak heights, convergence error and other instrumental errors were not made and therefore these ratios can be used only as a guide to the band assignments. The tracings of the Raman spectrum for this compound are shown in Figure 6.5. The infrared and Raman spectral data are listed in Table 6.2.

#### DISCUSSION

In the absence of any structural data for triallyl amine (TAA), it seems reasonable to assume that the three carbon atoms of the  $-\text{CH}_2$  groups\* in TAA are coplanar forming an equilateral triangle with the nitrogen atom lying at the centre of this triangle in the pyramidal position. The symmetry of the molecule depends upon the position and orientation of the remaining atoms of the three allyl groups in TAA.

---

\*  $-\text{CH}_2$  represents methylene group attached to the nitrogen atom.

There are two axes for each allyl group about which internal rotation is possible; one being along the C-C bond and the other along C-N bond. Therefore the possibility of rotational isomerism, giving rise to 'trans', 'gauche' and 'gauche' forms about each of the three N-C bonds; and further, 'cis', 'gauche' and 'gauche' forms about each of the C-C bonds of the three allyl groups, in turn, would give rise to several possible conformations for TAA. The possible symmetry point groups, to which the different rotational conformers of TAA may belong, are  $C_1$ ,  $C_s$ ,  $C_3$  or  $C_{3v}$ . All the possible conformations may not be spectroscopically distinct and steric interactions among different atoms of the groups, the  $\pi$ -orbitals of the C = C double bonds and the lone pair electrons of nitrogen may eliminate the possibility of some of them to be thermodynamically stable at normal temperatures. Corresponding to internal rotation about any of the N-C bonds in TAA, the trans (T) or gauche (G) configuration is taken with respect to the lone pair orbitals of nitrogen atom. For rotations about the C-C bonds of allyl groups; the dihedral angle is taken to be zero for the 'cis' configuration of the N-C-C = C skeleton.

If the N-C-C = C skeletons for all the three allyl groups are assumed to exist in the 'cis' configuration, the TTT configuration of TAA with respect to internal rotation about the N-C bonds may have  $C_{3v}$  symmetry. Under this point group symmetry, the sixty-nine fundamental modes may be divided as  $15 a_1 + 8 a_2 + 23 e$ , all the vibrations, except  $a_2$  type, being active in both the infrared and Raman spectra. However, the steric considerations suggest that this form of the molecule will be highly strained and hence should make the structure unstable.

The GGG configurations of the molecule, for either the 'cis', 'gauche' or 'gauche' positions of the three N-C-C = C skeletons, with all the skeletons having the similar configuration at the same time, can have at most a  $C_3$  - axis of rotation as an element of symmetry. For different configurations of the three N-C-C = C skeletons, the GGG configurations may have different point group symmetries other than  $C_3$ . The three GGG configurations, with all the N-C-C = C skeletons existing in either the 'cis', 'gauche' or 'gauche' positions simultaneously, may be designated as GGG(I), GGG(II) and GGG(III) respectively for convenience. The rotational constants are calculated for these three GGG forms of TAA by assuming the following parameters<sup>6</sup>:  $r_{C-N} = 1.472 \text{ \AA}$ ,  $r_{C-C} = 1.488 \text{ \AA}$ ,  $r_{C=C} = 1.333 \text{ \AA}$ , all the  $r_{C-H} = 1.09 \text{ \AA}$ ,  $\angle C_1 C_2 C_3 = 124^\circ 30'$ ,  $\angle C_2 C_3 H_4 = 121^\circ$ ,  $\angle C_3 C_2 H_3 = \angle C_2 C_3 H_5 = 119^\circ$ ,  $\angle H_4 C_3 H_5 = 120^\circ$ ,  $\angle C_1 C_2 H_3 = 116^\circ 30'$  and all other bond angles tetrahedral. The rotational constants and the calculated PR separation<sup>7</sup> for the three GGG forms are given in Table 6.1. The numbering of the atoms is shown in Figure 6.1. Within this  $C_3$  point group symmetry, the sixty-nine fundamental vibrations should divide into symmetry species as

$$\Gamma_{\text{vib}} = 23 a + 23 e$$

with all vibrations being infrared and Raman active. The molecule is an oblate symmetric top in all the three GGG configurations and hence parallel and perpendicular type of bands (with their PR separation as shown in Table 6.1) are expected in the vapour phase.

In the most unsymmetrical forms of the molecule ( $C_1$  symmetry), all the sixty-nine normal modes should appear in both the infrared



and Raman, with all the lines appearing as polarized Raman lines. The other possible configurations with  $C_s$  symmetries could be those in which one allyl group is oriented such that the  $N-C-CH=CH_2$  atoms lie in a plane ('cis' position) and the other two allyl groups are having the symmetrical positions with respect to the third allyl group (being in 'trans' position corresponding to rotations along C-N bond). For these configurations with  $C_s$  point group symmetries, there must be 38  $a'$  and 31  $a''$  species of vibrations and all of them should show up lines in both the infrared and Raman spectra. The  $a'$  modes are expected to appear as polarized and  $a''$  modes as depolarized Raman lines.

A comparison of the infrared spectrum of the solid TAA with that of the liquid and vapour phases at different temperatures reveals a number of sets of bands displaying differences in relative intensities between the liquid or vapour and solid phases and thus suggesting the presence of rotational isomers in this molecule. Some major simplifications occur on freezing in the band pairs (557, 590); (848, 866), and (1074, 1108)  $cm^{-1}$  which are ascribed to different isomers. The relative intensities of the pair of bands are also affected in different solvents of varying polarity. In solutions with non-polar solvents ( $CCl_4$  and  $CS_2$ ), the intensity of the bands at 557 and 1074  $cm^{-1}$  increases relative to those at 590 and 1108  $cm^{-1}$ , while in polar solvents ( $CH_3CN$ ,  $CH_3Cl$  etc.), the intensity of the bands at 557 and 848  $cm^{-1}$  decreases in comparison with the other components of the pairs. This behaviour shows that the isomeric equilibrium of different conformers changes in various solvents differing in their polarity.

On heating above room temperature in the vapour phase (unto  $\sim 100^\circ C$ ), the components of the bands of each pair are broadened and their

relative intensities are altered so that the intensity of the lower frequency components at 557, 848 and 1074  $\text{cm}^{-1}$  increases relative to their companion bands. This is consistent with the low temperature spectra in which the other component of each pair is the one that remains in the solid phase.

Warming and recooling the initial deposit gave rise to a crystalline solid whose spectrum is virtually the same as that of the original deposit except for the presence of a number of very sharp doublets. No bands were found to disappear as a result of annealing suggesting thereby that only one of the possible isomers could have been present in the original deposit. In the crystalline state, the splitting of some of the bands into close doublets is typical to that expected for a molecule having three fold or higher rotation axis. This splitting may be due to crystal field effects or lower symmetry point group of the subgroups - the effect of which is to remove the degeneracy causing each pair of vibrations that would normally be degenerate to appear as a very close doublet (site-group splittings). The a-type non-degenerate vibrations appear as a single sharp line. We therefore assume that the molecular species in the crystalline state at low temperature possess the  $C_3$  point group symmetry. Now there are three possible conformations, the GGG(I), GGG(II) and GGG(III) of TAA which may exist with  $C_3$  symmetry of the molecular frame. By analogy with the situation in allyl halides<sup>8</sup>, the 'cis' configurations of the  $\text{N-C-C} = \text{C}$  frames would be expected to have higher energies than the 'gauche' configurations with increase in the size of the substitution at the methylene carbon atoms of allyl groups. Hence the GGG(I) configuration of TAA may be expected to have higher energy than the other

two conformations. The steric considerations suggest that the GGG(III) form, with all the three N-C-C = C skeletons in the 'gauche' positions, will be favoured over the GGG (II) form. The observed P-R separation for some of the bands in the spectrum of vapour phase is in agreement with the calculated values for the GGG(III) form. On the basis of these arguments, it may be said that the GGG(III) form with  $C_3$  symmetry is existing and contributing to the observed spectrum at liquid nitrogen temperature in the crystalline phase.

In fluid phases, along with the isomer(s) having  $C_3$  symmetry, other isomers of lower symmetries may also be present whose relative concentration is expected to vary with variation in temperature. Out of the four, three lines are depolarized in the liquid phase which disappear at low temperature and therefore suggest that these might be due to the presence of isomer(s) having  $C_3$  or  $C_s$  symmetries and not  $C_1$  symmetry. From the present data it is not clear whether there is only one other isomer or all those which are sterically alike and have nearly a similar spectrum. As an aid to the assignment of the observed spectral data, the modes of vibration of triallyl amine have been classified (Table 6.3) according to the approximate description in terms of the different subgroups in the molecule assuming  $C_3$  point group symmetry for the more stable form of the molecule.

In compounds of this complexity, a particular normal mode of vibration involves the motion of all the atoms in a molecule. However, to a certain approximation, the normal modes may be ascribed to the motion of a particular group of atoms in the molecule, the motion of these atoms being only weakly coupled with the motion of other atoms of the molecule. The internal modes of groups will be only slightly

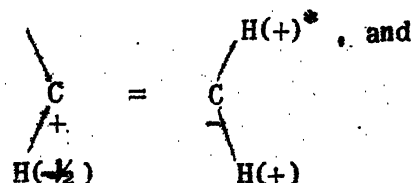
affected if the environment is similar in different molecules. The skeletal and out-of-plane bending modes will be more dependent on the geometry of the molecule, with normal vibrations not being localized to particular bonds, but involving motions of the whole skeleton. This leads to a large amount of coupling between the motions of adjacent bonds and bond angles in molecules. An unequivocal assignment of all the bands in this molecule is therefore difficult. The most probable agreement is tried by correlating the infrared band contours, polarization of Raman displacements, expected splitting in solid phase and the intensity of the bands.

In the vibrational assignment given in Table 6.2, the vinyl group frequencies are assigned on the basis of the revised work of Potts and Nyquist<sup>9</sup> on the out-of-plane modes and by Herzberg<sup>10</sup> and Torkington<sup>11</sup> on the in-plane modes of vinyl and ethylenic groups. The allyl group frequencies are assigned on the basis of the study made by McLachlan and Nyquist<sup>8</sup> on the allyl halides and Sheppard<sup>12</sup> on butene - 1 and Lord and Venkateswarlu<sup>13</sup> on propylene. These assignments are further aided by the present studies on allyl amine described in Chapter III. The fundamental frequencies for triallyl amine are given in Table 6.3 on the basis of  $C_3$  point group symmetry for the more stable form of the molecule.

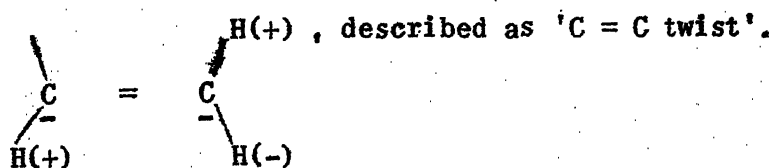
The vibrational assignment for most of the bands is given in Table 6.2 and there is no need to discuss them in detail, but a few bands require special comments. A weak band is observed at  $1296\text{ cm}^{-1}$  in the infrared spectrum and the corresponding Raman band at  $1292\text{ cm}^{-1}$  is very intense. Because of its high Raman intensity, this band is assigned to the in-plane  $=C-H$  deformation  $\nu_{33}$  in analogy with other related compounds. From the geometry of the molecule, it may be seen

that during this vibration, a little change of dipole moment is expected and hence will give rise to weak infrared bands.

According to the study made by Potts and Nyquist<sup>9</sup> on the out-of-plane modes of olefines, the mode giving rise to strong absorption at  $921\text{ cm}^{-1}$  in the infrared is essentially



is described as  $=\text{CH}_2$  wagging motion  $\nu_{39}$ . The same authors have also suggested that the presence of the first overtone of this mode in the infrared may be taken as a sustaining evidence for the correct band assignment. The band at  $1841\text{ cm}^{-1}$  in the infrared spectrum of vapour is probably the first overtone of this mode. Similarly, the strong band at  $998\text{ cm}^{-1}$  in the ir spectrum may arise due to the mode

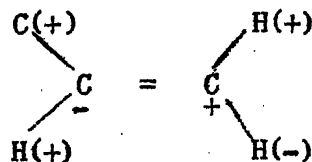


The medium strong band at  $1362\text{ cm}^{-1}$  in the infrared spectrum of the vapour phase shows a doublet nature in the solid state and has been ascribed to the  $-\text{CH}_2$  wagging modes  $\nu_9$  and  $\nu_{32}$  of the lower energy form. The weak band at  $1342\text{ cm}^{-1}$  in the vapour phase spectrum, which disappears in the solid phase, may belong to other isomer(s). In the frequency region  $1050$  to  $1200\text{ cm}^{-1}$ , three bands have been observed in the vapour phase spectrum at frequencies  $1082$ ,  $1115$  and  $1153\text{ cm}^{-1}$ . In this region, the expected modes may be the C-N stretching and the  $-\text{CH}_2$  twisting vibrations. In the solid phase, the band at  $1082\text{ cm}^{-1}$  disappears and the other two bands show up the doublet nature. The corresponding Raman lines are depolarized. The band at  $1115\text{ cm}^{-1}$  has

---

\* (+) and (-) indicate the motion of H - atoms above and below the plane of  $-\text{C}-\text{C}=\text{C}$  atoms respectively.

been assigned to the degenerate C-N stretching mode  $\nu_{36}$  in the GGG(III) form. The disappearing band at  $1062\text{ cm}^{-1}$  may be associated with the C-N stretching mode due to less stable conformer(s). The other bands in this region may be assigned to the  $-\text{CH}_2$  twisting modes with the help of their depolarization ratios in Raman effect and are given in Table 6.2. The medium weakband at  $650\text{ cm}^{-1}$  in the infrared spectrum of vapour may be associated with the vinyl hydrogen out-of-plane deformation  $\nu_{41}$ , described as "cis C-H" wagging mode,



The corresponding Raman line at  $652\text{ cm}^{-1}$  is depolarized. The polarized shoulder at  $642\text{ cm}^{-1}$  may belong to the other mode  $\nu_{18}$ . In 3-methyl butene -1 molecule, Ziomek and Forrette<sup>14</sup> have assigned the band at  $672\text{ cm}^{-1}$  to the similar type of mode.

The liquid phase infrared spectrum shows three bands at frequencies  $866$ ,  $854$  and  $848\text{ cm}^{-1}$ , with the last two lines appearing as a doublet having more intensity than the band at  $866\text{ cm}^{-1}$ . The Raman lines at  $846\text{ cm}^{-1}$  and  $862\text{ cm}^{-1}$  are medium intense and polarized. One of the lines of this doublet ( $854$ ,  $848\text{ cm}^{-1}$ ) may arise due to some overtone. In the solid phase, the intensity of the band appearing at  $855\text{ cm}^{-1}$  has reduced as compared to that of the band at  $870\text{ cm}^{-1}$ , at least by a factor of ten. In vapour phase at higher temperatures, the lower frequency component becomes more intense as compared to the higher frequency one. From their temperature dependence, it seems reasonable to associate the bands at frequencies  $848$  and  $866\text{ cm}^{-1}$  in liquid phase to the nondegenerate C-N stretching modes arising due to different rotational isomers. The weak shoulder at  $855\text{ cm}^{-1}$

in solid phase may then be interpreted as an overtone of  $\nu_{43}$  mode. In the vapour phase infrared spectrum, two bands are observed at  $953\text{ cm}^{-1}$  (weak) and  $978\text{ cm}^{-1}$  (medium strong). In the crystalline state, the band at  $953\text{ cm}^{-1}$  splits into three close components with frequencies at  $938$ ,  $947$  and  $956\text{ cm}^{-1}$ . This splitting may be due to resonance interaction of the second harmonic of the band at  $471\text{ cm}^{-1}$  and the combination tone  $355 + 588 = 943\text{ cm}^{-1}$  with nearby other bands. This splitting in liquid phase is probably obscured due to the weak intensity of the bands. The band at  $978\text{ cm}^{-1}$  splits into a very close doublet in the crystalline state and is ascribed to the degenerate C-C stretching mode  $\nu_{38}$ , as the corresponding Raman line at  $980\text{ cm}^{-1}$  is depolarized. The  $953\text{ cm}^{-1}$  infrared band and the  $950\text{ cm}^{-1}$  polarized Raman line have been associated with the non-degenerate C-C stretching mode  $\nu_{14}$ . The remaining in-plane vinyl hydrogen bending modes  $\nu_{11}$  and  $\nu_{34}$  have been attributed respectively to the bands at  $1236$  and  $1251\text{ cm}^{-1}$  in the infrared spectrum of solid phase.

In the frequency region below  $600\text{ cm}^{-1}$ , this molecule is expected to have fifteen fundamental modes, nine of them correspond to the skeletal bendings and six to the torsional modes. The pair of bands in the infrared spectrum at frequencies  $555$  and  $588\text{ cm}^{-1}$  shows a marked difference in the relative intensities of its components under different conditions. In the vapour phase, the band at  $555\text{ cm}^{-1}$  is more intense than the band at  $588\text{ cm}^{-1}$ . At higher temperatures, their relative intensity is altered but at low temperature in solid phase, the  $555\text{ cm}^{-1}$  band disappears completely. The band at  $588\text{ cm}^{-1}$  has been assigned to the CCN bending mode for the more stable isomer and the vanishing band at  $555\text{ cm}^{-1}$  to the less stable isomer(s). The other CCN deformation mode has been

associated with the polarized Raman band at  $349\text{ cm}^{-1}$ . The  $\text{-C-C}=\text{C}$  skeletal bending modes  $\nu_{19}$  and  $\nu_{43}$  have been placed at  $395$  and  $424\text{ cm}^{-1}$  in the vapour phase respectively in analogy with the assignment of Lord and Venkateswarlu<sup>13</sup> for propylene. The Raman line at  $394\text{ cm}^{-1}$  is polarized showing a depolarized shoulder at  $423\text{ cm}^{-1}$ . The weak and polarized Raman band at  $280\text{ cm}^{-1}$  has been assigned to the CNC deformation mode  $\nu_{21}$ . The other CNC deformation mode may be placed at  $471\text{ cm}^{-1}$  corresponding to the depolarized Raman line at  $467\text{ cm}^{-1}$ .

The assignment of the torsional modes is somewhat ambiguous and a tentative assignment for them is proposed in Table 6.2. It is also quite likely that some of the bands assigned to these torsional modes may arise due to less stable forms of the molecule. Besides the fundamentals discussed above, all the other observed bands may be satisfactorily explained as combinations and/or overtones of the fundamental vibrations and are given in Table 6.2.



## REFERENCES

1. C.H. Hine, J.K. Kodama, R.J. Guzman and G.S. Loquiam, Arch. Environmental Health 1, 343 (1960)
2. (a) R.J. Guzman et al., Arch. Environmental Health 2, 62 (1961);  
(b) K. Tsuda and T.H. Nakamura, J. Phrm. Soc. Japan 67, 107 (1947);  
(c) Gisele, Vex lea rschi and P. Rump, Compt. Rend. 236, 939 (1953);  
(d) J.C. Rapean, D.L. Pearson and H. Sello, Ind.Eng. Chem. 77A, 51(1959)  
(e) J.R. Parrish and R. Stevenson, Chem. and Ind. (London), 531 (1960)
3. L. Kahovec and K.W.F. Kohlrausch, Z. Physik. Chem. B-46, 165 (1940)
4. B. Gross and M.T. Forel, J. Khim. Phys. 62, 1163 (1963)
5. B.V. Thosar, Z. Physik. Chem. 107, 780 (1937)
6. E. Hirota, J. Chem. Phys. 42, 2071 (1965)
7. W.A. Seth-Paul and G. Dijkstra, Spectrochim. Acta 23A, 2861 (1967)
8. R.D. McLachlan and R.A. Nyquist, Spectrochim. Acta 24A, 103 (1968)
9. W.J. Potts and R.A. Nyquist, Spectrochim. Acta 679 (1959)
10. G. Herzberg, Infrared and Raman Spectra of Polyatomic Molecules, Van Nostrand Co., New York (1945)
11. P. Torkington, J. Chem. Phys. 17, 1279 (1949)
12. N. Sheppard, J. Chem. Phys. 17, 74 (1949)
13. R.C. Lord and P. Venkateswarlu, J. Opt. Soc. Amer. 43, 1079 (1953)
14. S. Ziomek and Forrette, J. App. Polymer Science 7, 1307 (1963)

TABLE 6.1

THE MOLECULAR PARAMETERS FOR THE GGG(I), GGG(II) AND GGG(III)  
CONFORMATIONS OF TRIALLYL AMINE CORRESPONDING TO ALL THE  
THREE N-C-C=C SKELETONS SIMULTANEOUSLY IN THE 'CIS',  
'GAUCHE' AND 'GAUCHE' POSITIONS RESPECTIVELY

Species	GGG(I)	GGG(II)	GGG(III)
$I_a(\text{a.m.u.} \cdot \text{\AA}^2)$	364.2	441.7	410.1
$I_b(\text{a.m.u.} \cdot \text{\AA}^2)$	364.2	441.7	410.1
$I_c(\text{a.m.u.} \cdot \text{\AA}^2)$	639.6	730.8	770.7
$\beta = \frac{C}{B} - 1$	-0.430	-0.396	-0.468
$\Delta \nu(\text{PR}) \parallel$ type bands	13.5 $\text{cm}^{-1}$	12.1 $\text{cm}^{-1}$	10.4 $\text{cm}^{-1}$
$\Delta \nu(\text{PR}) \perp$ type bands	10.0 $\text{cm}^{-1}$	9.5 $\text{cm}^{-1}$	7.7 $\text{cm}^{-1}$

TABLE 6.2

## INFRARED AND RAMAN SPECTRA OF TRIALLYL AMINE

Infrared						Raman			Assignment* (assuming poi group symmetr C <sub>3</sub> )
Vapour		Liquid		Solid (cryst.)		(Liquid)			
(cm-1)	Int.	(cm-1)	Int.	(cm-1)	Int.	(cm-1)	Int.	Qual. depol.	
				3780 } 3775 }	v w				v <sub>4</sub> + v <sub>16</sub>
3675	v w	3673	v w	3685 } 3677 }	v w				v <sub>24</sub> + v <sub>42</sub>
3295 } 3280 }	w	3287	m	3272 } 3268 }	w				2x v <sub>29</sub>
3090 } 3086 } 3081 }	11 + 1 ms	3078	s	3073 } 3069 }	m	3080	m	0.78	v <sub>1</sub> , v <sub>24</sub>
3024 } 3019 } 3014 }	1 m	3008	m	3004 } 3001 }	m	3010	s	0.13	v <sub>2</sub> , v <sub>25</sub>
2989	ms	2979	s	2969	m	2981	m	0.13	v <sub>3</sub> , v <sub>26</sub>
2942 } 2936 }	ms	2925	m	2914 } 2911 }	m	2926	s	0.24	v <sub>27</sub>
2922	sh	2913	sh						v <sub>4</sub>
2881	w	2882	w	2883 } 2880 }	w	2885	v w	D	v <sub>30</sub> + v <sub>31</sub>
2813	sh	2810	sh	2796	sh	2808	s	0.3	v <sub>5</sub>
2798	s	2791	s	2791 } 2788 }	s	2792	sh	P	v <sub>28</sub>
2769	mw	2760	w	2752	m	2765	v w	0.44	v <sub>29</sub> + v <sub>36</sub>
2708	w	2702	w	2702	v w				v <sub>31</sub> + v <sub>33</sub>
				2670	w				v <sub>31</sub> + v <sub>34</sub>
		1985	v w						2x v <sub>31</sub>

Contd...

Table 6.2 Contd...

169

				1892	w				$\nu_{38} + \nu_{39}$
1845 } 1841 } 1836 }	wm	1841	m	1845	w				$2X \nu_{39}$
1656	sh	1663	sh	1660	w				$\nu_{16} + \nu_{17}$
1651 } 1646 }	ms	1644	ms	1642 } 1636 }	m	(1638)	100	0.11	$\nu_{29}$
1641	sh	1639	sh	1630	sh	1636	100	0.11	$\nu_6$
1463	vw	1460	vw	1470	vw				$\nu_{37} + \nu_{44}$
1452	m	1449	s	1448 } 1444 }	m	1445	20	0.82	$\nu_{30}$
1440	sh	1439	sh						$\nu_7$
1424 } 1418 }	ms	1423	sh	1424 } 1420 }	m	1420	30	0.48	$\nu_{31}$
		1418	s	1410	w	1408	sh	?	$\nu_8$
1362	m	1354	m	1349 } 1345 }	ms	1352	vw	?	$\nu_9, \nu_{32}, \text{CH}_2 \text{ wag.}$
1342	sh	1333	sh			1332	5	0.92	Isomer(s), $\text{CH}_2 \text{ wag.}$
1296	w	1295	w, sh	1293 } 1289 }	vw	(1292)	90	0.32	$\nu_{33}$
				1280	vw	1292	90	0.32	$\nu_{10}$
1266	s	1259	s	1254 } 1248 }	ms	1258	20	0.85	$\nu_{34}$
				1236	w				$\nu_{11}$
		1163	sh	1161	w	1161	sh	?	$\nu_{12}$
1156 } 1150 }	ms	1147	ms	1155 } 1151 }	ms	1148	5	0.62	$\nu_{35}$
1121 } 1115 } 1109 }	s	1108	s	1102 } 1099 }	ms	1106	4	0.93	$\nu_{36}, \text{C-N str.}$
1082	mw	1074	m			1073	2	0.71	Isomer(s), $\text{C-N str.}$
				1011	w				$\nu_{13}$

Contd...

Table 6.2 Contd.

1002 } 1	s	996	s	997	s	1000	vw	?	v <sub>37</sub>
998 }									
993 }									
978	m, sh	976	ms	979 } 976 }	s	980	5	0.80	v <sub>38</sub>
953	vw	955	w	956	m	950	10	0.37	v <sub>14</sub>
				947	m				2X v <sub>44</sub>
				938	w				v <sub>20</sub> + v <sub>42</sub>
921 } 1	vs	918	vs	921	s	915	20	0.78	v <sub>39</sub>
917 }									
				910	sh				v <sub>15</sub>
858	w	866	m	870	ms	862	m	P	v <sub>16</sub> , C-N str.
		854	sh	855	w, sh				2X v <sub>43</sub>
845	w	848	sh			846	30	0.26	Isomer(s), C-N str.
795	vw			810 } 800 }	vw	778	vw		v <sub>17</sub>
						750	vw		v <sub>40</sub>
650	mw	653	mw	662	m	652	4	0.85	v <sub>41</sub>
				652	sh	642	w, sh	P	v <sub>18</sub>
588	w	590	w	587 } 582 }	m	586	w	0.2	v <sub>42</sub> , CCN def.
555	mw	557	mw			555	3	0.85	Isomer(s), CCN def.
471	w	470	vw	471	ms	467	5	0.91	v <sub>44</sub>
424	w	426	w	427 } 422 }	ms	423	sh	D	v <sub>43</sub>
395	w	399	vw	402	m	394	60	0.13	v <sub>19</sub>
355	vw	352	vw	353 } 348 }	mw	349	15	0.37	v <sub>20</sub>
						280	sh	P	v <sub>21</sub>
						228	20	0.87	v <sub>45</sub>
						192	30	P	v <sub>22</sub>
						~78	w	D	v <sub>46</sub>

\*The numbering of the modes is according to C<sub>3</sub> symmetry for the molecule (GGG (III) form).  
 Abbreviations: w, m, s, sh, v refer to weak, medium, strong, shoulder and very respectively.  
 ? means an uncertain assignment. P means Polarized and D means Depolarized Raman bands.

TABLE 6.3

FUNDAMENTAL VIBRATION FREQUENCIES (in  $\text{cm}^{-1}$ ) OF THE LOWER  
ENERGY GGG(III) FORM OF TRIALLYL AMINE

Species	Type	Approx. Description	Infrared			Raman (Liquid)
			Liquid	Vapour	Solid (Cryst.)	
a	$\nu_1$	$=\text{CH}_2$ stretch (asym.)	3078	3086	3073 } 3069 }	3080
	$\nu_2$	$=\text{CH}$ stretch (sym.)	3008	3019	3004	3010
	$\nu_3$	$=\text{CH}_2$ stretch (sym.)	2979	2989	2969	2981
	$\nu_4$	$-\text{CH}_2$ stretch (asym.)	2913	2922		2926
	$\nu_5$	$-\text{CH}_2$ stretch (sym.)	2810	2813	2796	2808
	$\nu_6$	C = C stretch	1639	1641	1630	1638
	$\nu_7$	$-\text{CH}_2$ deformation	1439	1440		1445
	$\nu_8$	$=\text{CH}_2$ deformation	1418		1410	1420
	$\nu_9$	$-\text{CH}_2$ wagging	1354	1362	1349 } 1345 }	1352
	$\nu_{10}$	Vinyl hydrogen in-plane bending			1280	1292
	$\nu_{11}$	Vinyl hydrogen in-plane bending			1236	
	$\nu_{12}$	$-\text{CH}_2$ twisting	1163		1161	1161
	$\nu_{13}$	Vinyl hydrogen out-of-plane bending			1011	1010
	$\nu_{14}$	C-C stretch	955	953	956	955
	$\nu_{15}$	Vinyl hydrogen out-of-plane bending			910	
	$\nu_{16}$	C-N stretch	866	858	870	862
	$\nu_{17}$	$-\text{CH}_2$ rocking				750
	$\nu_{18}$	Vinyl hydrogen out-of-plane deformation			652	642
	$\nu_{19}$	$-\text{C}-\text{C}=\text{C}$ bending	399	395	402	394
	$\nu_{20}$	CCN bending	352	355	353 } 348 }	349
	$\nu_{21}$	CNC bending				280

Contd...

Table 6.3 Contd...

172

	$\nu_{22}$	C-C torsion				192
	$\nu_{23}$	torsion along C-N bond				
e	$\nu_{24}$	=CH <sub>2</sub> stretch (asym.)	3078	3086	3073 } 3069 }	3080
	$\nu_{25}$	=CH stretch	3008	3019	3004	3110
	$\nu_{26}$	=CH <sub>2</sub> stretch (sym.)	2979	2989	2969	2981
	$\nu_{27}$	-CH <sub>2</sub> stretch (asym.)	2925	2936	2914 } 2911 }	2926
	$\nu_{28}$	-CH <sub>2</sub> stretch (sym.)	2791	2798	2791 } 2788 }	2792
	$\nu_{29}$	C=C stretch	1644	1646	1642 } 1636 }	1638
	$\nu_{30}$	-CH <sub>2</sub> deformation	1449	1452	1448 } 1444 }	1445
	$\nu_{31}$	=CH <sub>2</sub> deformation	1418	1418	1424 } 1420 }	1420
	$\nu_{32}$	-CH <sub>2</sub> wagging	1354	1362	1349 } 1345 }	1352
	$\nu_{33}$	Vinyl hydrogen in-plane bending	1295	1296	1293 } 1289 }	1292
	$\nu_{34}$	Vinyl hydrogen in-plane bending	1259	1266	1254 } 1248 }	1258
	$\nu_{35}$	-CH <sub>2</sub> twisting	1147	1156	1155 } 1151 }	1148
	$\nu_{36}$	C-N stretch	1108	1115	1102 } 1099 }	1106
	$\nu_{37}$	Vinyl hydrogen out-of-plane bending	996	998	997	1005
	$\nu_{38}$	C-C stretch	976	978	979 } 976 }	980
	$\nu_{39}$	Vinyl hydrogen out-of-plane bending	918	921	921	915
	$\nu_{40}$	-CH <sub>2</sub> rocking		795	810 } 800 }	778
	$\nu_{41}$	Vinyl hydrogen out-of-plane bending	653	650	662	652
	$\nu_{42}$	C-CN bending	589	588	587 } 582 }	586
	$\nu_{43}$	-C-C = C bending	426	424	427 } 422 }	423
	$\nu_{44}$	CNC bending	470	471	471	467
	$\nu_{45}$	C-C torsion				228
	$\nu_{46}$	torsion along C-N bond				78

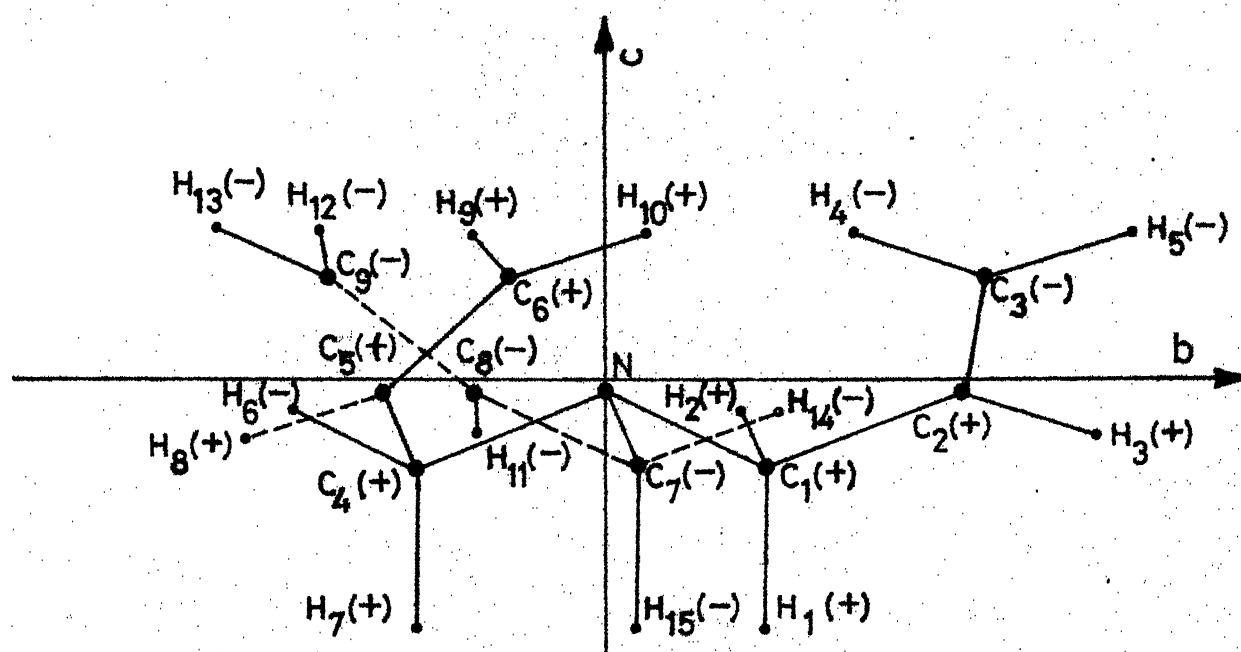
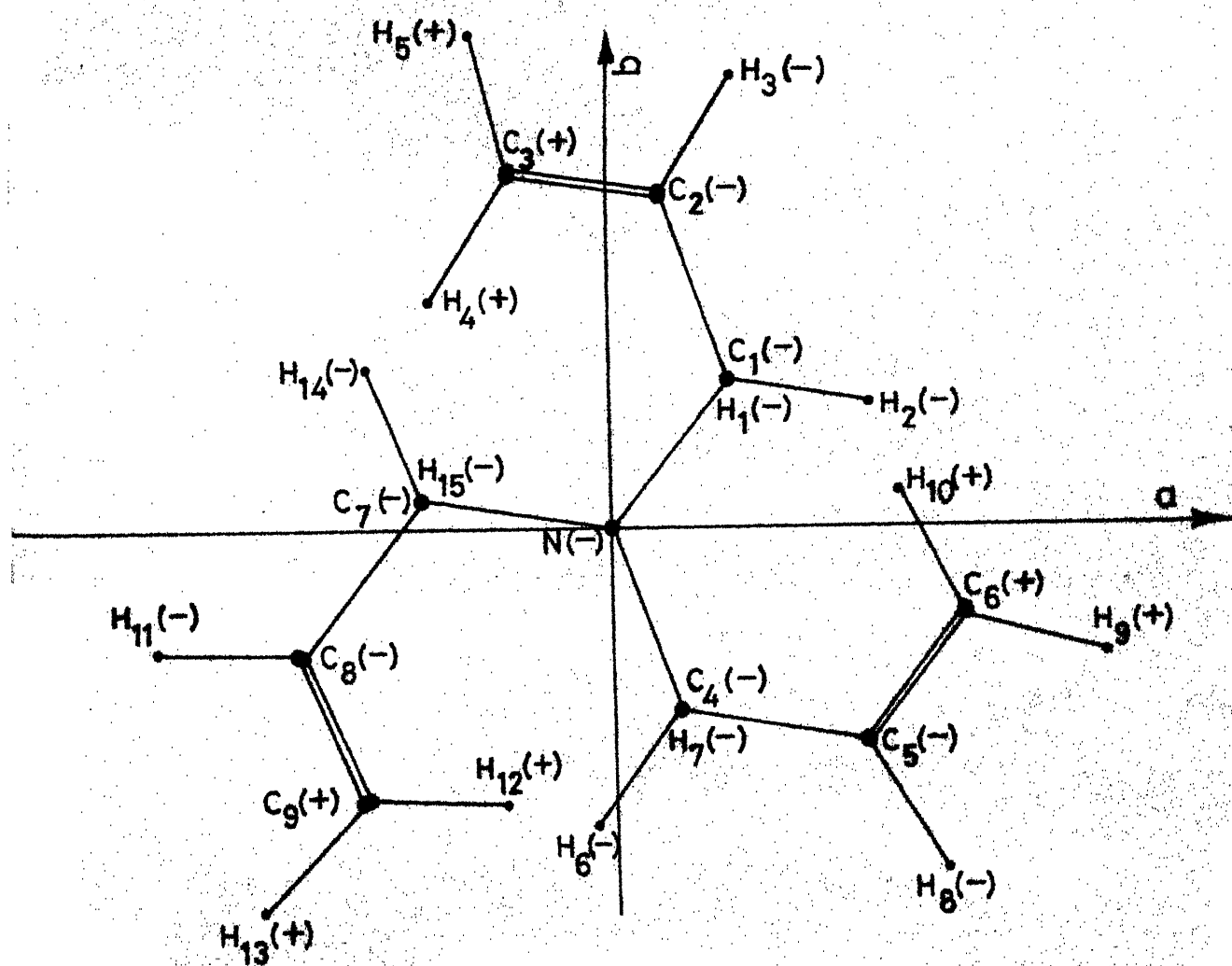
GGG (I) ( $C_3$ )GGG (I) ( $C_3$ )

Fig. 6. I(A): The projections of the GGG(I) form of TAA on the  $a$ - $b$  and  $b$ - $c$  planes of principal axes system. The + and - signs indicate the atoms above and below the planes respectively. (The description of these forms is given in the text).



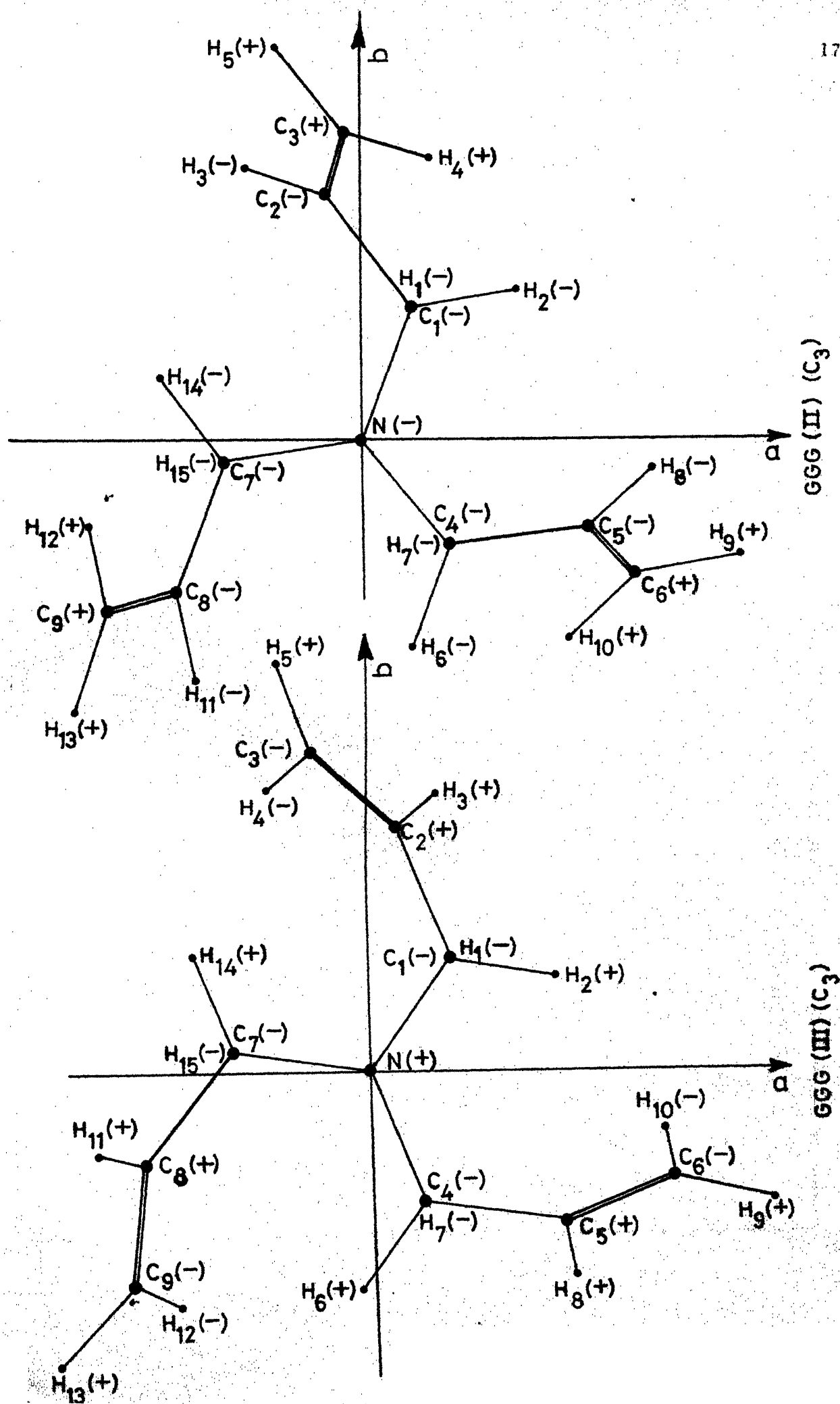


Fig. 6.1(B): The projections of the GGG(II) and GGG(III) forms of TAA on *a* - *b* plane of principal axes system.

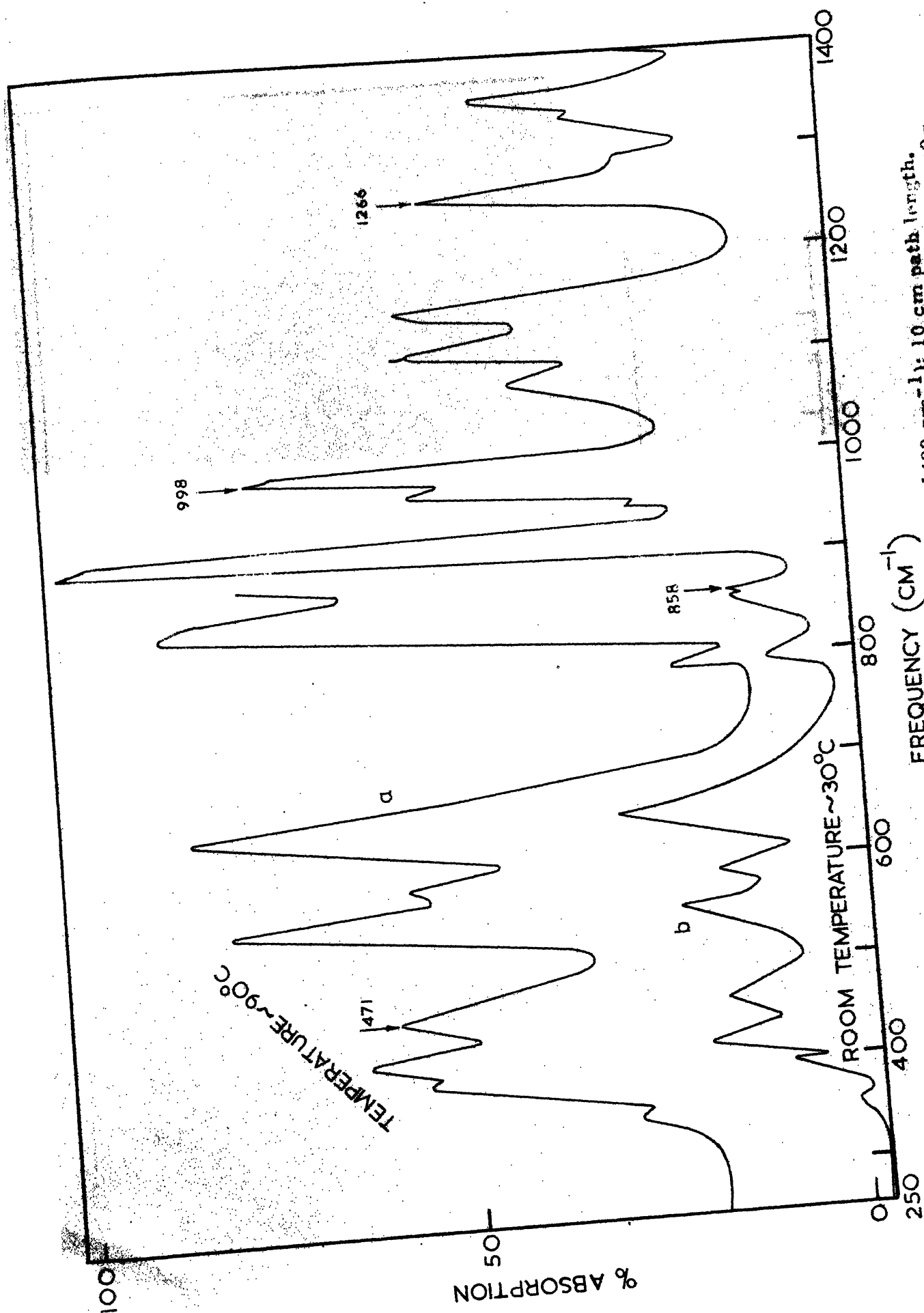


Fig. 6.2(A): The infrared spectrum of gaseous TAA (250-1400 cm<sup>-1</sup>); 10 cm path length. The letters a and b denote saturated vapour pressures at ~90°C and ~30°C respectively.

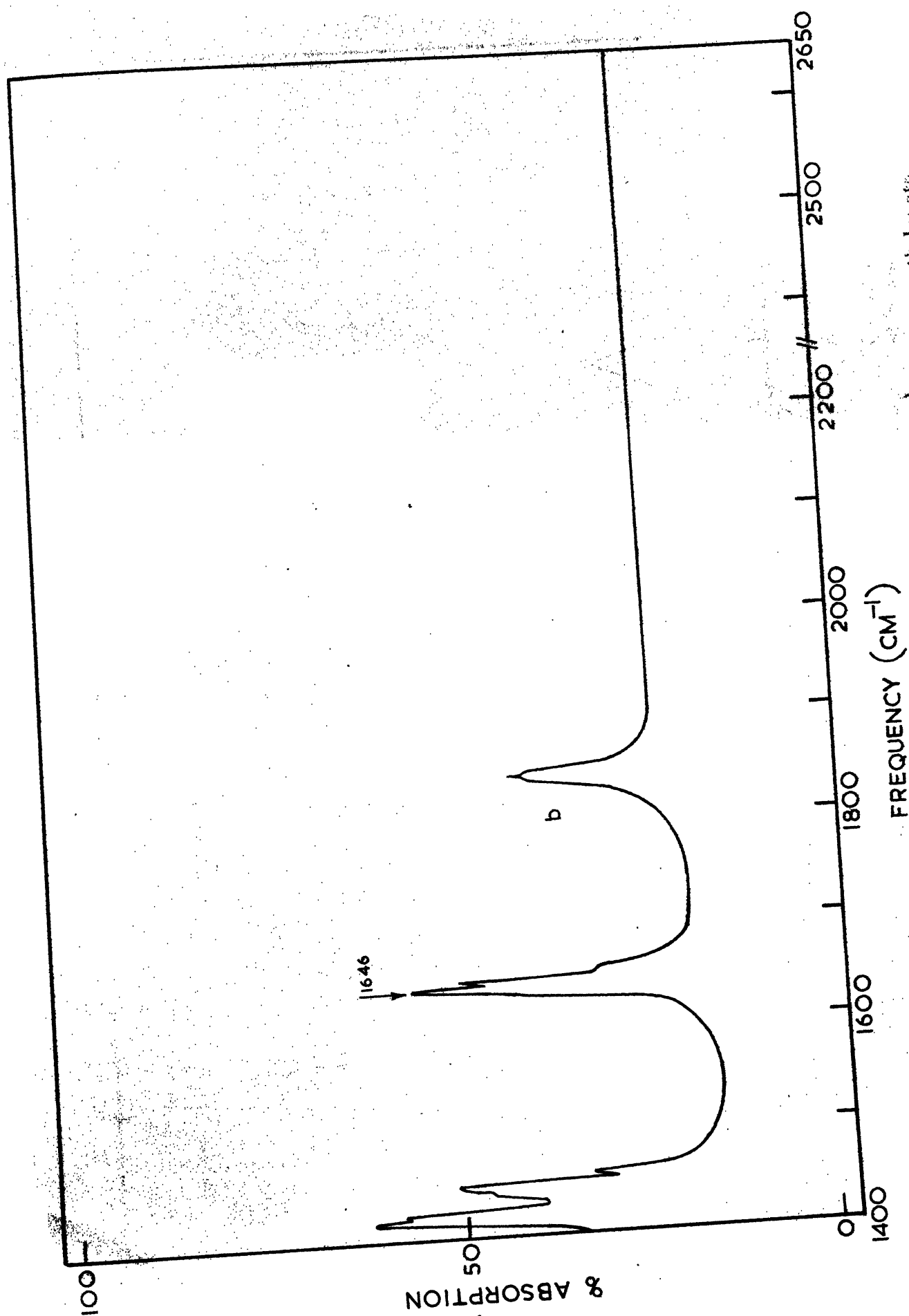


Fig. 6.2(3): The infrared spectrum of gaseous TAA ( $1400 - 2650 \text{ cm}^{-1}$ ); 10 cm path length. The letters a and b denote saturated vapour pressures at  $\sim 90^\circ\text{C}$  and  $\sim 20^\circ\text{C}$  respectively.

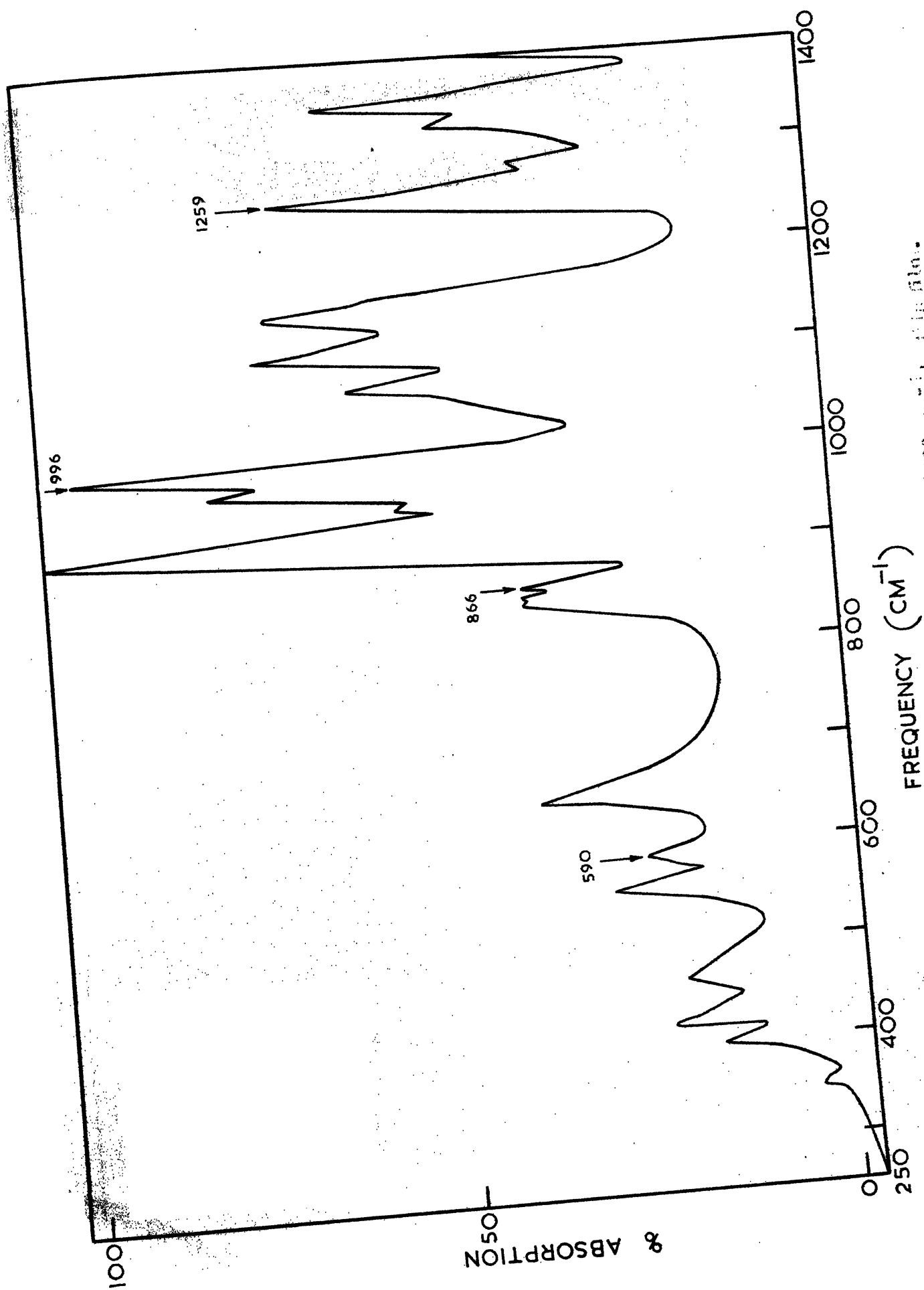


Fig. 6.3 A): The infrared spectrum of liquid TAA (250-1400  $\text{cm}^{-1}$ ) film flow.

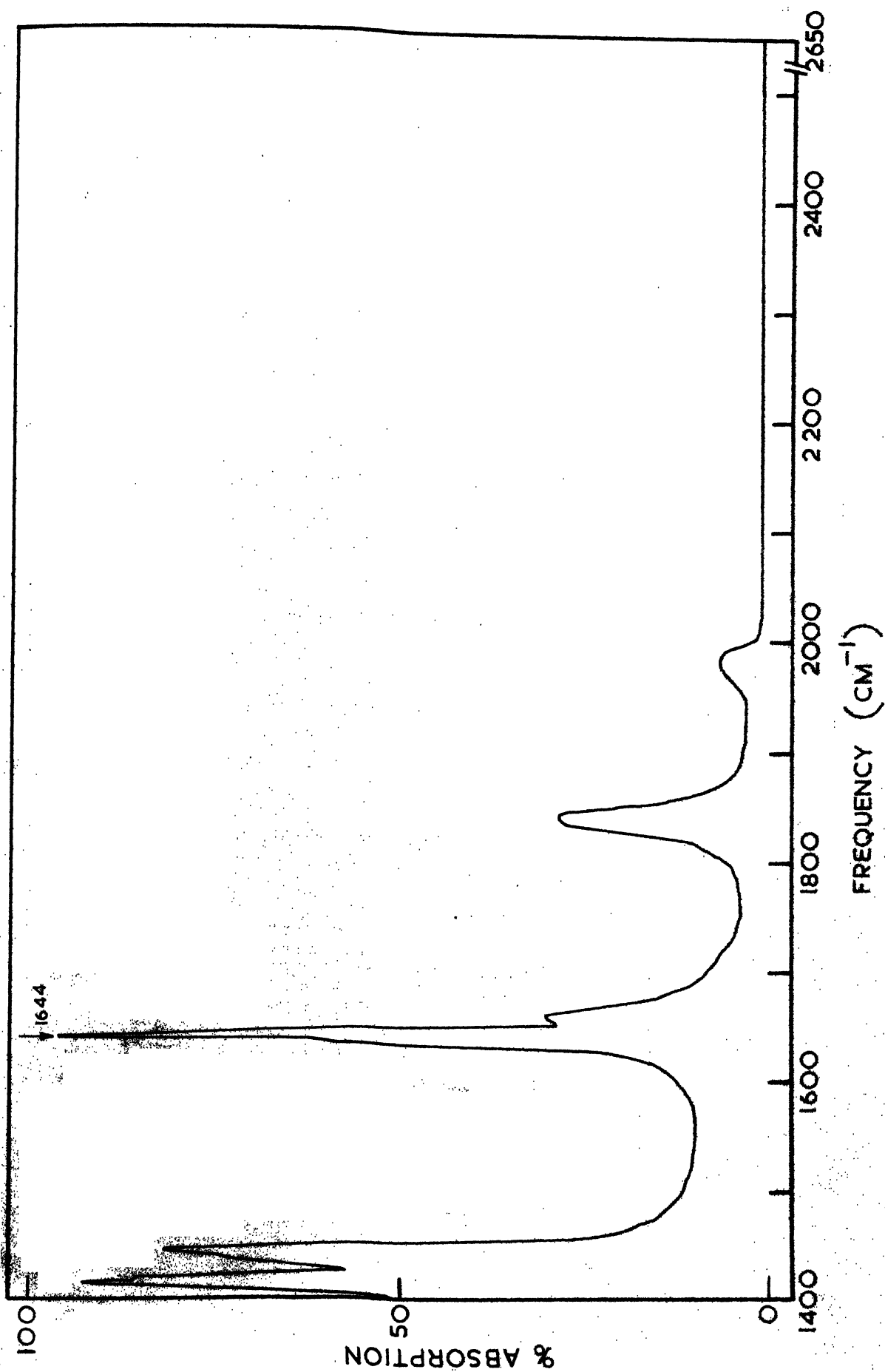


Fig. 6.35: The Infrared spectrum of liquid TAA (1400 - 2650 cm<sup>-1</sup>); thin film.

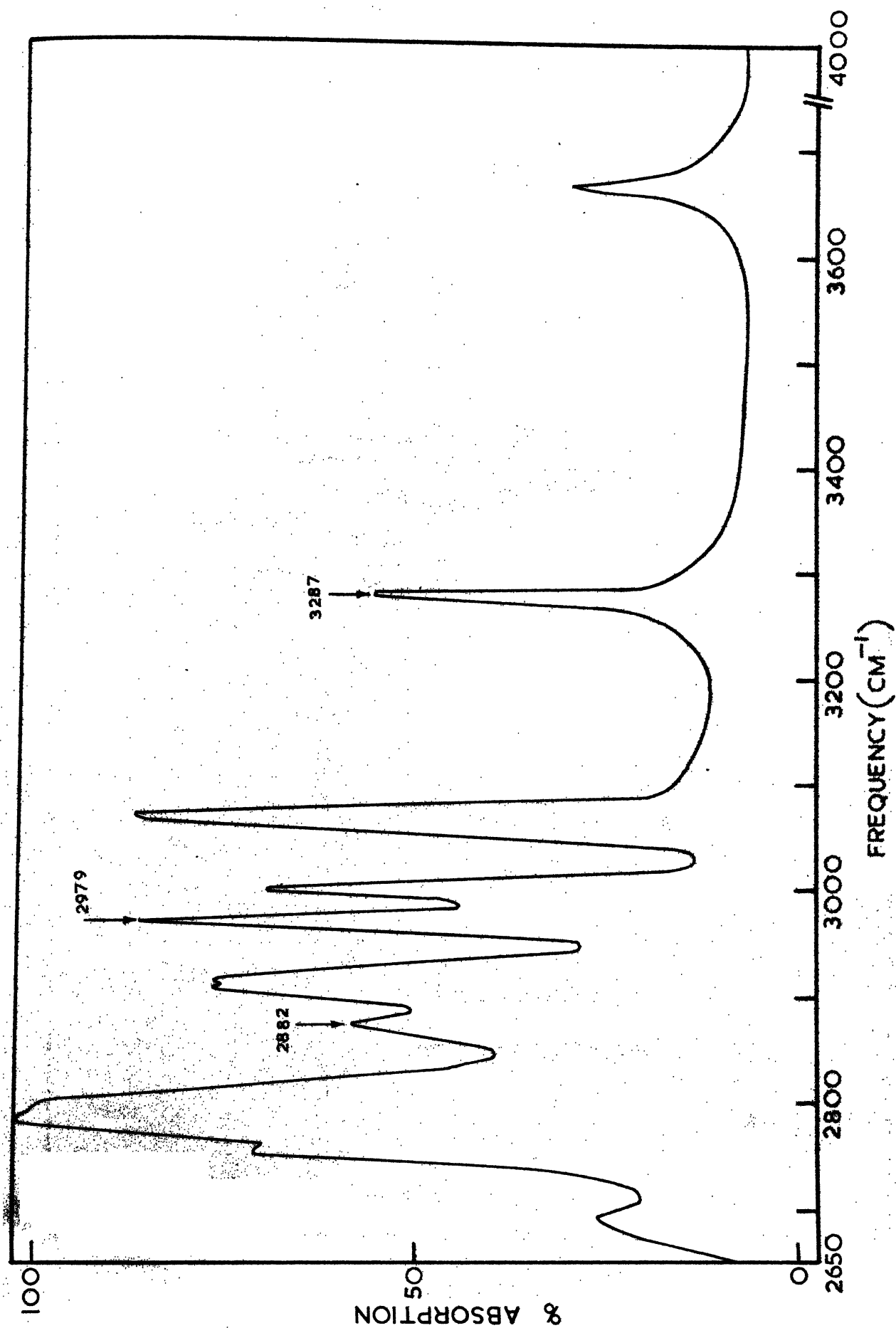


Fig. 9.3(C): The Infrared spectrum of liquid TAA (2650-4000  $\text{cm}^{-1}$ ); thin film.

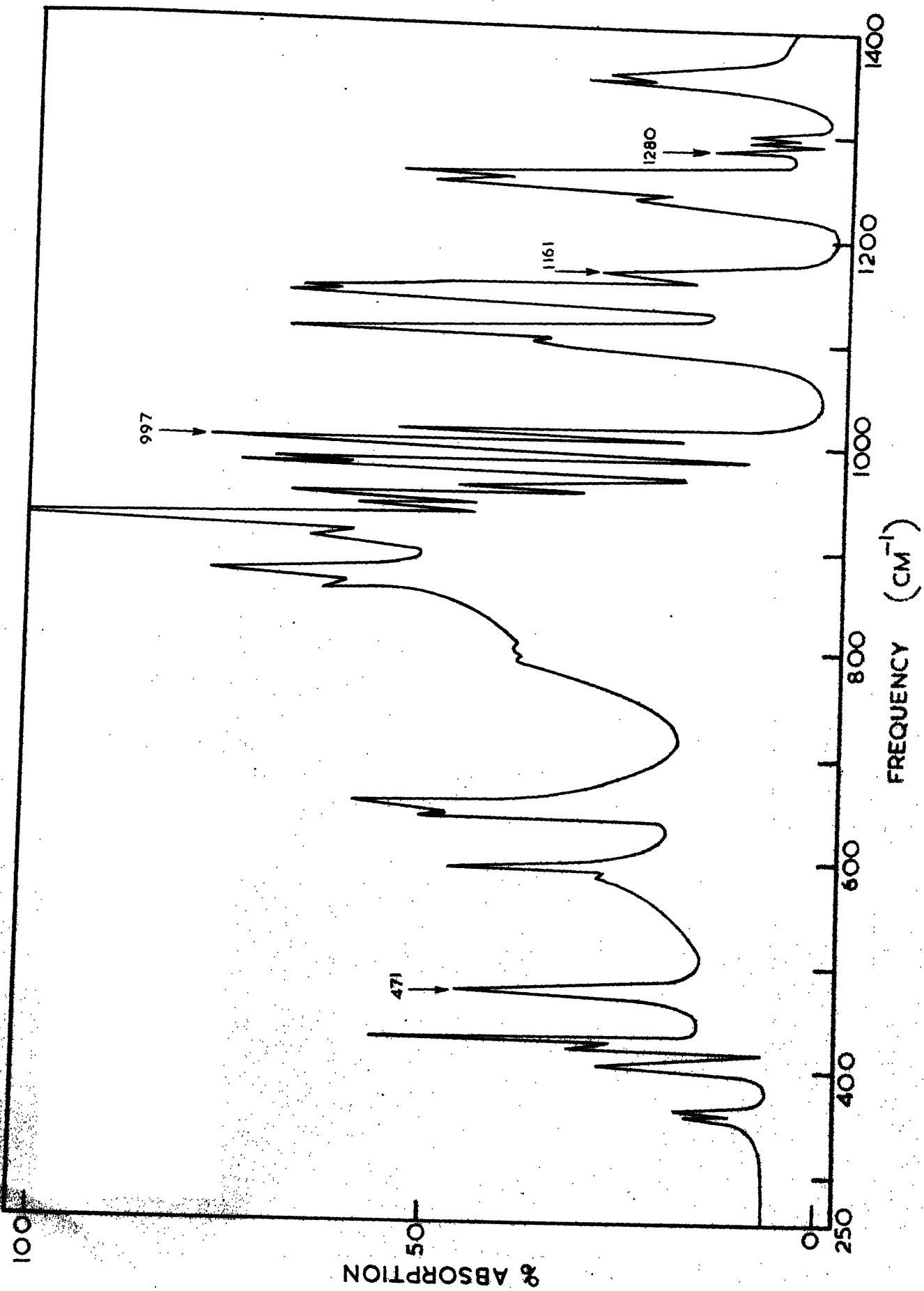


FIG. 6.4(A): The infrared spectrum of an annealed film of TAA near 77°K (250-1400 cm<sup>-1</sup>).

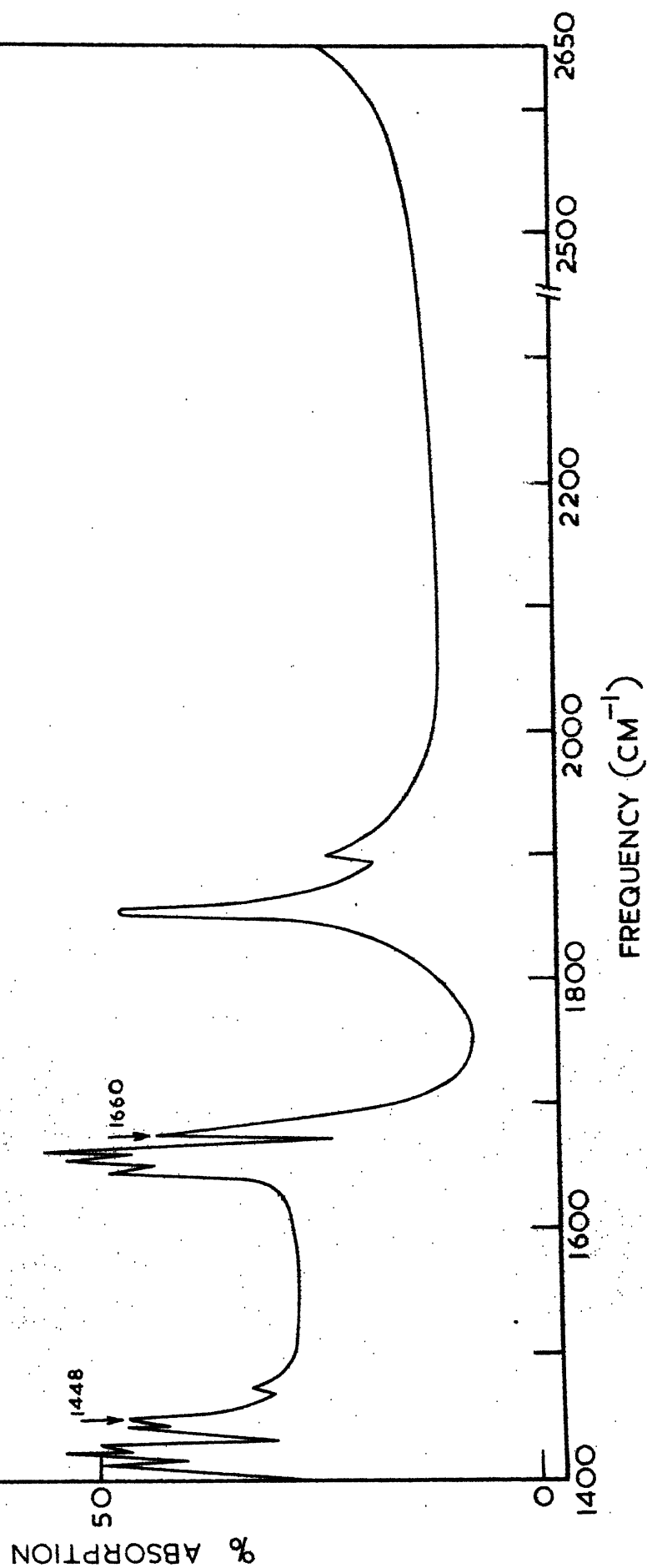


Fig. 6.4(B): The infrared spectrum of an annealed film of TAA near 77°K (1400-2650 cm<sup>-1</sup>).



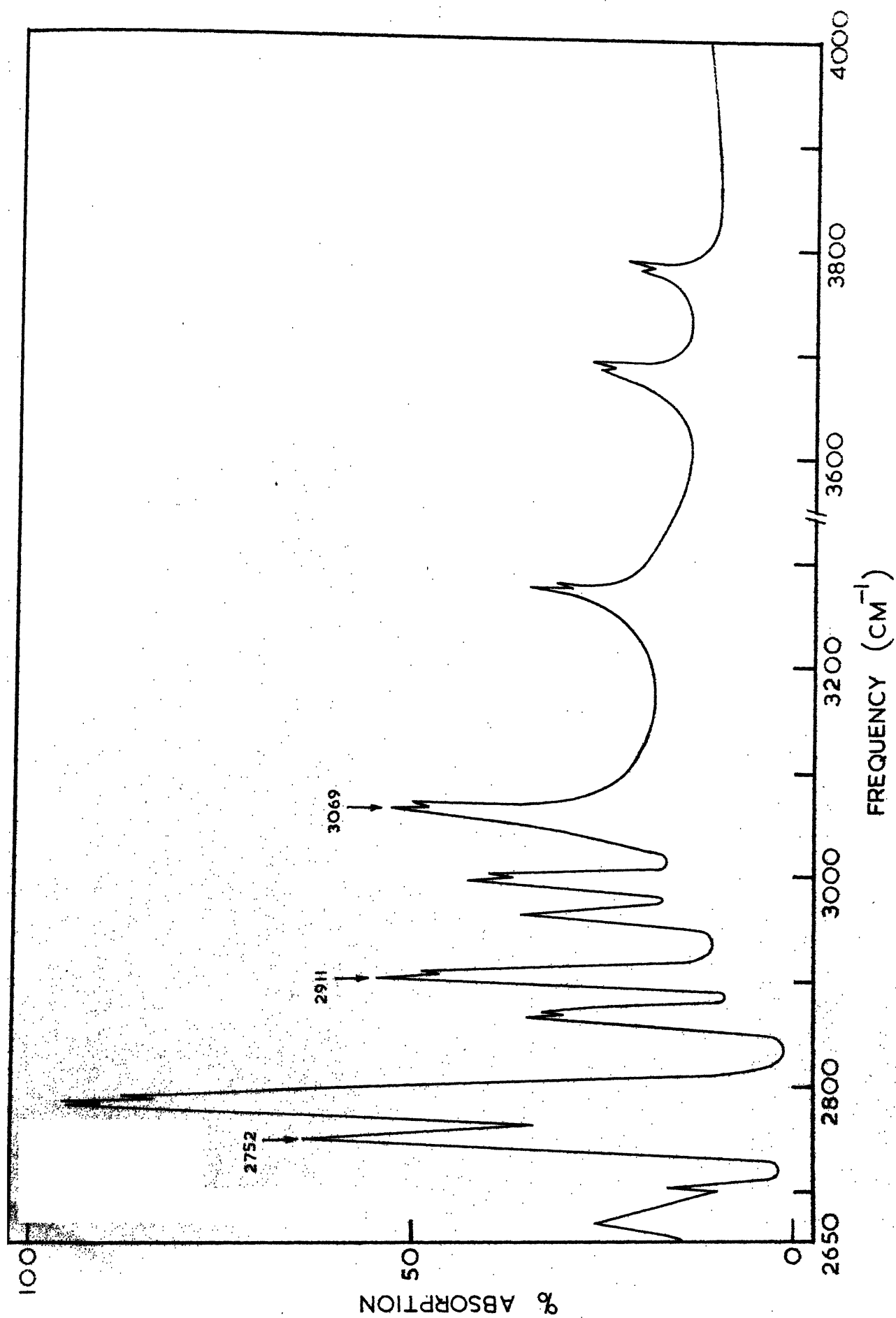


Fig. 6.4(C): The infrared spectrum of an annealed film of TAA near 77°K (2650-4000 cm<sup>-1</sup>).

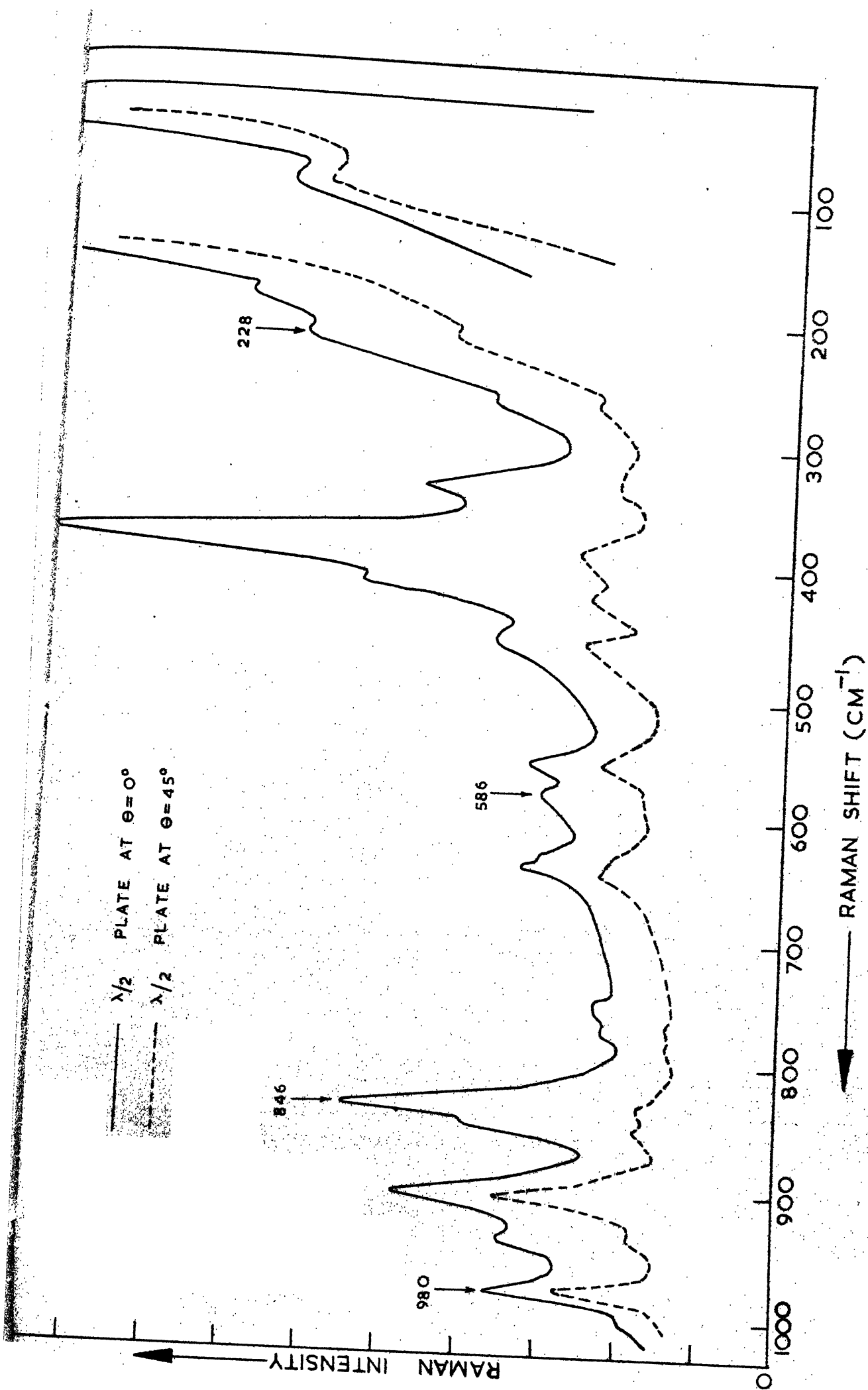


Fig. 6.5(A): The laser-Raman spectrum of liquid TAA (0-1050 cm<sup>-1</sup>).

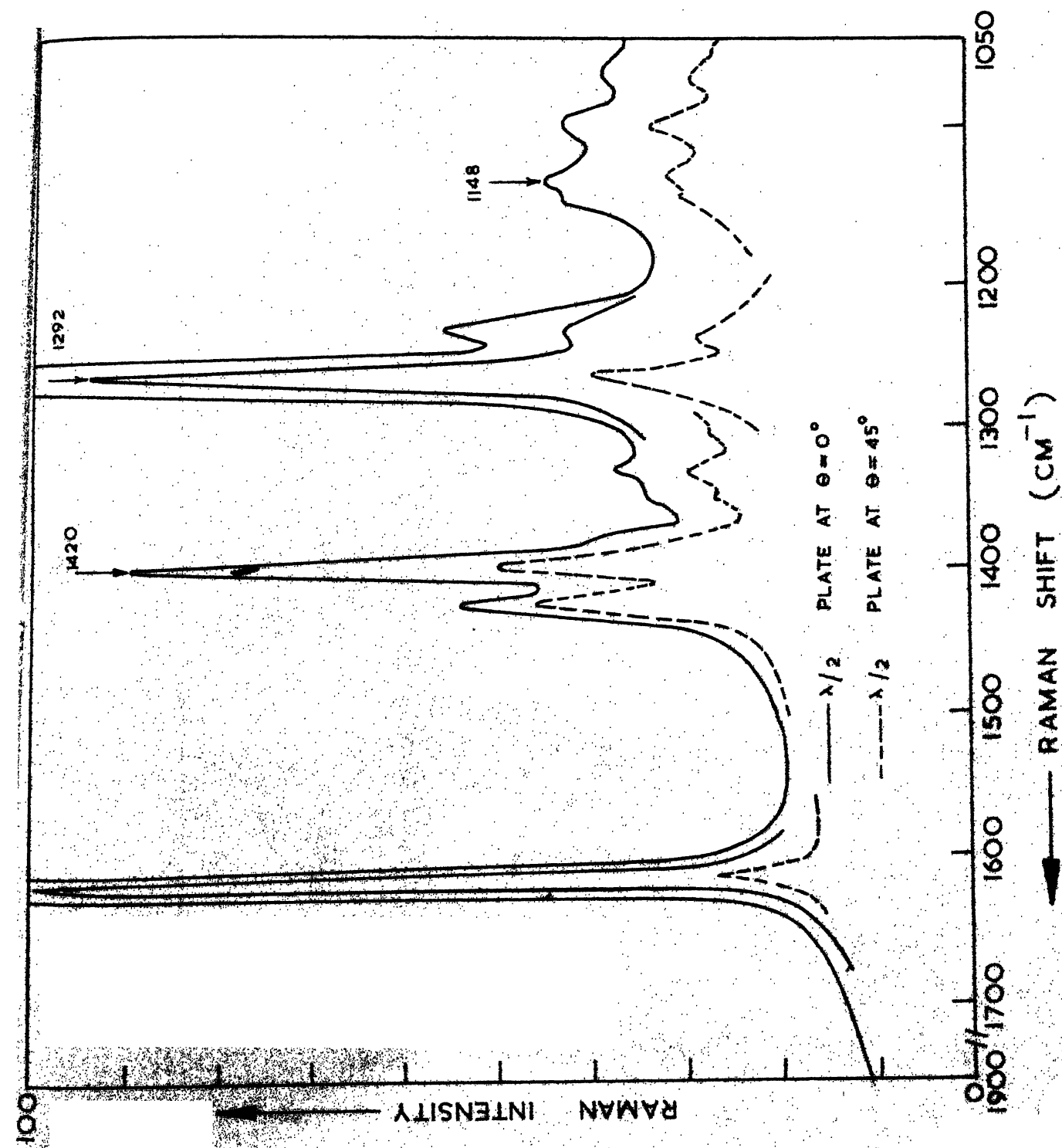


Fig. 6.5(B): The laser-Raman spectrum of liquid TAA (1050-1900 cm<sup>-1</sup>).

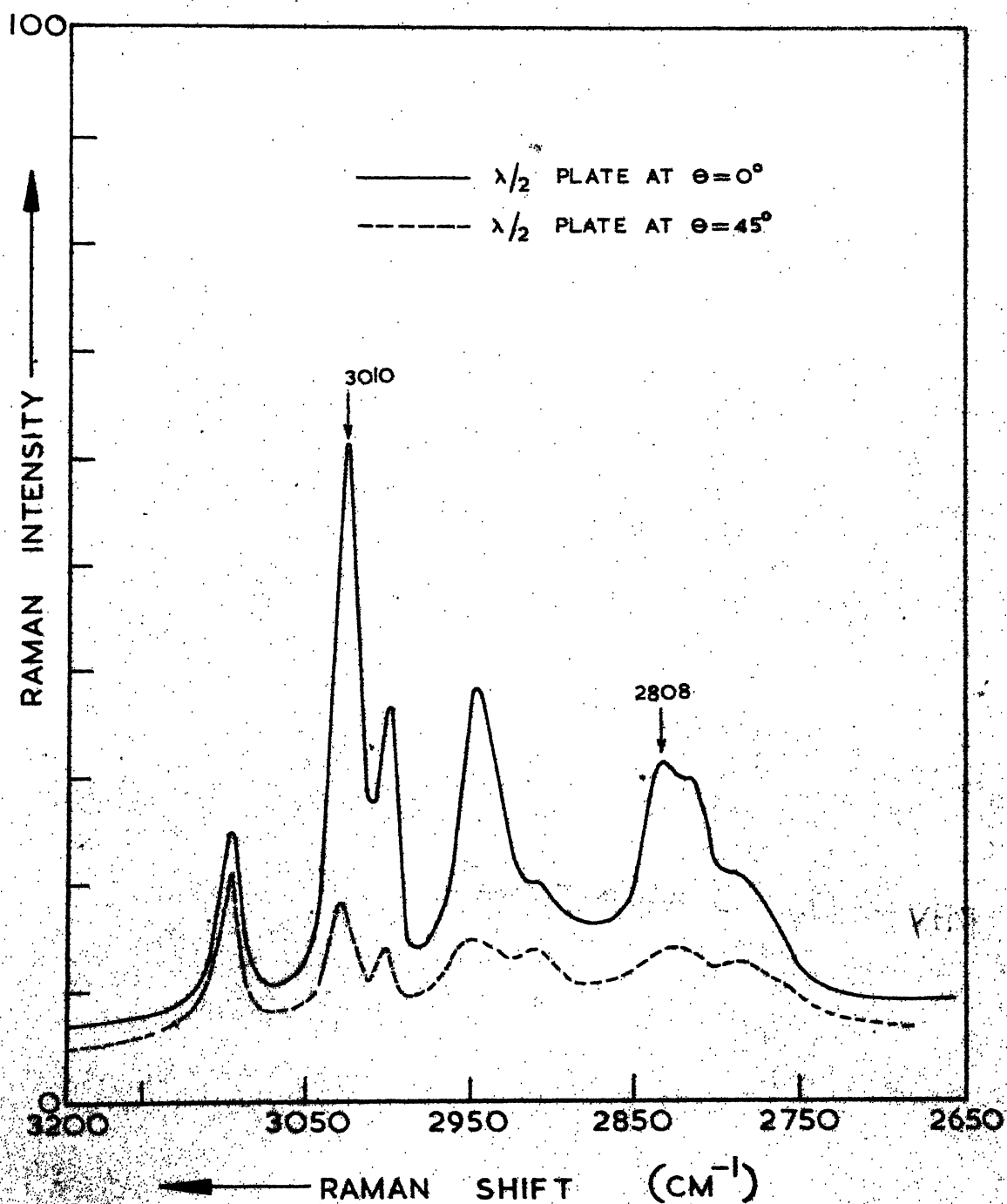


Fig. 6.5(C): The laser-Raman spectrum of liquid TAA (2650-3200 cm<sup>-1</sup>).